



**Investigation of chemoresistant mechanisms in triple negative breast
cancer cell lines and development of a nano-enabled Disulfiram for breast
cancer treatment**

A thesis submitted for the degree of

Doctor of Philosophy

By

Erebi Patricia Tawari B.Sc., M.Sc.

Faculty of Science and Engineering

March, 2016.

Investigation of chemoresistant mechanisms in triple negative breast cancer cell lines and development of a nano-enabled Disulfiram for breast cancer treatment

Erebi Patricia Tawari B.Sc., M.Sc.

A Thesis Submitted in partial fulfilment of the requirements of the University of
Wolverhampton for the degree of Doctor of Philosophy.

March 2016.

This work or any part thereof has not previously been presented in any form to the University or to any other body whether for the purpose of assessment, publication or for any other purpose (unless otherwise indicated). Save for any express acknowledgements, references and/or bibliographies cited in the work, I conform that the intellectual content of the work is the result of my own efforts and of no other person.

The right of Erebi P. Tawari to be identified as author of this work is asserted in accordance with ss.77 and 78 of the Copyright, Designs and Patents Act 1988. At this date copyright is owned by the author.

Signature:.....

Date:.....

Abstract

Cancer a global epidemic is a major cause of morbidity and mortality affecting populations in all nations and regions. Breast cancer (BC) is the second most common cancer in the world and the most fatal malignancy affecting women both in the developed and developing countries. Even with the improvement in overall survival of BC patients due to early detection and advancement with systematic therapy, triple negative breast cancer (TNBC), an aggressive subtype of BC still remains a major challenge as it lacks targetable receptors. Chemotherapy is the main treatment for TNBC. However, *de novo* and acquired resistance to conventional anticancer drugs is a major limitation and cause of therapeutic failure.

Cancer stem cells (CSCs) are believed to be responsible for chemoresistance and tumour relapse. My study demonstrates that hypoxia is involved in the development and maintenance of these CSCs traits in TNBC, as cells grown in hypoxia are significantly resistant to several first line anti-BC drugs. Hypoxia-induced activation of nuclear factor kappa B (NF κ B) and hypoxia inducible factors (HIFs) also play pivotal roles in chemoresistance. Forced expression of NF κ B and HIFs by transfection with p65 subunits of NF κ B and HIF1 α and 2 α subunits induced CSCs characters and resistance to a range of anticancer drugs in TNBC cell lines. My study also indicated a positive loop between the activation of NF κ B and HIFs. Therefore development of novel medicine to interfere the pathways of hypoxia and NF κ B may efficaciously target CSCs and reverse chemoresistance which will be of clinical significance for TNBC treatment.

Disulfiram (DS) is a commercially available anti-alcoholism drug. Recent studies demonstrate that it is highly cytotoxic in a wide range of cancer types and potentially repurposed as an anticancer drug. The anticancer mechanisms of DS were investigated in this study. The results from my study indicate that the cytotoxicity of DS is copper (Cu) dependent with a biphasic manner. The instant cytotoxic phase is induced by the extracellular reactive oxygen species (ROS) generated by the reaction between DS and Cu. The delayed killing is caused by the complex diethyldithiocarbamate (DDC) and Cu (DDC-Cu), the final product of the reaction. The cytotoxicity of both phases needs the intact DS. However, due to the extremely short half-life of DS in the bloodstream, the anticancer efficacy of DS has been severely hampered *in vivo* and in patients.

Nanotechnology-based drug delivery system is a rapidly evolving and expanding interdisciplinary field involving in an amalgamation of chemistry, engineering, biology and medicine. In the last part of my study, I have successfully encapsulated DS into polymeric micelle (PM) nanoparticles. The half-life of PM encapsulated DS (PM-DS) was extended to over 3 hours in horse serum. The PM-DS showed strong anticancer efficacy. Therefore this nano-enabled DS may be able to translate DS into cancer therapeutics in the future.

DEDICATION

This research work is dedicated to the Almighty God, for His protection and wisdom throughout this journey.

AKNOWLEDGEMENTS

I give the Almighty God all the glory for his unending grace to successfully complete this study. He has demonstrated to me in no small measure, through this programme that He is an ever-faithful and never failing God!

I sincerely thank the Nigerian Government through the management of Tertiary Educational trust funds (Tetfund) for providing me with a fully-funded 3-year scholarship for my studies at the University of Wolverhampton (UoW).

I thank the authority of the University of Wolverhampton for providing me with an enabling environment and erudite personnel for my PhD studies. On a very special note and with much heartfelt gratitude, I sincerely thank my supervisor Prof. Weiguang Wang for giving me the opportunity to undertake this project and for his careful and beneficial guidance, timely advice and frequent encouragement throughout the entire process. Prof. Juan Irache and Dr Krassi Yoncheva for introducing the concept of nano-encapsulation to me. I appreciate the time and effort of Dr Yoncheva for the preparation of micelles used for part of the study. Special thanks to Prof. Irache for making my stay at the University of Navarra a pleasant one and for his contribution to the successful completion of this this project.

For a great time in the lab, I would like to thank all the academic staff, technicians and researchers in RIHS for their support, encouragements and friendships. Dr. Angel Armesilla, Dr. Mark Morris, Dr. Zhipeng Wang and Dr Peng Liu for their help and encourage. Thanks to my colleagues, Dr. Vinodh Kannappan, Prasanna Channathodiyil, Kate Butcher and Sathishkumar Kurusamy for their strong support towards my study.

On a special note, I want to appreciate my husband Dr Chibueze Ikeh, his constant advice, encouragement and unceasing prayers. Your love and friendship means the world to me.

Thank you so much to my family and friends: Dad, Mum and siblings for their prayers, support and understanding over my long years of studies for various University degrees. Pastor (Dr) & Mrs Nonye Ezeah and members of RCCG (Hosanna House and Desire of Nations Parish) are well acknowledged for their encouraging and faith driven fellowships.

My sincere appreciation also goes to my dear friends Ayodele and Babale for your encouragement and friendships helped a lot, Adetoro, Richard Auta, Mandu, Olajumoke Adebayo-Oni, Adeniyi, and others. Thank you all.

TABLE OF CONTENTS

Contents	Page
Title page.....	i
Certification.....	ii
Abstract.....	iii
Dedication.....	v
Acknowledgements.....	vi
Table of Contents.....	viii
List of Tables.....	xxi
List of Figures.....	xxii
List of Abbreviations.....	xxviii

Chapter One

Introduction and literature review

1.1. Brief background on breast cancer.....	1
1.2. Classification and staging of breast cancer.....	2
1.3. Triple Negative Breast Cancer.....	5
1.3.1. Epidemiology and prevalence of triple negative breast cancer.....	5
1.3.2. Clinical and pathological features of TNBC.....	6
1.3.3. Classification of TNBC.....	6
1.3.4. Prognosis of TNBC.....	7
1.4. Treatment for Breast cancer.....	8
1.4.1. Chemotherapy.....	9
1.4.1.1. Cisplatin.....	11
1.4.1.2. Gemcitabine.....	13
1.4.1.3. Doxorubicin.....	15
1.4.1.4. Vincristine.....	17
1.4.1.5. Paclitaxel.....	18
1.5. Chemoresistance.....	19

1.5.1.	Drug efflux mechanisms.....	20
1.5.1.1.	P-glycoprotein.....	20
1.5.1.2.	Multidrug resistance associated protein (MRP).....	21
1.5.1.3.	Breast cancer resistance protein (BCRP).....	22
1.5.2.	Drug activation/ inactivation.....	23
1.5.3.	Defects in DNA damage repair.....	23
1.5.4.	Defects in apoptotic mechanisms.....	23
1.6.	Cancer stem cells	24
1.6.1.	Breast cancer stem cells	25
1.6.2.	Cancer stem cell markers.....	26
1.6.3.	Cancer stem cell in tumourigenesis	28
1.6.4.	Cancer stem cell and chemoresistance	29
1.6.5.	Cancer stem cell and hypoxia	30
1.7.	Hypoxia	31
1.7.1.	Hypoxia-inducible factors (HIFs).....	32
1.7.2.	HIF and cancer	34
1.8.	Nuclear factor kappa B (NFκB).....	34
1.8.1.	NFκB Family members	35
1.8.2.	Activation of NFκB Pathways.....	37
1.8.3.	NFκB and breast cancer.....	39
1.8.4.	NFκB and chemoresistance.....	40
1.8.5.	NFκB and hypoxia.....	41
1.9.	Disulfiram	44
1.9.1.	Metabolism of disulfiram	45
1.9.2.	Disulfiram and disease treatment	47
1.9.2.1.	Anti-alcoholism.....	47
1.9.2.2.	Anticancer treatment	48
1.9.3.	Cytotoxic mechanism of disulfiram	49
1.9.3.1.	Generation of reactive oxygen species (ROS).....	50
1.9.3.2.	ALDH inhibition	52
1.9.3.3.	Proteasome/ NFκB inhibition.....	53
1.9.3.4.	Overriding resistance mechanisms.....	54
1.10.	Encapsulation of chemotherapeutic drugs.....	55

1.10.1. Nanoencapsulation.....	55
1.10.2. Nanocarriers for anticancer drug delivery.....	56
1.10.3. Targeting strategies for effective drug delivery.....	58
1.10.4. Nanoencapsulation, a solution for chemotherapy delivery.....	59
1.11. Aim of the research.....	59
<u>Chapter Two</u>	
<u>Materials and Methods</u>	
2.0. Materials and Methods.....	60
2.1. Materials.....	60
2.1.1. General reagents, enzymes, kits, lab wares and equipments	60
2.1.2. Antibodies.....	63
2.1.3. Cell lines.....	64
2.1.4. Buffers.....	65
2.2. Methods.....	67
2.2.1. Cell culture.....	67
2.2.1.1. General cell line maintenance.....	69
2.2.1.2. Culturing cells under hypoxic conditions	69
2.2.1.3. Cell culture of resistant cell lines	70
2.3. Cytotoxicity assay	70
2.3.1. Time dependent Cytotoxicity of DDC-Cu and DS plus Cu (DS/Cu)...	72
2.4. Western blot.....	72
2.5. Flow cytometry.....	78
2.5.1. Stem cell marker determination	78
2.5.2. Detection of hypoxia in hypoxic cell cultures	79
2.6. Electrophoretic mobility shift assay (EMSA).....	79
2.7. Luciferase reporter gene assay.....	82
2.8. Stable transfection.....	83
2.8.1. Stable transfection of NF κ Bp65 subunits	84
2.8.2. Stable transfection of HIF proteins	84
2.9. Migration assay.....	85
2.10. Invasion assay.....	84
2.11. Growth curves and doubling time analysis	86
2.12. Confocal microscopy and image analysis.....	86

2.13. RNA extraction.....	87
2.14. Reverse transcriptase polymerase chain reaction.....	88
2.15. Purification of PCR products.....	89
2.16. Molecular biology protocols.....	89
2.17. Reactive Oxygen Species activity detection	93
2.18. Determination of metabolic kinetics of DS/Cu and DDC-Cu	94
2.19. Encapsulation of DS in polymeric micelles.....	94
2.19.1. Characterization of Disulfiram loaded Polymeric Micelle	95
2.19.2. Measurement of encapsulation efficiency (EE) and drug loading content (DLC) of DS loaded PM	95
2.19.3. Measurement of the half-life of DS <i>in vitro</i>	96
2.19.4. Cumulative release of Disulfiram from Polymeric Micelle	96
2.20. Statistical Analysis.....	97

Chapter Three

Hypoxia induces CSC, chemoresistance and migration/invasion traits in TNBC cell lines

3.1. Introduction.....	98
3.1.2. Hypoxia induced EMT.....	99
3.1.3. Rationale and aims of the study.....	100
3.2. Experimental design.....	100
3.2.1. Culturing cells under hypoxia.....	100
3.2.2. Detection of hypoxia in hypoxic cell culture.....	100
3.2.3. Determination of EMT properties of cells.....	101
3.3.4. CSC markers determination in hypoxic cells.....	101
3.2.5. MTT cytotoxicity assay for hypoxic cell cultures.....	101
3.2.6. Growth curves and doubling time analysis.....	102
3.3. Results.....	102
3.3.1. Increase proportion of hypoxic cells in hypoxic culture.....	102
3.3.2. Hypoxic cells significantly resistant to anticancer drugs.....	105
3.3.3. Increase population of CSCs in hypoxic cells.....	110
3.3.4. Hypoxia induces EMT in BC cell lines.....	113
3.3.5. Hypoxic cells display increase migration and invasive potential..	117
3.4. Discussion.....	121

Chapter Four

NF κ B: A key factor involved in hypoxia-induced chemoresistance and stemness of breast cancer cells

4.1. Introduction.....	124
4.1.1 Rationale and aims of this study.....	125
4.2. Experimental Design.....	126
4.2.1. Stable transfection of MDA-MB 231 cells with NFκB p65.....	126
4.2.2. MTT cytotoxicity assay in NFκB transfected cells.....	126
4.2.3. Determination of CSC markers in NFκB transfected cells.....	126
4.2.4. Determination of EMT characteristics in NFκB transfected cells..	127
4.3. Results.....	127
4.3.1. Stable transfection of NFκBp65 subunit in MDA-MB231 BC cell line	127
4.3.2. Hypoxia may be involved in NFκB activation.....	128
4.3.3. Cells overexpressing NFκBp65 were highly resistant to anticancer drugs.....	129
4.3.4. Overexpression NFκBp65 in BC cells induces CSC traits.....	132
4.3.5. NFκBp65 overexpression induced EMT in MDA-MB 231 cell line..	136
4.3.6. Increase in NFκBp65 expression induced higher migration and invasion.....	137
4.3.7. Inhibition of NFκBp65 expression decreased the migratory and invasive potential in MDA-MB231 cell line	138
4.3.8. NFκBp65 transfection induced HIF activity.....	141
4.4. Discussion.....	142

Chapter Five

The role of hypoxia inducible factors (HIF1 α and HIF2 α) in hypoxia induced EMT and chemoresistance in breast cancer

5.1. Introduction.....	145
5.1.2. Role of HIF in hypoxia induced EMT.....	146
5.1.3. Rationale and aims of the study.....	147
5.2. Experimental Design	147
5.3.1. Stable transfection of HIF1α and HIF2α subunits in MDA-MB 231 cell line	147
5.3.2. Determination of CSC markers in HIF transfected cells.....	147

5.3.2. Determination of EMT characteristics in HIF transfected cells.....	147
5.3.3. MTT cytotoxicity assay for HIF transfected cells.....	148
5.4. Results	148
5.4.1. Stable transfection of HIF1 α in MDA-MB 231 BC cell line	148
5.4.2. Overexpression of HIF1 α in MDA-MB231 cell line induced an increase CSC markers expression.....	149
5.3.3. Increase in HIF1 α activity induces resistance to anticancer drugs.	153
5.3.4. Cells with increase HIF1 α activity displayed mesenchymal properties.....	156
5.4.1. Stable transfection HIF2 α in MDA-MB 231 BC cell line	157
5.4.2. Overexpression HIF2 α in MDA-MB 231 cell line induced an increase in CSC markers expression.....	158
5.4.3. Increase HIF2 α activity induced chemoresistance.....	162
5.4.4. Cells with increased HIF2 α activity show mesenchymal properties.....	164
5.5. Discussion.....	166

Chapter Six

The cytotoxic mechanisms of Disulfiram in pan-chemoresistant breast cancer cell lines

6.0. Characterization of resistant breast cancer cell lines (T47D _{Dox100nM} and MDA-MB 231 _{Gem 100nM})	169
6.1. Introduction	169
6.1.2. Rationale for the study.....	170
6.2. Experimental Design.....	171
6.2.1. Cytotoxicity of DDC-Cu and DS plus Cu (DS/Cu)	172
6.2.4. Determination of CSC markers in resistant cell lines.....	172
6.2.5. Reactive Oxygen Species activity detection.....	172
6.2.6. Determination of metabolic kinetics of DS/Cu and DDC-Cu.....	172
6.3. Results.....	173
6.3.1. Morphological features.....	173
6.4.2. Resistant cell lines show cross and pan-resistance to anticancer drugs.....	174
6.3.3. Resistant cell lines displayed an increase in CSC markers.....	179

6.3.4. Resistant cell lines displayed an increase in embryonic stem cell markers.....	184
6.3.5. Resistant cell line have longer doubling time.....	187
6.3.6. Western blot analysis of antiapoptotic proteins.....	188
6.3.7. Resistant cells exhibit reduce cytotoxic apoptotic induced death....	188
6.4.1. Cytotoxicity of DDC-Cu and DS plus Cu (DS/Cu) was observed in cancer cell lines.....	191
6.4.2. Time dependent cytotoxicity of DDC-Cu and DS plus Cu (DS/Cu) in BC cancer cell lines.....	192
6.4.3. ROS was responsible for the cytotoxic killing of DS/Cu.....	194
6.4.4. DS/Cu is unstable in medium.....	195
6.5. Discussion.....	199
<u>Chapter seven</u>	
Encapsulation of DS in Polymeric micelles	
7.1. Introduction.....	203
7.1.2 Rationale and aims of this study.....	204
7.2 Experimental design.....	205
7.2.1. Preparation and Characterization of DS loaded PM.....	205
7.2.2. Cumulative release of DS from PM Measurement of the half-life of DS <i>in vitro</i>	205
7.3. Results.....	205
7.3.1. Physicochemical characterization of DS loaded PM NP.....	205
7.3.2. <i>In vitro</i> half-life of DS in serum.....	207
7.3.3. <i>In vitro</i> release studies.....	208
7.3.4. MTT cytotoxicity assay of PMDs in TNBC cell lines.....	209
7.4. Discussion.....	214
<u>Chapter Eight</u>	
8.1. General Discussion.....	217
8.2. Conclusion.....	224
8.3. Recommendation and future work.....	225
References.....	227
Appendices.....	270

LIST OF TABLES

Tables	Page
Table 1.1. Staging of Breast Cancer	3
Table 1.2. Commonly Recognized Molecular Subtypes of Breast Carcinoma..	4
Table 1.3. Clinical and Pathologic features of TNBC.....	6
Table 1.4. Some Commonly used Drugs in BC Chemotherapy.....	11
Table 1.5. Resistance Mechanisms to Some Anticancer Drugs.....	24
Table 1.6. CSC Markers in Solid Tumours.....	26
Table 2.1. Primary Antibodies.....	77
Table 2.2. Primers Target.....	89
Table 5.1. IC ₅₀ values for anticancer drugs in HIF1 α transfected cells	155
Table 5.2. IC ₅₀ values for anticancer drugs in HIF1 α transfected cells	163
Table 6.1. IC ₅₀ value for Resistant Cell Line T47D _{Dox100nM} and Sensitive Cell Line T47D Wild Type.....	179
Table 7.1. Influence of PMDS ratio on Encapsulation efficiency and drug loading content	206
Table 7.2. Size, Polydispersity and Zeta potential of PMDS	206
Table 7.3. IC ₅₀ Value of Several Resistant BC Cell Lines.....	214

LIST OF FIGURES

Figures	Page
Figure 1.1. Structure of Cisplatin.....	12
Figure 1.2. Structure of Gemcitabine.....	14
Figure 1.3. Structure of Doxorubicin.....	16
Figure 1.4. Structure of Vincristine.....	17
Figure 1.5. Structure of paclitaxel.....	19
Figure 1.6. HIF pathway in normoxic and hypoxic conditions.....	32
Figure 1.7. Members of the proteins in Rel/NFκB and IκB families.....	36
Figure 1.8. Classical and alterative pathway of NFκB activation.....	38
Figure 1.9. Cross-talk between HIF and NFκB in hypoxia.....	43
Figure 1.10. Structure of disulfiram.....	45
Figure 1.11. Metabolism of disulfiram.....	47
Figure 1.12. Disulfiram as an antialcoholism agent.....	48
Figure 1.13. Structure of a multilaminar liposome.....	56
Figure 1.14. Structure of Polymeric micelle.....	57
Figure 3.1.9(A) A FACS Representative Plot of expression of hypoxic population in BC cell lines	103
Figure 3.1(B) Bar chart representation of hypoxic and normoxic populations in BC cell lines	104
Figure 3.2 A Representative Western blot of hypoxia-inducible factors (HIFs) in BC cell lines	104
Figure 3.3. (A) A Representative Drug Concentration Curve of MDA-MB 231 in normoxic and hypoxic culture	106
Figure 3.3. (B) A Representative Drug Concentration Curve of BT 549 in normoxic and hypoxic culture	108
Figure 3.4. (A1) A FASC Representative Plot of ALDH expression in normoxic and hypoxic cultures measured by ALDEFLUOR assay.....	111
Figure 3.4. (A2) Bar chart representation of ALDH+ cells in hypoxic and normoxic populations in BC cell lines.	112
Figure 3.4. (B) A FASC Representative Plot of CD133 expression in normoxic and hypoxic cultures measured using CD133-PE conjugated antibody	113
Figure 3.5. A FASC Representative Plot of Embryonic CSC markers Expression in normoxic and hypoxic cultures of MDA-MB 231 cell line.....	114

Figure 3.6. A FASC Representative Plot of Embryonic CSC markers Expression in normoxic and hypoxic cultures of BT 549 cell line.....	115
Figure 3.7. A Representative Growth curves of MDA-MB 231 and BT549 cancer cell lines cultured in normoxia and hypoxia.....	116
Figure 3.8. A Representative Western Blot of EMT markers in hypoxic cells using whole cell lysates of NOR and HYP cultures of breast cell lines.....	117
Figure 3.9. A Representative of Matrigel Invasion assay of TNBC hypoxic cells.....	119
Figure 3.10. A Representative of Matrigel Migration assay of TNBC hypoxic cells.....	120
Fig 4.1 A Representative Western Blot of NFκBp65 transfected cells using whole cell lysates and nuclear extracts of MDA-MB 231 breast cell line transfected with NFκBp65 subunit.....	128
Figure 4.2 Figure 4.2 A Representative Western Blot of NFκBp65 in hypoxic cells using whole cell lysate and nuclear extracts of normoxic and hypoxic cultures of breast cell lines.....	129
Figure 4.3 A Representative Drug Concentration Response Curve of Mock and NFκB p65 transfected cells.	131
Figure 4.4. (A). A FASC Representative Blot of ALDH expression in MDA-MB 231 NFκBp65 transfected cells measured by ALDEFLUOR assay	133
Figure 4.4. (B) A FASC Representative Plot of CD133 expression in MDA-MB 231 NFκBp65 cell line measured using CD133-PE conjugated antibody.....	134
Figure 4.5. (A) A FASC Representative Plot of Embryonic Stem cell markers Expression in MDA-MB 231 NFκBp65 BC cell line	135
Figure 4.5. (B) Bar Chart Representative of Expression of Embryonic markers in MDA-MB 231 NFκBp65 cell line.	136
Figure 4.6. A Representative Western Blot of EMT markers in Mock and NFκBp65 transfected cell	137
Figure 4.7. Representative Migration (wound healing) assay of Mock and NFκBp65 transfected cell	138
Fig 4.8 Representative Matrigel Invasion assay of Mock and NFκBp65 transfected cells	139
Figure 4.9. (A) A Representative Migration assay of Mock and NFκBp65 transfected cells inhibited with small molecules and DS/Cu	140

Figure 4.9. (B) Representative Matrigel Invasion assay Image of Mock and NFκBp65 transfected cells inhibited with small molecules and DS/Cu	141
Figure 4.10. A Representative Western Blot of HIF1α and HIF2α expression in NFκBp65 MDA-MB 231 transfected cell	142
Figure 5.1. A Representative Western Blot of Mock and HIF1α transfection cells	148
Figure 5.2. A Representative FASC Plot of CD133 expression in MDA-MB 231 mock and HIF1α transfected cells measured by PE-CD133 immunostaining assay	150
Figure 5.3. A Representative FASC Plot of Embryonic Stem cell markers expression in MDA-MB 231 HIF1α transfected cell	151
Figure 5.4. A Representative Drug Concentration Response Curve of Mock and HIF1α transfected cells after treatment with anticancer drugs	154
Figure 5.5. A Representative Western blot of EMT markers in Mock and HIF1α transfected cells using whole cell lysates.	156
Figure 5.6. A Representative Matrigel Invasion assay Image of Mock and HIF1α transfected cells.	156
Figure 5.7. A Representative Migration (wound healing) assay Image of Mock and HIF1α transfected cells	157
Figure 5.8. A Representative Western Blot of Mock and HIF2α transfection cells.....	158
Figure 5.9. A Representative FASC Plot of ALDH expression mock and HIF2α transfected cells measured by ALDEFLUOR assay	159
Figure 5.10. A Representative FASC Plot of CD133 expression in MDA-MB 231 in mock and HIF2α transfected cells measured by PE-CD133 immunostaining assay.....	160
Figure 5.11. A Representative FASC Plot of Embryonic Stem cell markers expression in MDA-MB 231 mock and HIF2α transfected cell	161
Figure 5.12. Representative Drug Concentration Response Curve of Mock and HIF2α transfected cells after treatment with CDDP, VCR, PTX, dFdC and DOX	162
Figure 5.13. A Representative Western blot of EMT markers in Mock and HIF2α transfected cells using whole cell lysates.	164
Figure 5.14. A Representative Matrigel Invasion assay of Mock and HIF1α transfected cells	165
Figure 5.15. A Representative Migration (wound healing) assay Mock and HIF2α transfected cells	165
Figure 6.1. A Representative Image of Morphology of wild type and resistant cells.	173

Figure 6.2. (A) Representative Drug Concentration Response Curve of MDA-MB 231 and MDA-MB 231_{GEM100nM} cell line.	174
Figure 6.2. (B) Representative Drug Concentration Response Curves of MDA-MB 231 and MDA-MB 231_{GEM100nM} cell line	176
Figure 6.3. (A) A Representative Drug Concentration Response Curve of T47D and T47D_{Dox100nM} cell line.....	177
Figure 6.3. (B) Figure 6.3.B Representative Drug Concentration Response Curves of T47D and T47D_{Dox100nM} cell line to conventional anticancer drugs	178
Figure 6.4. (A) A Representative FASCS Plot of ALDH expression in MDA-MB 231 WT and MDA-MB 231_{GEM100nM} BC cell line.	180
Figure 6.4. (B) A FASC Representative Plot of CD133 expression in MDA-MB 231 WT and MDA-MB 231_{GEM100nM} BC cell line by PE-CD133 immunostaining assay	181
Figure 6.5. (A) A Representative FASC Plot of ALDH expression in T47D WT and T47D_{Dox100nM} BC cell line measured by ALDEFLUOR assay.....	182
Figure 6.5. (B) A Representative FASC Plot of CD133 expression in T47D WT and T47D_{Dox100nM} BC cell line measured by PE-CD133 immunostaining assay... 	183
Figure 6.6.(A) A Representative FASC Plot of Embryonic Stem cell markers expression in MDA-MB 231 MDA-MB 231 Wild Type and MDA-MB 231_{GEM100nM} cell line.	184
Figure 6.6. (B) Bar chart representation of embryonic stem cell markers in MDA-MB 231 WT and MDA-MB 231_{GEM100nM} BC cell line.....	185
Figure 6.7. A Representative FASC Plot of Embryonic Stem cell markers expression in T47D WT and T47D_{Dox100nM} cell line.....	186
Figure. 6.8. Representative Growth curves of MDA-MB-231 and MDA-MB-231_{GEM100nM} cells and T47D and T47D_{DOX100nM} cell lines.....	187
Figure 6.9. Representative Western Blot of MDR1 P-pg expression in T47D wild type and T47D_{Dox100nM}	188
Figure. 6.10. (A) MDA-MB-231_{GEM100nM} cell line is resistant to gemcitabine-induced apoptosis.....	190
Figure 6.10. (B) T47D_{Dox100nM} cell line is resistant to doxorubicin-induced apoptosis.....	190

Figure 6.11. (A) A Representative Drug Concentration Response Curve of MCF7 cells treated with DS/Cu and DDC-Cu	191
Figure 6.12. . Representative Drug Concentration Response Curves of DS/Cu and DDC-Cu at different time points	193
Figure 6.13. Representative Plot of ROS activity detected in DS, Cu, DS/Cu, DD-Cu and H ₂ O ₂ containing cell culture medium	195
Figure 6.14.(A) Representative HPLC Peaks DS and DDC-Cu in cell medium.	196
Figure 6.14(B)Representative Calibration Curves of DS and DDC-Cu in cell medium	197
Figure 6.15. Representative HPLC profile Plots of DS/Cu and DDC-Cu	198
Figure 6.16. Representatative Plots on Time dependent trend of DS-Cu and DDC-Cu in culture medium.....	198
Figure 7.1. Representative Scan Electron Microscopy (SEM) images of PMDS	207
Figure 7.2. (A) Representative Plots of <i>In vitro</i> half-life of free DS and DS loaded PM in horse serum	208
Figure 7.2. (B) Representative Bar chart of half-life of free DS and DS loaded PM in horse serum	209
Figure 7.3. Representative Plot of <i>In vitro</i> cumulative release of DS from PM in PBS.....	210
Figure 7.4.(A) Representative Drug Concentration Response Curves of PMDS and Anticancer Drugs on cells in Hypoxic culture.....	211
Figure 7.7(B) Representative Drug Concentration Response Curves of PMDS and Anticancer Drugs on cells in cells resistant cell lines.....	212

LIST OF ABBREVIATIONS

5-FU: 5-Fluorouracil

A/MBC: advanced/metastatic breast cancer

ABC: ATP-binding cassette

ABCG2: ATP-binding cassette G2

ADP: Adenosine diphosphate

AJCC: American Joint Committee on Cancer

ALDH: aldehyde dehydrogenase

AML: acute myeloid leukaemia

ATP: Adenosine triphosphate

BAFF: B cell activating factor

BAX: BCL2-associated protein

BC: breast cancer

BCL-2: B-cell leukemia/lymphoma

BCRP: breast cancer resistance protein

BCSCs: breast cancer stem cells

BSA: bovine serum albumin

CDDP: cisplatin

CDK: cyclin dependant kinase

CMC: Critical micelle concentration

CMC: Critical micelle temperature

CRUK: cancer research UK

CSC: cancer stem cell

Cu: copper

Cu(DDC)₂: bis(diethyldithiocarbamate)copper complex

CXCR4: chemokine receptor type 4

dCK: deoxycytidine kinase

DDC: diethyldithiocarbamic acid

DEAB: diethylaminobenzaldehyde

DER: Disulfiram-alcohol reaction

DEPC: diethylpyrocarbonate

dFdC: 2', 2'-difluorodeoxycytidine

DMEM: Dulbecco's modified Eagle's medium

DNA: deoxyribonucleic acid

dNTP: deoxynucleoside triphosphate

Dox: doxorubicin

DS: Disulfiram

DTT: dithiothreitol

ECL: Enhanced chemiluminescence

EDTA: Ethylenediaminetetraacetic acid

EGFR: Epidermal growth factor receptor

EMSA: electrophoretic mobility shift assay

EMT: epithelial to mesenchymal transition

ER: oestrogen receptor

ERK: extracellular-signal related kinase

FCS: fetal calf serum

FLIP: FLICE-inhibitory protein

GAPDH: glyceraldehydes-3-phosphate dehydrogenase

GSH: Oxidation of glutathione

GST: Glutathione-S-transferase

GTP: Guanosine-5'-triphosphate

H₂O₂: hydrogen peroxide

hCNT: the equilibrative (hENT) and the concentrative

HER2: human epidermal growth factor-2

HIF: Hypoxia inducible factor

HLH: helix-loop-helix domain

hNT: human nucleoside transporters

HRE: hypoxia-response elements

IKK: I κ B kinase

I κ B: Inhibitors of NF κ B

JNK: c-Jun N-terminal kinases

LRP: lung resistance-related protein

MAPK: mitogen-activated protein kinase

MDR: Multiple drug resistance

MEK: MAPK/ERK kinase

MMPs: matrix metalloproteinases

MRP-1: multidrug resistance associated protein.

MMTV-neu: Mouse mammary tumour virus–neu

MTT: 3-(4, 5-Dimethylthiazol-2-yl)-2, 5-diphenyltetrazolium bromide

NAC: N-acetyl cysteine

NaCl₂: Sodium chloride

NaOH: Sodium hydroxide

Nanog: homeodomain-containing transcription factor

NDDS: Nanotechnology-based drug delivery system

NEMO: Nuclear factor kappa B essential modulator

NFκB: Nuclear factor kappa B

NIK: Nuclear factor kappa B inducing Kinase

NPs: Nanoparticles

Oct4: octamer-binding transcription factor 4

PTX: Paclitaxel

PARP: poly (ADP-ribose) polymerase

PBS: Phosphate-buffered saline

PCR: Polymerase chain reaction

Pgp: P-glycoprotein

PHDs: prolyl-hydroxylases

PR: progesterone receptor

PM: Polymeric micelles

PM-DS: Polymeric micelle encapsulated disulfiram

PVDF: Polyvinylidene difluoride

RHD: rel homology domain

RNA: Ribonucleic acid

ROS: Reactive oxygen species

RR: ribonucleotide reductase

RRM1: Ribonucleotide reductase M1 polypeptide

RT-PCR: Reverse transcriptase polymerase chain reaction

SEM: Scanning electron microscope

SDS: sodium dodecyl sulphate

SDS PAGE: sodium dodecyl sulfate polyacrylamide gel electrophoresis

siRNA: small interfering RNA

SOD: superoxide dismutase

Sox2: SRY (sex determining region Y)-box 2

TAE: Tris-acetate-EDTA

TBST: Tris-tween buffered saline

TEMED: Tetramethylethylenediamine

TGF- β 1: transforming growth factor β 1

TNF: receptor-associated factors

TNM: Tumour, Node, and Metastasis

VEGF: vascular endothelial growth factor

VHL: von Hippel-Lindau

WT: Wide type

Chapter One

1.0. Introduction

1.1. Brief background on Breast cancer

Cancers, one of the leading causes of death worldwide, comes in many different types and forms in which uncontrolled cell growth can spread to other parts of the body. It is rapidly becoming a global pandemic with cancer-related death exceeding death caused by stroke and coronary heart diseases (Ferlay *et al.*, 2014). It was predicted that the global cancer burden is anticipated to increase to 23.6 million cases and 13 million deaths by 2030 (IARC- World cancer report, 2014). The most frequently diagnosed carcinomas worldwide are lung, female breast cancer, colorectal and stomach cancers representing about 40% of cancer cases.

Breast cancer (BC) is a heterogeneous malignant disease consisting of a cluster of breast diseases affecting the same anatomical organ and arising from the same anatomical structure; differing in risk factors, clinical manifestations, histopathologies, genetic and genomic variations, therapeutic and clinical outcomes (Weigelt and Reis-Filho, 2009). BC is the second most common cancer in the world and the most fatal malignancy affecting women both in the developed and developing world. It is a major culprit associated with cancer-related deaths occurring in women worldwide (Kamangar, 2006).

1.2. Classification and Staging of breast cancer

Breast cancer (BC) is not a single disease but represents a heterogeneous group of tumours with diverse morphologic and biological features, behaviour and responses to treatment (Weigelt and Reis-Filho, 2009). The treatment decisions of Breast cancer patients depend on variables such as the site of the primary tumour, the size and number of tumours, cell type and tumour characteristics and grade. BC Staging is based on the size of the tumour, nature of the tumour (invasive or non-invasive) and lymph node involvement (Sobin *et al.*, 2009; Elston and Ellis 1993) (Table 1.1).

BC can be histopathologically divided into invasive and non-invasive cancers. Invasive cancer is further subdivided into invasive ductal carcinoma (80%) arising from the breast ducts, invasive lobular carcinoma (10%) arising from the breast lobules and an inflammatory breast cancer (incidence 1-3%) an uncommon form of invasive breast cancer which has poorer prognosis. Using gene expression profiling BC is divided into three biological types according to the expression status of oestrogen receptor (ER), progesterone receptor (PR) and human epidermal growth factor receptor -2 status (HER2) (Moulder *et al.*, 2008). BC can be also divided into luminal A (ER+ and/or PR+, HER2-, low Ki67), luminal B (ER+ and/or PR+, HER2+), HER2-enriched (ER-, PR-, HER2+), and basal-like (ER-, PR-, and HER2-) BCs (Perou *et al.*, 2000; Sorlie *et al.*, 2003) (Table 1.2).

Table 1.1: Staging of Breast Cancer (Cancer Research UK, 2012)

Stage	Staging criteria
Stage IA	Tumour is 2cm or less and has not spread outside the breast
Stage IB	Tumour is 2cm or less and a few cancer cells in nearby lymph nodes
Stage 2A	<ul style="list-style-type: none">no tumour can be found in the breast, but cancer (larger than 2 mm) is found in 1 to 3 axillary lymph nodes or in the lymph nodes near the breast bone (found during a sentinel node biopsy) orthe tumour measures 2 cm or smaller and has spread to the axillary lymph nodes orthe tumour is larger than 2 cm but not larger than 5 cm and has not spread to the axillary lymph nodes
Stage 2B	<ul style="list-style-type: none">the tumour is larger than 2 cm but no larger than 5 cm; small groups of breast cancer cells -- larger than 0.2 mm but not larger than 2 mm -- are found in the lymph nodes ORthe tumour is larger than 2 cm but no larger than 5 cm; cancer has spread to 1 to 3 axillary lymph nodes or to lymph nodes near the breastbone (found during a sentinel node biopsy) ORthe tumour is larger than 5 cm but has not spread to the axillary lymph nodes
Stage 3A	<ul style="list-style-type: none">the tumour may be any size and has spread to the chest wall and/or skin of the breast and caused swelling or an ulcer AND may have spread to up to 9 axillary lymph nodes ORmay have spread to lymph nodes near the breastbone
Stage 3B	<ul style="list-style-type: none">the tumour may be any size and has spread to the chest wall and/or skin of the breast and caused swelling or an ulcer AND may have spread to up to 9 axillary lymph nodes ORmay have spread to lymph nodes near the breastbone
Stage 3C	<ul style="list-style-type: none">there may be no sign of cancer in the breast or, if there is a tumour, it may be any size and may have spread to the chest wall and/or the skin of the breast ANDthe cancer has spread to 10 or more axillary lymph nodes ORthe cancer has spread to lymph nodes above or below the collarbone ORthe cancer has spread to axillary lymph nodes or to lymph nodes near the breastbone
Stage 4	The tumour can be any size and has spread (metastasized) to other parts of the body such as the brain, bone, liver or lungs.

Table1.2: Commonly Recognized Molecular Subtypes of Breast Carcinoma (Schnitt, 2010; Tang, *et al.*, 2009; Sorlie, *et al.*, 2003)

Molecular Subtype	Representative Gene Expression Signature	Representative Immuno phenotype	Associated Histologic Features	Associated Clinical Features
Luminal A	ESR1 (estrogen receptor 1) Estrogen receptor–associated transcription factors	ER+ and/or PR+, HER2/neu2, low Ki-67	Usually low grade	Tend to be sensitive to endocrine therapy, variable response to chemotherapy, overall good prognosis
Luminal B	ESR1 Estrogen receptor–associated transcription factors	ER+ and/or PR+, HER2/neu+	Usually higher grade than luminal A subtype	Tend to be sensitive to endocrine therapy, variable response to chemotherapy, prognosis poorer than that of luminal A subtype
Basal-like	KRT5 (keratin 5) KRT17 (keratin 17) LAMC2 (laminin, g 2)	ER2-, PR2-, HER2/neu2, CK 5/6+, and/or EGFR+	Often high grade	Tend to be insensitive to endocrine therapy, variable response to chemotherapy, overall poor prognosis
HER2/neu Enriched	ERBB2 (HER2/neu) ERBB2 amplicon	ER2-, PR2-, HER2/neu+	Often high grade	Tend to respond to biologic therapy (trastuzumab), variable response to chemotherapy, overall poor prognosis

1.3. Triple Negative Breast Cancer

Triple-negative breast cancer (TNBC) is defined as invasive carcinoma of the breast that does not express the genes for oestrogen receptor, progesterone receptor and Her2/neu (Sorlie *et al.*, 2003; Lehmann *et al.*, 2010). TNBC and basal-like breast cancer (BLBC) have significant similar characteristics; however these breast cancer subtypes are not identical (Oakman *et al.*, 2010).

1.3.1. Epidemiology and prevalence of triple negative breast cancer

TNBC is diagnosed in approximately 15-20% of all breast cancer cases encountered and is usually of the invasive ductal carcinoma subtype (Carey *et al.*, 2006). Globally, approximately 170,000 cases of TNBC (ER⁻/PR⁻/HER2⁻) phenotype is detected in the estimated 1 million breast cancer incidences identified annually (Anders and Carey 2009). The incidence and prevalence of TNBC also vary with race. African American and Hispanic premenopausal women have the highest incidence rate of TNBC (Carey *et al.*, 2006). Asian women have a TNBC prevalence of about 12% to 19% (Tsang *et al.*, 2009), Hispanic women about 24% while black women have the highest prevalence of TNBC ranging from 26% in all ages which are elevated to about 39% in premenopausal black females (Carey *et al.*, 2006). Apart from premenopausal status and African ancestry, other associated risk factors linked with the development of TNBC include early menarche, higher parity, younger age at first term birth, not breastfeeding, intake of pharmacological lactation suppression, and increased waist-to-hip ratio (Dolle *et al.*, 2009).

1.3.2. Clinical and Pathological features of TNBC

TNBC have been shown to present as an interval cancer in which detection occurs more frequently through clinical examination rather than with a mammogram or an ultrasound (Dent *et al.*, 2007), which is suggestive of rapid growth and tissue density similar to that of normal tissue. Common clinical and pathologic features of TNBC are summarized in Table 1.3.

Table 1.3: Clinical and Pathologic features in TNBC

Prevalent in premenopausal African and Hispanic women	Azim <i>et al.</i> , 2012
BRCA 1 mutations present	Oakman <i>et. al.</i> , 2010
High grade invasive tumours	Dent <i>et al.</i> , 2007; Cheang <i>et al.</i> , 2008
High risk of early recurrence	Dent <i>et al.</i> , 2007
Rapid progression from the onset of metastasis to death	Kim <i>et al.</i> , 2006
High prevalence of brain and lung metastasis	Dent <i>et al.</i> , 2007
Chemoresistant tumours	Liedtke <i>et al.</i> , 2008
High expression of Ki-67, Vimentin and p53	Han <i>et. al.</i> , 2008
Loss of PTEN	Hu <i>et. al.</i> , 2009
Copy number alteration and amplified NFkB expression	Hu <i>et. al.</i> , 2009
Expression of epidermal growth factor receptor	Collins <i>et. al.</i> , 2009

1.3.3. Classification of TNBC

TNBC can be classified into two (2) major intrinsic subtypes

- The basal-like subtype

➤ The claudin-low subtype

However, the basal-like subtype constitutes the majority of TNBC incidence as it represents about 50-70% of TNBC encountered (Prat and Perou, 2011). The basal-like triple-negative breast cancer subtypes also have increased rates of p53 mutations (Sorlie, 2003). The claudin-low subtypes of TNBC are typically comprised of high grade invasive ductal carcinomas often having amplified frequency of metaplastic and medullary differentiation properties. The claudin-low subtypes of TNBC have lower expression of proliferation-related genes, such as Ki67 (Prat *et al.*, 2010) but are greatly enriched in mesenchymal features (ZEB1, twist, and snail) and stem cell-like biological processes epithelial–mesenchymal transition (EMT) (Prat and Perou, 2011; Prat *et al.*, 2010) when compared to the basal-like subtypes. The claudin-low tumours lack cell-cell junction protein E-cadherin and are known to have intense immune cell infiltrations. The report by Prat *et al.*, 2010 demonstrated that there was no difference in the survival rates between the basal-like and claudin-low subtypes of TNBCs however, the pathologic complete response (pCR) rates of the claudin-low subtype of TNBC was observed to be lower after preoperative anthracycline/ taxane-based chemotherapy in a cohort of 133 patients. There is also the existence of other TNBC subtypes such as the mesenchymal-related, proliferation-related and immune-related subsets (Lehmann *et al.*, 2010).

1.3.4. Prognosis of TNBC

Triple negative breast cancer (TNBC) patients generally have poorer prognosis when compared to other subtypes of breast cancers (Nofech-Mozes

et al., 2009). During diagnosis, TNBCs are often identified to be of larger tumour size, having high mitotic grade and are biologically more aggressive with low Bcl-2 but high p53 and Ki67 expressions (Tian *et al.* 2008). Altogether, these factors have been suggested to cause the poorer overall survival (OS), breast-cancer-specific survival (BCSS) and relapse-free survival (RFS) observed in patients with TNBC. Patients with TNBC have a greater risk of tumour recurrence and are more likely to die of cancer relapse when compared to patients with non-TNBC subtypes (Mersin *et al.*, 2008).

1.4. Treatment for Breast Cancer

There are several treatment regimens available for breast cancer and the choice of treatment is dependent on certain factors such as the type of breast cancer, the size of the breast tumour, the stage and grade of the tumour, the menstrual status of the patient, expression of certain proteins and endocrine receptors and general health of the patient. Five treatment options available in clinics include surgical resection, radiotherapy, immunotherapy, molecular based therapy (endocrine and biological therapy) and chemotherapy.

Surgery is usually the first type of treatment for breast cancer that has not spread to the axillary lymph nodes. Surgery also provides samples for further molecular and histological analysis to confirm diagnosis and may help in treatment and prognosis of cancer. Radiotherapy is the use of high energy x-ray radiation to kill cancer cells usually given in controlled doses. Hormone therapy involves the use of additional hormones to treat breast cancer to prevent relapse. Endocrine therapy is not effective against cancers that lack hormone receptors such as TNBC.

1.4.1. Chemotherapy

Despite the advancement in early detection of breast cancer, a small proportion of women present with metastatic disease at the first time of presentation (Early Breast Cancer Trialists' Collaborative Group, 2005) or are prone to develop distant metastasis even though their initial diagnosis was non-metastatic breast cancer. Metastatic breast cancer though not curable has improved in survival due to the introduction of new chemotherapeutic regimen (Gennari *et al.*, 2005; Chia *et al.*, 2007; Dafni *et al.*, 2010). Normal cell growth is tightly controlled where cells undergo apoptosis to avert excessive growth, however cancer cells have lost this control mechanism and thus are usually antiapoptotic in nature. Chemotherapeutic drugs target cancer cells via circulation in blood by inhibiting cancer cell proliferation and inducing apoptosis in cancer cells.

Chemotherapy is a treatment that involves the use of a drug or a combination of drugs that are cytotoxic to rapidly growing and dividing cells such as cancer cells. Rapidly dividing normal cells can also be affected by these cytotoxic drugs but are more likely to undergo repair. Anti-cancer drugs work by disrupting the growth of cancer cells. Chemotherapy is the standard care for patients with node-positive cancer and is of great benefit to patients with hormone receptor negative tumours (Goldhirsch *et al.*, 2007). Chemotherapy can be a neoadjuvant therapy given before surgery to shrink the tumour, adjuvant therapy given after surgery to prevent cancer spread or relapse or given to already relapsed tumour. The use of chemotherapy is largely based

on the age, tumour size or grade, type of receptors and status, lymph node involvement and risk of spread of cancer (Howell *et. al.*, 2005).

Chemotherapy is not recommended for stage I BC except in case with unfavourable features or at high risk of recurrence due to the adverse effects of chemotherapy drugs. Anthracycline-based regime (doxorubicin and epirubicin) are usually the standard chemotherapy drug used for such patients (Takeda *et. al.*, 2007). Stage II/III BCs are usually larger and involve spread to nearby lymph nodes, chemotherapy is either given before or after surgery to decrease the risk of recurrence. Standard chemotherapy treatment followed by paclitaxel (PTX) is usually recommended for such patients. In stage IV BC where spread is beyond the breast and lymph nodes to other parts of the body, patients are treated with a selection of chemotherapeutic drugs including the standard epirubicin or gemcitabine (dFdC), PTX or docetaxel, platinum agents, cyclophosphamide, vinorelbine, nucleotide analogue and ixabepilone (Ross and Cubby, 1994; McArthur and Hudis, 2007). Chemotherapy drugs can be classified into several groups based on the chemical structure, mechanism of action and interaction with other drugs. They can be grouped into alkylating agents, antimetabolites, Taxanes (mitotic inhibitors), antitumour antibiotics, monoclonal antibodies, topoisomerase inhibitors platinum and anthracyclines (Raina *et al.*, 2007). Most of which can be used to treat advanced breast cancer.

Table 1.4: Some Commonly used Drugs in BC Chemotherapy (Chorawala, *et al.*, 2012).

Drugs	Mechanism of action
Docetaxel	Stabilizes polymerization of tubulins and inhibits the disassembly of microtubules
5-Fluorouracil	Interferes with DNA synthesis
Paclitaxel	Stabilize microtubules and inhibition of cells in the anaphase stage
Cisplatin/Carboplatin	Reacts with proteins and nucleic acid, disrupts DNA synthesis by forming DNA adducts and cross-links
Gemcitabine	Incorporates into DNA inducing steric hinderance and inhibits DNA synthesis
Vincristine	Binds to tubulin, disrupts mitotic spindle and arrest cell growth
Doxorubicin	Disrupts DNA helical structure, Inhibits DNA and RNA polymerases, generates ROS
Vinorelbine	Binds to tubulin, disrupts mitotic spindle and arrest cell growth

1.4.1.1. Cisplatin

Cisplatin (*cis*-diamminedichloroplatinum(II)) is a heavy metal complex containing a central atom of platinum surrounded by two chloride molecules and two ammonia molecules in the cis position (Figure 1.1). It was first synthesized by Peyrone in 1844 and its chemical structure elucidated by Alfred Werner in 1893. It was until the 1960s when Rosenberg *et al.*, (1965) observed that cisplatin was capable of inhibiting cell division in *Escherichia coli* that it gained scientific interest as an anticancer agent.

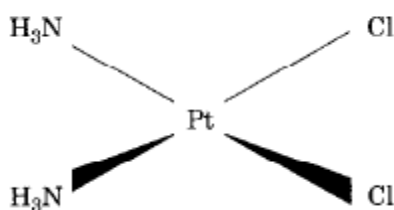


Figure 1.1 Structure of Cisplatin

Since its introduction in clinical trials cisplatin has changed the course of therapeutic management of several solid malignancies such as testicular, ovarian, bladder, head and neck and non-small cell lung cancers. Cisplatin predominantly targets the DNA by inducing DNA damage through inhibition of DNA synthesis, suppression of RNA transcription and induction of apoptosis. The cytotoxic effects of cisplatin occur after cisplatin undergoes hydrolysis within the cell producing a highly reactive platinum complex $[Pt(NH_3)_2ClH_2O]^+$ which combines with DNA forming adducts and DNA cross-linkages (DNA intra-strand and inter-strand links) which unwind the DNA helix and interferes with cell division and replication and triggers apoptosis if repair mechanisms are unsuccessful (Gonzalez *et al.*, 2001; Fuertes *et al.*, 2002). Cisplatin is not routinely used in breast cancer treatment but can be used in TNBC especially BRCA 1 tumours which are particularly susceptible to cisplatin (Garbe *et al.*, 2006; Byrski *et al.*, 2009; Hastak *et al.*, 2010; Silver *et al.*, 2010).

One major limitation associated with the use of cisplatin is the development of resistance. There are two types of resistance to cisplatin (intrinsic and acquired) however the molecular basis involved are not fully elucidated. Acquired resistance can develop in patients undergoing chemotherapy or in

cell lines after exposure to increasing dose of cisplatin after a high tolerance dose is reached. An initial response of up to 70% occurs with ovarian cancer, however, this response is not durable where the 5-year patient survival rate is only about 15 -20 % and the primary tumour becomes resistant to therapy (Ozols, 1991). Similar response also occurs in small cell lung cancer, where relapse rate is as high as 95% (Giaccone, 2000). Other analogs of platinum-containing drugs used in clinic include carboplatin, oxaliplatin, ormaplatin and enloplatin.

1.4.1.2. Gemcitabine

Gemcitabine (2', 2'-difluoro 2'-deoxycytidine, Gemzar, dFdC) (Figure 1.2) is a deoxycytidine analogue with metabolic similarities to cytarabine (Ara-C) but differs structurally due to its fluorine substituents on position 2' of the furanose ring. dFdC was synthesized in the 1980s at Lilly Research Laboratories (Eli Lilly and Co., Indianapolis, IN) as an antiviral agent because it was observed to inhibit DNA and RNA viruses (Bergman *et al.*, 2005) but then developed as an anticancer agent because of its *in vitro* and *in vivo* antitumoural effects. Gemcitabine is a first-line treatment for advanced pancreatic cancers (Burris *et al.*, 1997) and used in combination therapy in non-small cell lung cancer, ovarian, bladder, breast, and head and neck squamous cell cancers with response rates ranging from 13% to 29% (Sandler *et al.*, 2000; Albain *et al.*, 2004; Mini *et al.*, 2006).

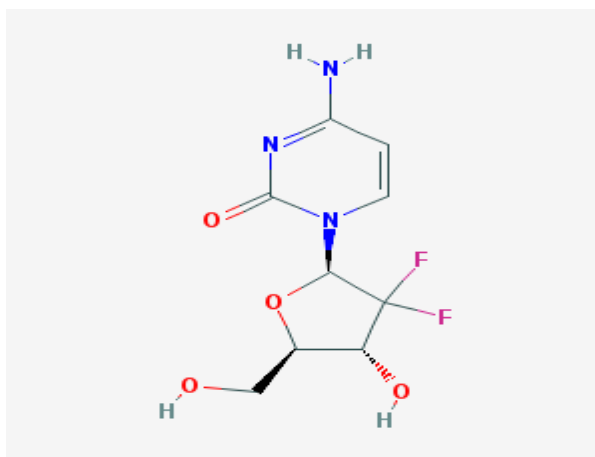


Figure 1.2: Structure of Gemcitabine.

dFdC is a prodrug which requires cellular uptake and intracellular phosphorylation for its activation. Being hydrophilic in nature, dFdC is transported across cell membrane via specialized carriers called human nucleoside transporters (hNT) which facilitate its uptake into cells. There are two hNTs; concentrative hNT (CNT) which is the sodium dependent and equilibrative hNT (ENT) sodium independent (Shah *et al.*, 2007). dFdC has affinity for five hNTs, two of which are of the equilibrative type (hENT1 and hENT2) and three concentrative type (hCNT1, hCNT2 and hCNT3)(Ritzel *et al.*, 2001). Once inside the cell dFdC is phosphorylated by deoxycytidine kinase (dCK) to gemcitabine monophosphosphate (dFdCMP), which is further phosphorylated to active drug metabolites diphosphate (dFdCDP) and triphosphate (dFdCTP) by nucleoside monophosphate kinase and nucleoside diphosphate kinase respectively (Ueno *et al.*, 2007; Galmarini *et al.*, 2004). dFdC can also be phosphorylated by thymidine kinase 2 but has a low substrate affinity of only 5% to 10% (Wang *et al.*, 1999).

The cytotoxic activity of dFdC is mediated by its phosphorylated derivatives which are inhibitors of DNA synthesis. dFdCTP competes with deoxycytidine triphosphate (dCTP) as an inhibitor of DNA polymerase (Gandhi and Plunkett, 1990), once incorporated into the DNA and after the incorporation of one more nucleotide, dFdCTP leads to DNA polymerization termination and single strand breakage (Ross and Cuddy, 1994). The extra nucleotide is able to prevent dFdCTP from being recognized by DNA repair enzymes which induce apoptosis. dFdCDP is a potent inhibitor of ribonucleotide reductase and indirectly inhibit DNA synthesis by depletion of the deoxyribonucleotide pools and prevents the conversion of RNA nucleotides to DNA nucleotides. Resistance to dFdC is correlated with CdR kinase levels in tumours, increased ribonucleotide reductase expression as well as inhibition of nucleoside transporters which prevents influx dFdC into cells.

1.4.1.3. Doxorubicin

Doxorubicin (Dox) is a member of the anthracycline drug family isolated from a metabolite of *Streptomyces peucetius* in the 1960s (Woodruff *et al.*, 1960) (Fig. 1.3). It is routinely used as treatment in a wide range of solid tumours, lymphomas and leukaemia (Kostrzewa-Nowak *et al.*, 2005; Cortes-Funes and Coronado, 2007) and is considered as one of the potent therapeutics for breast cancer. Dox is a first-line therapy for metastatic breast cancer and has a response rate of about 29% to 43% with a median survival time of 2 years (Henderson, 1991).

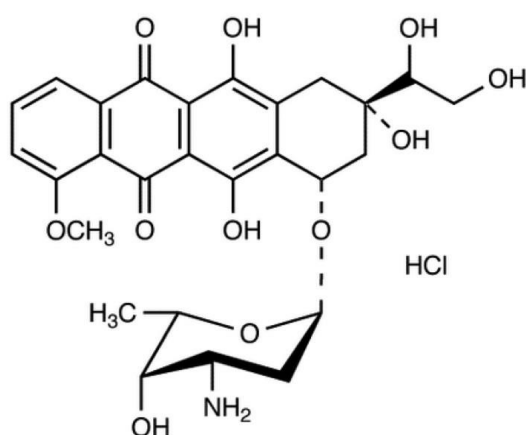


Figure 1.3 Structure of Doxorubicin

The two proposed mechanisms by which Dox carries out its anticancer effects are by intercalation to DNA which disrupts topoisomerase-II-mediated DNA repair and by the generation of free radicals which damage cellular membrane, DNA and proteins (Gewirtz, 1999). Dox is rapidly taken up into the nucleus of cells, once inside the cell, it binds with high affinity to DNA by classical intercalation between base pairs of the super-coiled double helix which impairs topoisomerase II activity resulting in uncoiling of the helix and DNA breakage. (Gewirtz, 1999). Topoisomerase II is a DNA superhelix control enzyme that controls the supercoiled structure of DNA by making a nick and rejoining the two adjacent DNA strands (D'Arpa and Liu, 1989). Once its activity is disrupted DNA replication and RNA transcription are compromised leading to permanent DNA cleavage (D'Arpa and Liu, 1989). Dox can also undergo a one-electron reduction by oxidoreductases such as mitochondrial NADH dehydrogenase, cytoplasmic NAD(P)H dehydrogenases, xanthine oxidase and endothelial nitric oxide synthase to form a Dox-semiquinone radical, an unstable metabolite which can be reoxidized back to Dox by same enzymes and in the process releases reactive oxygen species (ROS) which leads to lipid peroxidation,

membrane damage, DNA damage, oxidative stress, and triggers apoptotic pathways of cell death (Adama *et al.*, 2003). Although a potent antineoplastic drug, resistance to Dox is a problem limiting its use. Mechanisms of Dox resistance involves transporters such as ATP-Binding Cassette Sub-Family B -1 (ABCB1) an ATP-dependent drug efflux pump and ATP-Binding Cassette Sub-Family C -1 (ABCC1).

1.4.1.4. Vincristine

Vincristine (VCR) is a naturally occurring alkaloid isolated from the leaves of the plant *Catharanthus roseus* also known as Madagascar periwinkle (formerly classified as *Vinca rosea*) (Kufe *et al.*, 2003). This plant was first used for the treatment of diabetes and high blood pressure and later used in cancer treatment due to its cytotoxic effects (Gidding *et al.*, 1999).

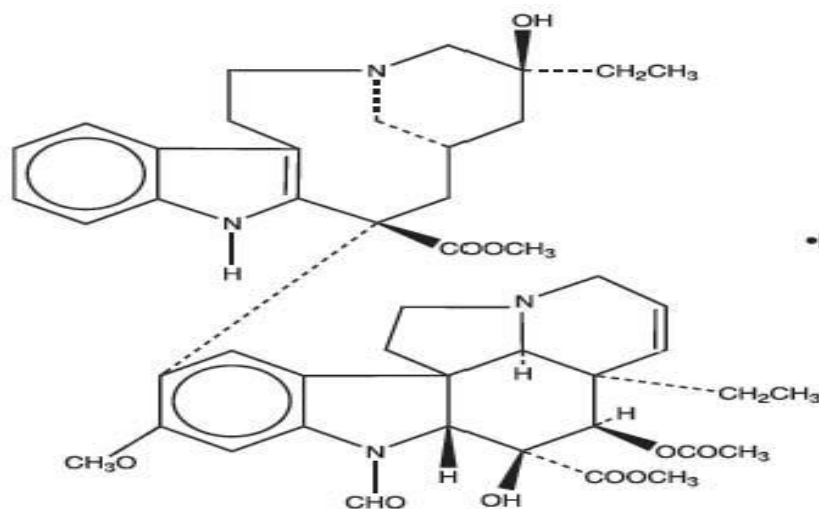


Figure 1.4 Structure of Vincristine.

VCR is one of the vinca alkaloids used in clinic. VCR is effective against a wide spectrum of cancers (Gascoigne and Taylor, 2009) and made up of two multi-ring structures: vindoline and catharanthine (Figure 1.4). The exact mechanisms

of action of vincristine is not fully understood, its cytotoxicity is due to interactions with tubulin and disruption of microtubule function, particularly of microtubules (hollow rigid dynamic structures that play a vital role in cell shape and cell movements) comprising the mitotic spindle apparatus which directly causes metaphase arrest (Himes, 1991). VCR binds to β -tubulin dimers at the vinca domain site located adjacent to the Guanosine-5'-triphosphate (GTP) binding site in tubulin forming a paracrystalline aggregate tubulin–drug complex which reduces the dimer and causes shrinkage of the microtubules. This shrinkage alters the alignment and movement of chromosomes during mitosis disrupting spindle fibre generations.

1.4.1.5. Paclitaxel

In 1967 Monroe E. Wall and Mansukh C. Wani isolated a mitotic inhibitor from the bark of *Taxus brevifolia* (northwest Pacific Yew Tree) which they called taxol. Paclitaxel (PTX) a taxol drug was first isolated from extracts of the bark of *Taxus Brevifolia* the Pacific yew or the English yew and in 1971 was discovered to have anti-leukemic effects (Wani *et al.*, 1971). PTX is now a first line anticancer drug for several cancers such as ovarian, liver, metastatic breast and non-small cell lung carcinomas (Rowinsky *et al.*, 1992; Yen *et al.*, 2004). PTX obtained from a non-renewable source the bark of Taxus tree was not widely used for patients until scientists developed a semisynthetic derivative based on the molecular structure of paclitaxel (Figure 1.5).

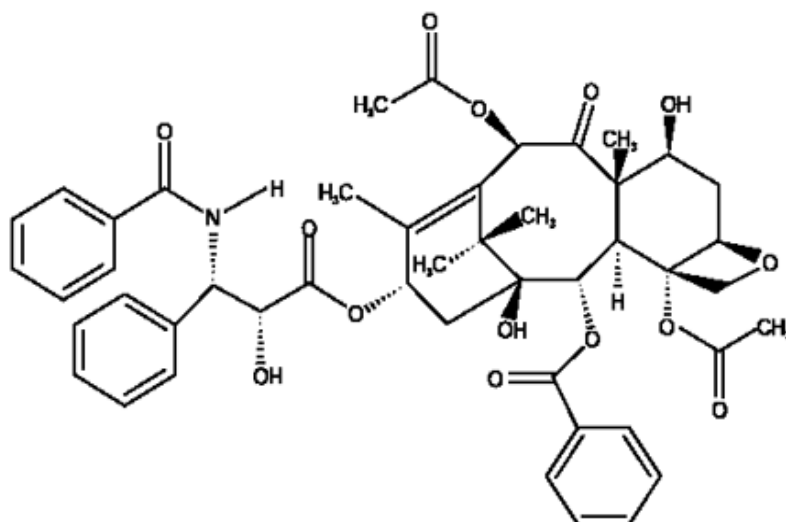


Figure 1.5 Structure of paclitaxel.

The main cytotoxic mechanism of PTX is its ability to stabilize microtubules and inhibition of cells in the anaphase stage. The microtubules are cylindrical assembly of tubulin dimers composed of α and β tubulin subunits (Chretien *et al.* 1992). The main function of microtubules is the formation of mitotic spindles during cell division. It also maintains cell structure, mobility and cytoplasmic movement and is in a state of dynamic equilibrium with the α and β subunits arranged in a head to tail pattern. The β -subunit of microtubule has a binding site for PTX, binding of PTX to the β -unit of tubulin forms structurally abnormal microtubules which do not depolymerize and cells are arrested in the anaphase (G2/M) stage and inevitably undergo cell death (Ganguly *et al.*, 2010).

1.5. Chemoresistance

Chemotherapy is one of the main strategies for breast cancer treatment. Even with the advancement in treatment and outcome of patients in recent times, drug resistance of tumour cells is a major factor limiting the effectiveness of chemotherapeutic treatment in most human tumours. There are two

categories of drug resistance, e.g. intrinsic (innate) and acquired resistance which may be applicable to a single agent or a group of agents with similar mechanisms of action (Longley *et al.*, 2005). Intrinsic chemoresistance is the *de novo* resistance of cancer cells prior to the commencement of treatment regimen which originates in cells capable of limiting drug uptake by enhanced efflux and activation of detoxification of the drugs (Gottesman, 2002). Acquired resistance occurs when tumour cells are initially sensitive to anticancer drugs but undergo genetic and epigenetic alteration that make them resistant. Chemoresistance is a multifactorial process involving numerous interrelated and independent mechanisms. Relevant mechanisms that contribute to cellular resistance in cancer cells include high expression of defence factors reducing intracellular drug concentrations, the involvement of cancer stem cells, modifications in drug-target interactions, defects in apoptotic pathways and increased cellular ability for DNA repair damage and increase tolerance to unfavourable cellular environment (Longley *et al.*, 2005).

1.5.1. Drug efflux mechanisms

1.5.1.1. P-glycoprotein

P-glycoprotein (P-gp) is an active, efflux, membrane bound transport protein pump discovered in 1976 (Juliano and Ling, 1976). P-gp also known as multidrug resistance protein 1 (MDR1) is a 170 kDA membrane protein encoded by the ATP binding cassette B1 (ABCB1) gene and belongs to the ATP binding cassette super family (ABC) transporters. P-gp is a physiological barrier protecting susceptible tissues from toxic compounds, preventing entry into the cytosol and extruding them to the exterior (Fortuna *et al.*, 2011). P-gp

is predominantly found in epithelial cells with excretory function such as the apical surface of epithelial cells lining the colon, small intestine, adrenal gland, bile ductules, pancreatic ductules and proximal kidney tubules (Melaine *et al.*, 2002; Edwards *et al.*, 2005). It is also found in the endothelial cells of the blood brain barrier (Ma *et al.*, 2010). Many solid tumours overexpress P-gp (Thomas and Coley, 2003). The efflux action of P-gp requires an ATP active process, where hydrolysis of ATP releases the energy needed for the extrusion process. This efflux occurs unidirectionally with the transfer of one molecule per time out of the cell to the extracellular space. A second hydrolysis of the ADP bound P-gp takes place to the bound ADP from P-gp which then returns to its original state. Substrates for P-gp transporter include cationic, hydrophobic cytotoxic drugs and amphipathic natural products such as taxanes, doxorubicin, paclitaxel, vinca alkaloids, anthracyclines and mitomycin C (Krishna and Mayer, 2000). P-gp overexpressed on the surface of cancer cells precludes the accumulation of anticancer drugs in the tumour preventing them from reaching their intended targets through the efflux pump. There are conflicting results on the influence on P-gp on breast cancer therapeutics, some studies showed a positive correlation between reduced P-gp expressions and improvement in response rate while others did not find such relationship (Verrelle *et al.*, 1991; Chevillard *et al.*, 1996).

1.5.1.2. Multidrug resistance associated protein (MRP)

Multidrug resistance associated proteins (MRPs) are members of the ATP-binding cassette (ABC) superfamily of transmembrane transporters found in many mammalian tissues. They are 180 to 195 kDa membrane proteins

associated with resistance of tumours to anticancer drugs. They primarily transport anionic drugs such as methotrexate and neutral drugs conjugated with acidic ligands (glutathione (GSH), glucuronate, or sulphate). 9 MRPs have been characterized in human tumours (MRP 1-9). MRPs 1-3 have also been found to confer resistance to neutral organic drugs not bound to acidic ligand by transporting drugs with free glutathione. MRP 1 is overexpressed in breast carcinoma (Zaman *et al.*, 1994) but their clinical relevance is still not fully understood. Anticancer drug resistance to anthracyclines (Doxorubicin), antifolates and vinca alkaloids are associated with MRP1 (Zhou *et al.*, 2001). The relevance of other members of the MRP family have not been linked to breast cancer.

1.5.1.3. Breast Cancer Resistance Protein (BCRP)

Breast cancer resistance protein (BCRP) is a 72kDa 655 amino acid peptide transporter encoded by the ATP-binding cassette ABCG2 gene with similarities to both P-gp and MRP but contain only one transmembrane domain and one nucleotide binding domain. BCRP overexpression confers resistance to cisplatin, paclitaxel and vinca alkaloids in BC cell lines (Brinkhuis *et al.*, 1999).

1.5.2. Drug activation/inactivation mechanisms

Drug resistance can occur due to decreased drug activation. For instance, the antifolate drug methotrexate is first polyglutamated by folypolyglutamate synthase to increase cellular retention and elevate substrate binding activity. Several studies have noted positive correlation between decrease

polyglutamation and antifolate resistance in cell line models (Barnes *et al.*, 1999; Wang *et al.*, 2003).

1.5.3. Defects in DNA damage repair

The anticancer mechanism of many chemotherapeutic agents is by induction of DNA damage which leads to cell cycle arrest, DNA damage repair and eventually death. Mutation in DNA mismatch repair (MMR) mechanisms has been associated with drug resistance. The MMR are important for the maintenance of the stability of the genome by scanning newly produced DNA to correct replication errors, excising single-base mismatches and inserting deletion loops (Fink *et al.*, 1998). Deficiency of MMR gene has been linked to resistance to DNA damaging agents. A research by Plumb *et al.*, 2000 demonstrated that resistance to cisplatin was attributed to hypermethylation of the *hMLH1* promoter which resulted in defects in the mutation in DNA mismatch repair. .

1.5.4. Defects in apoptotic mechanisms

During normal development and maturation cycle, cell death is a relevant aspect and a balance between the rate of proliferation and cell death is important for maintenance of normal physiological processes (Jacobson *et al.*, 1997). Apoptosis is a physiological programmed cell death characterized by cell shrinkage, blebbing of plasma membrane, condensation and fragmentation of the DNA control cell number during development and in disease states. Apoptosis is via the extrinsic or intrinsic pathway, the extrinsic pathway is a receptor mediated killing while the intrinsic pathway is regulated by the mitochondria mediated killing. Impairment of the apoptotic pathway

results in chemoresistance. Disruptions in mechanisms such as loss of p53 function, overexpression of Bcl2 or Bcl-XL and upregulation of epidermal growth factor receptor (EGFR) dysregulates the apoptotic pathway (Blagosklonny, 2001).

Table 1.5: Resistance Mechanisms to some Anticancer Drugs

Drug Efflux mechanism	Anti-cancer drugs
P-gp overexpression	doxorubicin, paclitaxel, docetaxel, vinca alkaloids, anthracyclines
Impair DNA repair mechanisms	Cisplatin
Multidrug resistance associated proteins (MRPs)	Doxorubicin, antifolates and vinca alkaloids

1.6. Cancer Stem cells

Stem cells are a small and distinct population of undifferentiated cells capable of differentiating into specialized cells and also divide through mitosis to produce more stem cells. Stem cells have major characteristics namely the ability for self-renewal and production of progenitor cells which differentiate into more mature and specialized cells. Cancer stem cells (CSCs) are defined as a rare group of cells within the tumour population capable of self-renewal and differentiation to produce diverse cells that drive tumourigenesis (Jordan, 2004). CSCs are also known as tumour initiating cells or tumourigenic cells. Normal stem and cancer stem cells share certain similar characteristics such as the ability to self-renew, differentiate to progenitor cells and utilize common

pathways (Jordan, 2004). Evidence for the concept of cancer stem cell was first documented in haematological malignancies, where a small population of cancer cells were able to generate tumours in *in vivo* mice models after transplantation of human acute myeloid leukaemia cells in immunodeficient mice (Bonnet and Dick, 1997). In recent years, there has been growing interest in the role of stem cells in cancer biology. CSCs have been identified in numerous solid tumours such as the breast, brain, colon, liver and pancreatic cancers (Li *et al.*, 2007; O'Brien *et al.*, 2007; Prince *et al.*, 2007). CSCs are believed to play crucial roles in tumour initiation, relapse, metastasis and resistance to therapy (Coker and Allan, 2008).

1.6.1. Breast cancer stem cells

Two cell types make up the breast epithelium: the luminal epithelial and the myoepithelial cells. Mammary stem cell population are located in the luminal but not in the myoepithelial compartment of the breast (Gudjonsson and Magnusson, 2005). CSCs in human BC were first identified in 2003 (Al-Hajj *et al.*, 2003) when a CD44^{+/high}CD24^{-/low} lineage subpopulation of tumours from human patients initiated tumour growth in immunodeficient mice. Injections of few cells (100 tumourigenic cells) resulted in palpable tumours within 12 weeks, serial passaging from these cells gave similar results, while CD 44⁻ cells were non-tumourigenic even after injection of 10,000 cells. The exact origin of breast CSCs though not clearly identified is suggested to occur from accumulation of oncogenic insults on normal breast stem/progenitor cells inducing mutations.

1.6.2. Cancer stem cell markers

Cancer stem cells (CSCs) have been isolated from several tumours such as the breast, brain, blood (leukemia), skin (melanoma), head and neck, thyroid, cervix, lung, organs of the gastrointestinal and reproductive tract (Mimeault *et al.*, 2007). Selective markers found on the cell surface can be used for detection and identification of CSCs. Specific surface markers used for identification of breast CSCs includes CD44, CD24, CD133 and Aldehyde Dehydrogenase (ALDH).

Table 1.6 CSC markers in solid tumours (Medema *et al.*, 2013)

Breast	Glioma	Colon	Liver	Lungs	Ovarian	Prostate	Pancreatic
ALDH	CD15	CD24	CD13	ABCG2	CD24	ALDH	ALDH
CD24	CD90	CD26	CD24	ALDH	CD44	CD44	CD24
CD44	CD133	CD29	CD44	CD90	CD117	CD133	CD44
CD133	Nestin	CD44	CD90	CD117	CD133	CD166	CD133
CD90		CD133	CD133	CD133		Trop2	Nestin
ESA		CD166					ABCG2
		LGR5					C-met
		ABCB5					
		ALDH					

Aldehyde Dehydrogenase (ALDH), a family of enzymes involved in the oxidation of aldehydes into their corresponding carboxylic acids is a functional marker of CSCs (Ginestier *et al.*, 2007). Nineteen isoforms of ALDH have been identified in humans, important for physiological and toxicological functions. High ALDH activity is seen in normal stem cells particularly the human haemopoietic stem cells. Increase in ALDH activity has also been reported in

many solid tumours such as breast, lung, pancreas, liver and head and neck cancers (Clay *et al.*, 2010; Hellsten *et al.*, 2011). The role of ALDH in chemoresistance was identified by Hilton *et al.*, (1984) in cyclophosphamide-resistant L1210 leukemic cell line. They observed that in early passage colon cancer xenograft tumours more, ESA+, CD44+, ALDH positive cell populations survived after exposure to cyclophosphamide. When these surviving ESA+, CD44+, ALDH positive cell CSCs were treated with ALDH inhibitors, sensitivity to cyclophosphamide was induced (Dylla *et al.*, 2008). Aldefluor a BIODIPY flurochrome attached to an aminoacetaldehyde moiety (a substrate of ALDH) when cleaved, fluoresces and remains within the cell and can therefore be used in the measurement of ALDH activity (Storms *et al.*, 1999). CSCs in breast, lung, liver, head and neck tumours and in cell lines have been identified using Aldefluor (Jiang *et al.*, 2009; Chen *et al.*, 2009).

CD 44 is an 85 to 90 kDa transmembrane glycoprotein containing 10 standard exons. CD44 plays vital role in adhesion, motility, proliferation and cell survival (Marhaba and Zoller, 2004; Afify *et al.*, 2008). The exact function of CD44 in breast CSCs is not fully understood, it is postulated to be involved in the metastasis characteristics of CSCs (Charafe-Jauffret *et al.*, 2009) and play protective roles against apoptosis (Bourguignon *et al.*, 2009).

CD24 is a 30 to 70 kDa glycosylated protein first identified on the surface of B-cell. It is expressed in a range of epithelial cancers and is an indicator for metastasis. *In vitro* assay and *in vivo* studies show that CD24 play important roles in the migration and invasion of cancer cells (Lim, 2004; Sano *et al.*, 2009). CD24⁺ expressing cells show increase growth and cell adhesion by

enhanced interactions between integrins and fibronectin proteins. CD24 expression also represents mesenchymal phenotypes in breast cancer by regulation of the chemokine receptor type 4 (CXCR4) response. CSC population in breast cancer cells have been well defined by CD44^{+(high)}/CD24^{-(low)} expression (Al-Hajj *et al.*, 2003). Cells with High ALDH expression in combination with CD44^{+(high)}/CD24^{-(low)} expression in primary breast cancer xenografts had enhanced ability to induce tumours in immunodeficient mice (Al-Hajj *et al.*, 2003).

CD133 is a 120kDa glycosylated protein consisting of five transmembrane domains with two large extracellular loops, was first discovered in haemopoietic stem cell (Miraglia *et al.*, 1997). CD133 positive phenotype was used in the identification and isolation of stem cells in brain tumour, it has been used to identify CSC populations in other tumours such as breast, liver and prostate cancers (Singh *et al.*, 2004). D133⁺ cells are expressed in tumour-initiating population of brain cancers as well as in CSC populations of the lung, pancreatic, liver, prostate, gastric, colorectal, and head and neck cancers (Singh *et al.*, 2004). High CD133 expression in *in vivo* and *in vitro* studies shows resistance to treatment with cisplatin, etoposide, doxorubicin, and paclitaxel (Chen *et al.*, 2008; Zhang *et al.*, 2009). Stemness genes Nestin, Olig2, and Nanog are upregulated in CD133⁺ population in the brain, lung, liver, and prostate tumours (Miki *et al.*, 2007; Ma *et al.*, 2008).

1.6.3. Cancer stem cell in tumorigenesis

Cancer stem cells (CSCs) have been implicated in the initiation and formation of cancer. Carcinogenesis, a multistep process depends on sequential

accumulation of mutation within tissue cells over a long period of time. However, only a subset of cells is vital for tumour initiation (Reya *et al.*, 2001; Al-Hajj and Clarke, 2004). These tumourigenic cells are believed to be the driving force in tumour progression and heterogeneity of breast cancer (Pardal and Clarke, 2003). CSCs therefore provides the cellular mechanism for genetic and epigenetic changes with resultant cancer initiation, progression, invasion, and metastasis.

1.6.4. Cancer stem cell and chemoresistance

Even with the improvement in Breast cancer (BC) treatment in recent times, the relapsed advanced/metastatic breast cancer has very poor prognosis and survival rate because it is usually pan-resistant to an ample range of anticancer drugs. Understanding the mechanisms of resistance is crucial for the development of new therapeutic approaches for BC management. BC contains a very small fraction (1%) of CSC population with stem cell characters e.g. self-renewal, development into the original tumors in immune deficient mice, differentiation into several lineages of progenies (Dalerba *et al.*, 2007). Evidence show that these CSCs play a vital role in resistance to chemotherapy and radiotherapy in several cancers (Phillips *et al.*, 2006; Tang *et al.*, 2007; Kakarala and Wicha, 2008). Most anticancer drugs target rapidly proliferative cells, CSCs are often quiescent and remain in the G0 phase and are able to evade killing by chemotherapeutic agents (Ishikawa *et al.*, 2007). Others resistant mechanisms of breast CSCs include the expression of cell surface drug pump such as ATP-binding cassette G2/ Breast cancer resistance protein1 (ABCG2/BCRP1), which increases the expulsion of

chemotherapeutic drugs from cancer cells (Engelmann *et al.*, 2008). The high ALDH expression in breast cancer cells metabolizes cytotoxic agents (Moreb, 2008) and overexpression of antiapoptotic molecules such as BCL2 and survivin can prevent cell death (Madjd *et al.*, 2009).

1.6.5. Cancer stem cell and hypoxia

Stem cell “niche” is a specialized microenvironment within tumours which maintains self-renewal and multi-potency. The stem cell niche contains cellular and non-cellular components. The stem cell niche contains a distinct population of cells that maintain stemness, these cells are anchored to the niche by adhesion molecules which interacts with the extracellular matrix. The niche also generates extrinsic factors that regulate that proliferative and differentiated rate of cell growth. The cells within the stem niche are in a hypoxic state. Both normal stem cell and CSC are quiescent in the niches which protect them from chemotherapy. CSCs in the niche have been implicated in tumour formation (Simsek *et al.*, 2010). Hypoxia has also been implicated in the development and maintenance of CSCs within the niche (Panchision, 2009). Hypoxia also triggers cancer stemness genes such as (sex determining region Y)-box 2 (Sox2), octamer-binding transcription factor 4 (Oct4) and Nanog resulting in tumour aggressiveness. The HIF proteins regulate the hypoxia-mediated phenotype and functions of CSCs by upregulation of HIF targeting genes such as Oct4, Nanog, c-Myc, Notch-1, and CD133 (Li and Rich, 2010; Bar *et al.*, 2011).

1.7. Hypoxia

Hypoxia, a reduction of oxygen levels insufficient to meet the metabolic requirement is a common feature of solid tumours (Vaupel and Mayer, 2007). The physiological oxygen concentration in normal tissue is maintained at 3-9%, tumours with an oxygen concentration at or below 1% are considered to be hypoxic. Tissue hypoxia occurs where there is an imbalance between oxygen supply and consumption. Cancer characterized by dysregulation in growth pattern with increased cell division and reduced cell death results in decreased O₂ availability. Oxygen supply to the respiring neoplastic and stromal cells are frequently compromised due to structural abnormalities of the tumour microvasculature and disturbed microcirculation (Vaupel *et al.*, 1989). Hypoxic areas within tumours are heterogeneously distributed with oxygen diffusion being greater in cells closer to the vessels (Vaupel *et al.*, 2004). Tumour hypoxic response could be acute, intermediate or chronic. Acute response to hypoxia induces disturbances in ionic homeostasis with decrease in intracellular adenosine triphosphate/adenosine diphosphate (ATP/ADP) ratios causing enhanced K⁺ efflux and Na⁺ and Ca²⁺ influx (Hammarstrom and Gage, 2002). To ensure survival and maintenance of oxygen homeostasis in tumours during chronic hypoxic conditions, several cellular responses are triggered such as metabolic reprogramming, *de novo* synthesis of new blood vessels or the activation of epithelial to mesenchymal transition (EMT) to escape the hostile hypoxic environment and metastasis to colonize a different environment. Hypoxia (1% or less O₂) or anoxia (<0.01% or no detectable O₂) is a predominant feature in more than 60% of locally advanced solid tumours which clinically contributes to high risk of metastasis, tumour recurrence,

reduced overall survival rate and high mortality (Harris, 2002; Vaupel *et al.*, 2004; Sullivan and Graham 2007).

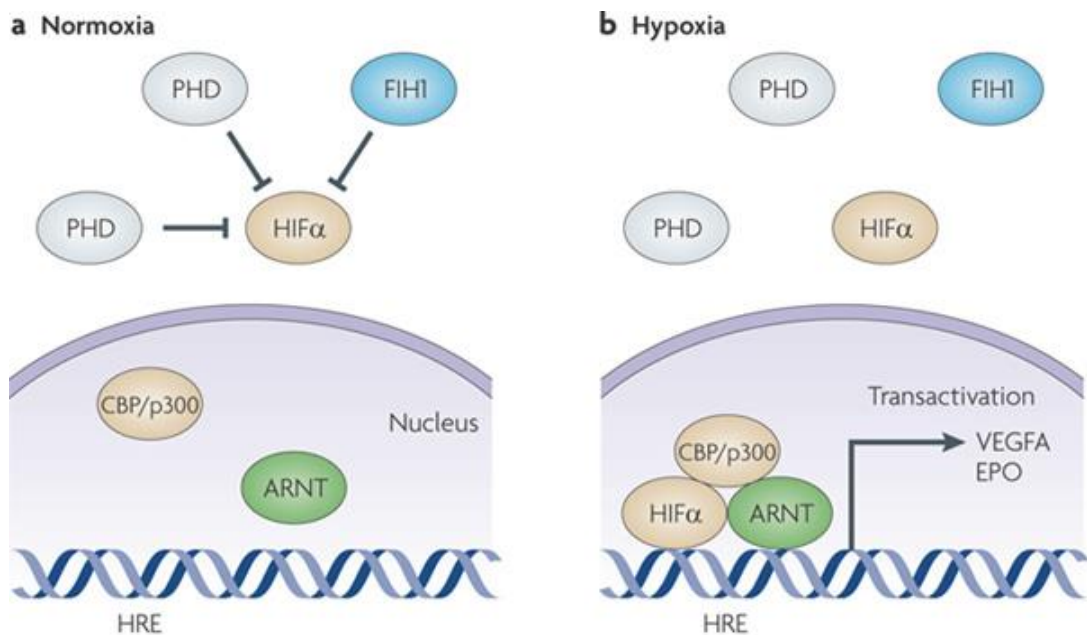


Figure 1.6: HIF pathway in normoxic and hypoxic conditions. Under normoxia hypoxia-inducible factor alpha (HIF α) subunits are hydroxylated by prolyl hydroxylase domain (PHD) enzymes leading to their degradation. In hypoxic conditions, HIF α is accumulated and translocated to the nucleus where combines with its β subunit inducing transcription of downstream target genes (Ohh *et al.*, 2000).

1.7.1. Hypoxia-inducible factors (HIFs)

Neoplastic cells respond to hypoxic microenvironments through the activation of hypoxia-inducible factors (HIFs). HIFs are DNA-binding transcription factors that respond to changes in oxygen levels specifically during hypoxia. They are the key regulator of hypoxia-inducible genes implicated in many different cellular functions such as cell survival, cell proliferation, apoptosis, glucose metabolism, and angiogenesis. HIF is a heterodimer consisting of an oxygen-labile α -subunit (HIF α) closely regulated by PHDs (prolyl-hydroxylases) and a

constitutively expressed β -subunit (HIF β or ARNT) (Gordan *et al.*, 2008). Three HIF alphas isoforms (HIF1 α , HIF2 α and HIF3 α) have been identified in humans with HIF1 α been the most established of the HIF family. HIF1 α protein levels are low in normoxic conditions, HIF1 α is hydroxylated by an oxygen sensitive prolyl-hydroxylase (PDH) in one or both conserved proline residue sites: a carboxyl terminal (CODO) and amino terminal oxygen-dependent degradation domains (NODO) (Ivan *et al.*, 2001). The hydroxyl-HIF1 α complex binds to the β -domain of von Hippel-Lindau tumour suppressor protein (pVHL) and is subsequently ubiquitinated by the breast cancer/Cul2/pVHL ubiquitin–ligase complex assembled via the pVHL α domain, where it is then degraded by 26S proteasomes (Ohh *et al.*, 2000). Under hypoxia, HIF1 α is stabilized and accumulates, it is then translocated to the nucleus, binds to HIF β and the co-activators p300/CBP to induce gene expression by binding to the conserved [A/G]CGTG hypoxia-responsive element (HRE) (Semenza, 2010) including PHD2 (Metzen *et al.*, 2005) and PHD3 (Pescador *et al.*, 2005).

HIF2 α is structurally similar to HIF1 α and is also rapidly induced by hypoxia. It is a heterodimer composed of HIF2 α and HIF2 β subunits. Expression of HIF2 α is cell-type specific and expressed in endothelial cells particularly important in renal cancer and vascular system (Bertout *et al.*, 2008). HIF2 α share numerous transcriptional targets with HIF1 α such as vascular endothelial growth factor (VEGF), Tie-1, Tie-2, Ang-2 and Flt-1 (Raval *et al.*, 2005; Carroll and Ashcroft, 2006). HIF2 α has recently been found to play vital roles in tumorigenesis and maintaining CSC phenotype in certain cancers.

Not much is known about the biology and function of HIF3 α . Several splice variants of HIF3 α has been identified (Maynard *et al.*, 2003). A non-functional complex is formed when pro-apoptotic activity Per/Arnt/Sim domain proteins bind to HIF1 α in the nucleus thus disrupting the expression of HIF1 target genes under hypoxia (Makino *et al.*, 2001).

1.7.2. HIF and cancer

Solid tumour has areas of limited oxygen availability due to structural and functional abnormalities in newly formed vessels resulting in poor perfusion. Hypoxia-inducible factors (HIFs) proteins are overexpressed in several solid tumours (Talks *et al.*, 2000). Tumour hypoxia is a common feature of many cancers and essentially occurs when the growth of the tumour outstrips the accompanying angiogenesis. The HIF proteins are activated by hypoxia which upregulates expression of proteins that promote angiogenesis, anaerobic metabolism, and antiapoptotic cell proliferation survival pathways. Many tumours including BC have high expression of HIF proteins which has been associated with poorer prognosis due to the aggressive, invasive and resistant phenotype of such cancer (Talks *et al.*, 2000).

1.8. Nuclear Factor kappa B (NF κ B)

NF κ B comprises a family of structure-related transcription factors that regulate a large number of normal cellular processes such as the immune and inflammatory responses, developmental processes, cellular growth and apoptosis. It is persistently activated in several disease states such as cancer, arthritis, chronic inflammation, asthma, neurodegenerative and heart

diseases. NF κ B was first discovered in the nucleus of activated B cells as having a DNA-binding activity with strong affinity for the transcriptional enhancer of kappa (κ) light-chain gene of immunoglobulin (Sen and Baltimore, 1986). NF κ B is ubiquitously expressed in almost all cell types and tissues and is a stimulus-responsive pleiotropic regulator of gene control which regulates several genes that have NF κ B binding sites in their promoters or enhancer regions (Oeckinghaus *et al.*, 2009) thus is important in several physiological and biological processes.

1.8.1. NF κ B Family members

The NF κ B family consists of five closely related transcription proteins namely RelA (p65), RelB, c-Rel, NF κ B1 (p50/p105), and NF κ B2 (p52/p100) which share a 300 amino acid N-terminal DNA binding domain called the Rel homology domain (RHD) (Moynagh, 2005; Hoffmann *et al.*, 2006). The RHD is the basis by which NF κ B family members can form homodimers and heterodimers allowing them to bind to promoters and enhancer gene regions which control their expression. The C-terminal transcriptional domain (TADs) located in RelA, cRel and RelB activates target gene expression while p50 and p52 lack C-terminal TADs and are suppressed unless they are bound to proteins containing TADs. NF κ B proteins are not produced *de novo* but are activated by signals that trigger Nuclear factor NF-kappa B inhibitor kinase (IKK) which cause the kappa light polypeptide gene (I- κ B) of nuclear factor to undergo phosphorylation which degrades and releases NF κ B from its dimer

form which then translocated to the nucleus to activate target genes (Liang *et al.*, 2004). The nuclear–cytoplasmic localization of NF κ B is tightly controlled.

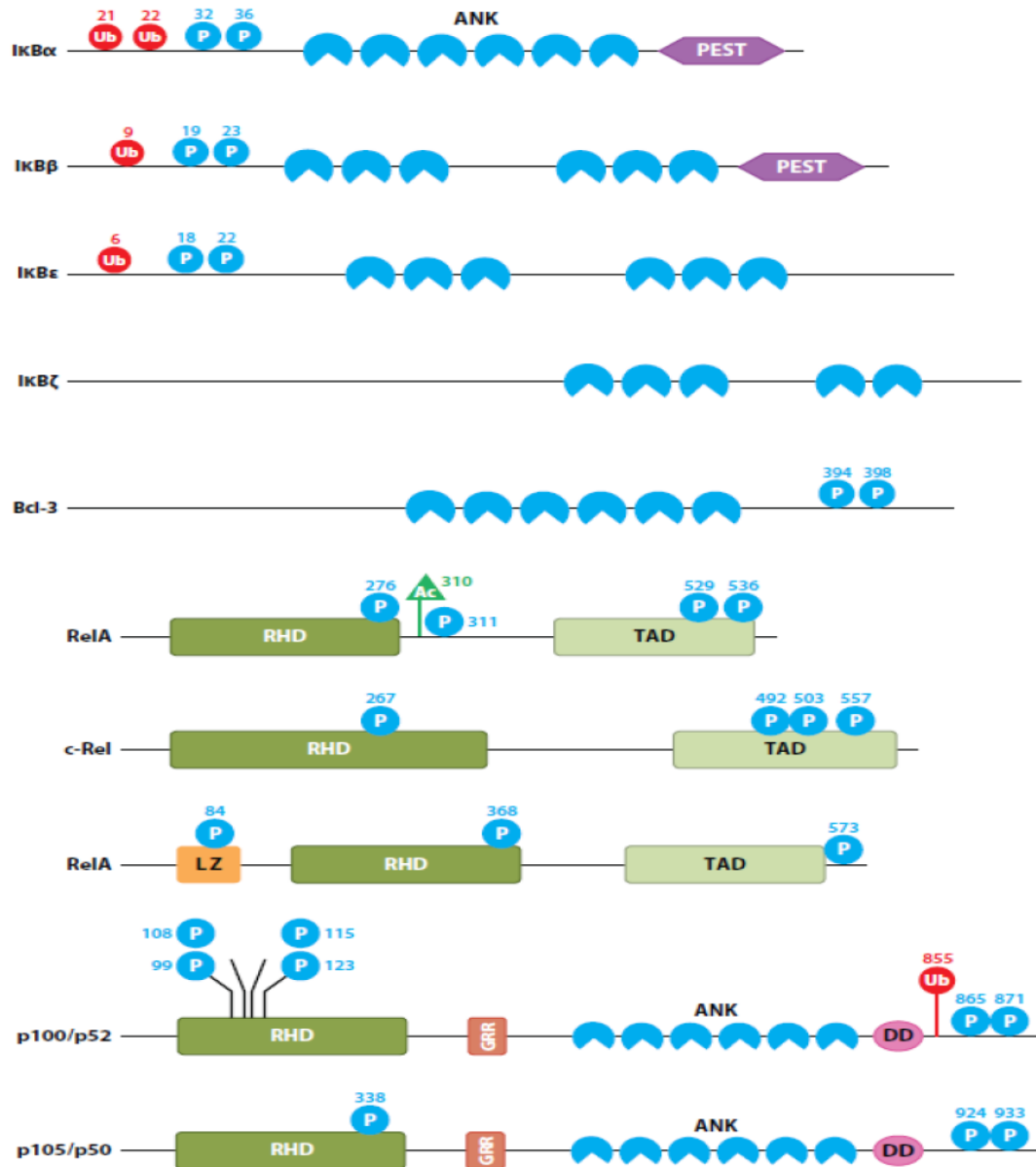


Figure 1.7. Members of the Rel/NF κ B and I κ B families of proteins.

The red boxes indicate the endoproteolytic cleavage sites of p105 and p100 which give rise to p50 and p52, respectively. Purple boxes indicate the PEST domains (polypeptide sequences enriched in proline, glutamic acid, serine, and threonine). Abbreviations: RHD, Rel homology domain; ANK, ankyrin repeat; SS, signal-induced phosphorylation sites. N, nuclear localization sequence.

1.8.2. Activation of NF κ B Pathways

NF κ B is usually bound to its co-repressor molecule I κ B in the cytosol in normal resting conditions. Degradation of I κ B protein occurs through specific phosphorylation mediated by I κ B kinase (IKK) (Ghosh and Karin, 2002). The IKK complex plays vital roles in upstream NF κ B signal transduction cascade. I κ B kinase (IKK) enzyme complex comprises of two catalytic kinase subunits I κ B α (IKK1) and I κ B β (IKK2) and a nonenzymatic regulatory scaffold protein NF κ B essential modulator (I κ B γ). Two primary signalling pathways (Figure 1.8) are involved in the activation of NF κ B namely the classical (canonical) and the alternative (non-canonical) pathways (Tergaonkar, 2006; Scheidereit, 2006). The canonical pathway activates NF κ B dimers RelA, c-Rel, RelB and p50 while the noncanonical pathway activates p100/RelB complexes. The classical NF κ B pathway is triggered when cells are stimulated by TNF α , T-cell receptors (TCR), B-cell receptors (BCR), Toll-like receptor (TLR) or interleukin-1 receptors (IL-1R) (Karin and Ben-Neriah, 2000). I κ B β is important for the phosphorylation of I κ B α at Ser32 and Ser36. Phosphorylation of I κ B α triggers rapid polyubiquitination at Lys21 and Lys22 sites of I κ B α and stimulates subsequent degradation of this cytoplasmic inhibitor by 26S proteasome complex, that liberates NF κ B (RelA/p50) and unveils the nuclear localization signal present on RelA promoting the nuclear translocation of NF κ B dimers to the nucleus (Karin and Ben-Neriah, 2000). The alternative pathway is largely dependent on IKK α subunits and is responsible for the activation of p100/RelB complexes. Signals from NF κ B inducers such lymphotoxin B and B cell activating factor (BAFF) initiate the activation of

NF κ B inducing kinase (NIK), which phosphorylates and activates the IKK α complex that in turn phosphorylates p100 by 26S proteasome liberating p52/RelB active heterodimer. This generates RelB/p52 heterodimers that are translocated into the nucleus as transcription factors (Bonizzi *et al.*, 2004).

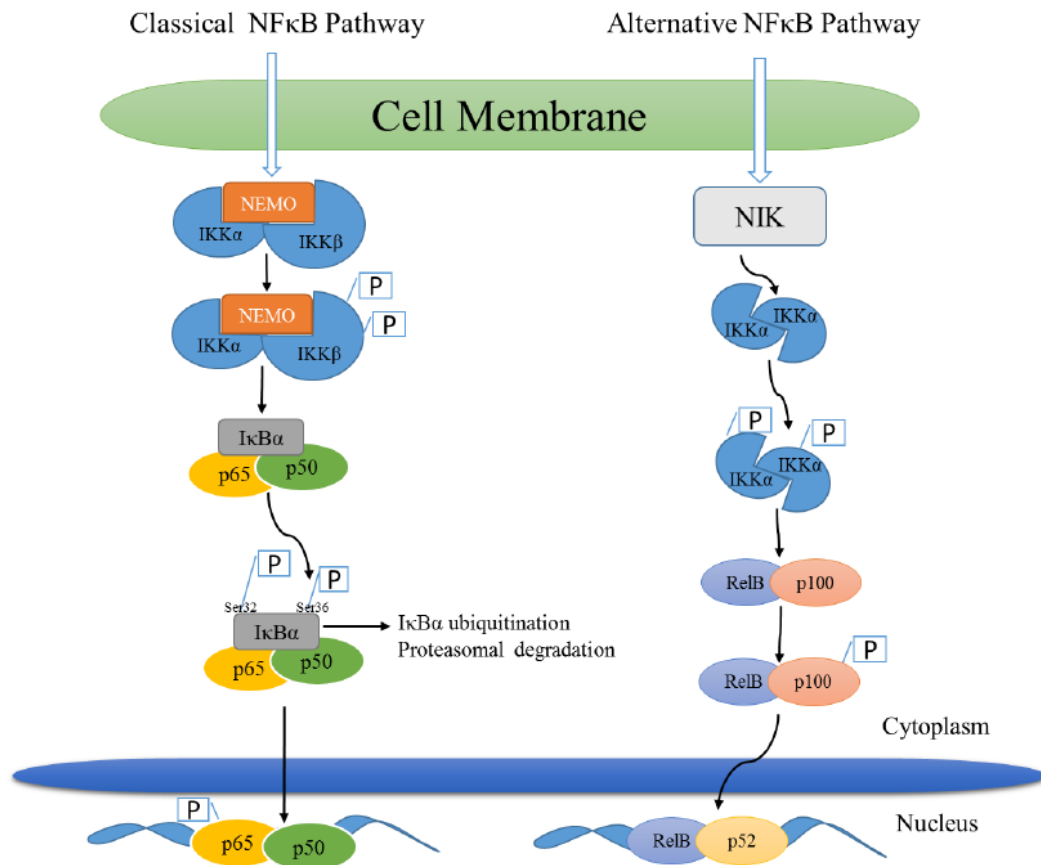


Figure 1.8: Classical and alternative pathway of NF κ B activation. The classical pathway is mediated by IKK β leading to the phosphorylation of I κ B. Activators of classical pathway include TNFR1/2, TCR and BCR and TLR/IL-1R. The alternative pathway involves NIK activation of IKK α and leads to the phosphorylation p100 liberating of p52/RelB heterodimer (Abbreviations NEMO: Nuclear factor kappa B essential modulator, NIK: Nuclear factor kappa B inducing Kinase, TNFR:, TCR:, IKK β : I κ B kinase, I κ B: Inhibitors of NF κ B) (Scheidereit, 2006).

1.8.3. NF κ B and Breast Cancer

Breast cancer (BC) is affiliated with dysregulated expression of growth factors, kinases and transcription factors. NF κ B activation is strongly associated with oncogenesis, its activation induces proliferation, inflammation, cell invasion and suppression of apoptosis (Basseres and Baldwin, 2006; Karin, 2006). Several reports have shown that NF κ B is activated in human breast cancer cell lines as well as in primary breast tumours (Cogswell *et al.*, 2000; Nakshatri and Goulet, 2002; Biswas *et al.*, 2004). NF κ B is an upstream regulator of many cellular signalling pathways involved in BC promotion, Its activation up-regulates antiapoptotic genes in BC cells resulting in cell survival mechanisms and resistance to therapeutic regimens. Constitutive activation of NF κ B in BC cells occurs through abnormal signalling of the epidermal growth factor receptor, cytokines (interleukin-1) or the heregulin pathways (Bhat-Nakshatri *et al.*, 2002). Mechanisms involved in NF κ B activation in mammary tumours is not fully understood, cyclin D1 a regulator of the cell cycle is activated by NF κ B gene. Cyclin D1 promoter has an NF κ B binding site, and experiments done on mice models reported that overexpression of cyclin D1 in the mammary gland of mice increased the incidence of mammary carcinoma and knock out of the cyclin D1 gene protected development of BC by the induction of mouse mammary tumour virus MMTV-neu or MMTV-v-Ha-ras (Wang *et al.*, 1994; Yu *et al.*, 2001). The basal-like subtype, a subgroup of TNBC, exhibits high levels of constitutively active NF κ B signalling. There is a cross-link between NF κ B and the oestrogen receptor pathway, according to the reports by Biswas and colleagues NF κ B activation is predominantly in oestrogen

receptor-negative breast tumours, thus TNBC patients have poorer prognosis (Biswas *et al.*, 2000).

1.8.4. NF κ B and Chemoresistance

NF κ B a ubiquitous transcription factor represents a class of dimeric proteins regulating over 400 genes involved in immunoregulation, growth regulation, inflammation, carcinogenesis, apoptosis and cell survival pathway. Activation of the NF κ B pathway protects tumour cells from apoptosis through the expression of antiapoptotic proteins as well as the suppression of proapoptotic protein expression in many tumours (Kato *et al.*, 2003; Panta *et al.*, 2004). Several studies have reported that NF κ B plays vital role in preventing apoptosis induced by radiation and chemotherapeutic agents. Most solid tumours including BC have high expression of NF κ B which can be further increased by exposure to cytotoxic agents resulting in cell growth, survival and resistance to therapeutic agents (Karin *et al.*, 2002; Arlt *et al.*, 2003).

Chemotherapeutic agents result in NF κ B-induced expression of antiapoptotic genes such as IAP, IEX-1L, FLICE, cFLIP, Bcl-XL, Bfl-1, TNF receptor (TNFR) associated factor TRAF1 and TRAF2. IAPs (c-IAP1, c-IAP2, and XIAP) inhibits caspases which suppress the extrinsic and intrinsic apoptotic pathways. Anti-apoptotic members of the Bcl-2 family (Bcl-XL, A1) prevents the release of cytochrome-c and inhibit caspase-9 activity (Wu *et al.*, 1998; Wang *et al.*, 1998). Genes for tumour growth and survival, including cyclin D1 and c-Myc, are also regulated by NF κ B and contribute to the chemoresistance. Furthermore, multidrug resistance genes such as multidrug resistance

associated protein, P-gp, and breast cancer resistance protein have NF κ B binding sites within their promoter regions (Bentires-Alj *et al.*, 2003), therefore activation of NF κ B induces these resistance gene. Thus regulation of the NF κ B signalling pathway could be a potent target for improving the chemosensitivity of tumour cells. Down regulation of constitutive activation of NF κ B by curcumin sensitize human multiple myeloma cells to vincristine and melpahan (Bharti *et al.*, 2003). Triptolide a potent inhibitor of NF κ B also enhance the chemosensitivity to doxorubicin (Yinjun *et al.*, 2005).

1.8.5. NF κ B and hypoxia

Hypoxia, a decrease in O₂ availability triggers several cellular and molecular responses required for adaptation of cells to the low oxygen conditions. Activation of a number of genes occurs during hypoxia, such as the hypoxia-inducible factor (HIF), an oxygen dependent transcription factor responsible for the upregulation of genes involved in different cellular functions such as cell survival, cell proliferation, apoptosis, glucose metabolism and angiogenesis (Semenza, 2009).

NF κ B is another important transcription factor activated during hypoxia. It consists of a 5 membered family of proteins namely (RelA (p65), RelB, c-Rel, NF κ B1 (p50/p105), and NF κ B2 (p52/p100). Studies have demonstrated that a cross-talk exists between NF κ B and HIF signalling pathways (Figure 1.9). Human HIF1 α promoter has a NF κ B binding site at -197/-188 base pairs upstream of the transcriptional start site, the mutation of which leads to a loss of hypoxic HIF1 α up-regulation. Studies showed that NF κ B stimulates the

transcription of HIF1, and HIF1 expression regulates the activation of NF κ B (Scortegagna *et al.*, 2008). Therefore, inhibition of NF κ B may influence the activity of HIF1 α and *vice versa*.

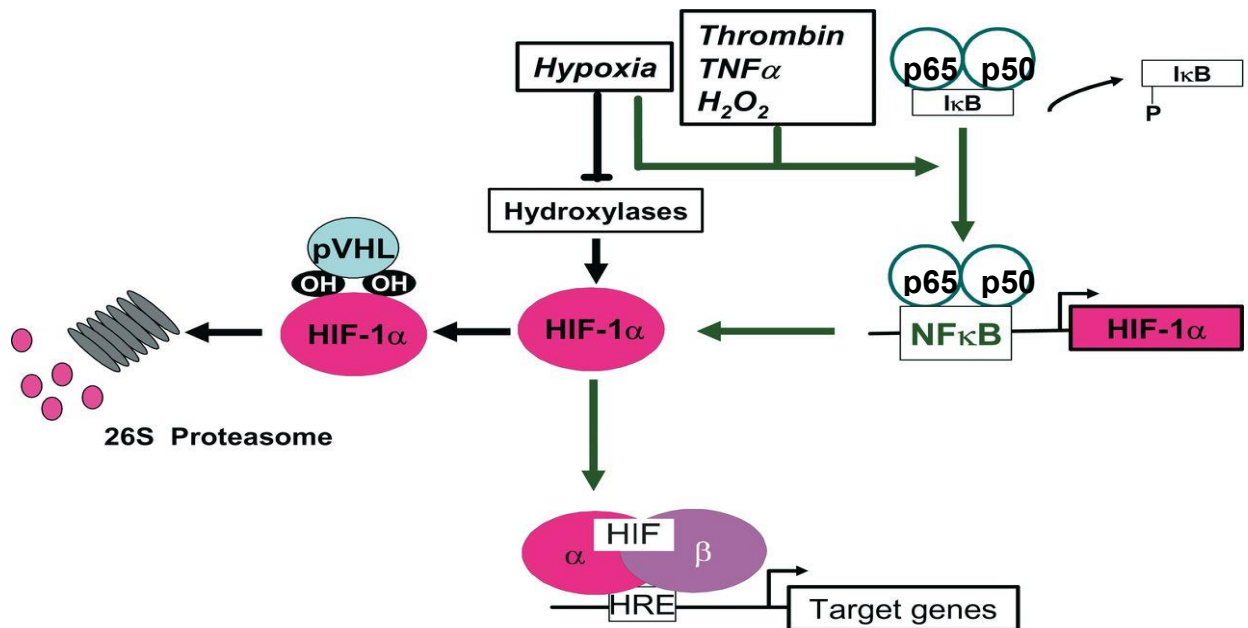


Figure 1.9 Cross-talk between HIF and NFκB in hypoxia. Under normoxic conditions, activated HIF1α binds to pVHL and is followed by proteasomal degradation. Hypoxia leads to phosphorylation of IκB, releasing NFκB to the nucleus, where it binds to a distinct element at HIF1α promoter site. (Abbreviations; HIF: hypoxia-inducible factor, NFκB: Nuclear factor kappa B, HRE: Hypoxia-response element, pVHL: von Hippel-Lindau, TNF: tumour necrosis factor, H₂O₂: Hydrogen peroxide) (Scortegagna *et al.*, 2008).

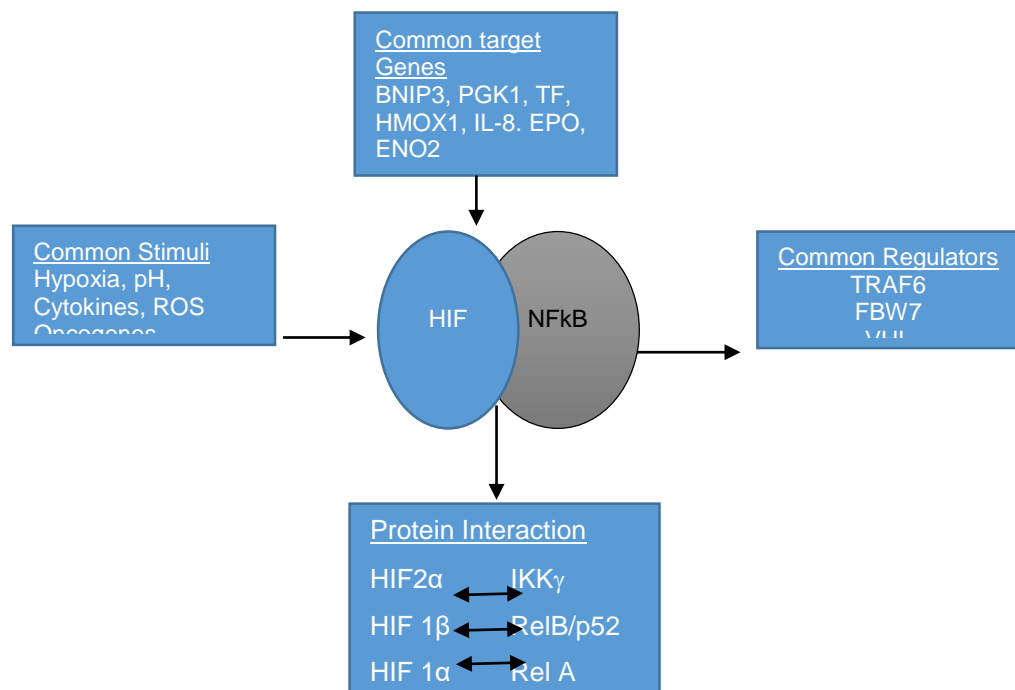


Figure 1.9B Cross-talk between HIF and NFκB. Figure displays some common stimulators and targets genes of HIF and NFκB proteins.

1.9. Disulfiram

Disulfiram (DS) also known as tetraethylthiuram disulfide was developed in 1881 by M. Grodzki a German chemist (Grodzki *et al.*, 1881). He synthesized DS from thiocarbamide with a stoichiometric formula of $C_{10}H_{20}N_2S_4$. This new formulation did not get much attention until some twenty years later when it was introduced in the rubber industry to accelerate the vulcanization of natural and synthetic rubber (Twiss *et al.*, 1992; Eneanya *et al.*, 1981). In the early 1940s, DS was also used as a scabicide. Two British physicians discovered that DS was an effective treatment against scabies in domestic animals (Gordon and Seaton, 1942). In 1945, two Danish physicians Hald and Jacobsen while testing the effects of DS as a vermicide observed that ingestion of alcohol after treatment with DS lead to the development of extreme unpleasant reactions which paved the way for the use of DS as an antialcoholism drug (Eneanyyn *et al.*, 1981). The clinical use of DS over a long period of time has shown it to be a very safe drug with minimal and manageable toxic effects, even when fairly high doses of 300 to 500 milligrams per day are administered. DS also has a high bioavailability of more than 80% with 20% still detected in the body after two weeks administration (Sauna *et al.*, 2005). DS is also found to have potent anticancer effects after it was observed that alcoholic patients with cancer being treated with DS had regression in cancer growth, this lead to further investigations on the use of DS as a potential anticancer agent (Wang *et al.*, 2003).

was quickly reduced to its thiols within 4 minutes (Cobby *et al.*, 1977). The DDC formed is a substrate for phase II metabolism and is further metabolised by four different reactions namely glucuronidation, nonenzymatic degradation, methylation, and oxidation.

Glucuronidation: This is the major detoxification mechanism of DS which involves the conjugation of DDC with glucuronic acid in mammals. 50% of the given dose of DS is excreted in urine as a glucuronide metabolite (III) (Eneany *et al.*, 1981).

Nonenzymatic degradation: The decomposition of DDC is pH dependent where DDC is rapidly converted to diethylamine (IV) and carbon disulfide (V) in an acidic environment (Stromme *et al.*, 1966). Diethylamine undergoes further degradation to ammonium and acetaldehyde. Carbon disulfide is oxidatively desulfurated to carbonyl sulfide (VII) and sulphur by NADPH and cytochrome P450 (Dematteis, 1974). Carbonyl sulfide undergoes further oxidation to carbon dioxide and sulphur, which can be metabolized to sulfate by the sulfoxidases (Faiman *et al.*, 1978).

Methylation: A small amount about 0.05% of DS and its DDC form can be methylated forming methyl ester of DDC (MeDDC) (X). DDC can also be methylated by S-methylation accounting for about 27% of the given dose (Gessner and Jakubowski, 1972). The MeDDC derivative can be targeted by esterases which generate mercaptan which is further oxidized to sulfate and formaldehyde.

Oxidation: oxidation of DS is an uncommon process where DDC is reoxidized back to DS under atmospheric oxygen conditions. This process accounts for

only 4% of DDC and is mostly affected by oxidases in the body (Strume *et al.*, 1965).

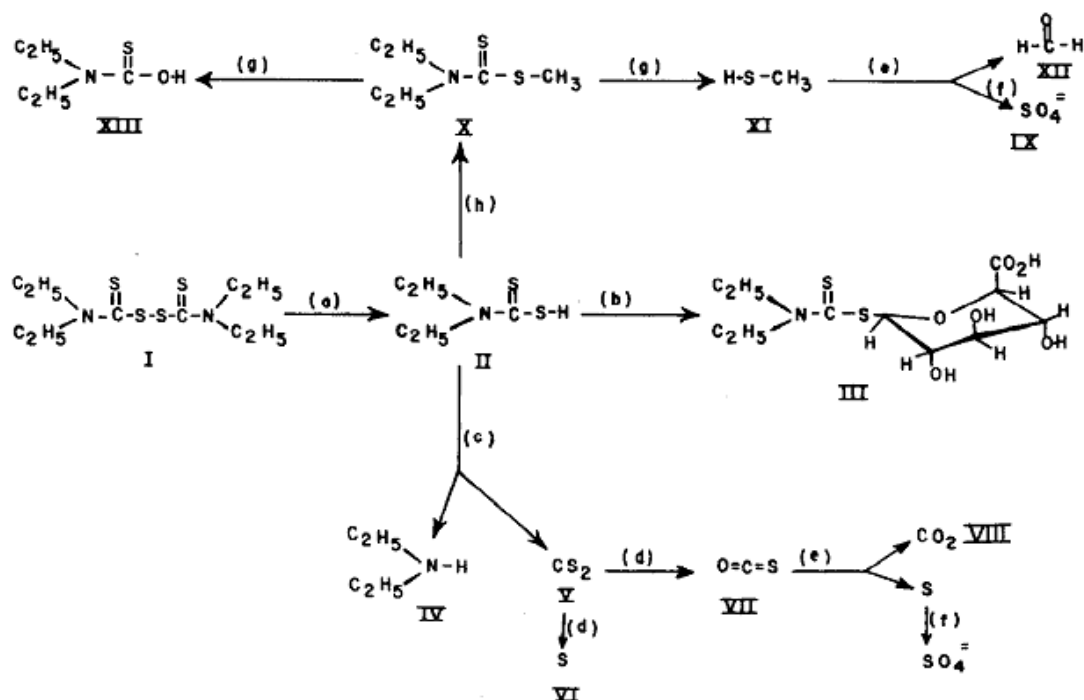


Figure 1.11: Metabolism of disulfiram. Tetraethylthiuram disulfide (disulfiram), II. Diethyldithiocarbamic acid, III. Glucuronide of diethyldithiocarbamate, IV. Diethylamine, V. carbonyl disulfide, VI. Sulfur, VII. Carbonyl sulfide, VIII. Carbon dioxide, IX. Sulfate, X. methyl ester of diethyldithiocarbamate, XI. Methyl mercaptan, XII. Formaldehyde, XIII. thiocarboxylic acid. (a) Glutathione reductase, (b) conjugation, (c) nonenzymatic degradation, (d) oxidative desulfuration (C-P450), (e) oxidation, (f) sulfoxidase, (g) esterases, (h) S-methylation: S-adenosyl methionine transmethylease (Eneany et al, 1981).

1.9.2. Disulfiram and Disease Treatment

1.9.2.1. Anti-alcoholism

Ethanol is metabolised by the liver by alcohol dehydrogenase (ADH) into acetaldehyde. Acetaldehyde is highly toxic and is promptly converted to

acetate a less toxic compound by acetaldehyde dehydrogenase (ALDH) (Deitrich *et al.*, 2007) (Figure 1.12), which then enters the citric acid cycle.

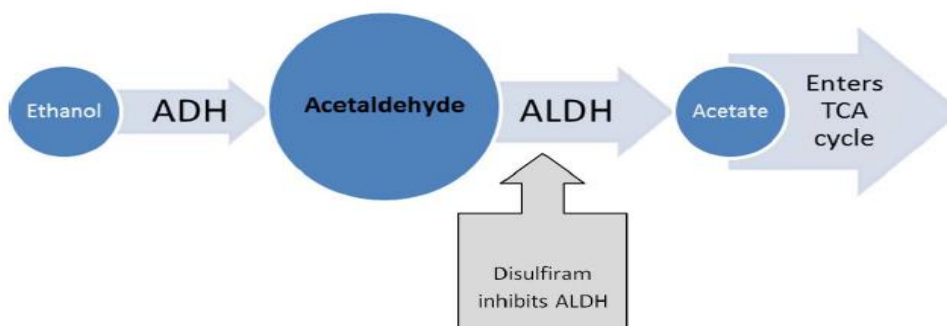


Figure 1.12: Disulfiram as an antialcoholism agent.

DS and many of its metabolites (S-Methyl-N,N-diethylthiocarbamate sulfoxide (MeDTC-SO), S-Methyl-N,N-diethyldithiocarbamate sulfoxide (MeDDC-SO) and S-Methyl-N,N-diethyldithiocarbamate sulfine (MeDDC-sulfine) irreversibly inhibits ALDH by oxidation of sulfhydryl groups to form irreversible internal S-S bonds leading to the accumulation of acetaldehyde in the blood (Johansson, 1992; Pike *et al.*, 2001). Alcohol consumption after taking DS intake drastically increase the acetaldehyde levels in plasma manifestating in a condition called disulfiram-alcohol reaction (DER).

1.9.2.2. Anticancer treatment

The use of DS as a potential anticancer agent has been studied (Brar *et al.*, 2004). DS has been shown to inhibit the growth of several cancers including breast cancer cell lines *in vitro*. The use of DS as an anticancer treatment drew some attention after a case report by Lewison in 1977 reported that a breast cancer patient with multiple bone metastasis had been treated for alcohol dependence by the Antabuse-DS showed spontaneous cancer regression. *In*

vivo animal studies also demonstrated the anticancer activity of DS. Neoplasia induced on the forestomach of female mice by Benzo[α]pyrene administration, after a 30 week period more than 90% of treated animals developed tumours while in the group with 1% Antabuse in their diet, no tumour was developed at this site (Borchert and Wattenberg, 1976). Another animal study reported similar findings; urinary bladder cancer was distinctly inhibited when Wistar rats were fed with Antabuse in their diet of N-n-butyl-N-(4-hydroxybutyl) nitrosamine (BHBN) (Irving *et al.*, 1979; Irving *et al.*, 1983). In a patient with stage IV metastatic ocular melanoma being treated for alcoholism, reduction in hepatic metastasis was observed after an oral combination of DS and zinc gluconate was given continuously for a 53 month period, the patient experienced negligible side effects from the drug (Brar *et al.*, 2004).

1.9.3. Cytotoxic mechanism of disulfiram

The exact mechanism by which DS exerts its anticancer effects has not been elucidated. However, studies have shown that DS and its metabolites target several cellular pathways in the human body such as inhibition of DNA topoisomerase preventing DNA transcription and replication, inhibition of matrix metalloproteinases (MMPs) leading to the inhibition of tumour cell metastasis, inhibition of the proteasome leading to inhibition of the NF κ B signalling pathway and downstream expression of cancer survival genes, inhibition of superoxide dismutase (SOD) and increasing intracellular copper (Cu) levels leading to toxic build-up of reactive oxygen species (ROS) (Sauna *et al.*, 2005). A recent paper showed that DS in association with Cu mediates its cytotoxic action by the generation of ROS (in short term) and formation of

DDC-Cu which has a longer term toxic effect on cancer cells (Tawari *et al.*, 2015). A Randomized phase 2 trial of advanced non-small cell lung carcinoma with/without disulfiram and cisplatin; Navelbine showed that DS increased the tumour response disease free survival in many patients (Nechushtan *et al.*, 2015)

1.9.3.1. Generation of Reactive Oxygen Species (ROS)

Reactive oxygen species (ROS) are chemically reactive molecules containing oxygen. They usually have a single unpaired electron in their outermost shell of electrons thus are highly reactive. ROS include free oxygen radicals as superoxide ($O_2^{\cdot-}$), hydroxyl radical ($\cdot OH$), nitric oxide ($NO\cdot$) and non-radical derivatives of oxygen such as hydrogen peroxide (H_2O_2) and singlet oxygen (1O_2). ROS is generated through normal cellular metabolism processes and from activation of membrane bound enzymes system such as NADPH oxidase complexes. The mitochondrial electron-transport chain, a complex system involved in a series of oxidation-reduction reactions through the transfer of electrons from reductant to oxidant results in the generation of intracellular ROS when some electrons leak out of the respiratory chain and react directly with oxygen forming superoxide which can also be converted to other ROS. ROS can also be generated by reactions involving NADPH oxidase complexes or from biochemical reactions in peroxisomes and cytochromes (Bokoch and Knaus, 2003). A mild increase in ROS favours cell proliferation and differentiation, however a substantial increase results in irreversible damage to lipids, proteins and DNA, leading to cell death (Schafer and Buettner, 2001; Boonstra and Post, 2004). Therefore, maintaining the level of ROS is important

for cell growth and survival. Antioxidants and ROS-scavenging enzymes tightly regulate the ROS generated. These antioxidants and ROS-scavenging enzymes include superoxide dismutases (SOD1, SOD2, and SOD3), glutathione peroxidase, peroxiredoxins, glutaredoxin, thioredoxin and catalase (Boonstra and Post, 2004).

Cancer cells being metabolically active and under high oxidative stress have elevated ROS level due to increase in peroxisome activity, mitochondrial dysfunction, oncogenic activity, infiltration of immune cells and increased cellular receptor signals (Storz, 2005). The cancer cells adapt to the high ROS generated by increasing the expression of cell survival proteins, modification of protein structures, enhancing transcription factors and activate genes that control cell growth and differentiation (Davies, 1999). Cancer cells also express high levels of antioxidant enzymes such as the superoxide dismutase (SOD), catalase, peroxidases and activation of the glutathione system (GSSG/2GSH) and thioredoxin system which maintain cellular redox balance (Schafer and Buettner, 2001). Transcription factors such as NF κ B, HIF1 α , HIF2 α and signalling molecules MAPK and JNK are activated in cancer cells which favour their growth and survival (Martindale and Holbrook, 2002). Therefore, further increment in ROS level after exposure to anticancer drugs might be an “Achilles heel” for cancer cells leading to their death.

Copper (Cu) an essential trace element plays pivotal role in the biology of humans (Harris and Gitlin, 1996). Its unique electronic structure enables it to act as cofactors in a number of redox reactions of enzymes required for normal growth and development (Tapiero *et al.*, 2003). Cu generates ROS with

oxidizing agent through the Fenton's reaction damaging cellular components such as lipids, protein and DNA inducing apoptosis. The transport of Cu within cells is tightly regulated by copper transporters such as the human copper transporter (hCtr1). DS is a strong chelator of divalent metallic ions such as Cu, zinc (Zn), gold (Au) and iron (Fe) (Morrison *et al.*, 2010). The binding of DS with Cu increases the cellular uptake of Cu, which causes ROS accumulation and induces apoptosis. Elevated levels of Cu has been documented in a number of tumours such as breast (Kuo *et al.*, 2002), lungs (Diez *et al.*, 1989), cervix (Chan *et al.*, 1993) and ovaries (Chan *et al.*, 1993). Exposure of cancer cells to DS/Cu complex increase the Cu load in the cells inducing the generation of more ROS within the cell. The ROS activates NF κ B activity triggering antiapoptotic factors which diminish this effect. However DS is also a potent inhibitor of NF κ B and ALDH which acts as ROS-scavengers. This overall effect, inhibition of NF κ B and ALDH by DS/Cu complex and the induction of excess ROS by Cu causes cell damage or sensitize the cancer cells to chemotherapeutic drugs (Guo *et al.*, 2010; Liu *et al.*, 2012; Yip *et al.*, 2011). This selective target mechanism of DS/Cu complex on inducing death of cancer cells (elevated Cu, NF κ B and ALDH inhibition) may be why DS is not toxic to normal cell.

1.9.3.2. ALDH inhibition

Aldehyde dehydrogenases (ALDHs) are a superfamily of enzymes important for endogenous and exogenous metabolism of aldehydes. There are 19 isozymes in humans which perform important physiological and toxicological functions. ALDH1A play crucial role in embryogenesis and mediation of

retinoic acid signalling. ALDH2 is the main enzyme involved in the metabolism of aldehyde for alcohol metabolism; the other ALDH isozymes maintain cellular homeostasis by oxidizing reactive aldehydes from lipid peroxidation. High ALDH activity is used as a functional marker for CSCs (Ginestier *et al.*, 2007) and is a factor involved in chemoresistance and radiotherapy resistance in several human cancer and in BC cell lines MDA-MB-231 and MDA-MB-468 (Crocker and Allan, 2012). ALDH is also a scavenger of ROS thereby reducing the drug or radiation induced oxidative stress which could explain the high amounts of ALDH in CSCs and their resistant nature (Crocker and Allan, 2012). DS is a potent inhibitor of ALDH where it inhibits the ALDH enzyme activity. DS and its metabolites irreversibly inhibits ALDH. The molecular mechanism by which DS inhibits ALDH is through the reduction DS to DDC which is an inhibitor of ALDH *in vivo* but not *in vitro* (Lipsky *et al.*, 2001). DDC is converted to methyltransferases to S-methyl-*N,N*-diethyldithiocarbamate and S-methyl-*N,N*-diethyldithiocarbamate by hepatic thiols which are potent inhibitors of mitochondrial ALDH2 *in vivo*.

1.9.3.3. Proteasome / NF- κ B inhibition

Proteasomes are protein complexes inside cells that degrade damaged or unwanted protein by proteolysis. Enzymes called proteases located in the proteasome carry out this degradation reaction after the proteins are tagged with ubiquitin. The proteasome degradation pathway is vital for several cellular processes such as cell cycle, regulation of gene expression and responses to oxidative stress (Lodish *et al.*, 2004). The ubiquitin–proteasome system (UPS) is a complex and dynamic intracellular proteases, responsible for the degradation of about 90% of proteins in the cell and plays a crucial role in

maintaining normal cellular homeostasis. The proteasome pathway plays a vital role in the activation of NF κ B which is a predominant transcription factor activated in many malignant tumours. NF κ B is constitutively active and overexpressed in breast cancer cells and drives cancer cell survival, development and metastasis (Sovak *et al.*, 1997). Therefore, inhibition of NF κ B would result in the inhibition of cancer cell survival, development and metastasis. DS/Cu complex is a potent inhibitor of NF κ B pathway via the inhibition of E3 ubiquitin ligase of the proteasome pathway which prevents phosphorylation and degradation of I κ B (NF κ B inhibitor), thus NF κ B release and nuclei translocation is hindered (Cvek and Dvorak, 2007; Matsuno *et al.*, 2012). This would lead to the accumulation of proapoptotic target proteins and induces cell death (Rae *et al.*, 2013).

1.9.3.4. Overriding resistance mechanisms

P-gp an active drug efflux pump is overexpressed in many solid tumours (Krishna and Mayer, 2000; Thomas and Coley, 2003). DS was found to decrease the P-gp mediated drug resistance of vinblastine and colchicine *in vitro* by targeting the thiol groups in cysteine residues of P-glycoprotein (Loo and Clarke, 2000). DS and its metabolites DDC, MeDDC-sufoxide and MeDDC-sulfone were also found to inhibit the stimulated ATPase activity of P-gp in verapamil treated cells (Loo *et al.*, 2004).

Due to the unrestricted and uncontrollable growth of breast cancer cells, angiogenesis the formation of new blood vessels to meet the demand of the growing cells occurs. DS was found to inhibit angiogenesis in glioma and lung carcinoma tumours (Marikovsky *et al.*, 2002). Other research also showed that

DS suppressed angiogenesis in 10 day old chicken embryos. The authors demonstrated that DS directly interacts with matrix metalloproteinase MMP-2 and MMP-9 *in vitro*, inhibiting their proteolytic activity through zinc chelating mechanisms (Shiah *et al.*, 2003).

1.10. Encapsulation of Chemotherapeutic drugs

1.10.1. Nanoencapsulation

Nanomedicine the use of nanotechnology (manipulation of matter in an atomic or molecular scale) to diagnose, treat or prevent diseases in humans is an evolving discipline that has the potential to radically change medical science. Nanoparticles are particles in the nanometer size range. Nanoencapsulation can therefore be defined as technology involved in the packaging of molecules of solid, liquid or gas in a core-shell complex where the active compound is protected within the core of the nanoparticles. The nanoparticles acts as a reservoir that encapsulates an active substance protecting and isolating it from the surrounding environment and the properties of the nanoparticles can be adjusted to meet specific requirements. The principal aims of nanoparticles are for the provision of formulations with prolonged activity, protection against unfavourable conditions and to control the release of the active ingredient. Nanotechnology has been extensively used in the preparation of medicine, food stuff and cosmetics in the pharmaceuticals (Farokhzad and Langer, 2009; Shimoni, 2009), food (Fathi and Mohebbi, 2010; Neethirajan and Jayas, 2011) and cosmetic industries.

1.10.2. Nanocarriers for anticancer drug delivery

Chemotherapy is usually accompanied by severe adverse effects limiting the amount of drug given to patients, consequently tumours may not be sufficiently exposed to lethal doses of drugs. Nanocarriers have improved the treatment and management of breast cancer patients by increasing the efficacy, specificity and targeting ability of chemotherapeutic agents (Soppimath *et al.*, 2001). Nano vehicles used for encapsulation of anticancer drugs include liposomes, micelles, carbon nanotubes and dendrimers.

Liposomes: Liposomes are spherical nanocarriers composed of an aqueous core surrounded by one or more concentric lipid bilayers with size ranging from 50 nm to several micrometers (Figure 1.13). A Major limitation of liposomes is their short half-life due to unspecific interactions with macromolecules and cellular surfaces. Macrophages in the liver and spleen rapidly clear conventional liposomes.

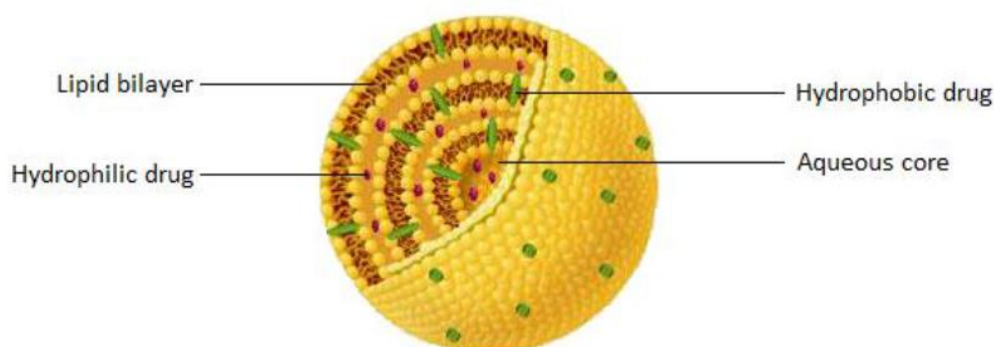


Figure 1.13 Structure of a multilaminar liposome

Polymeric micelles (PM): Polymeric micelles are nanoscopic amphiphilic block polymers formed from self-aggregation of amphiphilic polymers with the hydrophobic part of the polymer on the inside (core) and the hydrophilic part

on the outside (shell). Many anticancer drugs have been successfully encapsulated in micelles, Dox a very toxic anticancer drug when encapsulated in micelle, systemic uptake by normal tissue was reduced two fold compared to free drug (Marin *et al.*, 2002), the cytotoxic effect of PTX was greatly enhanced by encapsulation in amphiphilic block copolymers (Park *et al.*, 2005). Oxaliplatin loaded into poly(ethylene glycol)- β -poly(glutamic acid) polymeric micelles demonstrated enhanced antitumour activity (Cabral *et al.*, 2007). Surface modification of micelles such as conjugation with PEG increased blood circulation time by preventing opsonin adsorption and clearance by the mononuclear phagocytic system (Kwon, 2003).

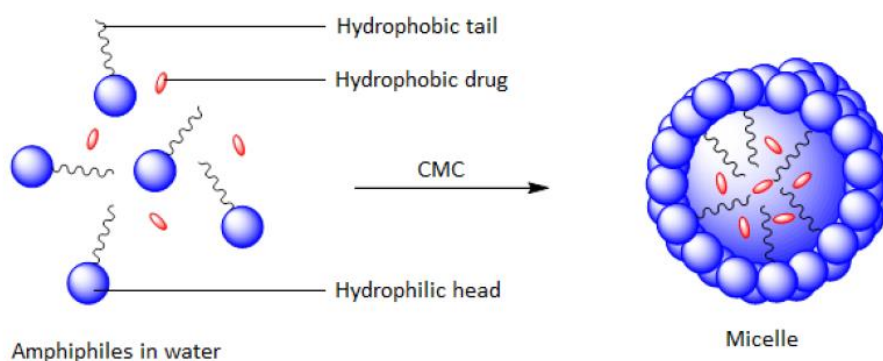


Figure 1.14 Structure of Polymeric Micelle.

Carbon nanotubes are graphite sheets rolled into cylinders with a hexagonal latticework. Anticancer drugs DOX and PTX have been successfully encapsulated in PEG-carbon nanotubes (Niu *et al.*, 2013)

Dendrimers are highly branched nanoscale molecules. They are the new class of polymeric molecules characterized by an extensively branched 3D structure composed of a central core, an interior dendritic structure and an exterior surface with functional groups. The core of dendrimers is suitable for

encapsulation of anticancer drugs while modifications to the surface groups affect solubility and chelating ability of dendrimers. Dendrimers have been used as delivery vehicles for Dox and PTX (Lai *et al.*, 2007).

1.10.3. Targeting Strategies for effective drug delivery

For effective delivery of chemotherapeutic drugs by nanocarriers, the drugs should be able to reach the desired tumour sites at optimal doses after administration, remain biologically active with minimal loss during blood circulation and exhibit selective killing of tumour tissues with minimal harmful effects to normal tissues (Sinha *et al.*, 2006). Two targeting strategies namely passive and active drug targeting are involved. The compromised lymphatic drainage system of tumour cells together with the 'leaky' vasculature of tumour vessels results in the enhanced permeability and retention (EPR) effects enabling macromolecules as low as 400nm to migrate into surrounding tumour tissues. The passive targeting takes advantage of the pathophysiological characteristics of tumour vessels (Smith *et al.*, 2008). However, not all tumours exhibit this EPR effect and different tumours cells have varying vessel permeability so the active targeting approach which involves the conjugation of ligands such as antibodies, peptides or small molecules to the surface of the nanodrug may overcome these limitations (Leamon and Reddy, 2004; Wu *et al.*, 2010). The conjugated nanodrug can then bind through ligand-receptor interactions to receptors or epitopes overexpressed on tumour cells but not on normal cells enabling accumulation of the nanodrugs inside the tumour cells. pH-sensitive delivery systems are stimulus responsive carriers that respond to pH changes in the body. The pH of solid tumour cells is acidic (4-6) unlike

blood pH which is alkaline 7.4. This pathophysiology of tumours serves as a trigger for delivery of pH sensitive nanocarriers (Rofstad *et al.*, 2006).

1.10.4. Nanoencapsulation, a solution for chemotherapy delivery

The efficacy of most chemotherapeutic agents in clinics are hindered by barriers such as severe adverse effects due to nonspecific killing of both cancerous and normal cells, poor solubility, macrophage uptake and the multidrug resistance. Nanocarriers can improve the solubility of hydrophobic anticancer drug enhancing their efficacy. Macrophages detect, capture and digest foreign materials circulating in the blood and transfer them to the liver, polyethylene glycol nanocarriers enables anticancer drug to escape phagocytosis by macrophages increasing cellular uptake and prevents liver damage (van Vlerken *et al.*, 2007).

1.11. Aim of the research

The goal of this study was to develop and examine a novel drug delivery system for treatment of drug-resistant breast cancer cells with disulfiram. This project was designed to achieve the following aims.

1. To examine the roles of hypoxia and hypoxia-induced transcription factors in stemness and chemoresistance of triple negative breast cancer cell lines. (Chapters 3, 4 and 5).
2. To characterise the resistant *in vitro* cell systems for similarity to breast cancer cells (Chapter 6).
3. To develop a disulfiram loaded polymeric micelle nanoparticle and examine its *in vitro* efficacy in the resistant cell systems (Chapter 7).

Chapter Two

2.0. Material and Methods

2.1. Materials

2.1.1. General reagents, enzymes, kits, lab wares and equipment.

Enhanced Chemiluminescence Western Blot Signal Detection Kit (Amersham Biosciences, Buckinghamshire, UK).

BD FACSCalibur™ Flow Cytometer, CellQuest™ Pro (BD Biosciences, Oxford, UK).

Stuart® 3 block heater (Bibby Scientific Ltd., Straffordshire, UK).

EZ-ECL chemiluminescence detection kit for horse radish peroxidase Solution A and B (Biological Industries Beit Haemek Ltd., Isreal).

Bio-Rad protein assay kit II (Bio-Rad Laboratories, Hertfordshire, UK)

Dulbecco's Modified Eagle Medium (DMEM) with 4.5 g/L glucose, Foetal Calf Serum (FCS), L-Glutamate (200 mM) (BioWhittaker® Lonza, Walkersville, USA).

Penicillin-streptomycin mixture (10,000U/ml penicillin and 10,000U/ml Streptomycin) (BioWhittaker® Lonza, Walkersville, USA).

Sterile Phosphate Buffer Saline (PBS) (0.0067M PO₄) (BioWhittaker® Lonza, Walkersville, USA).

Trypsin-EDTA (10x) (BioWhittaker® Lonza, Walkersville, USA).

Microscope slide (ERIE SCIENTIFIC Company Portsmouth.N.H., USA).

Fuji Medical X-Ray Film Super RX (13x18) (Fujifilm UK Ltd., Bedfordshire, UK).

Amersham Hybond TM - P (PVDF membrane), Amersham Hybond TM - N+ (GE Healthcare, Buckinghamshire, UK).

30% acrylamide:bis-acrylamide (37.5:1) (GeneFlow Ltd, Staffordshire, UK)

10× Transfer buffer (GeneFlow Ltd, Staffordshire, UK).

10× Electrophoresis buffer (GeneFlow Ltd, Staffordshire, UK).

Semi-dry transfer unit (Hoefer, Inc., Holliston, USA).

NuPAGE [®] LDS Sample Buffer (4x), SeeBlue plus 2 pre-stained protein markers (Invitrogen Ltd., Paisley, UK).

10×TAE buffer, G418, Trizol, Optimem, Hygromycin B, Lipofectamine transfection reagent (Invitrogen Ltd., Paisley, UK).

Nalgene CryowareTM Cryogenic vials (Labware, Roskilde, Denmark).

Marvel dried milk (Marvel, Dublin, Ireland).

10, 25, 50 and 100 ml tubes (Merck Sharp & Dohme (MDS) Ltd., Hertfordshire, UK).

AccuGel 40% (19:1 acrylamide:bis), Running buffer (10X, contains distilled H₂O, Tris/Glycine/SDS) (National Diagnostics, Yorkshire, UK).

BamH I and Hind III enzymes and associated buffers (New England Biolabs, Hitchin, UK).

Restriction enzymes and associated buffers, pfu polymerase, Luciferase assay kit, Gel shifting assay kit, 1Kb DNA ladder, 100Kb DNA ladder, Dual Luciferase Assay reagents, Access RT-PCR system (Promega UK Ltd., Southampton, UK).

Qiaquick gel extraction kit, Qiafilter maxiprep kit, Qiafilter miniprep kit (Qiagen, West Sussex, UK).

RNase A (100 mg/ml) (Qiagen Ltd., West Sussex, UK).

Complete EDTA free protease inhibitor tablets, Rapid Ligation kit (Roche Diagnostics Ltd., East Sussex, UK).

Complete easy packs-Protease inhibitor cocktail tablets (Roche Diagnostics Ltd., West Sussex, UK)

96-well flat-bottom tissue culture plates with lids, Tissue culture Cell+ flasks with PE flat-bottom tissue culture plates with lids, Tissue culture Cell+ flasks with PE (Sarstedt Ltd., Leicester, UK).

Disulfiram, Copper Chloride (CuCl_2), minisapt plus (0.20 μm) filter, cisplatin (CDDP), paclitaxel (PTX) , doxorubicin (Dox) , gemcitabine (dFdC), 99.9% Dimethylsulfoxide (DMSO), Tris HCl, Tris Base, Tween 20, EDTA, Ammonium persulfate (APS), Sodium Dodecyl Sulfate (SDS, 98.5% GC grade), Methanol, Isopropanol, Glycine, HEPES, Sodium Chloride (NaCl), Thymidine, KH_2PO_4 , Sodium hydroxide (NaOH), Nonident p40, Ethidium Bromide, LB broth, polydIdC (PdIdC), Triton X-100, Agarose, 3MM paper, Propidium iodide (powder), Tetramethylethylenediamine (TEMED), fixer/replenisher,

developer/replenisher, DL-dithiothreitol (DTT) solution (1 M in H₂O) (Sigma Aldrich Company Ltd., Dorset, UK).

ϵ -caprolactone (CL) and methoxy-poly(ethylene glycol) (mPEG-OH, Mn=2000 g/mol) were purchased from Sigma-Aldrich Co. (Steinheim, Germany) and used as received. Chrysin(CHR) was purchased from Aladdin Co. (Aladdin, China) and used as received. Methylbenzenesulfonyl (TsCl) and triethylamine (TEA) were purchased from Asta Tech Pharmaceutical (Chengdu, China).

Multiskan Ascent and Multidrop 384 (Thermo Fisher Scientific Inc., Leicestershire, UK).

2.1.2. Antibodies

p-p65 (S276) antibody (ab106129, Abcam, Cambridge, UK) .

Sox2 (3578), Oct4 (2890) and Nanog (3580)(Cell Signalling, Herts, UK).

Enhanced ChemiLuminescence (ECL) TM anti-mouse antibody (RPN2232), ECL TM anti-rabbit antibody (RPN2232) (GE Healthcare, Buckinghamshire, UK).

HIF1 α (NB100-479) and HIF2 α antibody (NB100-122) (Novus Biologicals, CO, USA).

Anti-vinculin monoclonal antibody (V9130), Anti-tubulin monoclonal antibody (T9026), FITC-conjugated anti-mouse IgG antibody (Sigma Aldrich Company Ltd., Dorset, UK).

2.1.3. Cell lines

Human breast cancer cell lines: MDA-MB-231, MCF7, T47D, and BT 549.

Human normal breast epithelial cell line: MCF10A (American Tissue Culture Collection, Rockville, USA).

The normal human vascular endothelial cells, HeCV (Prof Wenguo Jiang, University of Cardiff, UK).

Human endothelial cell line: EAhy926 (Prof. Angel Armesilla, University of Wolverhampton, UK).

NF κ B p65 transfected (C1, C6) and mock transfected MDA-MB 231 triple negative breast cancer cell line (Prof. Weiguang Wang, University of Wolverhampton, UK).

HIF 1 α transfected (C3, C4) and mock transfected MDA-MB 231 triple negative breast cancer cell line (Prof. Weiguang Wang, University of Wolverhampton, UK).

HIF 2 α transfected (C4, C6) and mock transfected MDA-MB 231 triple negative breast cancer cell line (Prof. Weiguang Wang, University of Wolverhampton, UK).

Resistant cell lines (MDA-MB 231Gem 100nM and T47Ddox 100nM) (Prof. Weiguang Wang, University of Wolverhampton, UK).

2.1.4. Buffers

Complete protease inhibitor

A (25x) complete protease inhibitor (Roche Diagnostics Limited, West Sussex, UK) was prepared by dissolving 1 tablet of complete protease inhibitor in 25 ml of distilled water, and stored at -20°C until use.

Glycine Buffer

Glycine buffer solution (500 ml) was prepared by dissolving 3.75 g glycine and 2.92 g NaCl in distilled water. The pH of the glycine buffer was adjusted to pH 10.5 using 5 M NaOH. The glycine buffer solution was stored at room temperature until use.

RIPA Buffer for Whole Protein Extraction

10x RIPA Buffer was prepared as follows stored at -20°C until use.

Tris HCL 25 g/l

Sodium dodecyl sulphate 0.1% per ml

Triton-X 100 1%

NaCl 0.15 M

EDTA 1 mM

Protease inhibitor 0.001% per ml

Buffer A for Nuclear Protein Extraction

Lysis buffer (buffer A) was prepared by mixing 200 µl 500 mM HEPES, 50 µl 2 M KCl, 2 µl 500 mM EGTA (pH 8.0), 2 µl 500 mM EDTA (pH 8.0), 20 µl 0.5 M DTT, and 500 µl (25X) protease inhibitor in 9.2 ml water. Buffer A was stored at -20°C until use.

Buffer C for Nuclear Protein Extraction

Nuclear extraction buffer (Buffer C) was prepared by mixing 60 µl 500 mM HEPES, 120 µl 5M NaCl, 3 µl 500 mM EGTA, 3 µl 500 mM EDTA, 3 µl 0.5 M DTT, 75 µl (25X) protease inhibitor, and 75 µl 100% glycerol in 1161 µl water, and stored at -20°C.

Separating buffer

Separating buffer was prepared by mixing 90.8 g Tris base and 2g SDS in 500 ml of distilled water. The pH of the solution was then adjusted to pH 8.8 using HCl. The separating buffer was stored at room temperature until use.

Stacking buffer

Stacking buffer was prepared by mixing 30 g Tris base and 2 g SDS in 500 ml of distilled water. The pH of the solution was then adjusted to pH 6.8 using HCl. The stacking buffer was stored at room temperature until use.

Tris-buffered saline Tween-20 (TBS-T)

A stock (10x) TBS-T solution was prepared by dissolving 12.11 g Tris base and 81.8 g NaCl in 1 litre of distilled water. The (1x) TBS-T buffer was then prepared by mixing 100 ml (10x) TBS-T, 900 ml distilled water and 500 µl of Tween-20.

Blocking buffer

Blocking buffer was prepared by dissolving 5 g Marvel milk powder in 100 ml of (1x) TBS-T.

Transfer Buffer

Transfer buffer was prepared by mixing 100 ml of 10 x stock solution, 200 ml of methanol and 700 ml distilled water. This solution was stored at room temperature until use.

Running buffer

Running buffer was prepared by mixing 100 ml of 10X stock solution with 900 ml distilled water.

2.2. Methods

2.2.1. Cell culture

Serum-containing medium

Serum-containing medium consists of DMEM medium containing 1% (v/v) L-glutamate, 1% (v/v) penicillin-streptomycin and 10% Foetal Calf Serum (BioWhittaker® Lonza, Walkersville, USA).

Serum-free medium

Serum-free medium consists of DMEM medium containing 1% (v/v) L-glutamate, 1% (v/v) penicillin-streptomycin (BioWhittaker® Lonza, Walkersville, USA).

Trypsin

Working solution of trypsin (1x) was prepared by diluting stock solution of trypsin (10x) in sterile PBS (BioWhittaker® Lonza, Walkersville, USA).

Freezing Medium for cryogenic storage of cell samples

Freezing medium was prepared by mixing 90% foetal calf serum with 10% DMSO (Sigma Aldrich Company Ltd., Dorset, UK), and stored at 4°C until use.

Preparing Cell Lines for Liquid Nitrogen Storage

Cells were trypsinised, spun for 3 minutes at 1200rpm and the cell pellet collected. The cell pellet was then re-suspended in freezing medium and aliquot into 1 ml/labelled-cryovial. Each cryovial was then wrapped in tissue paper, put into a disposable labelled-glove and placed at -80°C overnight. The following day, the cryovials were removed from the gloves and tissue papers, and transferred into liquid nitrogen (-180°C) for long-term storage. The locations of the samples stored in liquid nitrogen are recorded in the liquid nitrogen storage log.

Recovering Cell Lines from Liquid Nitrogen Storage

A 75 cm² tissue culture flask (Sarstedt Ltd., Leicester, UK) was prepared by adding 19 ml of serum-containing medium. Cells were recovered from liquid nitrogen storage, rapidly defrosted at 37°C water bath, and transferring the 1 ml content of the cryovial into the prepared 75 cm² tissue culture flask. The recovered sample was stored in an incubator, in 37°C with 5% CO₂.

Trypsinization of Adherent Cell Lines

Cell culture medium was removed from the tissue culture flask, rinsed with 5 ml of sterile phosphate buffered saline (PBS), and 3 ml of trypsin added to the adherent cells and spread evenly. The flask was placed in the incubator and checked regularly, under the microscope and by gentle tapping of the flask, to determine that the cells were no longer adhered to the tissue flask. When the cells were no longer adhered to the tissue flask, 3ml of serum-containing medium were added to the cell and were re-suspended thoroughly by pipetting the 6ml volume up and down.

2.2.1.1. General Cell Line Maintenance

Cell cultures were regularly checked under the microscope (2-3 times a week) for cell density defined as percentage confluence, and changes in the colour of the medium. When there is a change in the colour of the medium but the cell density is low (less than 60% confluence) in which adhered cells are spread out and very few cells are touching each other, the medium is removed and replaced with fresh serum-containing medium. When there was a change in the colour of the medium and the cell density is high (greater than 80% confluence), and cells were overgrown leading to some cells no longer being adhered to the tissue culture flask and were in suspension, cells are sub-cultured. Sub-culturing was done by trypsinizing the cells. The 4 ml of cells were collected into a 15 ml falcon tube. In the case when cells were not needed, half of the cells (2 ml) were disposed of. In the case when cells were needed, the cells were centrifuged at 1200rpm for 3 minutes. The medium was removed and cell pellet was re-suspended in 2 ml of fresh serum-containing medium. Two 75 cm² tissue culture flasks were then prepared by adding 19 ml of serum-containing medium, and to this 1 ml of the cell suspension was then added. The cells were stored in an incubator at 37°C with 5% CO₂ with the tissue culture flask lying down.

2.2.1.2. Culturing cells under hypoxic conditions

Monolayer breast cancer cell lines MDA-MB 231 and BT 549 were grown under hypoxic conditions using STEMCELL Technologies Hypoxia incubator chamber gassed with mixture of 1%O₂, 5%CO₂ and remaining N₂ from a

custom made BOC gas cylinder. Cells were seeded in T75 flasks and placed into the chamber and sealed after purging O₂ into the chamber with the above mentioned low O₂ gas for 4 minutes. Cultured cells were placed in an incubator and grown for 5 days before any experiment was done with the cells. The cells were fed with fresh media every 2-3 days to make sure the residual O₂ in the media did not affect the experiment, the media in the flask was gassed before closing and then placed in the chamber to continue hypoxic conditions. An O₂ meter was also placed inside the chamber to monitor any leaks or increase in O₂ levels during the process.

2.2.1.3. Cell culture of resistant cell lines

The MDA-MB 231_{GEM100nM} and T47D_{Dox100nM} resistant cell lines were generated by from MDA-MB-231 and T47D (purchased from ATCC) by continuous culturing in medium containing gemcitabine (dFdC) and doxorubicin (Dox) respectively (Sigma, Dorset, UK) in a stepwise concentration-increasing procedure. The cell lines MDA-MB-231 and T47D were cultured with low concentration of drugs dFdC (20nM) and Dox (20nM) for 4 weeks and increased gradually to 50nM in time interval of 8 weeks, after which they were maintained in DMEM medium supplemented with 10% FCS, 50 µg/ml penicillin, and 50 µg/ml streptomycin containing 100nM dFdC for MDA-MB 231 cell line and 100nM Dox for T47D cell line.

2.3. Cytotoxicity assay

Stock MTT solution 5 mg/ml MTT solution (500 ml) (Sigma Aldrich Company Ltd., Dorset, UK) was prepared by adding 2.5 g of 3-(4,5-Dimethylthiazol-2-yl)-2,5-diphenyltetrazolium bromide in 500 ml of sterile PBS, mixed to dissolve

using a magnetic stirrer, with the bottle wrapped in foil to protect the 3-(4, 5-Dimethylthiazol-2-yl)-2, 5-diphenyltetrazolium bromide (MTT) from direct light. This MTT mixture was filtered using a vacuum filter connected to a pump. This filtered MTT solution, wrapped in foil, was stored at 4°C until use.

MTT assay is one of the widely used methods to evaluate the effect of anti-cancer drugs on cell viability. Cells were cultured in 96-well plates (5×10^4 /well) and left overnight to allow the cells attached to the bottom in the incubator at 37°C. Cells were exposed to different concentrations of anti-cancer drug prepared by a two-fold serial dilution using medium i.e. 10 µM, 5 µM, 2.5 µM, 1.25 µM, 0.625 µM, 0.3125 µM. There was also a negative control of cells which was untreated. After removing the spent media from the wells, the medium (200 µl) with different concentrations of drug was distributed in each well. Normally there are 3 wells with the same drug concentration and cell type in each plate at the same time to calculate the standard deviation. After incubation at 37°C for 72 hours, 50 µl of MTT (5 mg/ml) was added to the wells and the plates were wrapped in the aluminium foil to prevent the deterioration of MTT by light. The solution was removed after incubation for 4 hours at 37°C, and 80 µl of 99.9% DMSO and 20 µl glycine buffer were added. The readings were tabulated and half maximal inhibitory concentration (IC_{50}) values which indicates how much of the anticancer drug is needed to inhibit cell growth expressed as cell viability of the cell lines was calculated from the graph after reading the plates by a spectrophotometer at a wavelength of 540 nm.

Cells treated with PTX, VCR, DOX were exposed for 3 days while cells treated with CDDP and dFdC were exposed for 5 days.

2.3.1. Time dependent Cytotoxicity of DDC-Cu and DS plus Cu (DS/Cu)

MCF 7 breast cancer were cultured overnight in flat bottomed 96 well plates at a cell density of 5000 cells/well in triplicates and were exposed to equal molar ratio of DS (Sigma, Dorset UK) in DMSO and CuCl₂ in H₂O (DS/Cu) or DDC-Cu (TCI, Merseyside UK) in DMSO. The cells were treated for 72 hours and subjected to *in vitro* MTT analysis. The percentage cell viability at different concentrations was calculated and the corresponding IC₅₀ values were calculated.

To determine the time-dependent cytotoxicity of DS/Cu reaction and DDC-Cu. MCF 7 breast cancer cells were plated on 96-wellplates and exposed to DDC-Cu or DS/Cu (1:1 molar ratio). After 30 minutes, 60minutes, 180minutes, 360 minutes, 12 hours and 24 hours drug exposure, the drug-containing medium was discarded and the cells were cultured for another 72 hours in drug-free medium and then subjected to MTT assay.

2.4. Western Blot

10% Ammonium Persulphate (APS)

10% Ammonium Persulfate (APS) (Sigma Aldrich Company Ltd., Dorset, UK) was prepared by dissolving 0.1 g APS in 1 ml of distilled water. This was prepared fresh before use.

Preparation of Separating Gel

Separating gel was prepared by adding 5.5 ml of separating buffer to 6.5 ml of distilled water. To this mixture, 4.4 ml of 40% (19:1) acrylamide:bis (AccuGel) (Sigma Aldrich Company Ltd., Dorset, UK) was added, followed by 120 µl of 10% APS and 15 µl Tetramethylethylenediamine (TEMED) (Sigma Aldrich Company Ltd., Dorset, UK). 4 ml of this separating gel solution was added to the glass gel rack. A small amount of isopropanol, just enough to cover the top of the separating gel solution, was added on top of the separating gel. The gel was left to set.

Preparation of Stacking Gel

Stacking gel was prepared by adding 4.2 ml of stacking buffer to 6.6 ml of distilled water. To this mixture, 1.2 ml of AccuGel was added. The isopropanol (Sigma Aldrich Company Ltd., Dorset, UK) from the separating gel was removed and rinsed with distilled water when the gel was set. To the stacking gel mix, 250 µl of 10% APS and 20 µl TEMED was added. The final stacking gel mix was added on top of the separating gel. A comb was immediately placed on the top layer of the stacking gel, to form the protein loading wells, while avoiding bubbles. The gel was left to set before removing the comb.

Cytoplasmic and Nuclear Protein Extraction

Nuclear protein extracts were prepared by washing the cells in PBS, suspended in lysis buffer A and left on ice for 15 minutes, to which, 5 µl 10%

NP-40 (Sigma Aldrich Company Ltd., Dorset, UK) was added and then centrifuged for 5 minutes at 800 g. The supernatant was collected (cytoplasmic protein) and the pellet was re-suspended in 500 µl lysis buffer A, centrifuged for 5 minutes at 800 g, and the supernatant removed. The pellet was re-suspended in 100 µl of nuclear extraction buffer C, left to spin on a rotator at 4°C for 1 hour, centrifuged for 5 minutes at 12,000 g and the supernatant collected (nuclear protein).

Protein samples were diluted to a 1:10 or 1:5 ratio in distilled water depending on the size of the cell pellet when preparing the protein sample. 5 µl of the BSA standards (duplicates) and the diluted protein samples were pipetted into a 96-well flat-bottomed plate, in triplicates, to which 25 µl of reagent A/S was added. 200 µl of reagent B was then added, incubated at room temperature for 10 minutes and the absorbance read at 650 nm. The protein concentration of the samples was calculated from plotting the absorbance versus protein concentration of the Bovine serum albumin serial standard.

Protein Concentration Measurement

A BSA protein serial standard was prepared by serially diluting the 3.0 mg/ml BSA solution in RIPA buffer to the following concentrations: 3.0 mg/ml, 1.5 mg/ml, 1.0 mg/ml, 0.75 mg/ml, 0.50 mg/ml, 0.25 mg/ml and 0 mg/ml (30 µl RIPA buffer). The BioRad reagent A/S was prepared by adding 20 µl of reagent S to every ml of reagent A and mixed by vortex.

SDS-PAGE Electrophoresis

The prepared SDS-PAGE gels were assembled into the electrophoresis tank loaded with 1 x running buffer. The protein samples were prepared by mixing 0.5 ml of 16 μ l of loading buffer (4x), 1 μ l of 1 M DTT, 50 μ g of protein sample and distilled water to make up a final volume of 64 μ l in an eppendorf tube. This mixture was heated using a PCR block heater at 90°C for 10 minutes, then centrifuged at 10,000 g for 30 seconds and stored on ice until use. 10 μ l of pre-stained protein markers and 30 μ l of each protein mixture were loaded into the loading wells using a pipette. The gel was ran at 200 amperes of current for 1 hour.

Blotting

3MM paper (Sigma Aldrich Company Ltd., Dorset, UK) was cut into 12 x 12 cm size and wet with transfer buffer. PVDF membrane was cut into 7 x 9 cm size and wet with methanol. A semi-dry transferring unit was setup by placing the SDS-PAGE gel (Sigma Aldrich Company Ltd., Dorset, UK) on top of the PVDF membrane, which is sandwiched by 2 layers of 3 x 3 MM paper. Protein was transferred from the SDS-PAGE gel to the PVDF membrane by applying current for 1 hour and 20 minutes.

Blocking of the membrane

The TBS-T(1x) working solution supplemented with 5% fat-free milk was used to block the protein-containing PVDF membrane (Sigma Aldrich Company Ltd., Dorset, UK) for 1 hour along with agitation in order to prevent non-specific binding of primary and secondary antibodies.

Antibody Staining

5 ml of primary antibody (Table 2.1, for catalogue numbers refer to page 63) was prepared as described in the blocking buffer. After shaking the PVDF membrane in the blocking buffer for at least 1 hour, the membrane was placed in a plastic bag with the primary antibody, sealed, and left overnight at 4°C on a shaker. On the following day, the PVDF membrane was washed twice with TBS-T (1x) for 10 minutes. The PVDF membrane was then soaked in the secondary antibody at room temperature for at least 1 hour on a shaker. The PVDF membrane was washed twice with TBS-T (1x) for 10 minutes.

Table 2.1 Primary Antibodies

Target Molecule	Dilution	Source
p-p65 (S276)	1:1000	Abcam, Cambridge, UK
Sox2	1:1000	Cell Signalling, Herts, UK
Oct4	1:1000	Cell Signalling, Herts, UK
Nanog	1:1000	Cell Signalling, Herts, UK
HIF2 α	1:1000	Novus Biologicals, CO, USA
HIF1 α	1:1000	Novus Biologicals, CO, USA
p65	1:1000	Santa Cruz, Heidelberg, Germany
Nucleolin	1:1000	Santa Cruz, Heidelberg, Germany
I κ B α	1:1000	Santa Cruz, Heidelberg, Germany
Tubulin	1:8000	Sigma Aldrich, Dorset, UK

Signal detection

In the dark room, 2 ml prepared EZ-ECL solution (Thermo Fisher Scientific Inc., Leicestershire, UK) which was a mixture of solution A and solution B at a 1:1 ratio was added to PVDF membrane. The PVDF membrane in the A/B mixture solution was left for 3-5 minute and the excess solution was removed by pouring onto a tissue paper. The PVDF membrane was then wrapped in cling film and exposed to a Fuji film. The length of exposure depends on the strength of the signal.

2.5. Flow Cytometry

Preparation of Ethanol

70% ethanol (Thermo Fisher Scientific Inc., Leicestershire, UK) was prepared by diluting in PBS from ethanol stock solution to improve the storage ability of ethanol.

After 72 hours incubation of cell cultures with the appropriate test drugs, the supernatant containing cells in suspension was collected into a 25 ml tube. In addition, adhered cells were trypsinised and also collected into the same 25 ml tube. The cells were pelleted by centrifugation at 800 g for 5 minutes. The supernatant was removed and the cells washed twice with 5 ml of sterile PBS. The final cell pellet was re-suspended in 0.5 ml of sterile PBS. Using a vortex mixing the 0.5 ml cell suspension, 2 ml of 70% ethanol was slowly added and left for 10 minutes. After 10 minutes have passed, the cell was pelleted by centrifugation at 800 g for 5 minutes, the ethanol was removed and the cell pellet re-suspended in 1 ml of sterile PBS. To this cell suspension, 1 µl of 100 mg/ml RNaseA was added followed by 50 µl of 1 mg/ml propidium iodide and incubation for 30 minutes at room temperature wrapped in foil. Samples were stored at 4°C until they were analysed by flow cytometry.

2.5.1. Stem cell marker determination

The ALDH positive population in breast cancer cell lines were detected by ALDEFLUOR kit (StemCell Tech., Durham, NC, USA) following the supplier's instruction. The cells (2.5×10^5) were analyzed after being stained in ALDH substrate containing assay buffer for 30 min at 37°C. The negative control was

treated with diethylaminobenzaldehyde (DEAB), a specific ALDH inhibitor. For CD133 detection cells were incubated with PE 133 antibody (BD Pharmingen, Oxford, UK) for 20 minutes at 4°C. Unbound antibodies were washed off with PBS (Sigma). For the determination of embryonic markers Sox2, Oct4 and Nanog, after trypsinization the cells fixed by acetone/methanol and permeabilized by 0.1% triton-X100 and then blocked with 3% BSA for 1 hour the cells were stained with primary (1:50 dilution) and FITC-conjugated secondary antibodies respectively for 1 hour at RT. The positively stained population was detected using a FACS Calibur flow.

2.5.2. Detection of hypoxia in hypoxic cell cultures

The hypoxic status of cells grown in hypoxic conditions was determined using HypoxyprobeTM-1 plus Kit supplied by Hypoxyprobe Inc (Burlington, MA, USA) following the supplier's instruction. Flow cytometry was used for the analysis; the cells were cultured in 25cm² flasks in both normoxia (NOR) and hypoxia (HYP), after treatment with HP reagent they were trypsinized, counted, fixed with methanol and stained with the FITC anti-HP antibody. The hypoxic population was detected using a FACS Calibur flow cytometer with 488 nm blue laser and standard FITC 530/30 nm bandpass filter.

2.6. Electrophoretic mobility shift assay (EMSA)

Gel preparation

10 x TAE-10 ml of 50 x TAE + 40 ml of dH₂O (Invitrogen Ltd., Paisley, UK)

30% polyacrylamide Protogel, TEMED 10% Ammonium persulfate (APS)-1 g of APS + 1 ml of dH₂O (10% APS) (Thermo Fisher Scientific Inc., Leicestershire, UK).

Sample preparation

10 x Binding Buffer, 1 µg/µl Poly (dl-dC), 50% Glycerol, Biotin End-Labelled Target DNA, 5 x Loading Buffer (Thermo Fisher Scientific Inc., Leicestershire, UK).

Probes Preparation

Wild Type (WT) Unlabelled Target DNA (sense and anti-sense probes) 40 µm. Mutant (MUT) Unlabelled Target DNA (sense and anti-sense probes) 40 µm. The probes were heated at 100°C for 10 minutes and were cooled down to room temperature.

Samples Preparation

10 x Binding Buffer, 1 µg/µl Poly (dl-dC), 50% Glycerol, wild type (WT) unlabeled target DNA, mutant unlabeled target DNA, and Biotin End-Labelled target DNA were thawed on ice. Nuclear proteins from samples were added to biotin-labeled oligonucleotide binding buffer consisting of 10 mM Tris at pH 7.5, 50 mM KCl, 1 mM DTT, 2.5% glycerol, 5 mM MgCl₂, and 50 ng of poly (dl-dC). The samples incubated on ice for 15 minutes and then 10 minutes at room temperature. The other samples were prepared without Biotin End-Labelled Target DNA. 1 µl of Biotin End-Labelled Target DNA of added to all samples and incubated on ice for 15 minutes followed by 10 minutes incubation at room temperature. 5 µl of 5 x Loading Buffer were added into each sample.

Electrophoresis

All samples (23 µl/well) were loaded into their designated wells respectively, and then the gel was run for 45 minutes at 120 voltage on ice.

Blotting

The nylon membranes (Amersham Hybond TM-N+, GE Healthcare, UK) and 3MM papers were soaked in 1 xTAE for a minimum of 5-10 minutes. The probes were transferred from the gel to the nylon membrane using wet or semi-dry units following manufacture protocol at 200 amperes of current for 1 hour.

Cross-link

The membranes were wrapped in cling film and were exposed for 10-15 minutes on a trans-illuminator equipped with a 312 nm bulb (Ingenious Syngene Bio-Imaging).

Blocking

The blocking buffer and the 4 x wash buffer (Thermo Fisher Scientific Inc., Leicestershire, UK) were pre-warmed to 37-50°C to dissolve any precipitation, then the membranes were soaked in blocking buffer for 15 minutes at room temperature on a shaker. At the same time, 30 µl Stabilized Streptavidin-Horseradish Peroxidase Conjugate were added to 10 ml Blocking Buffer. The membranes were soaked in the blocking buffer for 15 minutes at room temperature on a shaker.

Washing

1 x wash solution (40-60 ml) (Thermo Fisher Scientific Inc., Leicestershire, UK) were prepared for washing the membranes for 10 minutes twice in a clean

tray, then the membranes were transferred to a new container adding 10 ml Equilibration Buffer for 5 minutes at room temperature on a shaker.

Signal detection

(Luminol/Enhancer Solution): (Stable Peroxide Solution) (Thermo Fisher Scientific Inc., Leicestershire, UK) were mixed in 1:1 ratio and were evenly spread on the membranes, for 5 minutes. The membranes were exposed to film in the dark room.

2.7. Luciferase reporter gene assay

Cell culture

Different cell lines were harvested by trypsinisation. Plate 5×10^4 /100 μ l of medium/well on to 96 well plates and allowed them to grow overnight at 37°C.

Lipofectamine Transfections

On the following day, the transfection solution I and II were prepared first, then the pGL3-Basic and other luciferase vectors (0.2 μ g of each vector/well) in triplicate and internal control pRL-SV40 (0.002 μ g/well) were co-transfected by using Lipofectamine 2000.

Solution I: 0.2 μ g of each Luciferase reporter plasmid DNA and 0.002 μ g pRL-SV40 (Renilla) DNA was diluted in 25 μ l of opti-MEM medium without serum.

Solution II: 0.5 μ l of lipofectamine 2000 was diluted in 250 μ l of opti-MEM for each DNA samples and incubated at room temperature for 5 minutes.

The equal amount of solution I and solution II were mixed for 20 minutes at room temperature and then were added to the cell culture. The cells were

incubated at 37°C, 5% CO₂ for 24 hours and were fed with fresh medium for further 24 hours incubation prior to luciferase assay test.

Luciferase assay test & analysis

The growth medium was removed after 48 hours, and the wells were washed with 1 x PBS. 100 µl of 1 x lysis buffer was added to each well and incubated at room temperature for 10 minutes with agitation. 20 µl of each lysate sample was transferred into a polypropylene plate to test. 30 µl of Luciferase assay reagent II was added and read in a luminometer. The reading corresponds to firefly luciferase activity. 30 µl Stop & Glo reagent was added and the reading was taken which corresponds to renilla activity. The process was repeated for each sample in a fresh plate each time. The luciferase activity of each well was normalized by the pRL-SV40 Renilla value using the formula: $Ln = L/R$ (Ln : normalised luciferase activity; L : luciferase activity reading and R : Renilla activity reading). Transcriptional activity of the control, pGL3-Basic, was used to further standardize Ln using the formula: $RLU = Ln/pGL3\text{-basic}$ (RLU : relative luciferase unit) (Promega UK Ltd., Southampton, UK).

2.8. Stable transfection

About 0.5-1 million cells/well were cultured in 6 well-plates with 2 ml medium overnight to about 70-80% confluence.

2.8.1 Stable transfection of NFκBp65 subunits

4µg of empty vector cDNA3.1 and recombinant vector with cDNA NFκBp65 were introduced into the cells separately using Lipofectamine™ 2000 reagent. The transfected cells were incubated at 37°C for 24 hours selected for 7-10

days in a selective medium containing hygromycin 150µg/mL. Colonies of cells were picked up, enlarged and screened for over-expression of target gene in comparison with mock transfected clones using western blot. Confirmation of the overexpression of NFκBp65 was done by analysing the nuclear translocation of NFκB using western blot from nuclear extract of transfected cells. At least two positive clones with high nuclear translocation of NFκB were selected for each gene and subjected to further analysis. The mock transfected cells containing empty vector was grown in parallel for all experiments and used as controls for NFκB expression. All cells were grown under the selecting medium containing hygromycin throughout culturing time.

2.8.2 Stable transfection of HIF proteins

MDA-MB 231 cells were cultured (1×10^6 cells/well) in 6 well plates without antibiotics overnight. 4µg of empty vector pcMV6 and recombinant vector with HIF1α and HIF2α were introduced into the cells separately using Lipofectamine™ 2000 reagent. The transfected cells were incubated at 37°C for 24 hours selected for 7-10 days in a selective medium containing G418 150ug/mL for HIF1α culture and 200ug/mL for HIF2α cultured cells. Colonies of cells were picked up, enlarged and screened for over-expression of target gene in comparison with mock transfected clones using western blot. Confirmation for the overexpression of HIF1α and HIF2α was done by analysing the nuclear translocation of HIF1α and HIF2α respectively using western blot from nuclear extract of transfected cells. At least two positive clones with high nuclear translocation of both HIF1α and HIF2α were selected for each gene and subjected to further analysis.

2.9. Migration assay

Scratch or wound healing assay is a popular cheap assay that can be used to study migration of cells. A confluent plate generated from initial seeding of 0.5×10^6 cells in 6 well plates of any type of attached cells control or test is “wounded” by scraping off a thin straight line area of cells using a 200ul plastic pipette tip. Pictures of the scratch area were taken at 0hr, 24hrs and 48 hrs. Cell migration can be monitored microscopically, as cells travel from the undamaged regions into the scratched region. %migration can be calculated by measuring the decrease of the uncovered region at different time points until the “wound” is closed using the image J software. Cell migration can be observed as single cells or loosely connected population (mesenchymal cells) or as sheets of cells (epithelial cells).

2.10. Invasion assay

300 µl of warm, serum-free media was added to the cell culture inserts and incubated at room temperature for 1 hour in order to rehydrate the basement membrane layer of the insert. The media was carefully removed after the incubation period. 300 µl of cell suspension with $0.5-1 \times 10^6$ cells/ml in serum-free media was added to the inside of each insert. 500 µl of media with 10% fetal bovine serum was added to the lower well of the plate. After incubation for 48 hours, media was carefully aspirated from the insert. Using wet cotton-tipped swabs, cells were removed from the interior of the insert. The insert was then dipped in a well containing 400 µl of cell stain solution and incubated for 10 minutes at room temperature. After several gentle washes in a beaker of water, the inserts were allowed to air dry. The inserts were then transferred to

a well with 200 µl of Extraction Solution and incubated for 10 minutes in an orbital shaker. 100 µl from each sample was transferred to a 96-well plate and the optical density was measured at 560nm.

2.11. Growth curves and doubling time analysis

The cells (3×10^3 /well) were cultured in 24-well plates in triplicate. The cells were collected by trypsinization and cell numbers in each of three wells were counted every 24 hours for 148 hours. The cell doubling time was calculated using the program from the Doubling Time Online Calculator <http://www.doubling-time.com/compute.php>.

2.12. Confocal microscopy and image analysis

Cell culture

Cells were harvested by trypsinisation. 5×10^4 cells were plated on a sterile 8-well chamber slide over night at 37°C for immunofluorescence experiment. Dose-dependent drug treatment or time-dependent treatment was conducted on the following day.

Fluorescence labelling of cells

The cells were washed twice with PBS gently to avoid the cells detachment from the surface of the chamber slide, and then the cells were fixed by adding 500 µl of methanol/acetone (Volume Ratio 1:1) for 5 minutes. The fixed cells were washed twice with PBS, then the cells were blocked with 5% BSA for 30 minutes at room temperature to block non-specific binding of immunoglobulin. The cells were incubated with the primary antibodies for 1 hour at room temperature, washed three times with PBS and then labelled with the

secondary antibodies for 1 hour in the dark, then the cells were washed three times in PBS. Coverslips were mounted onto slides using anti-fade mounting medium. Images were captured using laser-scanning microscope (Carl Zeiss Laser Scanning Systems LSM 510).

2.13. RNA extraction

1×10^6 cells were harvested and washed once with cold 1 x PBS, cell pellets were lysed in trizol in 1.5 ml eppendorf for 5 minutes at room temperature. The samples were mixed with chloroform and incubated for 5 minutes at room temperature. After centrifuge the samples at 10,000 g for 5 minutes, the aqueous phase was carefully pipetted off to another 1.5 ml eppendorf. The aqueous phase and 550 μ l of isopropanol were mixed gently for 5 minutes at room temperature, and mixtures were centrifuged again at maximal speed (14,000g) for 20 minutes. The isopropanol was discarded from mixtures and 1 ml of 75% ethanol in diethylpyrocarbonate (DEPC) treated H₂O was added for washing the pellet barely visible at the base of tube. The pellets were re-centrifuged at 8,000 g for 5 minutes and air-dried. Finally, the RNA pellets were dissolved by adding 30-50 μ l (depending on yield) of either DEPC treated TE buffer or water. RNA concentration was determined spectrophotometrically by measuring absorbance at 260 nm (1 absorbance = 40 ng/ml RNA). The 260/280 ratio should be greater than 1.8. If less than 1.5-1.6 or so, the RNA is partially degraded. Lower ratios also suggest DNA or thiocyanate contamination. The concentration is essentially the equivalent of the OD at 260 nm (in μ g/ μ l).

2.14. Reverse transcriptase polymerase chain reaction

In this study, a promega access real time-polymerase chain reaction (RT-PCR) system kit was used to perform the experiment. This system is one step RT-PCR in a single tube in which a reverse transcriptase produces first a strand of cDNA from RNA, then a thermostable DNA polymerase produces a second strand of DNA and amplifies the specific DNA of interest. A ratio of 1:2 oligodT primers: RNA template was used in a volume of 25 µl containing 5 µl of 5 x AMV/Tfl reaction buffer, 1 µl of TAMV-reverse transcriptase, 1 µl of Tfl DNA polymerase, 2 µl of 25 mM MgSO₄, 1 µl of dNTPs (10 mM of ATP, CTP, GTP and GTP) and nuclease free water up to 25 µl. Reverse transcription was performed at 45°C for 45 minutes, following inactivation of AMV RT and denaturation of the RNA/cDNA hybrid by incubation at 94°C for 2 minutes. The human housekeeping gene GAPDH was used as the RNA loading control, which was amplified by the same RT-PCR system. The table 2.2 shows the primers, which was used in RT-PCR in this study. Amplification was performed using standard cycling parameters: 94°C 30 seconds for denaturation, 58°C 1 minute for annealing and 68°C 1 minute for extension. After the final PCR cycle the final extension was at 68°C for 5 minutes and then kept at 4°C until further analysis. The room temperature-polymerase chain reaction products were separated on a 1% agarose gel and the bands visualized and photographed under UV light.

Table 2.2. Primers Target

Primer	Product Size	Forward primer 5' - 3'	Reverse primers 5' -3'
GAPDH	226bp	GAAGGTGAAGGT CGGAGTC	GAAGATGGTGAT GGGATTTTC
ALDH1A1	154bp	TGTTAGCTGATGC CGACTTG	TTCTTAGCCCGCT CAACACT
ALDH1A3	150bp	TCTCGACAAAGC CCTGAAGT	TATTCGGCCAAAG CGTATTC
ALDH2	193bp	AACCAGCAGCCC GAGGTCTT	AAGGTGAGCCCA GCTGGAAG
ALDH3A1	229bp	TGTTCTCCAGCAA CGACAAG	CTGACCTTCAGGC CTTCATC

2.15. Purification of PCR products

Polymerase chain reaction (PCR) products were purified using a StrataPrep® PCR Purification kit. An equal volume of DNA-binding solution was added to the aqueous portion of the PCR products. Transfer PCR product-DNA-binding-solution mixture to a micro-spin cup and spin at 12,000 g for 30 seconds. The PCR products remaining in the fibre matrix of the micro-spin were washed with 1× washing buffer then eluted using 50 µl of elution buffer.

2.16. Molecular Biology Protocols**Preparation of LB plates**

LB medium was prepared by dissolving 25 g LB broth powder and 20 g agar into 1 L of deionized water. This was autoclaved and allowed to cool to 50°C prior to the addition of ampicillin (50 µg/ml) or kanamycin (50 µg/ml). The

medium was mixed to ensure equal distribution of antibiotic and approximately 15 ml poured per 10cm² Petri dish. The plates were left to set at room temperature before being stored at 4°C.

Transformation of competent bacterial cells

Competent bacteria DH5α was purchased from invitrogen and kept at -80°C. An aliquot of 50µl competent bacteria DH5α was allowed to thaw on ice. 10 ng of DNA was added and incubated on ice for 15 minutes. The cells were subjected to a heat shock at for 42°C 90 seconds and returned to ice for 2 minutes. Added 1 ml of SOC medium to the cells and incubated at 37°C for 1 hour in a shaking incubator. One hundred microliters of the reaction was spread onto a LB plate containing the appropriate antibiotic and incubated overnight at 37°C.

Preparation of plasmid DNA

Mini-preps

Mini-prep purification was carried out using Qifilter miniprep kit following the manufactures instructions. Cells were harvested by centrifugation at 12,000 g for 5 minutes and re-suspended by pipetting in 100µl of re-suspension buffer I (50 mM Tris-HCl, 10 mM EDTA, pH 8.0 containing 100 µg/ml RNase A). Cells were treated with 100µl of lysis buffer II (200 mM NaOH, 1% (w/v) SDS), mixed and incubated for 5 minutes with gently up and down. Lysis was terminated by the addition of 100µl of neutralisation buffer III (3 mM potassium acetate, pH 5.5). After centrifuging for 10 minutes at 12,000 g, the supernatants of cell lysates were transferred to mini-prep columns. The columns were centrifuged

for 1 minute at 12,000 g and washed twice with 750 µl wash buffer (1.0 mM NaCl, 50 mM Tris-HCl, pH 7.0, 15% (v/v) isopropanol). After washing, bound DNA was eluted into a clean 1.5 ml eppendorf tube with 100 µl DNase, RNase-free H₂O.

Maxi-preps

The Qiagen Qiafilter kit was used to produce larger scale DNA samples. Purification of DNA was carried out according to the manufactures instructions (Qiagen Ltd., Manchester, UK). A 350 ml culture of transformed bacteria was pelleted by centrifugation for 15 minutes at 6,000 g at 4°C. The cell pellet was re-suspended in 10 ml of pre-cold buffer P1 (50 mM Tris-HCL pH 8.0, 10mM EDTA, 100 µg/µl Rnase A). 10 ml buffer P2 (200 mM NaOH, 1% (w/v) SDS) was added to the cells with gently up and down for incubating 10 minutes at room temperature. Neutralized the reaction by adding 10 ml of buffer P3 (3.0 M potassium acetate pH 5.5) and the solution was immediately applied to a QIAfilter cartridge and left for 10 minutes at room temperature to settle. Meanwhile, a Qiagen tip 500 was equilibrated by the addition of buffer QBT (750 mM NaCl, 50 mM MOPS pH 7.0, 15% (v/v) isopropanol). After 10 minutes, the lysed cells were added onto the equilibrated tip and allowed to filter through. The column was washed with 60 ml of buffer QC (1.0 M NaCl, 50 mM MOPS pH 7.0, 15% (v/v) isopropanol). The DNA was eluted by the addition of 15 ml of buffer QF (1.25 M NaCl, 50 mM Tris-HCl pH 8.5, 15% (v/v) isopropanol) to the tip. After adding 10.5 ml isopropanol, the DNA was precipitated by centrifuging at 12,000 g for 30 minutes at 4°C. The DNA pellet was washed with 5 ml of room temperature 70% (volume ratio) ethanol and

then centrifuged for 15 minutes at 12,000 g at 4°C. The supernatant was carefully removed and the pellet allowed to air dry prior to re-suspension in 0.5-1 ml of DNase, RNase-free H₂O.

Quantification of DNA

DNA measurement was performed by examining the absorbance of a 1:40 dilution of the sample at 260 nm. An optical density of 1 unit was taken to correspond to 50 µg/ml of double stranded DNA. The sample concentration could be determined using the following formula.

Sample concentration = OD 260 x dilution factor (40) x 50 µg/ml

Digestion of DNA with restriction endonucleases

One unit of restriction endonuclease activity was capable of completely digesting 1 µg of DNA depending on the manufacturer. 1 µg of DNA digests were prepared using the appropriate restriction enzyme (1-2 units) with a specified buffer providing by the manufacturer provided in a final volume of 20 µl. Reactions were incubated at 37°C for a minimum of 2 hours.

Agarose gel electrophoresis of DNA

Digested DNA samples or PCR reactions were examined using gel electrophoresis. Samples were diluted in 5 × DNA loading buffer. 1.0% (w/v) agarose gel was prepared by mixing agarose with 1 × TAE and 2.5 mg/ml ethidium bromide. The gels were set in a horizontal gel tank and once set immersed in 1 × TAE. Samples were loaded and the gels run at 100V for 1 hour. The DNA fragments were visualized under ultraviolet light. The size of each fragment was assessed by comparison with DNA molecular markers.

DNA Purification from agarose gels

The required DNA fragments were excised from the gel with a sterile disposable scalpel blade inside the UV transilluminator hood. Excised gel fragments were transferred to a sterile tube. The fragments were purified using the QiaQuick gel extraction according to the manufacturer's instructions. Excised DNA fragments were dissolved in buffer QG followed by the addition of isopropanol at 37°C. The solution was loaded onto a purification column. After centrifugation, DNA was eluted from the purification column using 30 µl of sterile water.

Ligation of DNA

When plasmid DNA and/or PCR fragments had been digested and purified as described above, ligation of digested PCR or DNA fragments to the digested vector DNA was achieved using a Rapid DNA ligation kit. A molar ratio of 1:3 to 1:8 vector, PCR product/DNA fragment was used in a volume of 10 µl containing 1 unit of ligase and the supplied buffer. The reaction was incubated at room temperature for 1 hour or at 4°C overnight.

2.17. Reactive Oxygen Species activity detection

The extracellular ROS levels were determined using Fc OxyBURST dihydro-2', 4, 5, 6, 7, 7'-hexafluorofluorescein (H2HFF) probe (Invitrogen, Paisley, UK). 60 µl of Fc oxyBurst dye was added to 3ml of serum free medium and 100 µl aliquoted into 96 well plate. 20µM of H₂O₂ was prepared in PBS and 100 µl added to 3 wells in the 96 well plate. Equal molar concentration (10 µM or 10 mM) of DS and CuCl₂ was mixed in culture medium. Fluorescence was measured in 96-well plates at excitation 490 nm and emission 520 nm using a

Fluoroskan Ascent UV fluorometer (Thermo Scientific, Northumberland, UK) at different time intervals.

2.18. Determination of metabolic kinetics of DS/Cu and DDC-Cu

MCF7 cells were treated with equal molar ratio of DS and CuCl₂ or DDC-Cu at a final concentration of 2µM. The medium and cells were separately collected after 30, 180 and 360 min. The reaction products in the whole cell lysate and medium were extracted in 0.25 and 1ml chloroform respectively and subjected to HPLC analysis. The separation was achieved using a C18 reverse-phase column at an injection volume of 20µl and a flow rate of 1ml/min. The wave length of 435nm and 275nm, mobile phase of 10:90% and 30:70% (water: methanol, v/v) were used for DDC-Cu and DS analysis respectively.

2.19. Encapsulation of DS in polymeric micelles

Preparation of DS loaded Polymeric micelles Nanoparticles

The DS loaded micelles is formed by solvent evaporation method. A dispersion of 100 mg of F127 micelles was made in 20ml of purified water under magnetic stirring and 50 mg DS dissolved in 20ml of absolute ethanol was slowly added to the aqueous dispersion of micelles. The mixture was kept under magnetic stirring for 24 hours (covered with parafilm). After the 24 hours incubation 20ml of ethanol was evaporated by rotary evaporation (temperature <40°C) and the aqueous dispersion containing the DS loaded micelles was filtered through a 0.20µm filter to eliminate the non-encapsulated DS. Sucrose (5%) was added to the micellar dispersion which was then frozen for subsequent lyophilization.

Empty polymeric micelles were also prepared using similar technique.

2.19.1. Characterization of Disulfiram loaded Polymeric Micelle

The mean particle size and size distribution of the PMDS were determined by dynamic light scattering (DLS) (Brookhaven Instruments Corporation, USA). Zeta potential was measured by the Laser Doppler Anemometry (LDA) on ZetaPlus Zeta Potential Analyzer (Brookhaven Instruments Corporation, USA). Samples were dispersed in distilled water and the lyophilized DS-micelles were reconstituted in water, and were analyzed for size by DLS, for drug loading by spectrophotometry. All measurements were performed at 25 °C. Experimental values were calculated from the measurements performed at least in triplicate.

2.19.2. Measurement of encapsulation efficiency (EE) and drug loading content (DLC) of DS loaded PM

The content of encapsulated DS was determined by HPLC Agilent 1260 in methanol using calibration curve obtained from DS/methanol solutions with different DS concentrations. C₁₈ column (250 mm×4.6 mm, 5 µm) was used with a mobile phase of methanol-water (70:30) and the flow rate was 1.0 mL/min. The detection wavelength was 275nm and column temperature was 25°C. Drug loading content (DLC) and drug loading efficiency (DLE) were calculated according to the following formulae:

$$\text{DLC}(\text{wt}\%) = \frac{\text{mass of DS in micelles}}{\text{mass of DS loaded micelles}} \times 100\%$$

$$\text{DLE}(\text{wt}\%) = \frac{\text{mass of DS in micelles}}{\text{mass of DS in feed}} \times 100\%$$

The amount of non-entrapped DS was determined by HPLC by UV detection set at 275 nm (SHIMADZU LC-20). The mobile phase was a mixture of methanol:water (70:30%) and the flow rate was set at 1 ml/min. Separation was achieved using a Phenomenex C18 column (250mm × 4.6 mm, 5µm). The amount of DS entrapped in the nanoparticles was determined after their dissolution in dichloromethane. After evaporation of dichloromethane at room temperature, DS was dissolved in pure ethanol. The supernatants were passed through a membrane filter (pore size 0.22 µm, Millipore) before HPLC measurements.

2.19.3. Measurement of the half-life of DS *in vitro*

Free DS or PM-DS (100 µl at a concentration of 3 mg/ml) was added into an eppendoff tube containing 300 µl of horse serum with shaking at 37°C. The eppendoff tubes were collected and protein precipitated by adding 300 µl of absolute methanol at different time intervals. The supernatant was subjected to HPLC measurement.

2.19.4. Cumulative release of Disulfiram from Polymeric Micelle

In vitro cumulative release of DS for the polymeric micelles were carried out in 0.1 M phosphate buffer solution (PBS) at pH 5 and 7.4 containing 0.5% Tween 80 (w/v) to enhance the solubility of DS, using the dialysis bag diffusion technique. A known amount of disulfiram loaded micelles was dispersed in 4ml phosphate- buffered saline (PBS) containing 0.5% Tween 80 (w/v). The mixture (2ml) was placed in a dialysis bag (MWCO 6000-8000, Sigma-Aldrich). The end-sealed bag was immersed in 50ml PBS (pH 7.4 and 5) containing 0.5% Tween 80 (w/v). Sample were maintained at 37°C and shaken at

100rpm. At appropriate intervals, 2ml of sample was collected from the medium and an equal volume of fresh medium was added to the release medium. The concentration of disulfiram in each sample was measured by ultraviolet- visible spectrophotometry at 275nm. Data obtained in triplicate were analysed graphically (the percent accumulative amount of DS released from micelles versus time plotted).

2.20. Statistical Analysis

All statistics used in analysing the data were conducted using Graphpad Prism (version 6.01; GraphPad Software, Inc) and Microsoft Excel 2010 data analysis tools. The cut-off for statistical significance between samples was set to $p=0.05$. Any statistical tests with $p<0.05$ defines “the results between the samples are statistically different”, $p<0.001$ “the results between the samples are statistically very different”, and $p\geq 0.05$ defines “there are no statistical significance between the samples”. The statistical Mann-Whitney U test: was used to determine the statistical significance between Breast Cancer (BC) cell lines that were tested under the exact same conditions. Two-sample assuming unequal variance’ was used to determine the statistical significance of the same BC cell line that was tested under different conditions. The statistical test “Kruskal-Wallis, Mood’s median test” was used to determine the statistical significance of the same BC cell lines that were tested under different condition.

Chapter Three

Hypoxia induces CSC, chemoresistance and migration/invasion traits in TNBC cell lines.

3.1 Introduction

Triple negative breast cancer (TNBC) is the subtype of breast cancer that does not express genes for oestrogen receptor (ER), progesterone receptor (PR) and human epidermal growth factor receptor 2 (HER2) (Curigliano and Goldhirsch, 2011; Penault-Llorca and Viale, 2012). Scientific advancement in BC research have improved BC management with resultant increase in survival rate, however TNBC is still a difficult cancer to treat because of the lack of targetable receptors and is an assemblage of different breast cancer subtypes.

Stem cell “niche” a specialized microenvironment within tumours maintains the properties of cancer stem cells (CSCs) self-renewal and multipotency (Keith and Simon, 2007; Hill *et al.*, 2009). The cells, blood vessel, matrix glucoproteins and three-dimensional space form the stem cell niche (Scadden, 2006). The stem cell niche contains CSCs and these cells are mostly in a hypoxic state. Reports by Ezashi *et al.*, (2005) showed that the low O₂ tension (1%) in the niche decreased cell proliferation and maintained pluripotency while higher oxygen tension (3-5%) maintained pluripotency of cells but had no effect on their proliferation rate. These results suggest that the hypoxic niche maintains slow-cycling proliferative rate and quiescence in relation to the oxygen tension within tumours. HIF protein activated under hypoxia also regulates signalling pathways that maintain stem cell self-renewal and

multipotency. CD133⁺ CSCs from gliomas were found to overexpresses HIF2 α and other HIF regulated genes compared to non-stem cells or normal neural progenitor cells, inhibition of HIF2 α reduced self-renewal, proliferation and survival *in vivo* with diminished tumour initiation potential of glioma CSCs (Li *et al.*, 2009). This finding was also confirmed by Franovic *et al.* (2009) in which inhibition of HIF2 α in colorectal, non-small cell lung cancer and glioblastoma that harboured CSCs population prevents *in vivo* growth and tumourigenesis irrespective of the mutational status and tissue origin (Franovic *et al.*, 2009).

3.1.2. Hypoxia induced EMT

High invasion and metastasis are the principal factors causing poor prognosis of patients with TNBC. Approximately 90% of cancer related death results from the metastatic spread of primary tumours (Christofori, 2006). Hypoxic response regulated by the HIF protein particularly HIF1 α activation correlates with tumour metastasis by promoting tumour cell metastatic potential. HIF1 α is suggested to mediate the repression of E-cadherin as overexpression of HIF1 α upregulates repression of E-cadherin repressors twist, Snail and SIP1 with associated loss of E-cadherin and overexpression of N-cadherin and Vimentin which promotes epithelial to mesenchymal transition (EMT) and metastatic phenotypes in human cancer cells (Evans *et al.*, 2007).

CSCs are widely accepted to be responsible for multidrug resistance in cancer cell and are believed to be one of the reasons for chemotherapeutic failure and cancer relapse. Previous studies have shown that hypoxia play key role in the induction and maintenance of CSCs traits, chemoresistance and metastasis in cancer cells (Li *et al.*, 2009, Franovic *et al.*, 2009).

3.1.3 Rationale and aims of the study

This study was carried out to confirm if hypoxia is able to induce CSCs traits in triple negative breast cancer (TNBC) cell lines, and to examine the response of these cells to conventional anticancer drugs. Hypoxia induced EMT was also examined to determine the process of cell metastasis.

3.2. Experimental design

General materials, products, labwares, manufacturers and methodologies used for the entire study have been described in details in chapter 2. Specific materials, methods and experimental design used for this part of this study are stated below.

3.2.1. Culturing cells under hypoxic conditions

Monolayer TNBC breast cancer cell lines MDA-MB 231 and BT 549 were grown under hypoxic conditions using STEMCELL Technologies Hypoxia incubator chamber (refer to Chapter 2, page 69).

3.2.2. Detection of hypoxia in hypoxic cell cultures

The hypoxic status of MDA-MB 231 and BT 549 cells grown in hypoxic conditions was determined using HypoxyprobeTM-1 plus Kit (refer to Chapter 2, page 79). Additional confirmation of the hypoxia status was done by western blot analysis of hypoxia-inducible factors (HIFs) (refer to Chapter 2, page 72).

3.2.3. Determination of EMT properties of cells

Hypoxia is believed to induce epithelial to mesenchymal transition (EMT). *In vitro* wound healing assay (scratch assay) for migration and transwell invasion assay (Boyden chamber assay) were performed in hypoxic and normoxic cultures to determine the invasive and migratory properties of the cells (refer to Chapter 2, page 85 and 86).

3.2.4. CSC markers determination in hypoxic cells

Increase in markers such as ALDH⁺, CD 133 and embryonic markers Sox2, Oct4 and Nanog are common feature of CSCs. If hypoxia induces EMT in cells, it was hypothesized that these markers would also be increased. These CSC markers were examined using immunofluorescence protocol for FACS where an increase in fluorescence indicates an increase in the expression of these markers (refer to Chapter 2, page 78).

3.2.5. MTT cytotoxicity assay for hypoxic cell cultures

Chemoresistance is a feature of CSCs and a major problem for chemotherapy. If cells under hypoxia show increase in CSC markers, it was hypothesized that hypoxic cells would show resistance to an ample range of anticancer drugs. To assess the effect of hypoxia on drug sensitivity cells, MTT cytotoxicity assay was performed in hypoxic and normoxic cultures after exposure to various anticancer drugs (refer to Chapter 2, page 70 and 71).

3.3.6. Growth curves and doubling time analysis

To examine the growth profile and proliferative rates of hypoxic cells, growth curve and doubling time analysis was performed on MDA-MB 231 and BT 549 cell lines (refer to Chapter 2, page 86).

3.3. RESULTS

3.3.1. Increase proportion of hypoxic cells in hypoxic culture

Monolayer breast cancer (BC) cells lines grown in hypoxic culture were compared with those grown under normoxia using hypoxyprobe. The results obtained from FACS analysis showed that a substantial number of cells grown in hypoxic culture had an increase in proportion of hypoxic cell (%) compared to those cultured in normoxia (Figure 3.1A and B). Further analysis for the confirmation of hypoxia was done by western blot and the results show an increase and nuclear translocation in HIFs in the hypoxic culture when compared to the normoxia culture of BC cell lines (Figure 3.2).

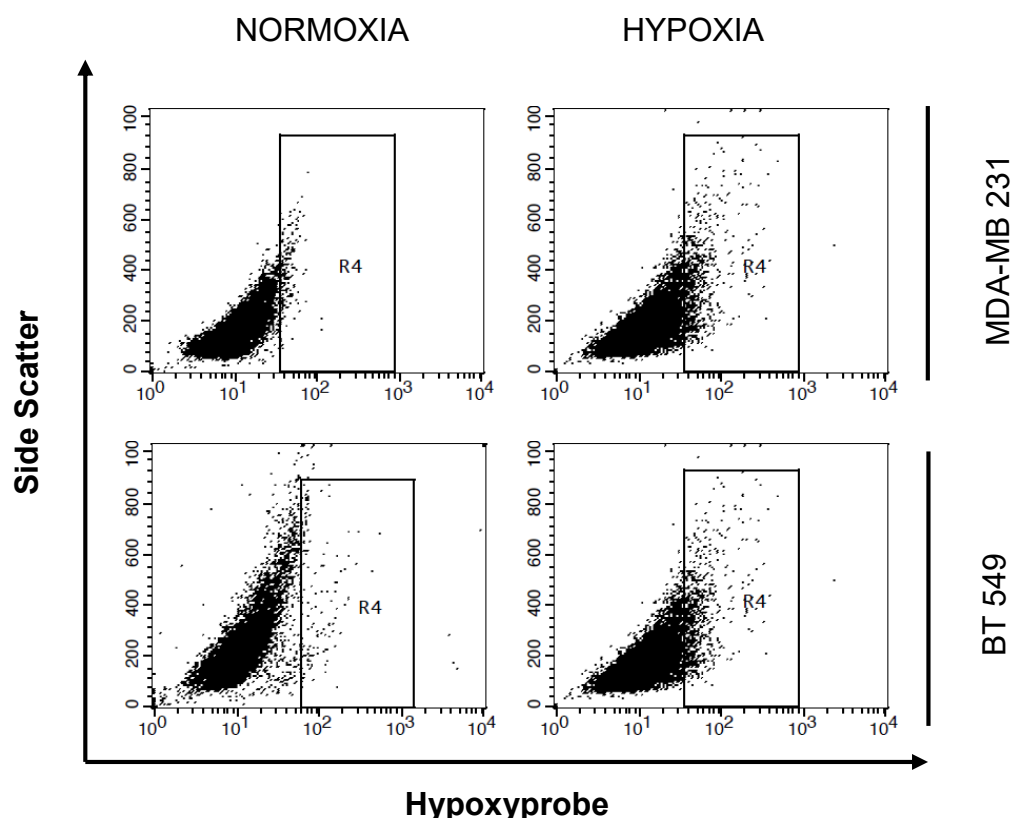


Figure 3.1(A) Representative FACS Plots of expression of hypoxic population in BC cell lines: Fluorescence Activated Cell Sorting (FACS) analysis using Hypoxyprobe kit staining shows increase in population of hypoxic cells in hypoxic culture compared to normoxic culture. This indicates the successful induction of hypoxia in our hypoxic culture system.

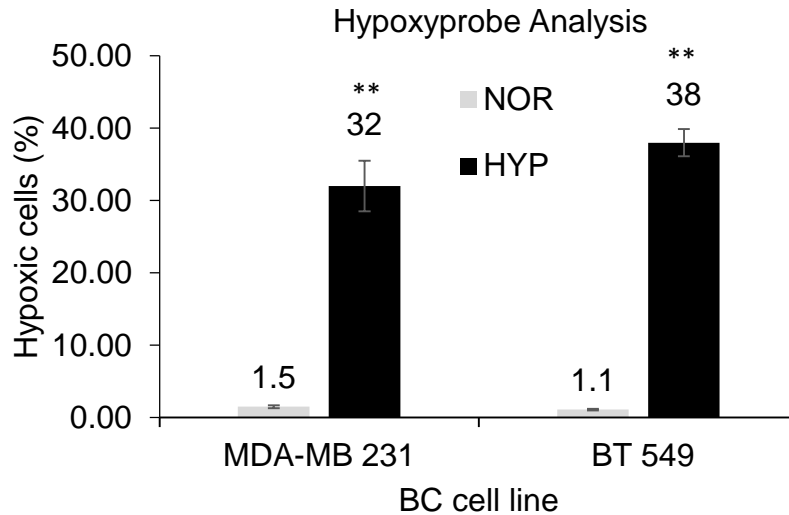


Figure 3.1B Bar chart representation of hypoxic and normoxic populations in BC cell lines. Histograms (Median \pm interquartile range) displayed an increase hypoxic cell population in cell lines grown under hypoxia in comparison to their respective normoxic cultures (Mann and Whitney U test, ** $p < 0.05$, $n=9$).

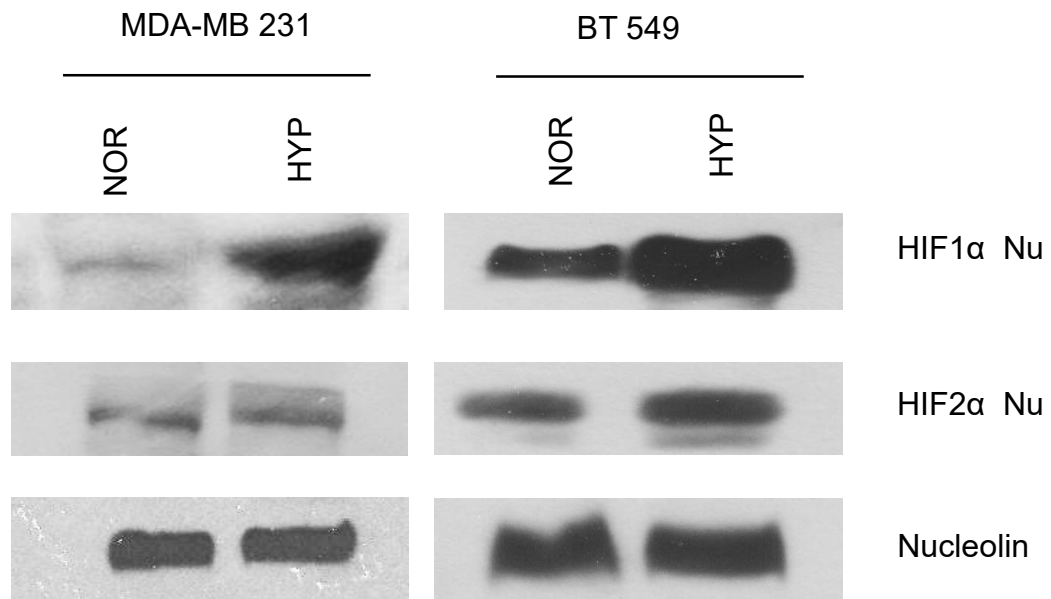


Figure 3.2. Representative Western blots of hypoxia-inducible factors (HIFs) in BC cell lines: Western blot analysis of nuclear extracts from NOR and HYP cells of MDA-MB 231 and BT 549 cell line shows that the hypoxic cultures have increased expression and nuclear translocation of HIF1 α and HIF2 α in comparison to the normoxic cells. Nucleolin was used as loading control. (NOR: normoxic culture, HYP: hypoxic culture, HIF: hypoxia-inducible factor).

3.3.2. Hypoxic cells significantly resistant to anticancer drugs

To study the effect of hypoxia in the induction of chemoresistance, cisplatin (CDDP), a first line drug for TNBC and four conventional anticancer drugs paclitaxel (PTX), doxorubicin (Dox), vincristine (VCR) and gemcitabine (dFdC) were tested on cells cultured in both hypoxic and normoxic conditions. MTT cytotoxicity results showed that the cells grown in hypoxic conditions were resistant to all five anticancer drugs tested, while the cells cultured in normoxic conditions were killed at low concentrations of the drugs. The hypoxic cells were able to survive at even high concentrations of anticancer drugs used. The half maximal inhibitory concentration (IC_{50}) values indicates how much of the anticancer drug is needed to inhibit cell growth expressed as cell viability. Figure 3.3 (A) and (B) shows that cell viability curves and bar charts (IC_{50} values) for MDA-MB 231 and BT 549 breast cell lines respectively grown in hypoxia were significantly higher than their normoxic culture.

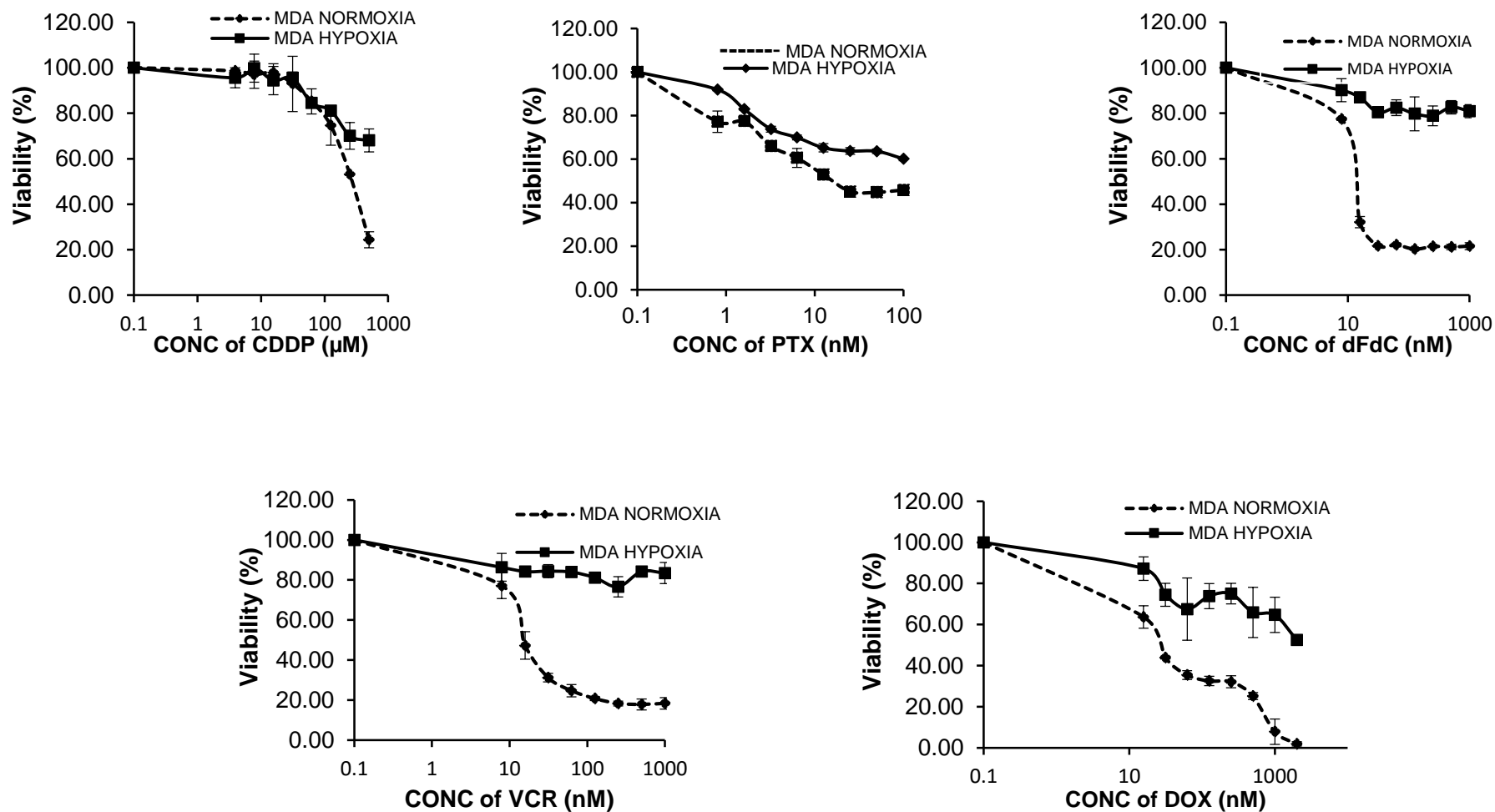


Figure 3.3(A1). Representative Drug Concentration Response Curves of MDA-MB 231 in normoxic and hypoxic culture. Cell viability curve shows difference in dose response between normoxia and hypoxia cultures. The hypoxic cells were highly resistant to the CDDP, DOX, PTX, dFdC and VCR while cell death was induced in the normoxic cells at much lower concentrations of these anticancer drugs. (MDA: MDA-MB 231 cell line, Cisplatin (CDDP), paclitaxel (PTX), doxorubicin (Dox), vincristine (VCR) and gemcitabine (dFdC))

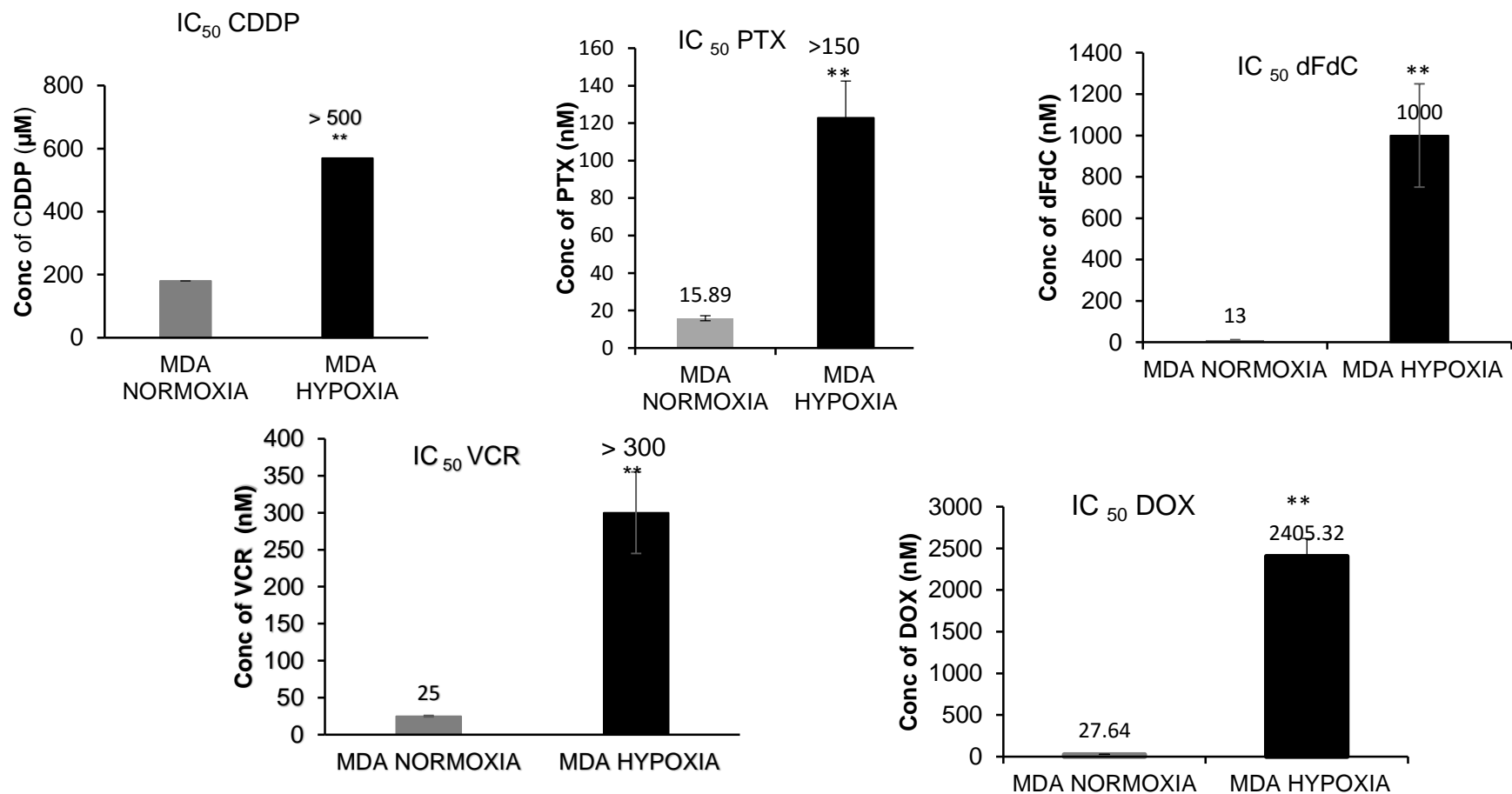


Figure 3.3(A2). Bar chart representative of IC_{50} values of normoxic and hypoxic cells treated with anticancer drugs. The histograms (median \pm interquartile range) shows the elevated half maximal inhibitory concentration (IC_{50}) values for hypoxic cells indicating increased drug to 5 anticancer drug tested cisplatin (CDDP), paclitaxel (PTX), doxorubicin (Dox), vincristine (VCR) and gemcitabine (dFdC), (Mann and Whitney U test, ** $p < 0.001$, $n = 9$).

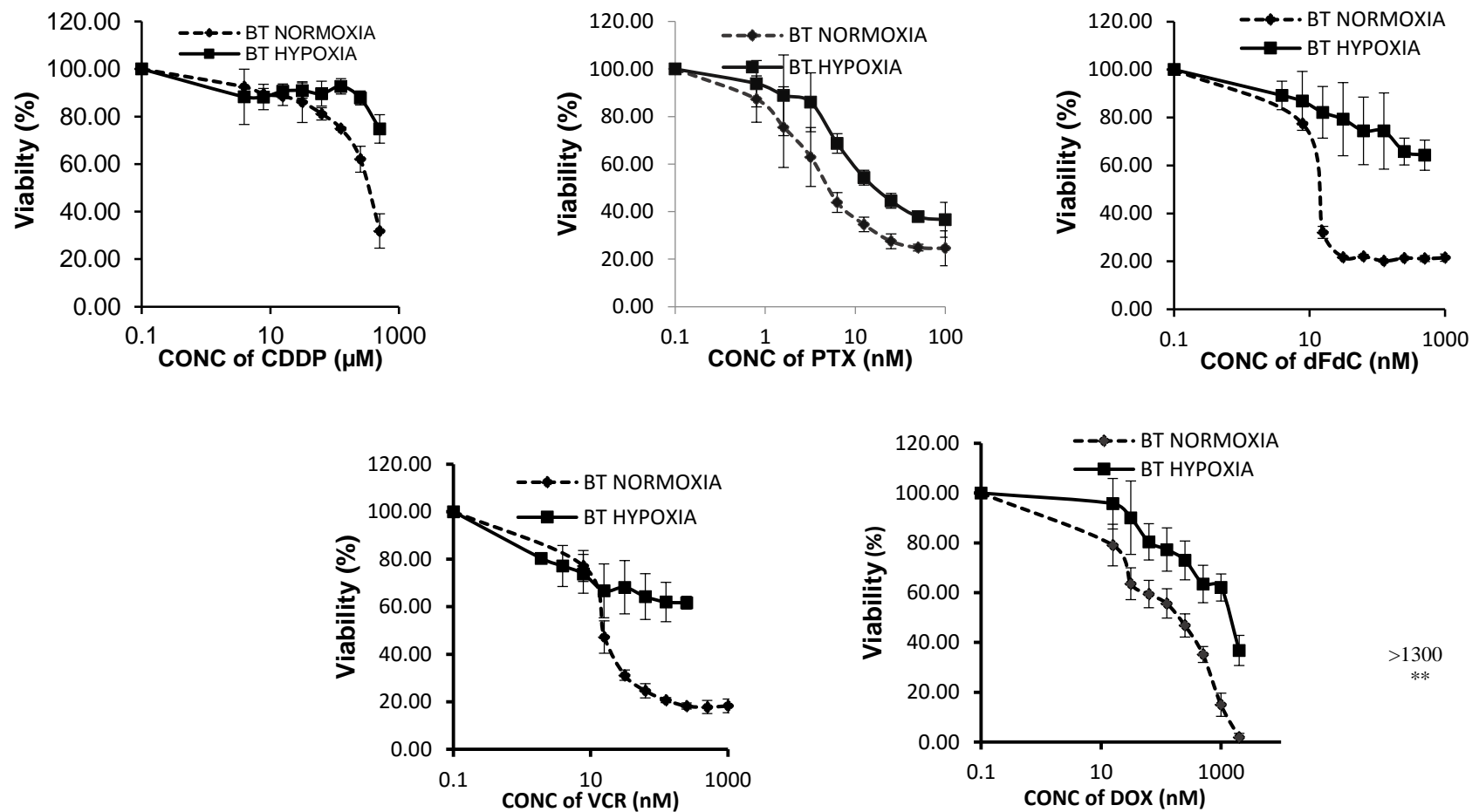


Figure 3.3(B1). Representative Drug Concentration Response Curves of BT 549 in normoxic and hypoxic culture. Cell viability curve shows difference in dose response between normoxia and hypoxia cultures. The hypoxic cells were highly resistant to the CDDP, DOX, PTX, dFdC and VCR while cell death was induced in the normoxic cells at much lower concentrations of these anticancer drugs. (BT: BT 549 cell line, Cisplatin (CDDP), paclitaxel (PTX), doxorubicin (Dox), vincristine (VCR) and gemcitabine (dFdC)).

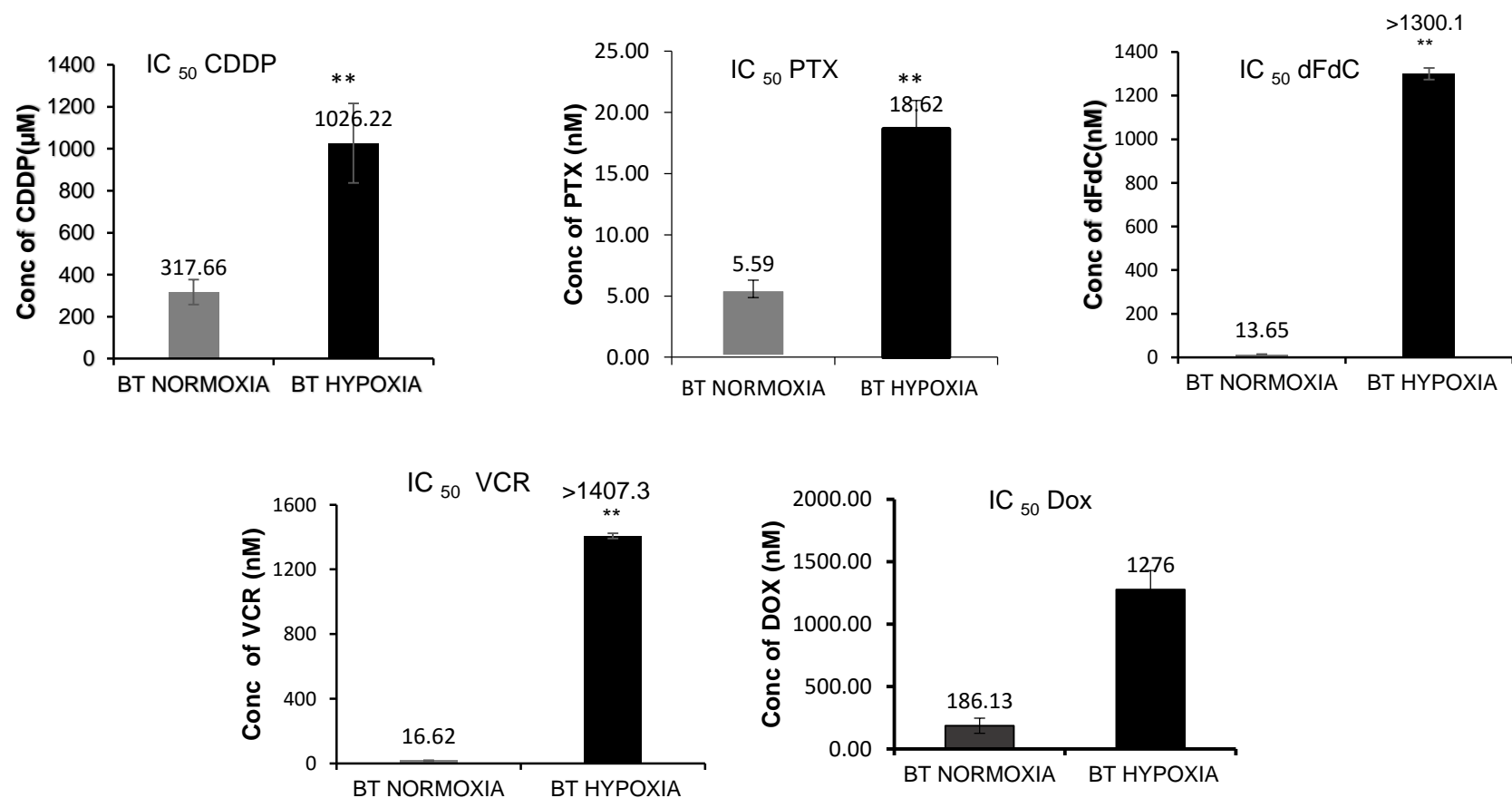


Figure 3.3(B2) Bar chart representative of IC_{50} values of normoxic and hypoxic cells treated with anticancer drugs. Histogram (median \pm interquartile range) shows elevated half maximal inhibitory concentration (IC_{50}) values for hypoxic cells indicating increased drug resistance to 5 anticancer drug cisplatin (CDDP), paclitaxel (PTX), doxorubicin (Dox), vincristine (VCR) and gemcitabine (dFdC) (Mann and Whitney U test, resistance, **p=<0.001, n=9).

3.3.3. Hypoxic cells express high CSCs markers

Fluorescence-activated cell sorting (FACS) analysis showed that BC cells grown under hypoxia had higher expression of CSC markers (ALDH⁺, CD133) (Figure 3.4 A and B) and embryonic markers (Nanog, Sox2, Oct4) when compared to cells cultured in normoxic conditions. The expression of embryonic stem cell proteins Sox2, Oct4 and Nanog regulates stemness, self-renewal and pluripotency of cells and are were found to be significantly increased in hypoxia in both MDA-MB 231 (Figure 3.5) and BT 549 (Figure 3.6). Growth curve experiments were also conducted and the results (Figure 3.7) obtained demonstrated that hypoxic cells had a significant decrease in growth rate and doubling time indicating quiescence which is an important stem cell feature.

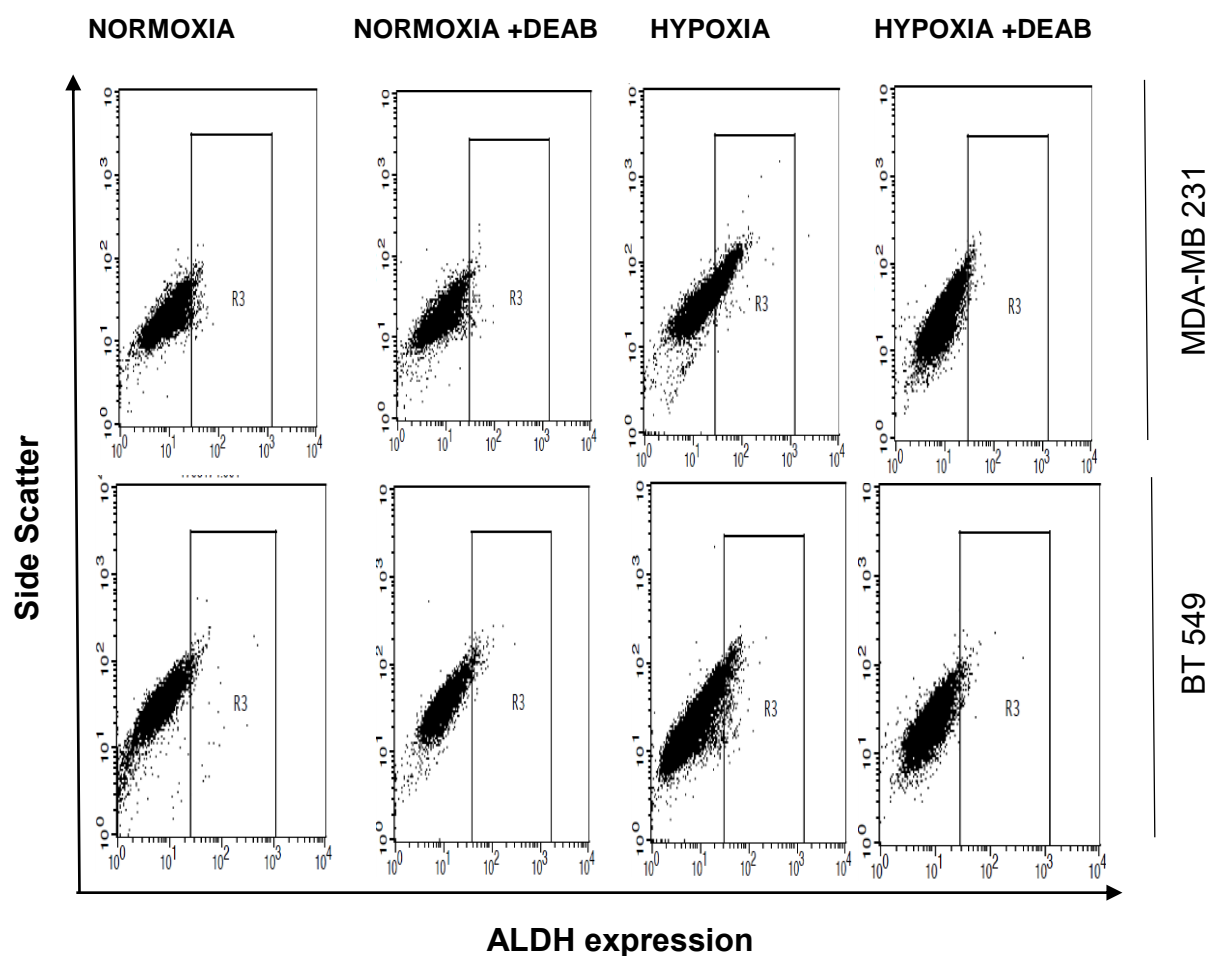


Figure 3.4(A1). Representative FACS Plots of ALDH expression in normoxic and hypoxic cultures measured by ALDEFLUOR assay. FACS results shows ALDH activity in hypoxic and normoxia cells with and without treatment with DEAB (30μM). Breast cancer cell line cultured under hypoxia expressed high percentage of ALDH⁺ compared to their respective normoxic cultures. (Abbreviations: DEAB: Diethylaminobenzaldehyde; ALDH: Aldehyde dehydrogenase activity, FACS: Fluorescence Activated Cell Sorting).

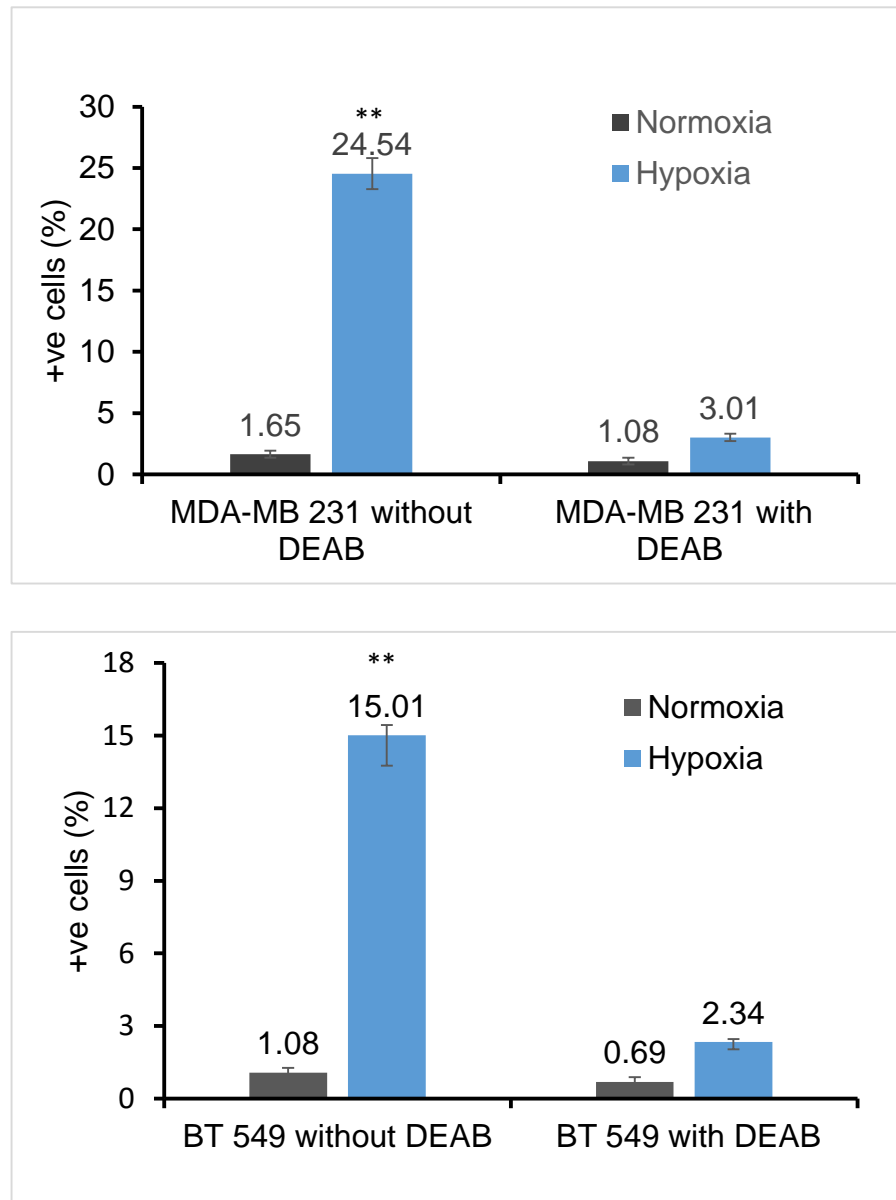


Figure 3.4(A2). Bar chart representation of ALDH+ cells in hypoxic and normoxic populations in BC cell lines. Histograms (median \pm interquartile range) displays statistically significant increase in the ALDH+ activity in hypoxic cultures in comparison to their respective normoxic cultures (Mann and Whitney U test, $**p < 0.0001$, $n=9$). After treatment with DEAB, there was no statistical difference in ALDH+ cell from both cultures (Mann and Whitney U test, $p > 0.05$). (Abbreviations ALDH: aldehyde dehydrogenase, DEAB: diethylaminobenzaldehyde).

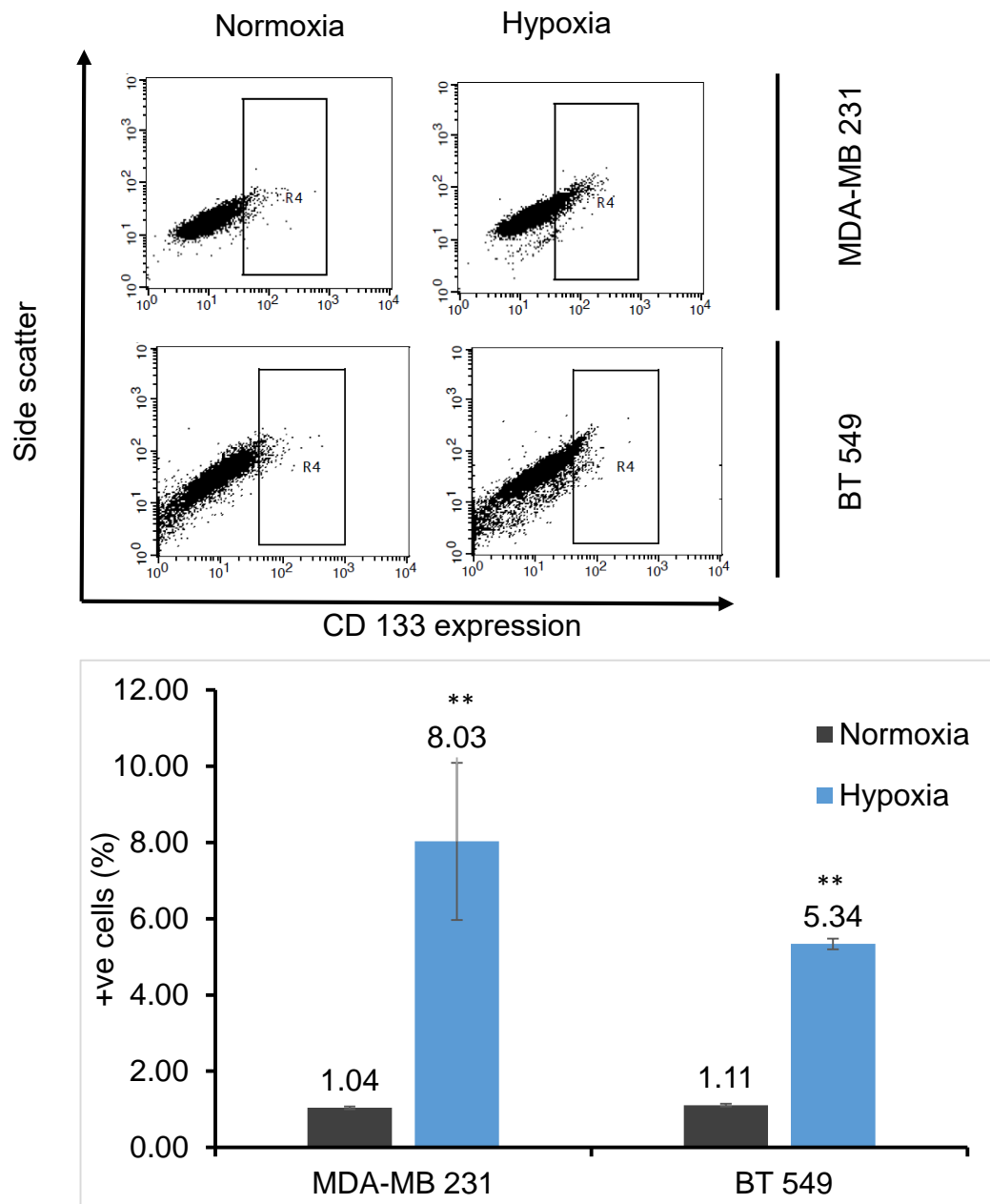


Figure 3.4 (B) Representative FACS Plots of CD133 expression in normoxic and hypoxic cultures measured using CD133-PE conjugated antibody. FACS data shows that higher expression of CD133 was observed in hypoxic culture compared to normoxic culture. Histograms (median \pm interquartile range) displays statistically significant increase in CD133 expression in Hypoxic cultures in comparison to their respective normoxic cultures. (Mann and Whitney U test, $**p < 0.001$, $n=9$). (Abbreviations FACS: Fluorescence Activated Cell Sorting).

MDA-MB 231

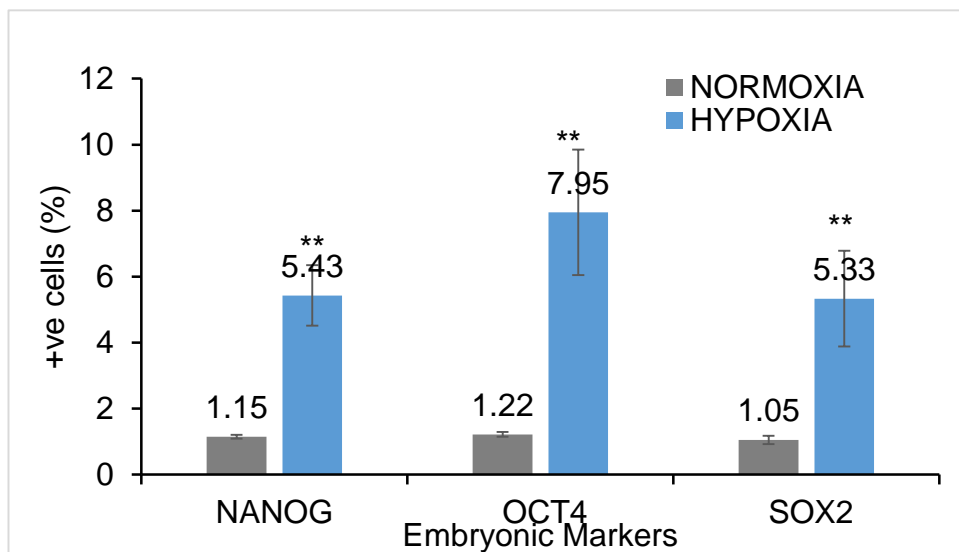
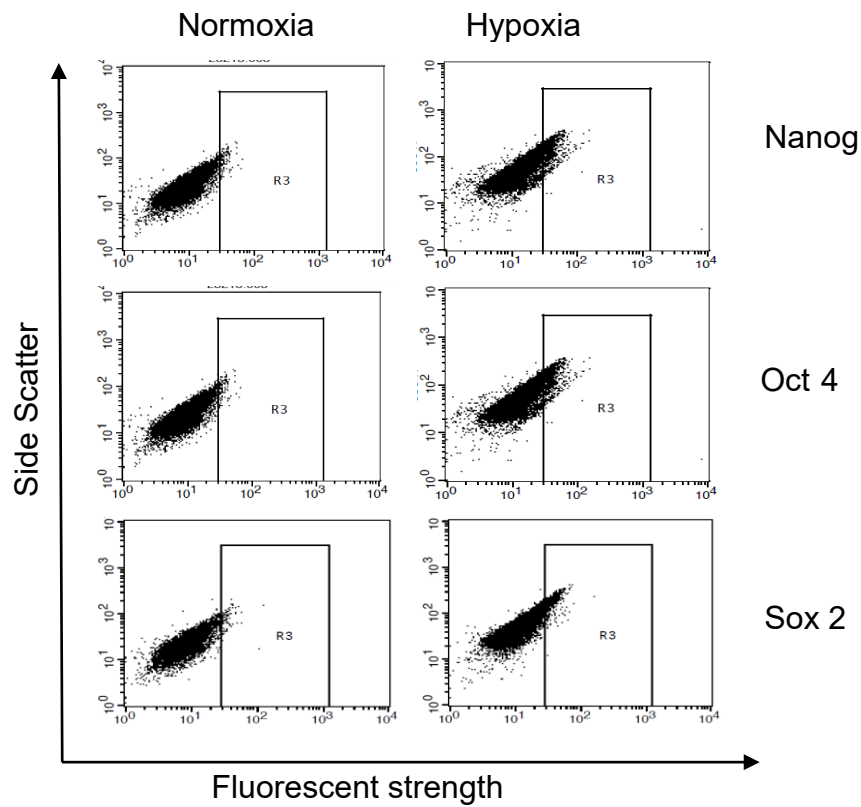


Figure 3.5. Representative FACS Plots of Embryonic CSC markers Expression in normoxic and hypoxic cultures of MDA-MB 231 cell line. FACS data shows that higher expression of embryonic stem cell markers (Nanog, Sox2 and Oct4) were displayed in MBA-MB231 hypoxic culture compared to normoxic culture. Histograms (median \pm interquartile range) above displays statistically significant increase in all three embryonic CSC markers in hypoxic cultures in comparison to normoxic culture. (Mann and Whitney U test, $**p < 0.001$, $n=9$). Abbreviation; FACS: Fluorescence Activated Cell Sorting expression

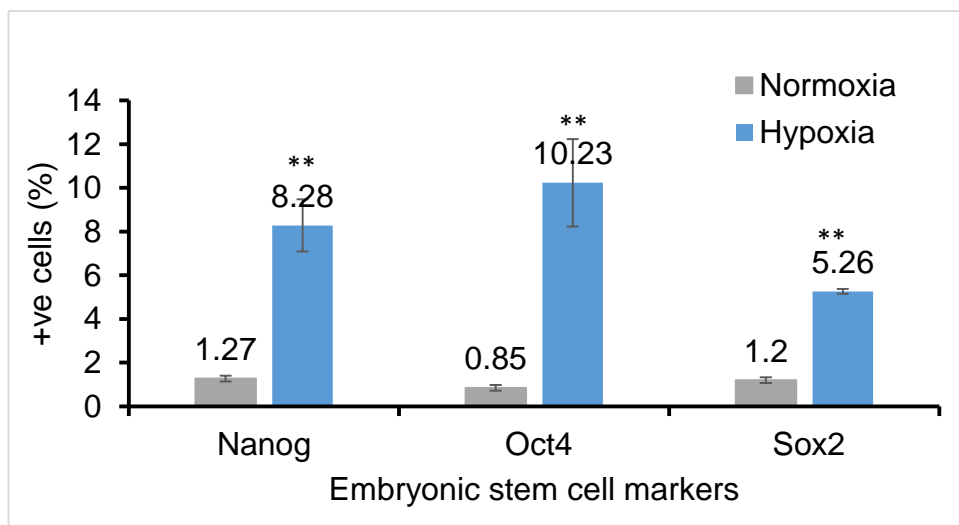
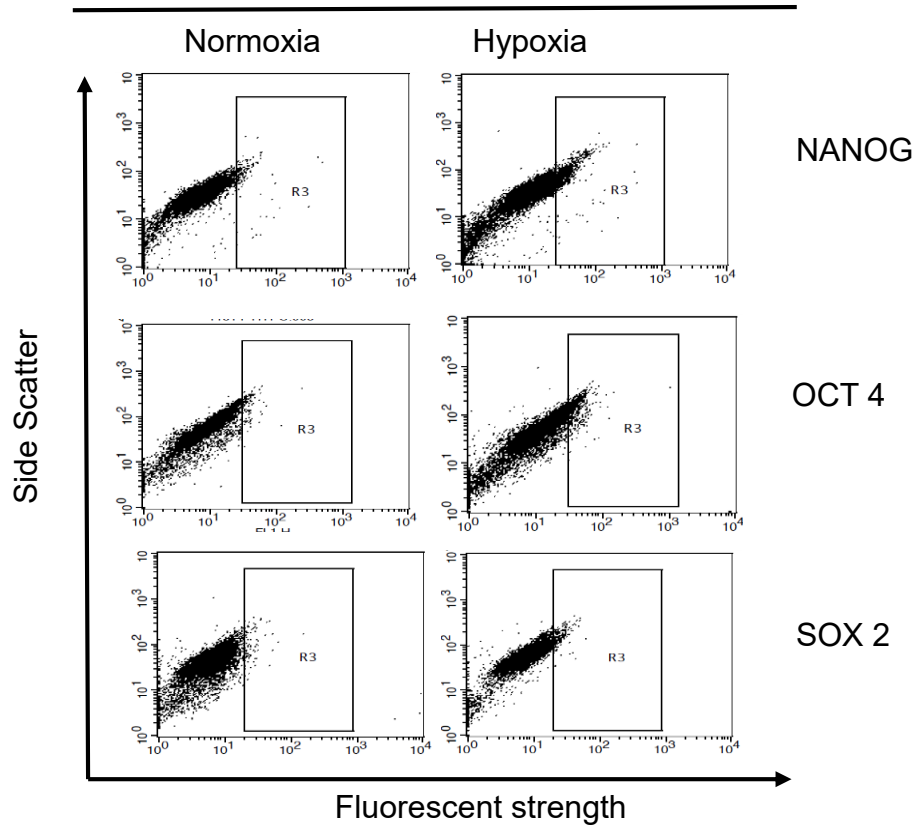


Figure 3.6. Representative FACS Plots of Embryonic CSC markers Expression in normoxic and hypoxic cultures of BT 549 cell line. FACS data shows that higher expression of embryonic stem cell markers (Nanog, Sox2 and Oct4) were displayed in BT 549 hypoxic culture compared to normoxic culture. Histograms (median \pm interquartile range) above displays statistically significant increase in all three embryonic CSC markers in hypoxic cultures compared to normoxic cultures. (Mann and Whitney U test, $**p < 0.001$, $n=9$).

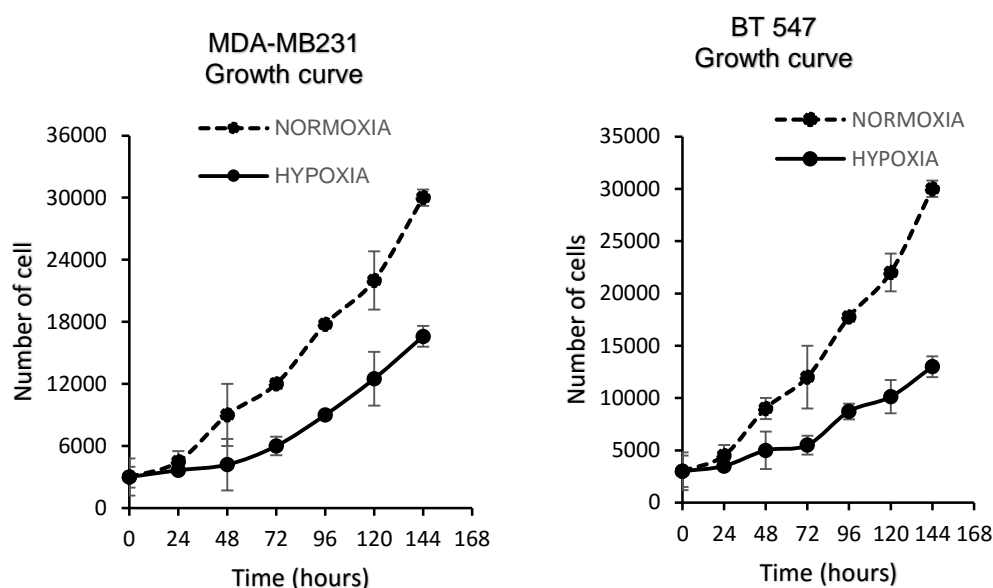


Figure 3.7. Representative Growth curves of MDA-MB 231 and BT549 cancer cell lines cultured in normoxia and hypoxia. Cells growth rate under hypoxia was slower than those grown in normoxia. This could be due to the acquisition of CSC characteristics leading to quiescence (Mean \pm SD, n=6).

3.3.4 Hypoxia induces EMT in BC cell lines

Results from western blot protein analysis showed that cells grown in hypoxia were found to have higher expression of EMT markers such as increase in N-cadherin and decrease in E-cadherin expressions, this switch indicates the cells obtained a more mesenchymal characteristic. Vimentin expression was also increased. Whereas in cells grown under normoxia there was no loss of E-cadherin and hence they remain epithelial in nature. These results suggest that hypoxia can transform the cells into a more mesenchymal phenotype and can be reversed to epithelial nature if the cells were to return to normoxia.

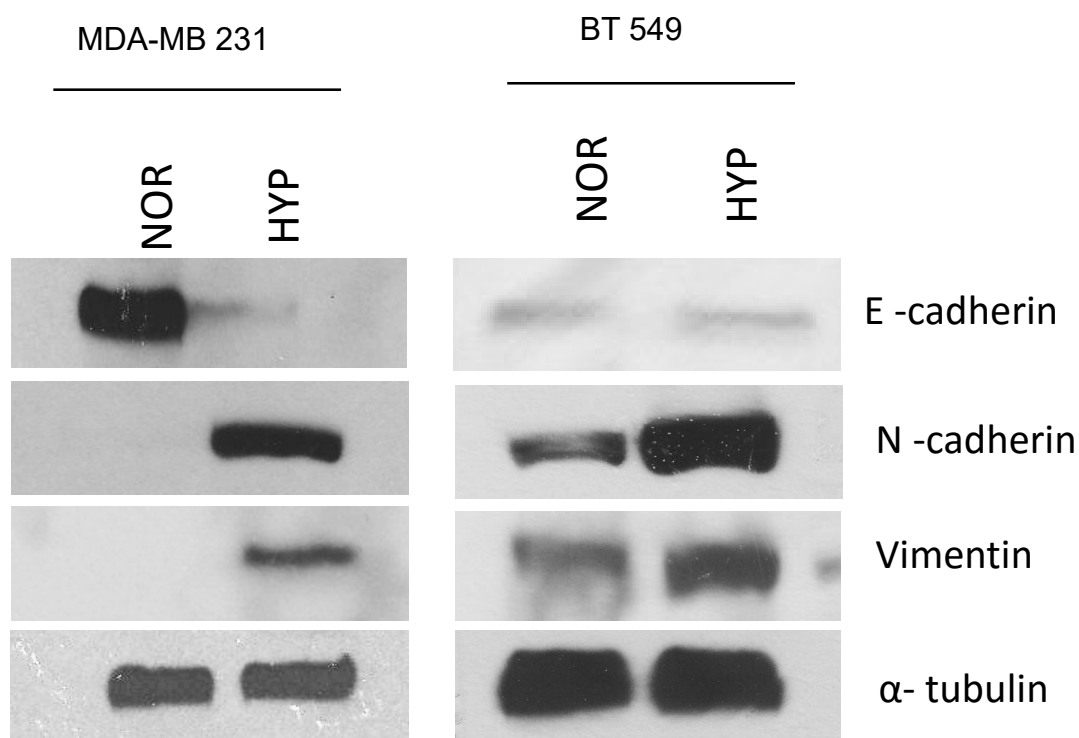


Figure 3.8. Representative Western Blots of EMT markers in hypoxic cells using whole cell lysates of NOR and HYP cultures of breast cell lines. The results shows that cells under hypoxia have decreased expression of epithelial marker E-cadherin and increased expression of mesenchymal markers (N-cadherin and vimentin) in comparison to that of normoxic cells indicating EMT activation in the HYP cells. Tubulin was used as loading control. (NOR-normoxic culture, HYP: hypoxic culture).

3.3.5. Hypoxic cells display increase migration and invasive potential

Further confirmation of hypoxia-induced EMT and transformation of cells into mesenchymal phenotype was done by analysing the migratory potential of cells under hypoxia. The images taken using the inverted microscope for Boyden chamber migration assay and the optical density (OD) measured from the experiment enabled determination of percentage migration between normoxic and hypoxic cell cultures. Results from the analysis (Figure 3.9) showed significant increase in the migratory potential of cells grown under hypoxic

conditions. Mesenchymal phenotypes are also known to have increased invasion potential that can be measured by transwell matrigel invasion assay. Cells with mesenchymal characteristics have the potential to produce matrix metalloproteinases that can digest the extracellular membrane or substance like matrigel that enables them to invade the gel and move out of the matrix towards chemoattractants like serum or growth factors. Images taken from the above experiment shown in Figure 3.10 indicate a remarkable increase in the invasion potential of cells grown under hypoxia. The results given as invasion index (%) confirm the increased invasion potential of hypoxic cell cultures which is statistically significant.

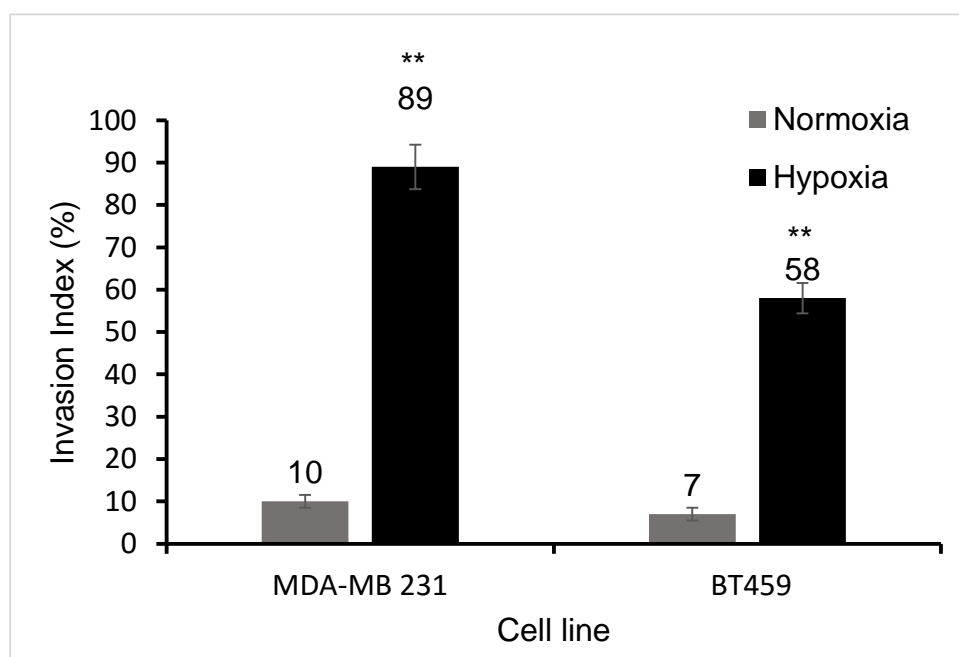
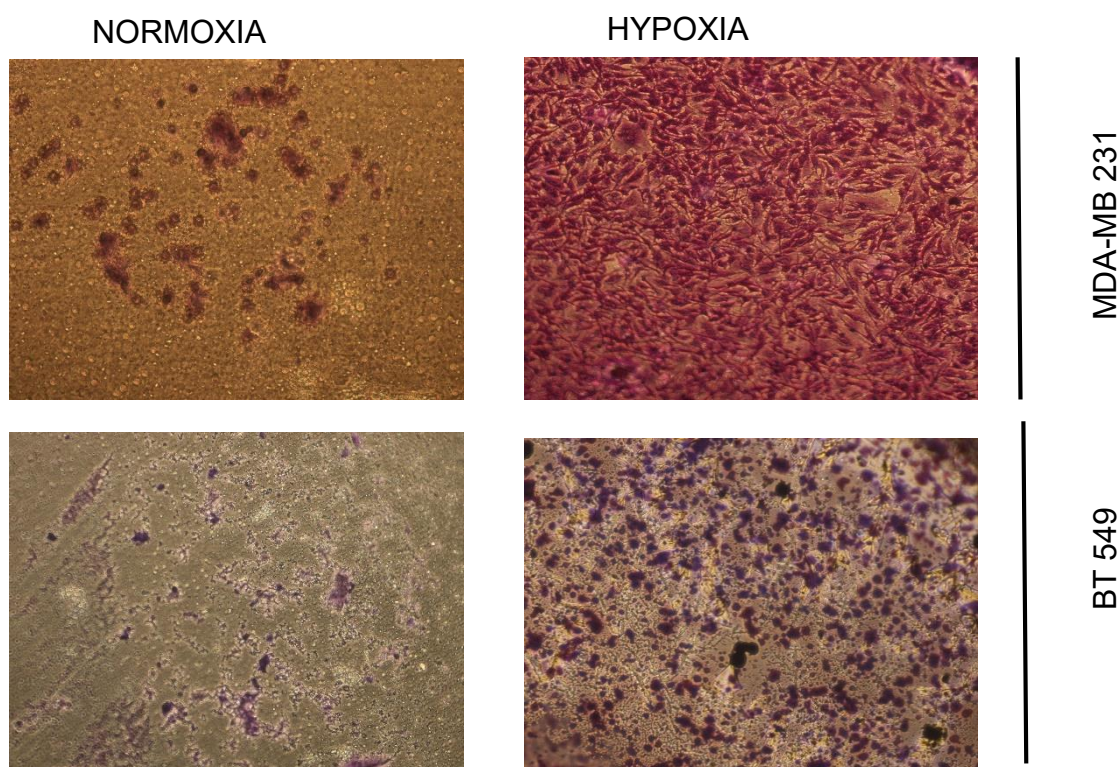


Figure 3.9. Representative Matrigel Invasion assay of TNBC hypoxic cells. Images (Magnification 20X) shows that the cells grown under hypoxic conditions are highly invasive in comparison to that of normoxic cells indicating EMT activation and mesenchymal characteristic of the hypoxic cells. Histograms (median \pm interquartile range) shows statistically significant invasive rate of hypoxic cells (Mann and Whitney U test, $**p < 0.0001$, $n=6$). (Abbreviations Triple negative breast cancer (TNBC). Epithelial to mesenchymal transition (EMT)).

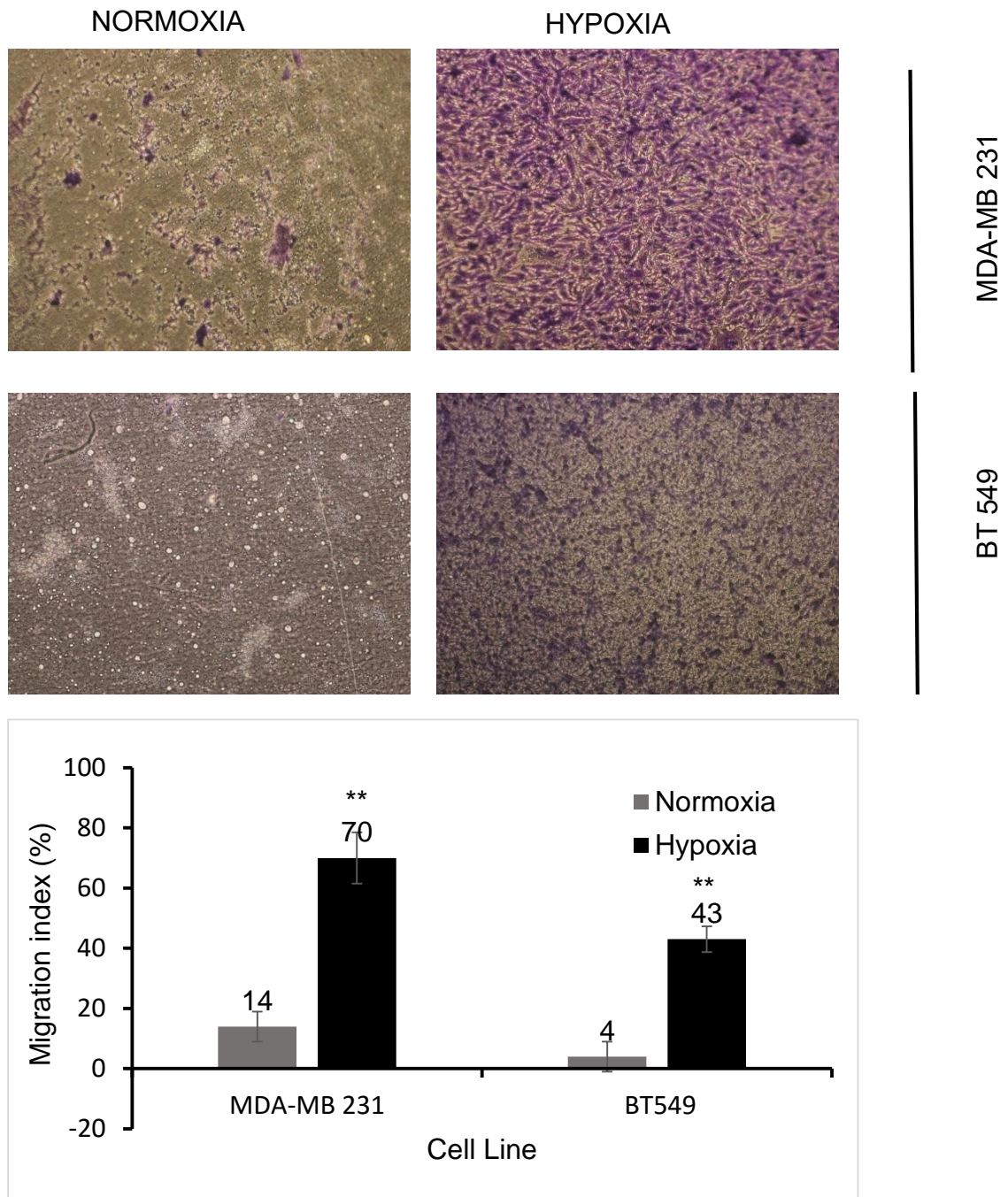


Figure 3.10. Representative Matrigel Migration assay of TNBC hypoxic cells. Images (Magnification 20X) shows that the cells grown under hypoxic conditions have increase migration in comparison to that of normoxic cells. The histograms (median \pm interquartile range) displayed statistically significant migratory potential of hypoxic cells indicating EMT activation and mesenchymal characteristic of the hypoxic cells (Mann and Whitney U test, $**p < 0.0001$, $n=6$). (Abbreviations Triple negative breast cancer (TNBC). Epithelial to mesenchymal transition (EMT)).

3.4. Discussion

Hypoxia, a reduction in tissue oxygen tension is a common feature associated with solid tumours (Vaupel and Mayer, 2007). Tumours adapt to these hypoxic changes by switching on genetic pathways that promote tumour aggressiveness, metastasis and chemoresistance; patients with hypoxic tumours generally have a poorer prognosis (Semenza, 2007; Keith and Simon, 2007). Increasing evidence show that cancer is a disease that involves stem cells as cells with stem-like features have been isolated from many solid tumours including the breast, brain, colon, liver and pancreatic cancers (Al-Hajj *et al.*, 2003; Singh *et al.*, 2004; Li *et al.*, 2007; O'Brien *et al.*, 2007; Prince *et al.*, 2007). Increased expression of certain cancer stem cell markers (CSC) markers such as ALDH⁺ and overexpression of embryonic stem markers (Sox2, Oct4, Nanog) have been used to identify stemness in BC cells (Tirino *et al.*, 2013).

Das *et al.*, (2008) reported that hypoxic tumour cells are poorly differentiated and express stem cell markers. Other studies also postulate that hypoxia may be responsible for the persistence of CSCs in tumours and the hypoxic niche provides a suitable microenvironment for the maintenance of these CSCs which are involved in promoting therapeutic failure and tumour relapse (Rosen and Jordan, 2009; Lin and Yun, 2010). With these facts in mind, it was hypothesized that hypoxia may be involved in the induction of CSCs traits and maintenance of CSCs in cancer cells. Breast cancer cell lines MDA-MB 231 and BT549 cultured in hypoxic chamber were observed to have higher population of hypoxic cells compared to those cells cultured in normoxia. HIF nuclear translocation was also increased in the hypoxic cultured cells (Figure 3.1 and 3.2). Data from this study (Figure 3.4 A and B) also showed that monolayer TNBC cells grown under

hypoxia had higher expression of CSCs markers (ALDH⁺, CD133) and embryonic markers (Sox2, Oct4, Nanog) compared to cells grown in normoxia, suggestive that hypoxia induces these CSC traits.

Breast cancer metastasis is one of the primary cause for cancer related deaths in TNBC patients (Gupta and Massagu, 2006; Steeg, 2006). Patients with primary tumours that contain high population of hypoxic cells have been reported to have a reduction in overall survival rate after surgical resection of the primary tumour (Vergis *et al.*, 2008), these suggests that hypoxia is able to promote a more aggressive tumour with metastatic phenotype. According to the report by Badve and Nakshatri, (2012) CSC phenotype represents tumours that are aggressive with inherent ability to adapt, lie dormant or rapidly proliferate and these CSC phenotype represents the plasticity of tumours to undergo EMT giving rise to metastasis. The results from this study shows that cells under hypoxia displayed an increase in vimentin and N-cadherin expression indicating a switching to a mesenchymal phenotype while losing E-cadherin which is the trademark of epithelial phenotype (Figure 3.8). Further confirmation from the invasion and migration assay (Figure 3.9 and 3.10) also demonstrated that cells cultured under hypoxia have significant increased migratory and invasion potentials compared to cells in normoxic culture indicating that there is a close relationship between stem cell induction and EMT phenotype in cancer cell lines.

Exposure of cells and tissues to hypoxia stimulates stress response pathways that enable self-preservation and anti-apoptotic phenotype in cells. There is strong association between tumour hypoxia and poor prognosis and resistance to therapies (De Milito and Fais, 2005; Li *et al.*, 2009). Data from MTT analysis reveal that cells grown under hypoxia were significantly resistant to the 5

conventional anticancer drugs (Cisplatin, vincristine, paclitaxel, Doxorubicin and gemcitabine) tested suggestive that hypoxia may be involved in the induction of these drug resistance indicative that hypoxia induces stemness of cells with resultant drug resistance.

Conclusion

Even with the advancement in treatment and outcome of patients in recent times, drug resistance of tumour cells is a major factor limiting the effectiveness of chemotherapeutic treatment in most human tumours. Hypoxia induces CSC-like characteristics in breast cancer cell line. The hypoxic cells show slow proliferation rate but displayed high migratory and invasive potentials. It is concluded that hypoxia induces these CSC-like phenotype leading to chemoresistance, therefore further understanding of the mechanisms of hypoxia-induced EMT will be beneficial in targeting these hypoxic stem cell.

Chapter Four

NF κ B: A key factor involved in hypoxia-induced chemoresistance and stemness of breast cancer cells

4.1 Introduction

NF κ B is a family of transcription factors important for the regulation of the immune and inflammatory responses, developmental processes, cellular growth and apoptosis (Li and Verma, 2002; Bonizzi and Karin, 2004). NF κ B is expressed in virtually all cell types and sequestered in cytoplasm by the inhibitor of NF-kappa B (I κ B) (Hayden and Ghosh, 2004). External stimuli such as oxidative stress, hypoxia, inflammatory cytokines, viral infections activates I κ B kinase (IKK) which triggers the phosphorylation of I κ B α with resultant proteasomal degradation of I κ B α , releasing NF κ B dimer form which then translocates to the nucleus where the NF κ B proteins bind to κ B sites as dimers, either homodimers or heterodimers, and exerts both positive and negative effects on target gene transcription (Liang *et al.*, 2004).

The inactive NF κ B-I κ B complex can directly or indirectly be activated by hypoxia which results in an increase in its expression. There is constitutive NF κ B in many solid tumours contributing to cancer cell survival and reduced sensitivity to anticancer drugs (Arlt and Schafer, 2002). Several reports have shown that NF κ B is activated in human breast cancer cell lines as well as in primary breast tumours (Cogswell *et al.*, 2000; Nakshatri and Goulet, 2002). Other studies also demonstrated that NF κ B activation results in tumour chemoresistance by exerting antiapoptotic effects by the up-regulation antiapoptotic genes in BC cells

resulting in cell survival mechanisms and resistance to therapeutic regimens (Arlt and Schafer, 2002; Montagut *et al.*, 2003).

Hypoxia induced NF κ B promotes signalling pathways involved in the inflammatory response through the regulation of gene expression of proinflammatory cytokines, adhesion molecules, enzymes, and pro-inflammatory enzymes. NF κ B activates the antiapoptotic process which inhibits apoptosis enabling survival of hypoxic insult in cancer cells (Taylor *et al.*, 2008). Hypoxia induced NF κ B activation is also believed to contribute to the maintenance of CSCs during the development and progression of tumours (Nakshatri and Goulet, 2002).

Result data from Chapter 3 revealed that hypoxia induced the overexpression of NF κ B in monolayer TNBC cultured under hypoxia with resultant stemness of cells.

4.1.1 Rationale and aims of this study

This study was therefore carried out to confirm if the overexpression of NF κ B induced CSCs traits in TNBC cell lines cultured in normoxia and to examine the link between hypoxia and NF κ B signalling pathway in chemoresistance and therapy failure. The effects of NF κ B in BC metastasis was also examined to reveal if overexpression of NF κ B increases the migratory and invasiveness of TNBC cells.

4.2 Experimental Design

General materials, products, labwares, manufacturers and methodologies used for the entire study have been described in details in chapter 2. Specific materials, methods and experimental design used for this part of this study are stated below.

4.2.1. Stable transfection of MDA-MB 231 cells with NF κ B p65 subunits

To determine the effects of NF κ B in maintenance of stem-like cell characteristics and chemoresistance, MDA-MB 231 cells were transfected with cDNA NF κ Bp65 vector and empty vector following the protocols for transfection as reported in Chapter two (page 84).

4.2.2. MTT cytotoxicity assay in NF κ B transfected cells

There is established proof that hypoxia induced chemoresistance in breast cancer cell as shown in chapter 3, to test if overexpression of NF κ B can also induce drug resistance, Mock and NF κ B transfected cells were exposed to anticancer drugs paclitaxel (PTX), vincristine (VCR), doxorubicin (DOX), cisplatin (CDDP) and gemcitabine (dFdC) and MTT assay performed (refer to Chapter 2, page 71).

4.2.3. Determination of CSC markers in NF κ B transfected cells

CSC markers ALDH, CD133, Sox2, Oct4 and Nanog were determined using immuno-fluorescence protocol for FACS. Over expression of the NF κ B protein should induce an increase in these CSC markers which was quantified by measuring increase in fluorescence (refer to Chapter 2, page 78).

4.2.4. Determination of EMT characteristics in NF κ B transfected cells

To examine the epithelial to mesenchymal transition (EMT) in NF κ B transfected cells, EMT markers vimentin, E-Cadherin and N-cadherin were determined by western blot (refer to Chapter 2, page 72). *In vitro* wound healing assay (scratch assay) for migration and transwell invasion assay (Boyden chamber assay) were also performed to determine the invasive and migratory properties of the cells (refer to Chapter 2, page 85 and 86).

4.3. Results

4.3.1. Stable transfection of NF κ B p65 subunit in MDA-MB 231 BC cell line

MDA-MB 231 cells were transfected with cDNA incorporating the NF κ Bp65 vector or the empty vectors in media containing hygromycin 150 μ g/mL. Two clones C1 and C6 with the highest expression of NF κ Bp65 were chosen for further testing. Western blot results (Figure 4.1) shows that clones C1 and C6 expressed higher levels of NF κ Bp65 from both nuclear and whole cell lysate extracts.

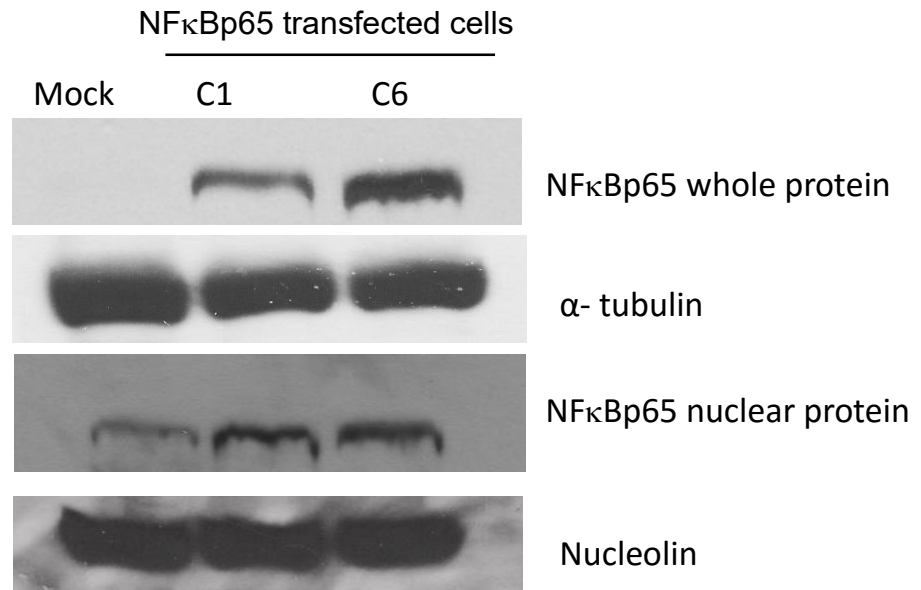


Figure 4.1. Representative Western Blots of NFκBp65 transfected cells using whole cell lysates and nuclear extracts of MDA-MB 231 cell line transfected with NFκBp65 subunit. The result shows that NFκBp65 overexpressing clones C1 and C6 had higher p65 expression and higher nuclear translocation of p65 in comparison to the mock. Tubulin and nucleolin were used as loading control.

4.3.2 Hypoxia may be involved in NFκB activation

BC cells cultured under hypoxia had higher of p65 expression and nuclear translocation of p65 from nuclear protein extracts (Figure 4.2).

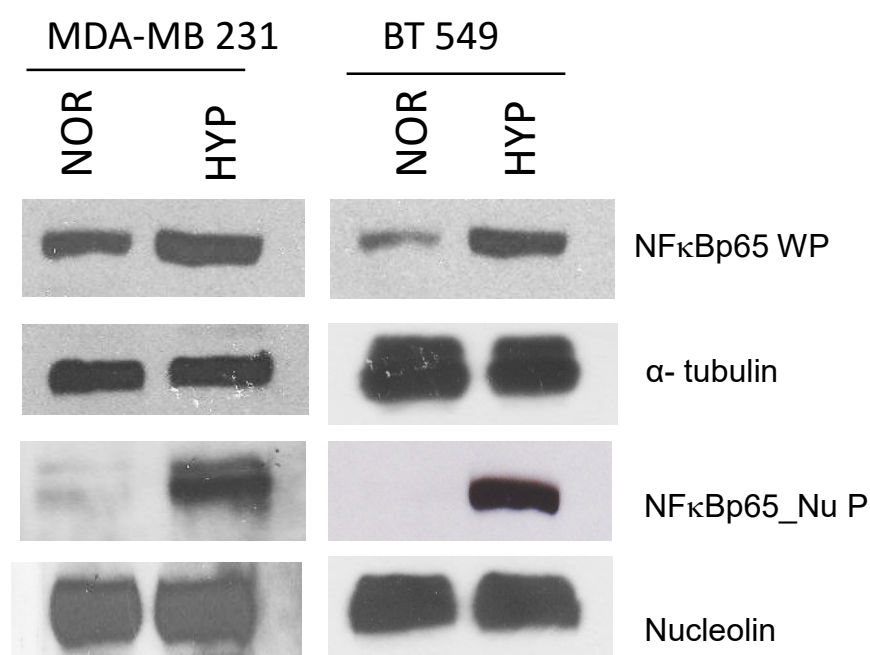
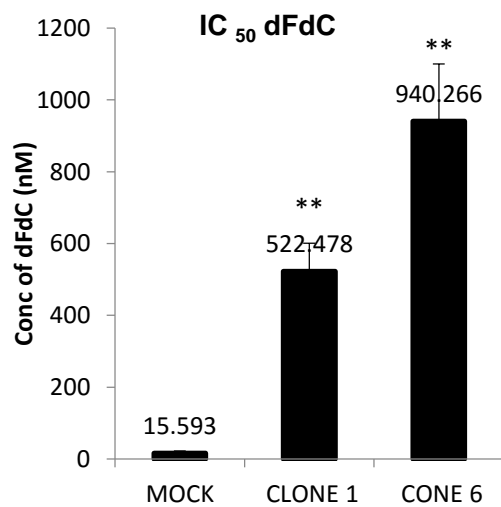
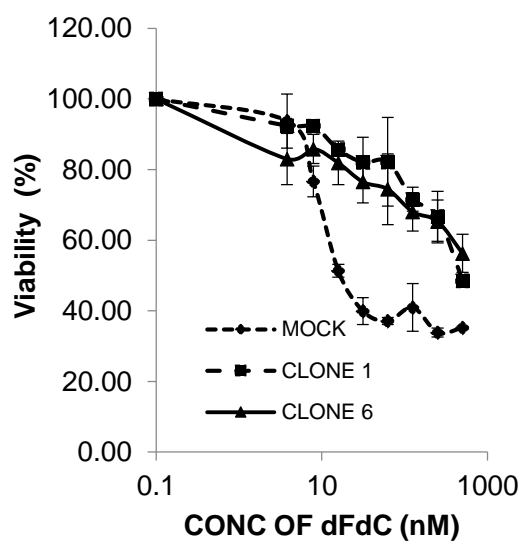
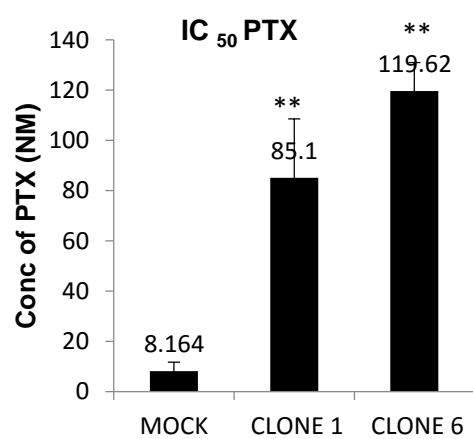
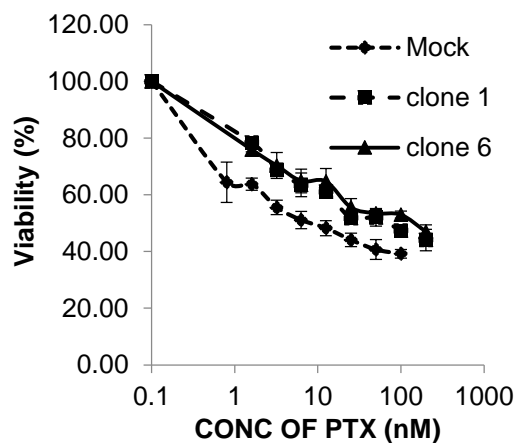
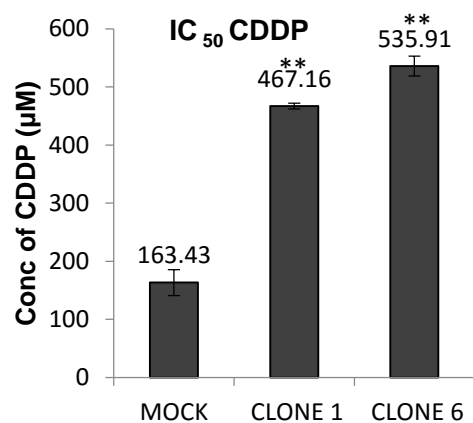
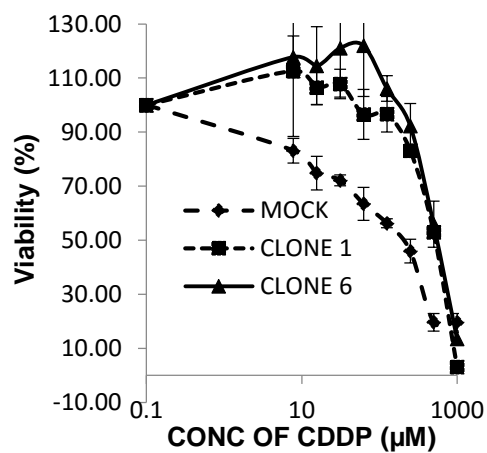


Figure 4.2. Representative Western Blots of NFκBp65 in hypoxic cells using whole cell lysate and nuclear extracts of normoxic and hypoxic cultures of breast cell lines. The results shows that cells cultured under hypoxia had increase of NFκBp65 and higher nuclear translocation of p65 in comparison to that of normoxic cells. Tubulin and nucleolin were used as loading control. (NOR- normoxia, HYP: hypoxia, WP – whole protein; NuP – nuclear protein)

4.3.3. Cells overexpressing NFκBp65 were highly resistant to anticancer drugs

Results from MTT cytotoxicity analysis show that NFκBp65 (C1 and C6) overexpressing cells were significantly resistant to 5 anticancer drugs tested (cisplatin, paclitaxel, doxorubicin, vincristine and gemcitabine) when compared to the Mock which were killed at lower concentrations of the drugs. The IC₅₀ (refer to chapter 2, page 71) of the NFκBp65 overexpressing cells were much higher than that obtained for the mock transfected cells (Figure 4.3).



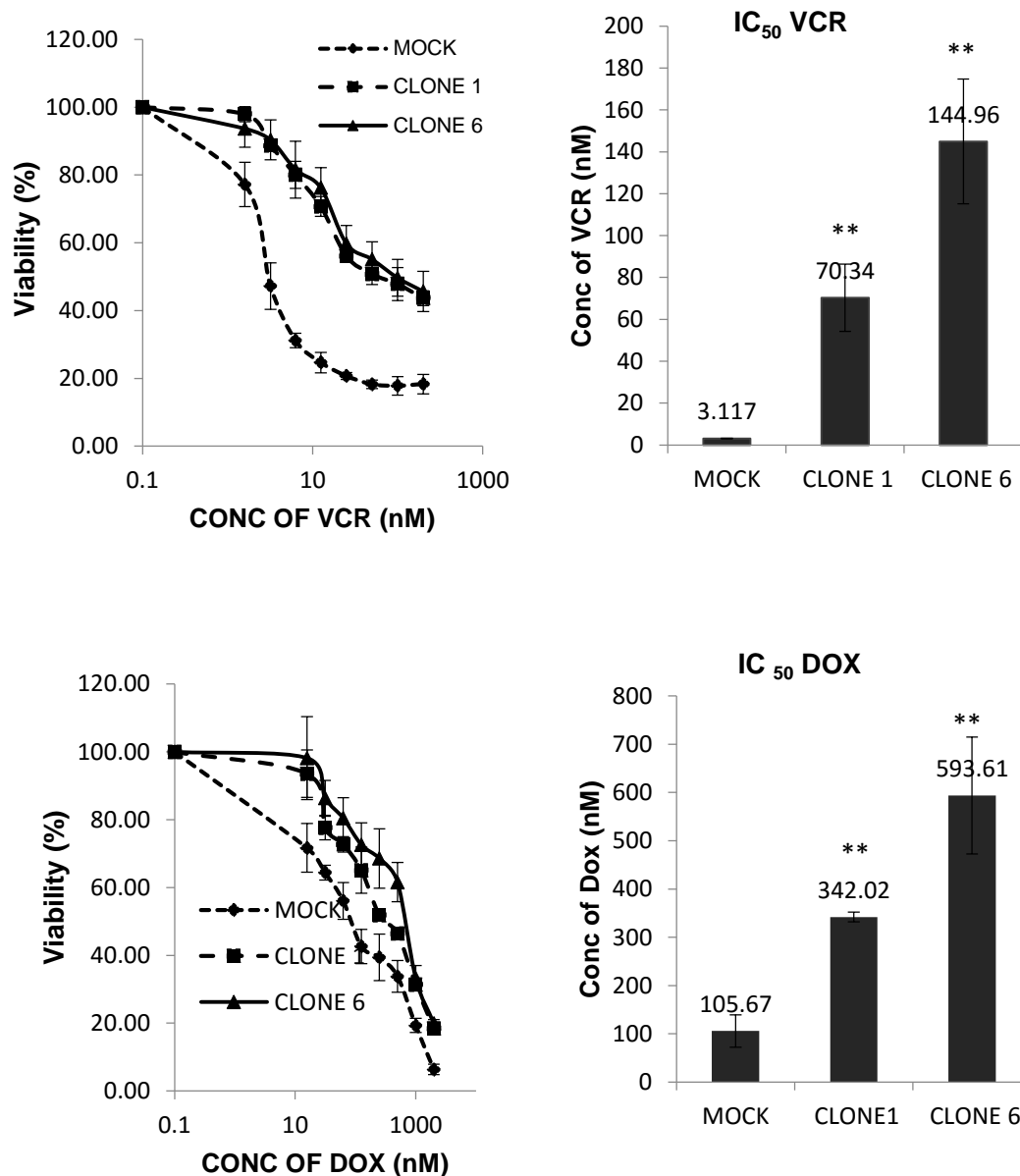


Figure 4.3 Representative Drug Concentration Response Curves of Mock and NFκB p65 transfected cells. Cell viability curve from MTT analysis shows difference in dose response between cells overexpressing NFκB p65 and the mock cells. The NFκB p65 overexpressing cells C1 and C6 were highly resistant to the CDDP, DOX, PTX, dFdC and VCR. Histograms (median ± interquartile range) shows elevated half maximal inhibitory concentration (IC₅₀) values for NFκB p65 overexpressing cells compared to mock cells indicating increased drug resistance. (Kruskal-Wallis test, ** $p < 0.0001$, $n = 9$) (Abbreviations; Cisplatin: CDDP, doxorubicin: DOX, paclitaxel (PTX), gemcitabine (dFdC) and vincristine (VCR))

4.3.4. Overexpression of NF κ Bp65 in BC cells induces CSC traits

Data from FACS analysis showed that the NF κ Bp65 over expressing positive clones (C1 and C6) had significantly higher expression of CSC markers (ALDH and CD 133) when compared to the Mock cells (Figure 4.4A and 4.4B). The expression of embryonic stem cell markers Sox2, Oct4 and Nanog were also increased in the NF κ Bp65 overexpressing clones compared to the mock cells (Figure 4.5 A and B).

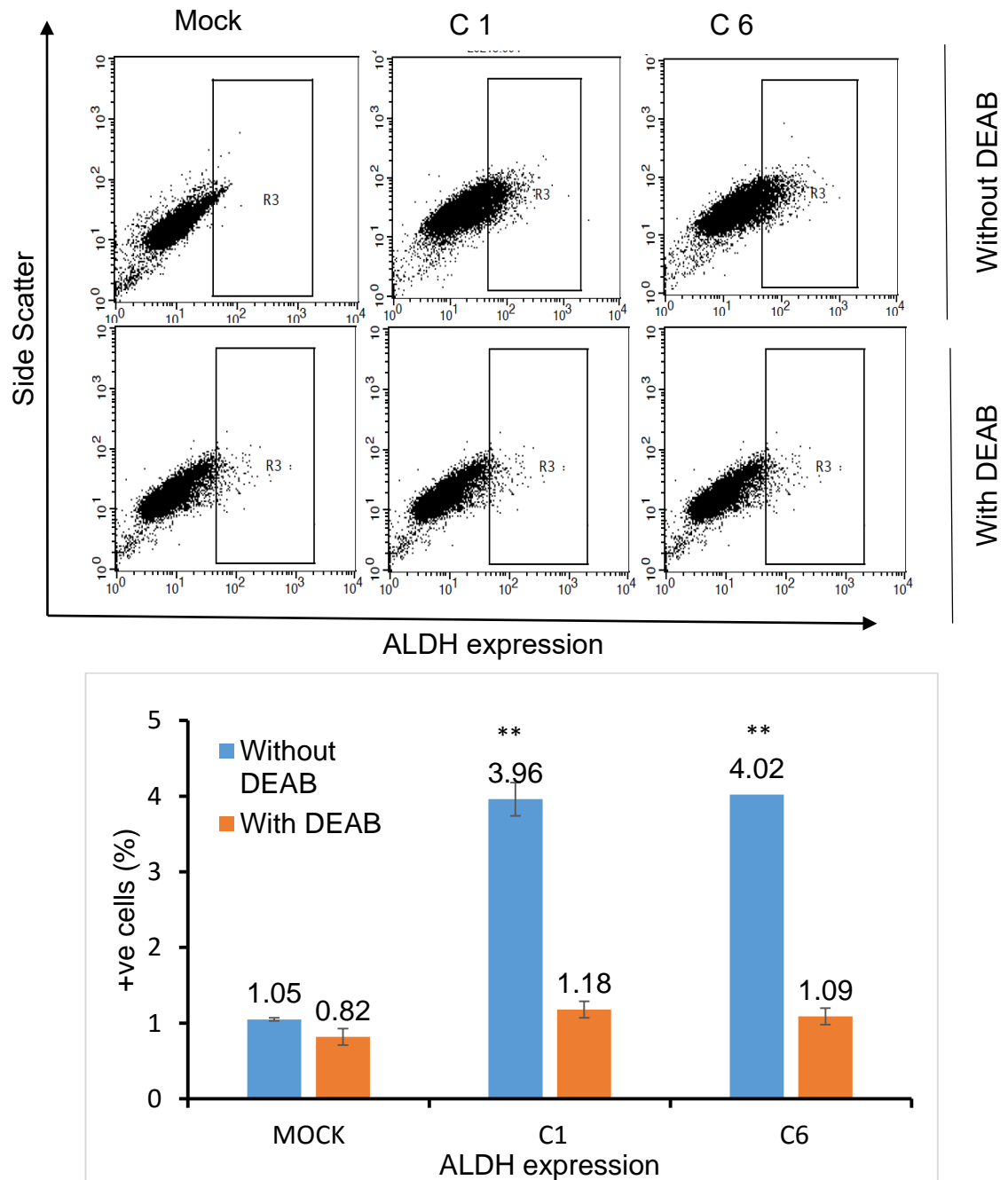


Figure 4.4.(A). Representative FACS Plots of ALDH expression in MDA-MB 231 NFκBp65 transfected cells measured by ALDEFLUOR assay. FACS data shows ALDH activity in mock and NFκBp65 transfected clones (C1 and C6) with and without treatment with DEAB (30μM). NFκBp65 transfected clones (C1 and C6) expressed high percentage of ALDH⁺ compared to the mock cells before treatment with DEAB. Histograms (median ± interquartile range) displays the statistically significant increase in the ALDH⁺ activity in NFκBp65 transfected clones (C1 and C6) in comparison to mock cells (Kruskal-Wallis test, ** $p < 0.0001$, $n = 9$). After treatment with DEAB, there was no statistical difference in ALDH⁺ cell from both cultures (Kruskal-Wallis test, $p > 0.05$). (Abbreviations: DEAB: Diethylaminobenzaldehyde; ALDH: Aldehyde dehydrogenase active).

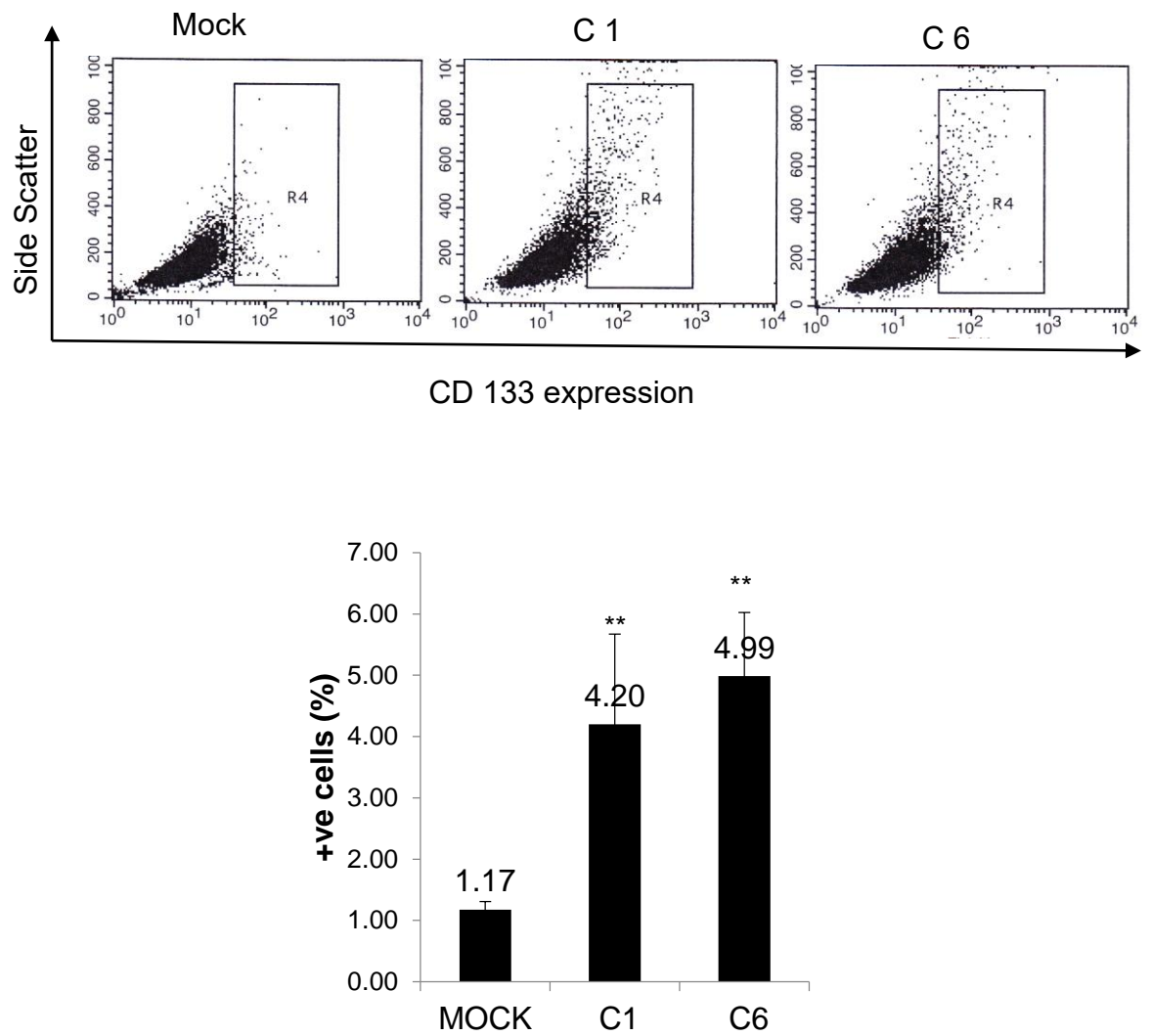


Figure 4.4B. Representative FACS Plots of CD133 expression in MDA-MB 231 NFκBp65 cell line measured using CD133-PE conjugated antibody. FACS data shows that CD133 expression was significantly higher in the transfected cells (C1 and C6) when compared to the Mock cells. Histograms (median \pm interquartile range) above displays statistically significant increase in CD133 expression in transfected cells (C1 and C6) compared to the mock (Kruskal-Wallis test, $**p < 0.001$ $n=9$).

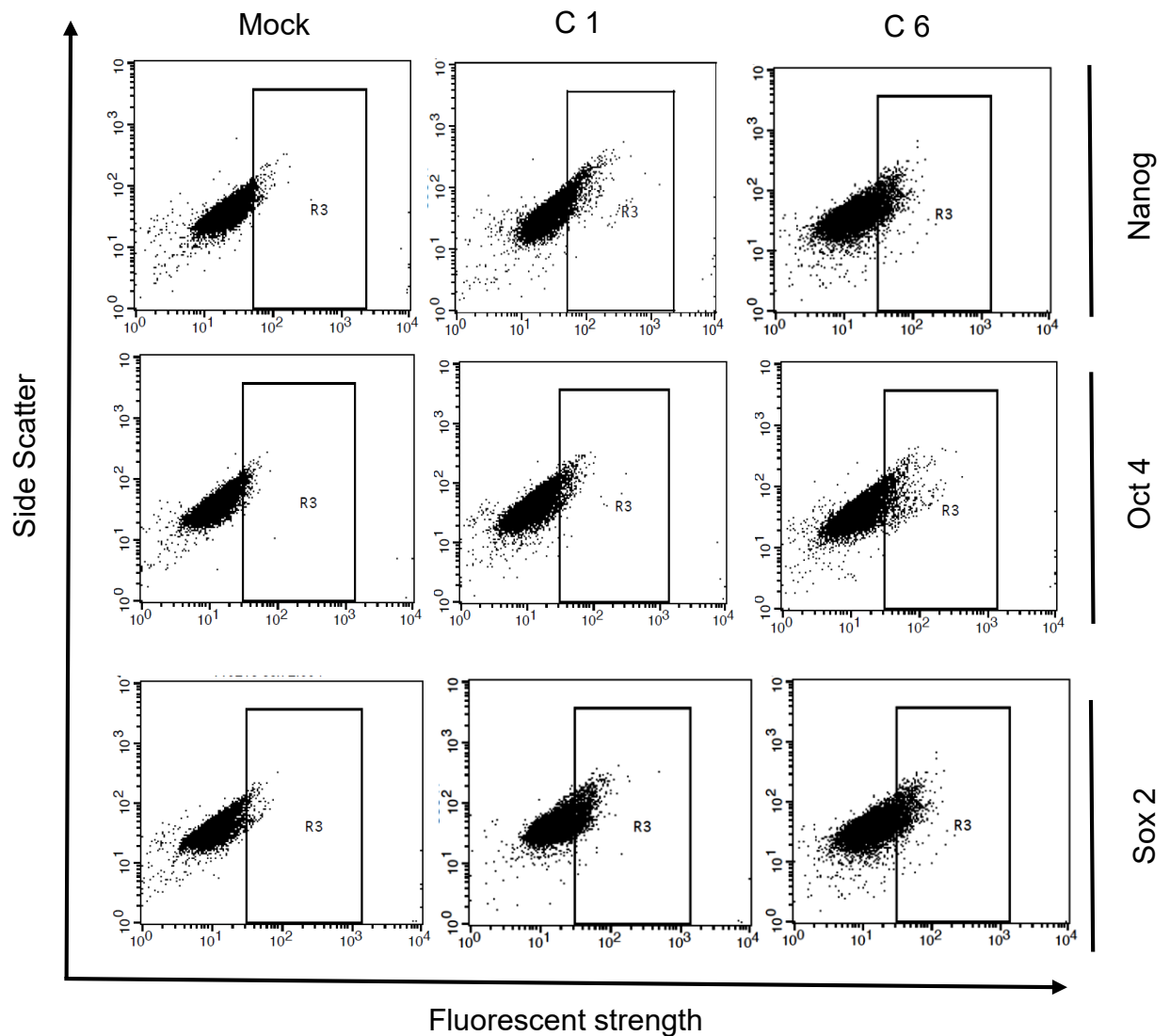


Figure 4.5(A). Representative FASC Plots of Embryonic Stem cell markers Expression in MDA-MB 231 NF κ Bp65 BC cell line. FASC data shows that higher expression of embryonic stem cell markers (Nanog, Sox2 and Oct4) were displayed in the NF κ Bp65 overexpressing clones (C1 and C6) compared to Mock cells.

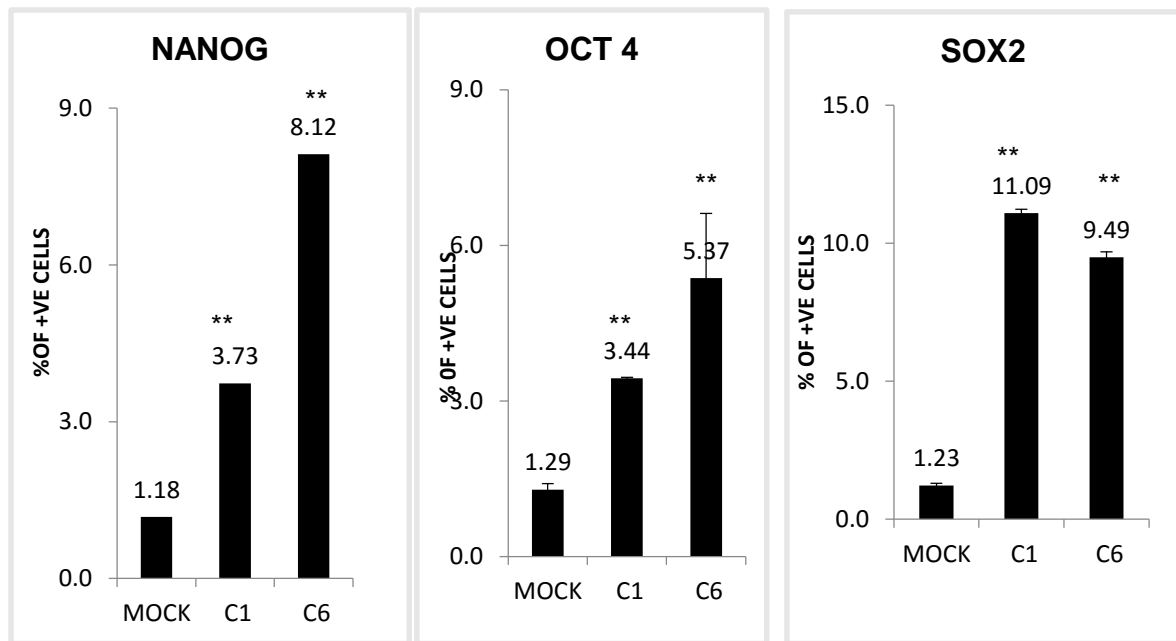


Figure 4.5B Bar Chart Representative of Expression of Embryonic markers in MDA-MB 231 NFκBp65 cell line. Histograms (median \pm interquartile range) above displays significant increase in all three embryonic markers (Nanog, OCT4 and Sox2) markers in transfected cells (C1 and C6) compared to the Mock cells (Kruskal-Wallis test, ** $p < 0.001$ $n=9$).

4.3.5. NFκBp65 overexpression induced EMT in MDA-MB 231 cell line

Results from Chapter 3 showed that EMT is induced under hypoxic conditions. Overexpression of NFκBp65 in TNBC cell line MDA-MB 231 also induced higher expression of EMT markers Vimentin and N-cadherin with accompanying decrease in E-cadherin expressions (Figure 4.6), this cadherin switch indicates the cells acquired a more mesenchymal characteristic.

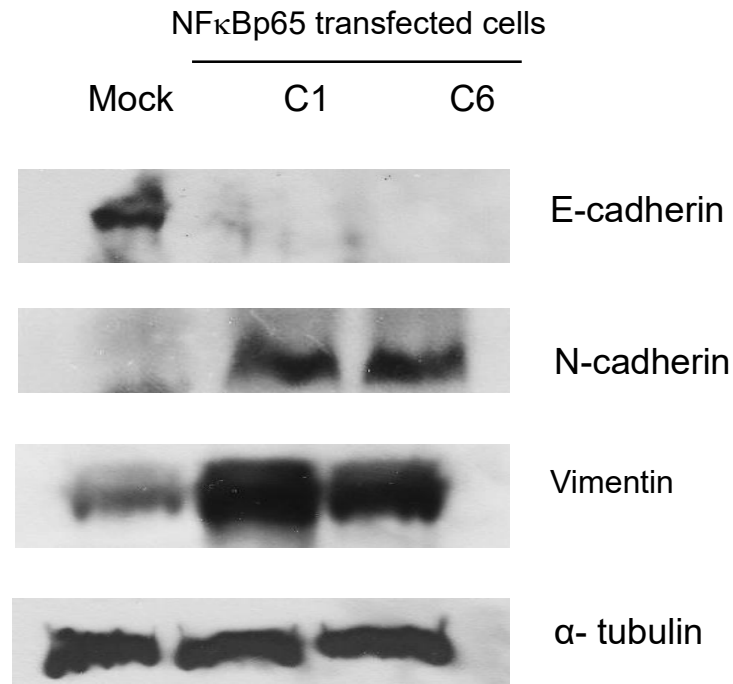


Figure 4.6. Representative Western Blots of EMT markers in Mock and NFκBp65 transfected cell. NFκBp65 overexpressing cells C1 and C6 exhibits EMT features displayed as decreased expression of epithelial marker E-cadherin and increased expression of mesenchymal markers (N-cadherin and vimentin) in comparison to Mock cells indicating EMT is induced by increase in NFκBp65 activity. Tubulin was used as loading control.

4.3.6. Increase in NFκBp65 expression induced higher migration and invasion

Further confirmation of hypoxia-induced EMT and transformation of cells into mesenchymal phenotype was done by analysing the migratory potential of cells under hypoxia. NFκBp65 overexpressing cells (C1 and C6) showed significant increase in migratory and invasive potentials compared to the Mock cells (Figure 4.7 and 4.8).

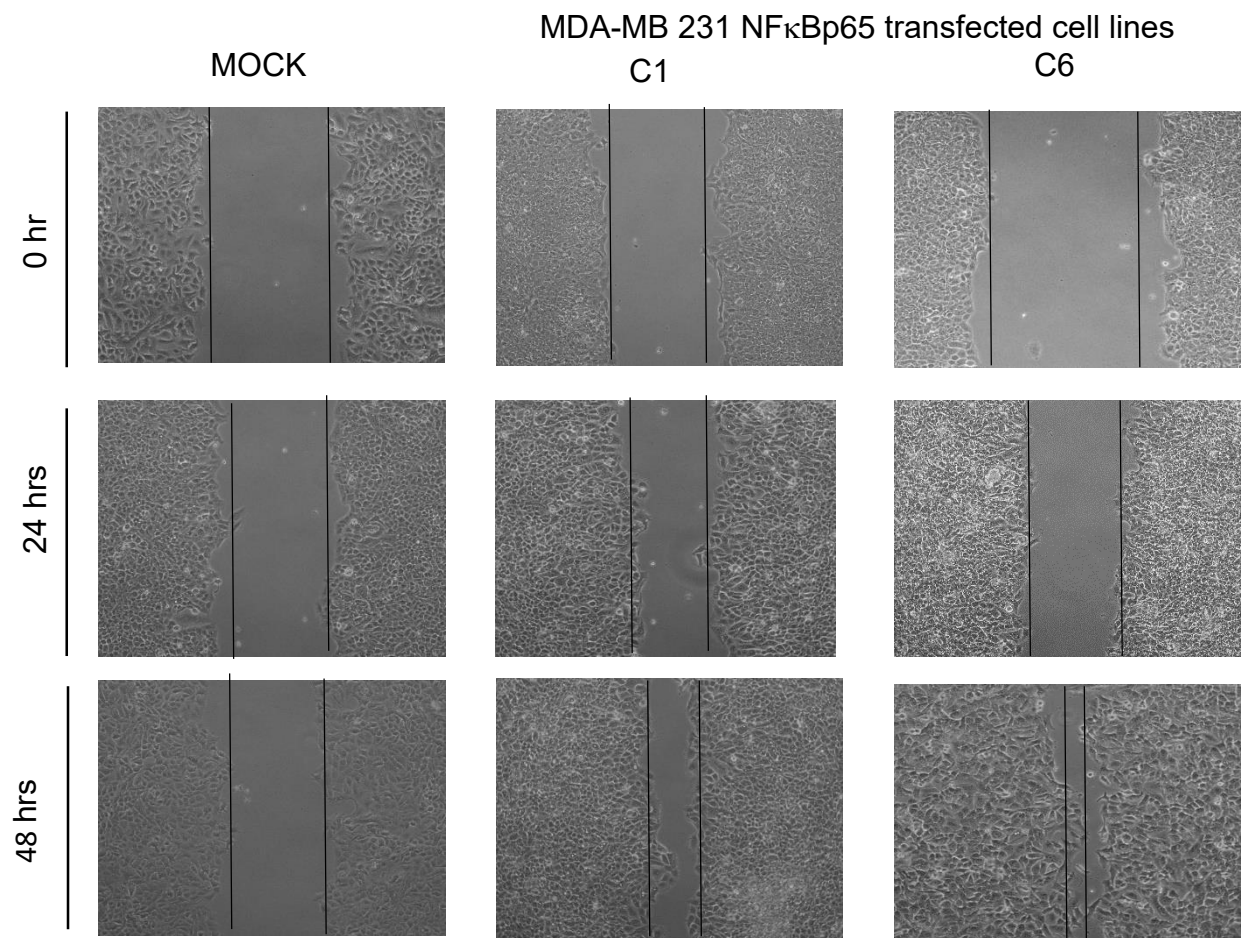


Figure 4.7 Representative Migration (wound healing) assay Images of Mock and NF κ Bp65 transfected cells. Images (Magnification 10X) taken shows that the cells overexpressing NF κ Bp65 are highly migratory compared to Mock cells. Images after 48 hours showed that NF κ Bp65 overexpressing cells (C1 and C6) had a higher migratory potential than Mock cells.

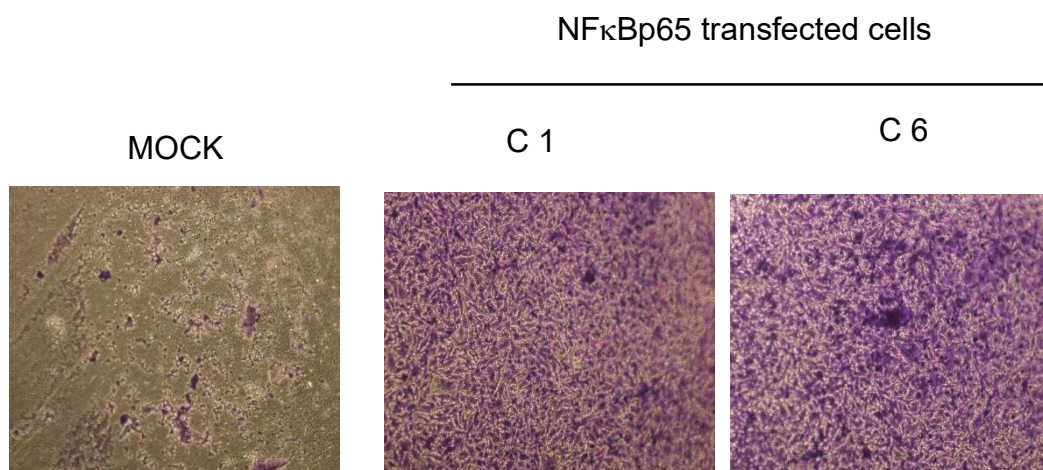


Figure 4.8 Representative Matrigel Invasion assay Images of Mock and NF κ Bp65 transfected cells. Images (Magnification 20X) taken after 3 days shows that the cells overexpressing NF κ Bp65 have high invasive properties in comparison to that of mock cells indicating EMT activation in these cells.

4.3.7. Inhibition of NF κ Bp65 decreased the migratory and invasive potential in MDA-MB231 cell line

Increase in NF κ Bp65 activity in BC cell line induced increase in migration and invasion potential as shown from our results above. Inhibition of NF κ Bp65 with an inhibitor resulted in a decrease in migratory potential of cells (Figure 4.9 A and B).

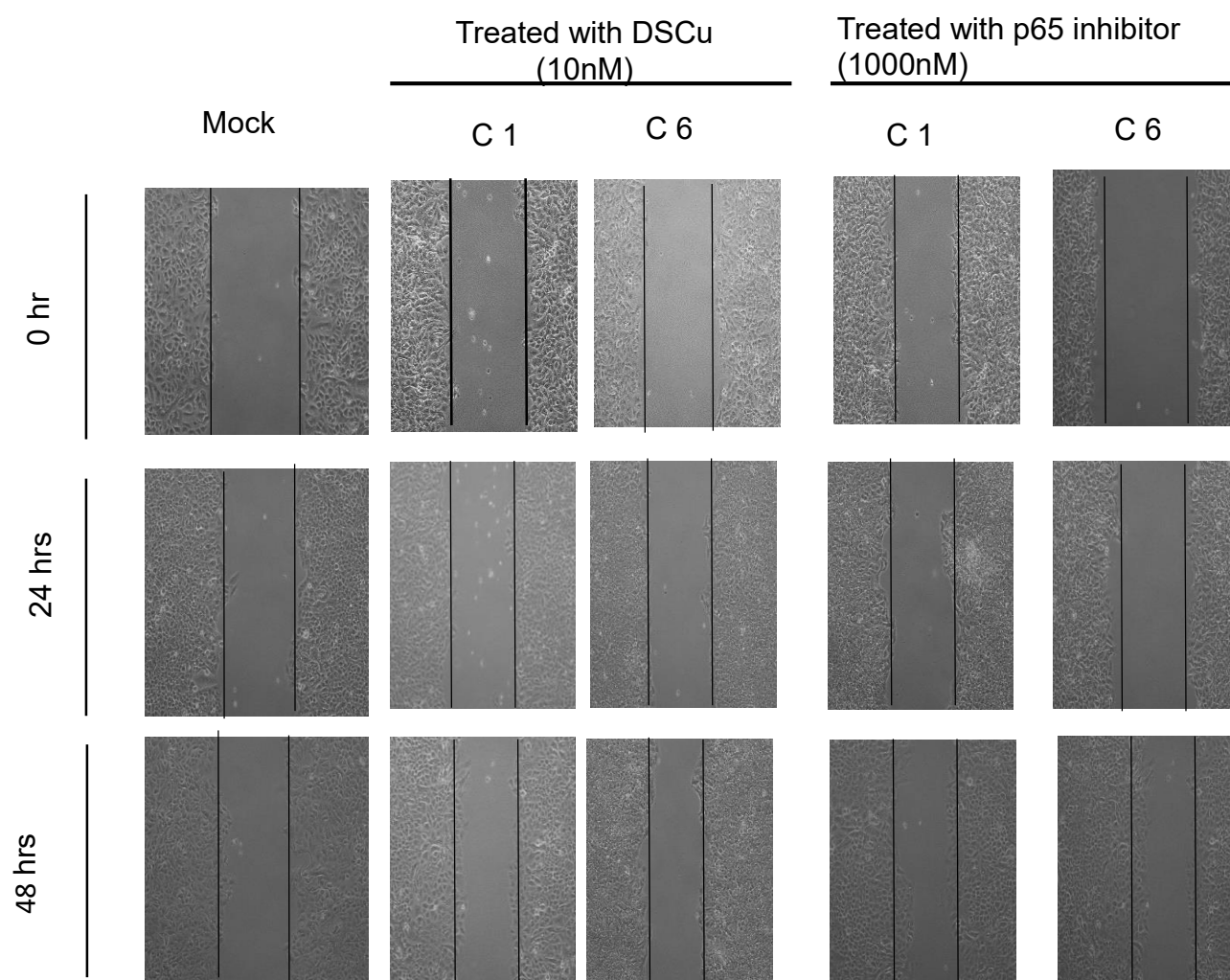


Figure 4.9. Representative Migration assay Images of Mock and NF κ Bp65 transfected cells inhibited with small molecules and DS/Cu. Images (Magnification 10X) taken shows that inhibition NF κ Bp65 subunit by p65 inhibitor or DS/Cu decreased the migration of NF κ Bp65 transfected cells even after 48 hours.(DS: disulfiram, Cu: copper).

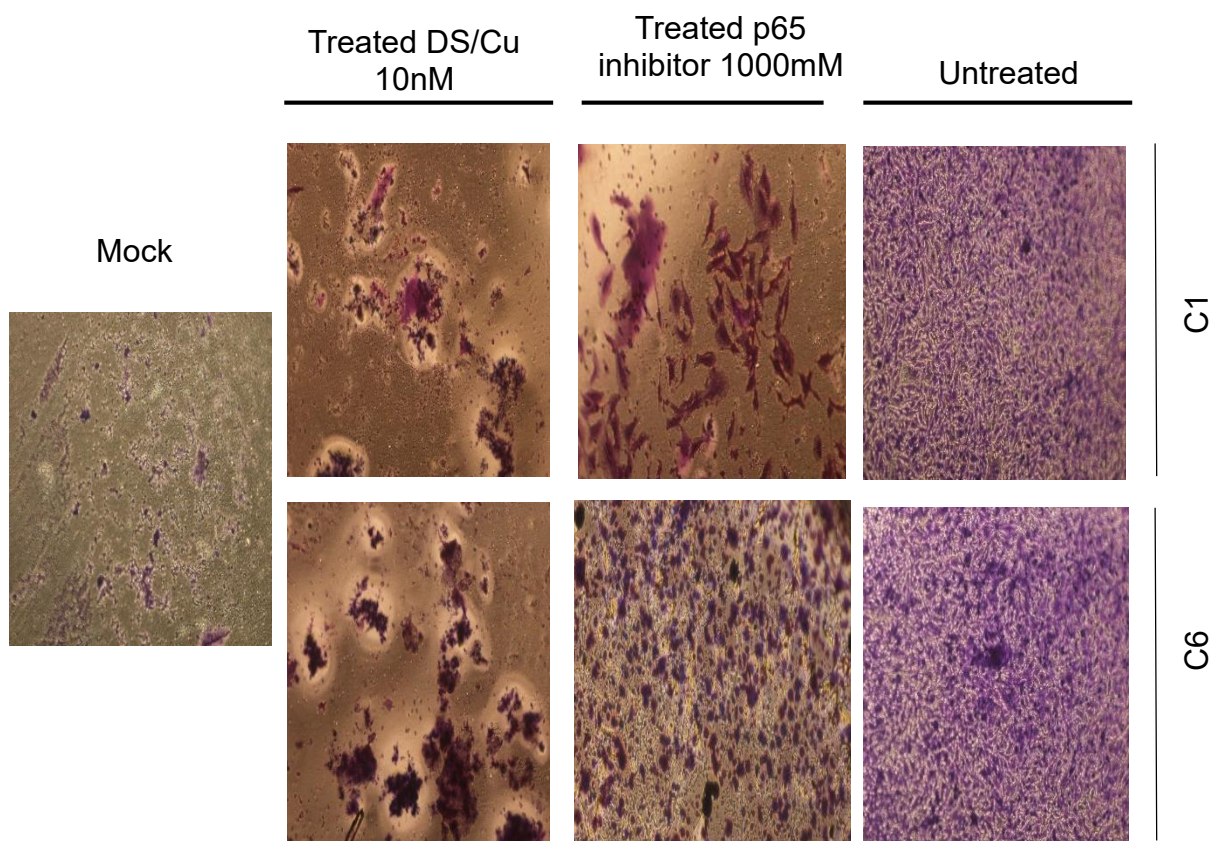


Figure 4.9B. Representative Matrigel Invasion assay Image of Mock and NF κ Bp65 transfected cells inhibited with small molecules and DS/Cu. Images (Magnification 20X) taken shows that inhibition of NF κ Bp65 decreased the invasiveness of NF κ Bp65 transfected cells after treated of cells with DS plus copper and p65 inhibitor (DS: disulfiram, Cu:copper).

4.3.8 NF κ Bp65 transfection induced HIF activity

Scortegagna *et al.*, (2008) reported that loss of HIF1 α activity decreased NF κ B activation and p65 expression while increase in HIF1 α expression resulted in hyperphosphorylation of I κ B and phosphorylation of p65 at Ser²⁷⁶ in keratinocytes. NF κ B also induces HIF2 α by the interaction between IKK γ and CBP/p300 (Tian *et al.*, 2012). Results from western blot analysis showed that HIF

proteins were overexpressed in the NF κ Bp65 positive clones C1 and C6 (Figure 4.10).

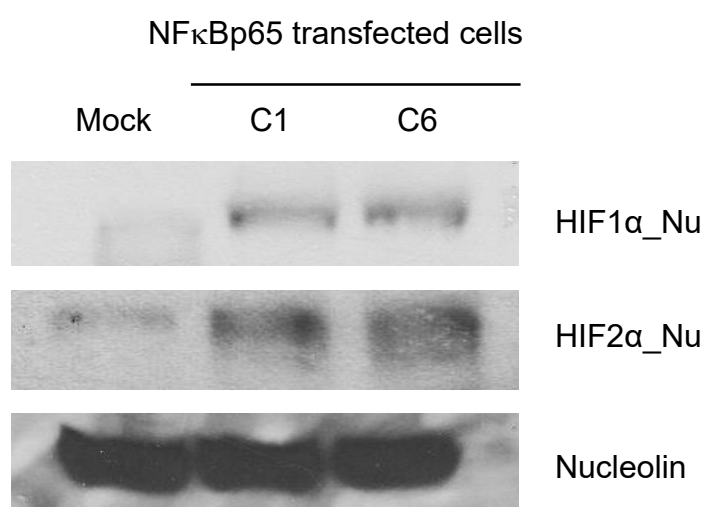


Figure 4.10. Representative Western Blots of HIF1 α and HIF2 α expression in NF κ Bp65 MDA-MB 231 transfected cell. Nuclear translocation of HIF1 α and HIF2 α was displayed in NF κ Bp65 overexpressing cells C1 and C6. Nucleolin was used as loading control (Abbreviation; HIF: hypoxia-inducible factor).

4.4. Discussion

Breast cancer stem cells (BCSCs) play pivotal role in the propagation of tumour existence, treatment resistance and cancer relapse (Kakarala and Wicha, 2008; Coker and Allan, 2008). Several reports revealed that hypoxia is crucial for stemness of cells as it provides a conducive environment 'Stem cell niche' for the maintenance of these self-renewing cells (Rosen and Jordan 2009; Lin and Yun, 2010). This is in line with my results as hypoxia induced a stem cell-like phenotype in triple negative breast cancer (TNBC). NF κ B, a family of transcription factors is one of the many transcription factors activated during hypoxia to ensure the survival of cells during hypoxic insults. Dysregulation of NF κ B activation results in persistent nuclear translocation of proteins such as p50, p52, p65, cRel

and RelB, which disrupts the balance between cell proliferation and death through the upregulation of anti-apoptotic proteins (Karin and Lin, 2002). NF κ B is widely overexpressed in many cancers such as pancreatic cancers, breast cancer, brain cancer, colon cancer (Biswas *et al.*, 2004).

Resistance in breast cancer (BC) is a complex process and several studies have revealed that BC cells with stem cell-like properties are highly resistant to cancer drugs (Al-Hajj *et al.*, 2003; Hambardzumyan *et al.*, 2006; Dave and Chang, 2009). These BC stem cells with stem cell phenotype are defined by expression of surface markers such as ESA+, CD44+, CD24- (Clarke and Fuller, 2006; Lynch *et al.*, 2006; Polyak and Hahn, 2006). Data from this study reveal that that hypoxia induced the activation and expression of NF κ B in monolayer cells cultured under hypoxia (Figure 4.2). Flow cytometry analysis of my data showed that the transfected cells (C1 and C6) displayed higher expression of stem cell markers ALDH, CD133 and embryonic stem cell markers (Nanog, Oct4 and Sox2) compared with mock cells. These results suggest that NF κ B activation can induce stem-like features in cancer cells which is consistent with the report by Takase *et al.*, (2013) which demonstrated that NF κ B, especially p65, play crucial role in the maintenance of pluripotency of cells.

NF κ B is the main chemoresistant anti-cancer factor activated during chemoresistance in many human tumours. Constitutively elevated NF κ B levels have been reported in oestrogen receptor negative primary tumours which can be further increased by chemotherapy (Biswas *et al.*, 2000). A studies by Wang *et al.*, (2003) demonstrated that high NF κ B activity is linked with chemoresistance as it triggers the upregulations of antiapoptotic genes that block the induced

apoptosis by anticancer drugs. Results from my study showed that NF κ B induced resistance to anticancer drugs (Figure 4.3), which is consistent with other studies (Guo *et al*, 2009; Wang *et al.*, 2003). This elevated NF κ B activity in TNBC has been suggested to be responsible for chemoresistance and metastatic growth.

Metastasis the spread of primary tumours to secondary organs and sites contributes to over 90% of cancer mortality (Christofori, 2006). EMT features induces the loss of epithelial markers (E-cadherin and α and γ catenin), with associated gain in mesenchymal cell markers (fibronectin, vimentin, and N-cadherin), leading to the acquisition of migratory and invasive properties (Huber *et al.*, 2005). NF κ B signalling has been associated with EMT as evidence show that activation of NF κ B pathway is required for the induction and maintenance of Ras and transforming growth factor (TGF) β -dependent EMT. Furthermore, NF κ B binds to a promoter in E-cadherin repressor ZEB-1/2 resulting in regulation of the EMT phenotype (Chua *et al.*, 2007). The NF κ B transfected cells were observed to have higher migratory and invasive potential indicating that NF κ B may indeed be essential for metastasis (Figure 4.6, 4.7 and 4.8). This hypothesis was further confirmed as inhibition of NF κ B with small molecule inhibitor and DS reduced the invasive and migratory potentials in the transfected cell lines (Figure 4.9 A and B). This is consistent with the reports by Huber *et al.*, (2004) as blocking of NF κ B activity revoked the metastatic potential of mammary epithelial cells in a mouse model system.

Conclusion

NF κ B promotes expression of antiapoptotic proteins protecting cells from apoptosis induced by chemotherapeutic agents contributing to chemoresistance of tumours. Hypoxia induced NF κ B activation may be important for the maintenance of CSCs during the development and progression of tumours. TNBC lacks targetable receptors, NF κ B may be considered as a potential therapeutic target for TNBC as inhibition of NF κ B increases the sensitivity of cancer cells to chemotherapeutic drugs.

Chapter Five

The role of hypoxia inducible factors in hypoxia induced EMT and chemoresistance in breast cancer

5.1 Introduction

Many human cancers have significantly lower O₂ concentration when compared to surrounding normal tissues. This persistent reduction in O₂ availability induces the HIFs, HGF, 'SNAIL', 'TWIST', Notch and NFκB pathways which regulates several cancer biological processes such as cell immortalization and stem cell maintenance, glucose and energy metabolism, vascularization, genetic instability, invasion and metastasis and resistance to therapy (Xia *et al.*, 2009; Semenza, 2010). A study reported that there are regions of hypoxia or anoxia within solid tumours caused by poor or altered vascularization and deterioration of diffusion geometry which results in limited oxygen diffusion and delivery (Vaupel and Mayer, 2007). This decrease in oxygen tension may be detrimental to some tumour cells however hypoxia can contribute to a selection of cells that are more aggressive and promote tumour growth (Semenza, 2000; Harris, 2002), leading to poor prognostic outcome and an increased risk for metastasis that may escape therapy (Tatum *et al.*, 2006). Neoplastic cells surviving in hypoxia display increased invasive tendency suggesting that hypoxia may favour cancer progression (Semenza, 2002; Le *et al.*, 2004).

Under hypoxia, several transcription factors are activated, one of such is the hypoxia-inducible factors (HIF-1 and HIF-2) referred to as the master regulators for hypoxia. HIF1α and HIF2α are commonly over expressed in malignant cells and is greatly associated with poor prognosis in many breast cancers (Schindl *et al.*, 2002; Bos *et al.*, 2003).

5.1.3 Rationale and aims of this study

This study was carried out to investigate the role of HIF1 α and HIF2 α in hypoxia induced EMT and related stemness and to find out if HIF1 α or HIF2 α functions as the driving force behind chemoresistant CSCs in TNBC.

5.2 Experimental Design

General materials, products, labwares, manufacturers and methodologies used for the entire study have been described in details in chapter 2. Specific materials, methods and experimental design used for this part of this study are stated below.

5.3.1 Stable transfection of MDA-MB 231 cell line with HIF1 α and HIF2 α

HIF1 α and HIF2 α were overexpressed in breast cancer cell line after transfection with HIF1 α and HIF2 α pCMV6 subunits respectively. The mock transfected cells containing empty pCMV6 vector were controls for HIF expression (refer to Chapter 2, page 84).

5.3.2 Determination of CSC markers in HIF transfected cells

Over expression of the HIF protein should induce an increase in CSC markers which were measured by flow cytometry (refer to Chapter 2, page 78).

5.3.3 Determination of EMT characteristics in HIF transfected cells

Pervious results from chapter 3 show that EMT features were induced in cells grown under hypoxia. I expect the HIF transfected cells to also follow the same trend with cells overexpressing both HIF1 α and HIF2 α displaying mesenchymal characteristics. EMT markers were determined by western blot, *in vitro* wound

healing assay and transwell invasion assay were performed (refer to Chapter 2, page 85 and 86).

5.3.3 MTT cytotoxicity assay for HIF transfected cells

The drug sensitivity of Mock and HIF transfected cells were determined by MTT assay (refer to Chapter 2, page 71).

5.4 Results

5.4.1 Stable transfection HIF1 α in MDA-MB 231BC cell line

Mock cells and two clones (C3 and 4) with the highest expression of HIF1 α cultured in media containing 150 μ g/ml of G418 were chosen for further testing. Western blot results (Figure 5.1) show that clones 3 and 4 expressed higher levels of HIF1 α .

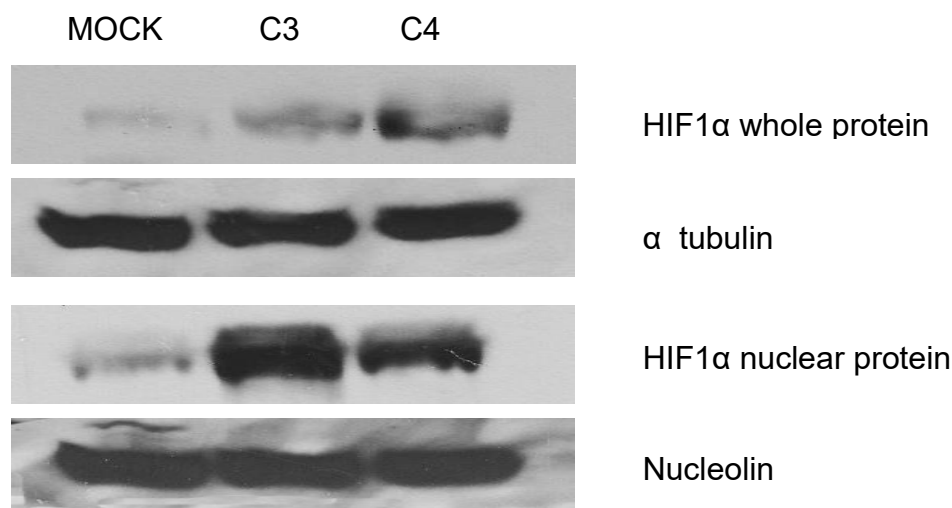


Figure 5.1. Representative Western Blots of Mock and HIF1 α transfection cells:

MDA-MB 231 cell line was successfully transfected with pCMV6-HIF1 α to increase the expression of HIF1 α protein. Western blot analysis of whole cell lysates and nuclear protein from mock transfected cells and two clones (C-3 and C-4) revealed an increased expression and nuclear translocation of HIF1 α in the positive clones in comparison to that of Mock cells. Tubulin and Nucleolin were used as loading control.

5.4.2 Overexpression HIF1 α in breast cancer cells induces higher expression of CSC markers.

Data from FACS analysis (Figure 5.2 and 5.3) showed that the HIF1 α over expressing clones C3 and C4 had significantly higher expression of CSC markers (ALDH and CD 133) and embryonic stem cell markers (Sox2, Oct4 and Nanog) when compared to the mock (Figure 5.4).

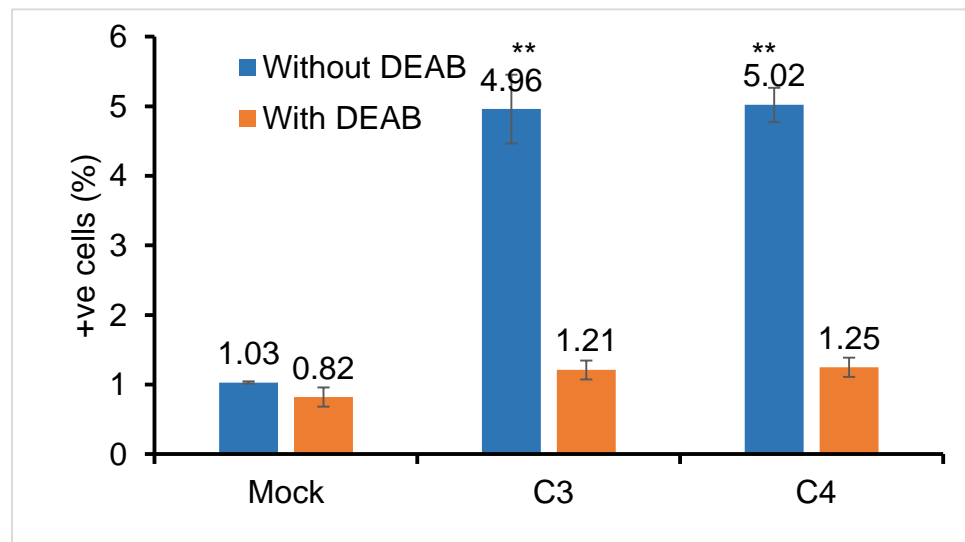
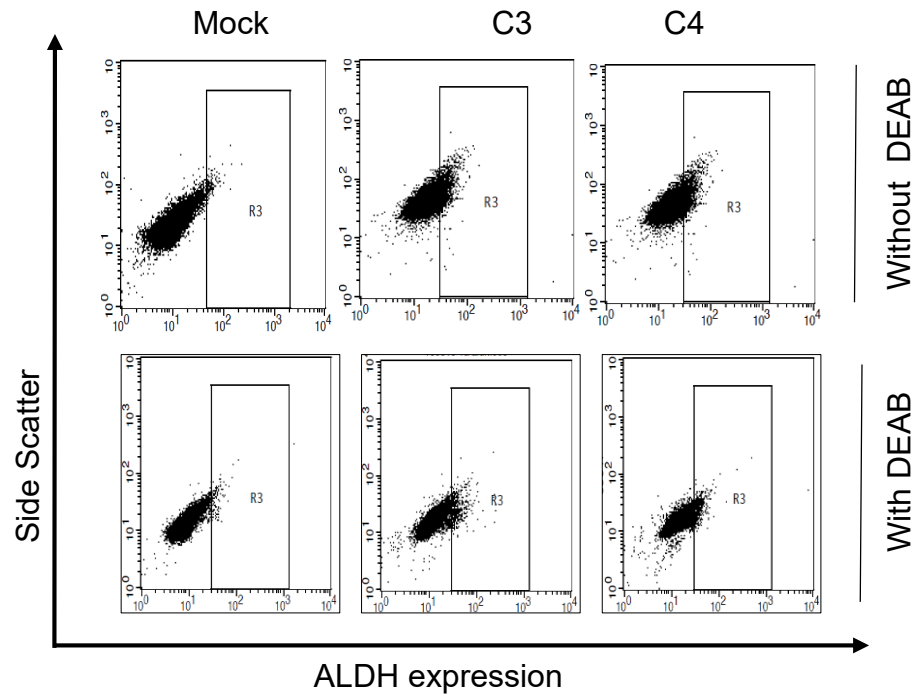


Figure 5.2. Representative FACS Plots of ALDH expression in MDA-MB 231 HIF1 α transfected cells measured by ALDEFLUOR assay. FACS results shows ALDH expression in Mock and HIF1 α transfected clones (C3 and C4) with and without treatment with DEAB (30 μ M). HIF1 α transfected clones (C3 and C4) expressed high percentage of ALDH⁺ compared to the mock cells before treatment with DEAB. Histogram (median \pm interquartile range) displays the statistically significant increase in the ALDH⁺ activity in HIF1 α transfected clones (C3 and C4) in comparison to mock cells (Kruskal-Wallis test, ** p < 0.0001, n = 9). After treatment with DEAB, there was no statistical difference in ALDH⁺ cell from both cultures (Kruskal-Wallis test, p > 0.05). (Abbreviations: DEAB: Diethylaminobenzaldehyde; ALDH: Aldehyde dehydrogenase active)

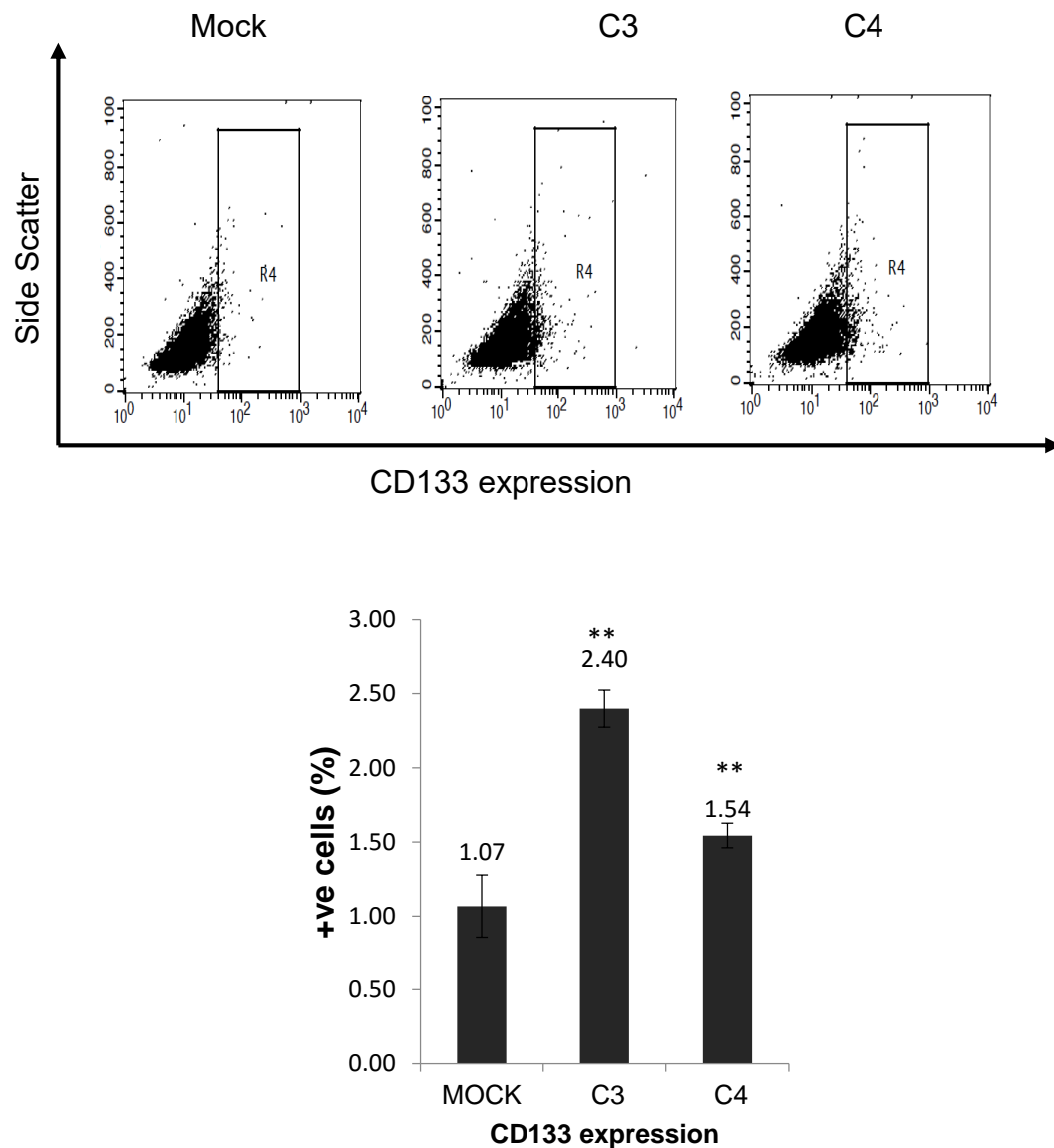


Figure 5.2. Representative FACS Plots of CD133 expression in MDA-MB 231 mock and HIF1 α transfected cells measured by PE-CD133 immunostaining assay. FACS data shows CD133 expression in mock and HIF1 α transfected clones (C3 and C4). There was an increase in the expression of CD133 in the HIF1 α overexpressing clones (C3 and C4) compared to mock cells. Histograms (median \pm interquartile range) displays the statistically significant increase in the CD133 expression in HIF1 α positive clones C3 and C4 in comparison to mock transfected cells (Kruskal-Wallis test, ** $p < 0.05$ $n = 9$).

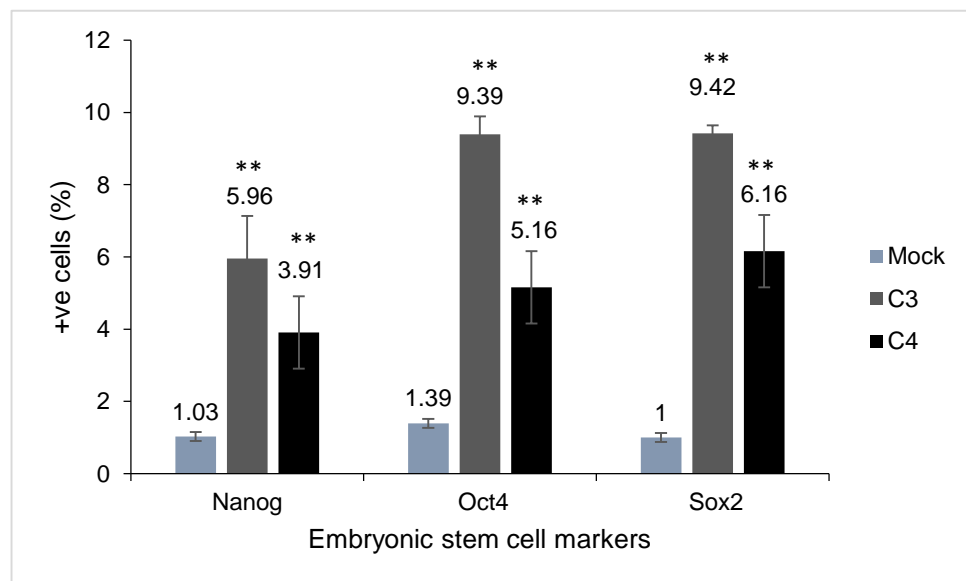
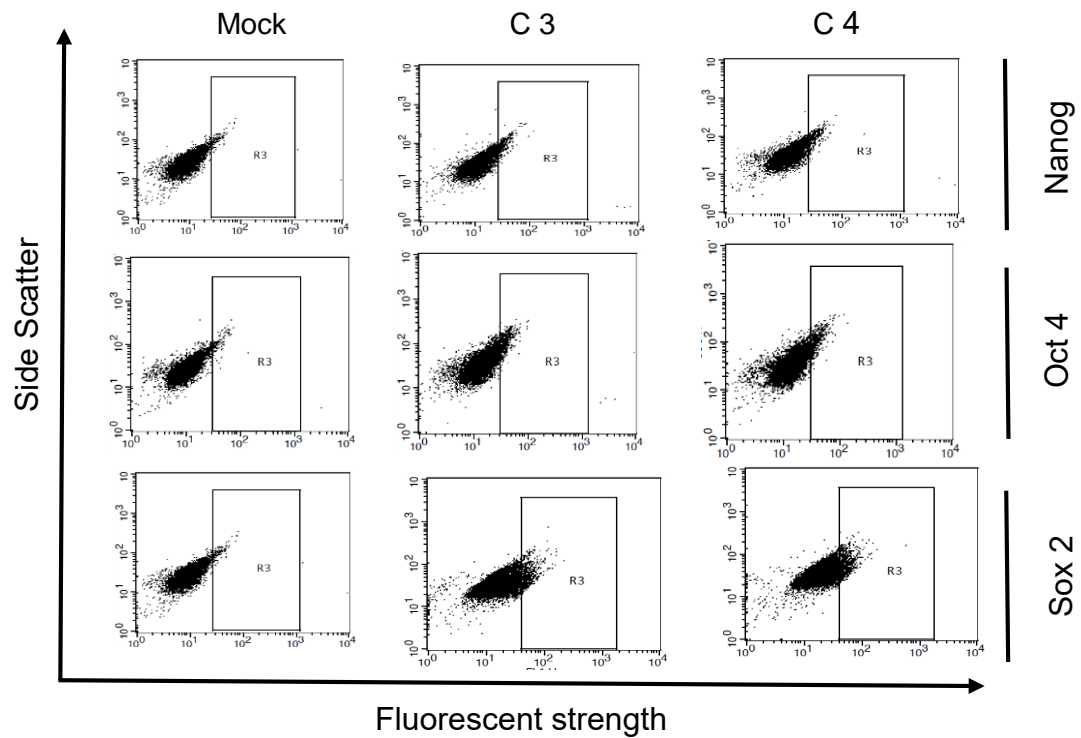
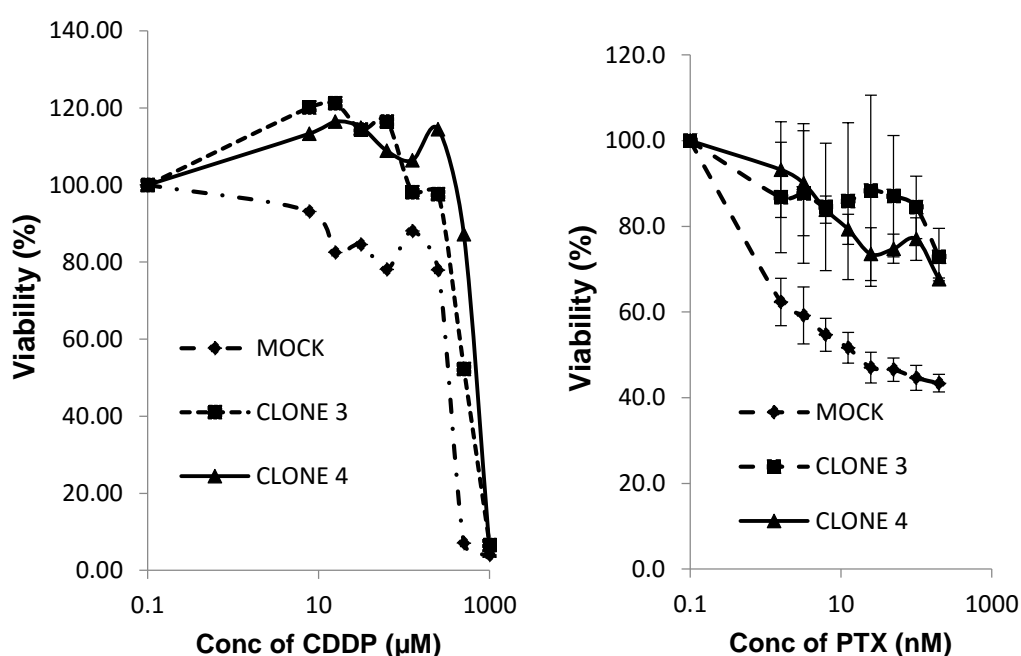


Figure 5.3. Representative FACS Plots of Embryonic Stem cell markers expression in MDA-MB 231 HIF1 α transfected cell. Fluorescence Activated Cell Sorting (FACS) data shows data shows that higher expression of embryonic stem cell markers nanog, Sox2 and Oct4 were displayed in HIF1 α transfected clones (C3 and C4) compared to mock cells. Histograms (median \pm interquartile range) above displays statistically significant increase in all three embryonic markers (Nanog, Oct4 and Sox2) markers in transfected transformed cells (C3 and 4) when compared to the mock (Kruskal-Wallis test, ** $p < 0.05$ $n = 9$).

5.3.3 Increase in HIF1 α activity induces resistance to anticancer drugs

Results from chapter 3 and 4 already show that both hypoxia and NF κ Bp65 overexpression induce chemoresistance to anticancer drugs. MTT cytotoxicity results showed that HIF1 α positive clones C3 and C4 were extremely resistant to all five anticancer drugs (cisplatin, doxorubicin, vincristine, paclitaxel and gemcitabine) tested compared to the Mock cells. Figure 5.4 shows the cell viability curves and bar charts for the IC₅₀ values for the five anticancer drugs indicating that increase HIF1 α protein is able to drug resistance in cells.



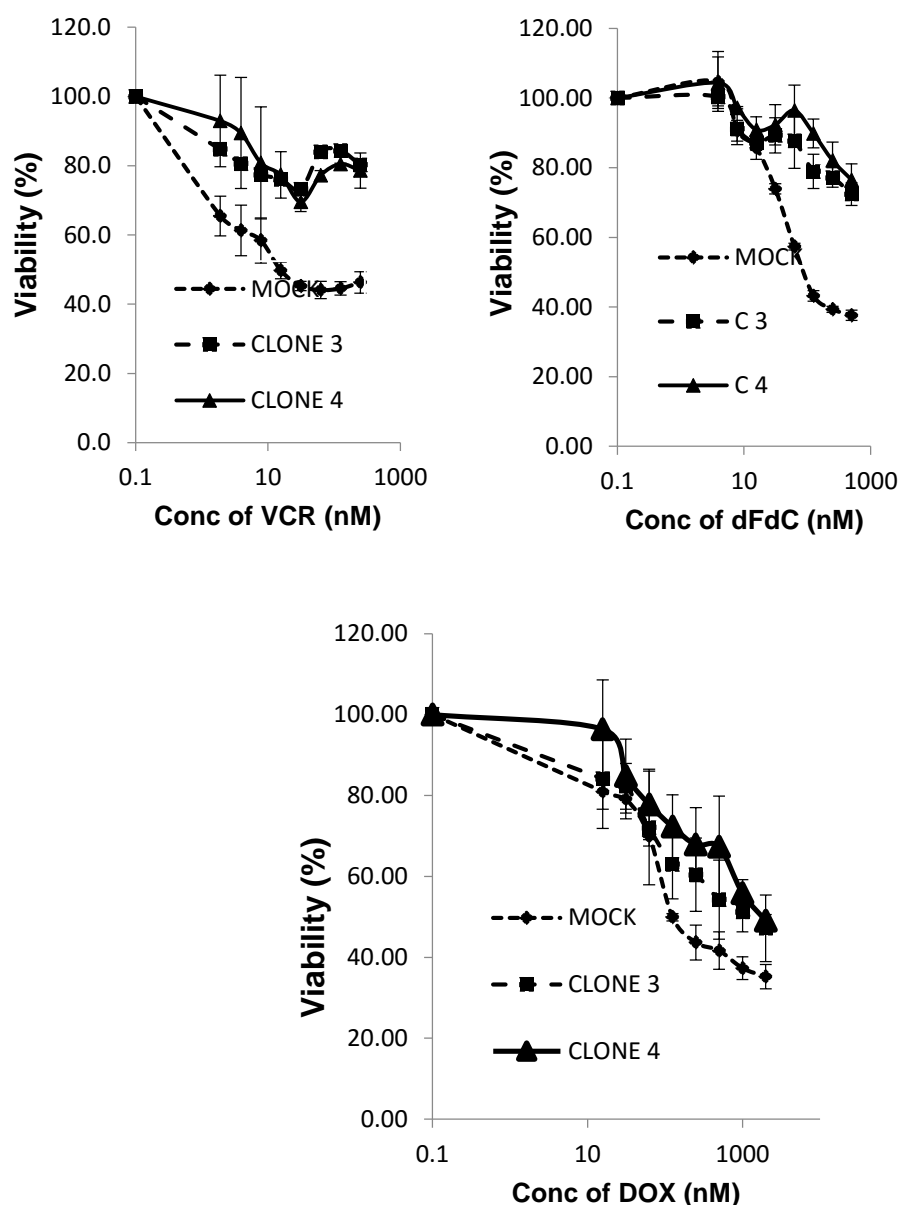


Figure 5.4. Representative Drug Concentration Response Curves of Mock and HIF1 α transfected cells after treatment with anticancer drugs CDDP, VCR, PTX, dFdC and DOX. The cell viability curves from MTT analysis shows the dose response of mock and HIF transfected cells (C3 and C4) to conventional anticancer drugs CDDP, VCR, PTX, dFdC and DOX. (Abbreviations; CDDP: cisplatin, VCR: vincristine, PTX paclitaxel, dFdC: gemciatbine and Dox: doxorubicin).

Table 5.1 IC₅₀ values of some Anticancer Drugs in Mock and HIF1 α Transfected Cells

Anti -cancer drug	IC ₅₀ Mock	IC ₅₀ HIF1 α C3	IC ₅₀ HIF1 α C4	H- value	p-value
Cisplatin (μ M)	201 \pm 20.61	> 500	> 500	19.53	0.002**
Paclitaxel (nM)	20.56 \pm 10.67	> 200	> 200	26.32	0.0001**
Vincristine (nM)	16.89 \pm 5.33	> 150	>150	22.67	0.0001**
Gemcitabine (nM)	30.49 \pm 9.81	> 500	> 500	38.78	0.0001**
Doxorubicin (nM)	300.11 \pm 8.73	> 1000	> 1000	27.10	0.0001**

Table 5.1 displays the results (median \pm interquartile range) of half maximum inhibitory concentration (IC₅₀) values of HIF1 α transfected cells and mock cells. The HIF1 α transfected cells were found to have higher IC₅₀ and were significantly resistant to these conventional anticancer drugs compared to the mock cells. (Kruskal-Wallis test, ** p<0.05, n=9).

5.3.4 Cells with increase HIF1 α activity displayed mesenchymal properties.

Expression of mesenchymal proteins vimentin and N-cadherin in HIF1 α positive clones were observed as shown from western blot analysis in Figure 5.5, with a loss of the epithelial marker E-cadherin. In the mock cells the E-cadherin expression was high with decreased expression of vimentin and N-cadherin suggesting an epithelial phenotype in these cells.

Images taken from wound healing scratch assay and matrigel invasion assay in HIF1 α transfect clones and mock cells showed that the HIF1 α clones C3 and C4 have increased invasive potential when compared to the mock transfected cells

(Figures 5.6 and 5. 7). These results show that HIF1 α overexpression in cells is able to induce a more mesenchymal phenotype.

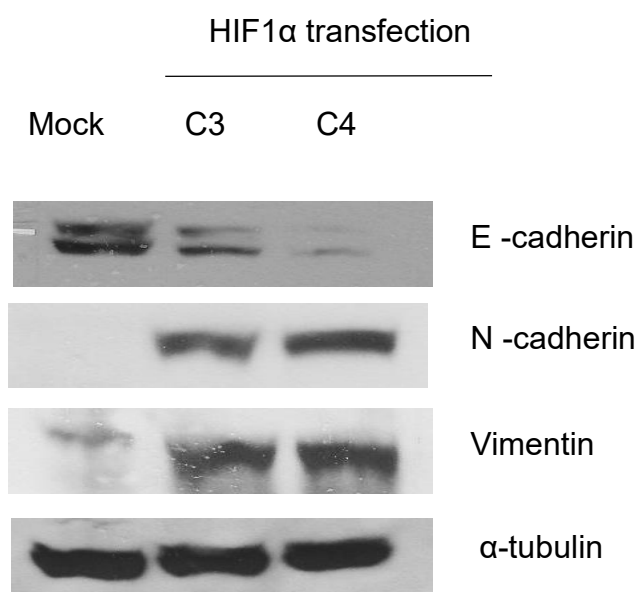


Figure 5.5. Representative Western Blots of EMT markers in Mock and HIF1 α transfected cells using whole cell lysates. The results shows that expression of E-cadherin was decreased in HIF1 α transfection clones and increased expression of mesenchymal markers (N-cadherin and vimentin) in comparison to that of Mock cells indicating epithelial to mesenchymal transition (EMT) activation in the these cells. Tubulin was used as loading control.

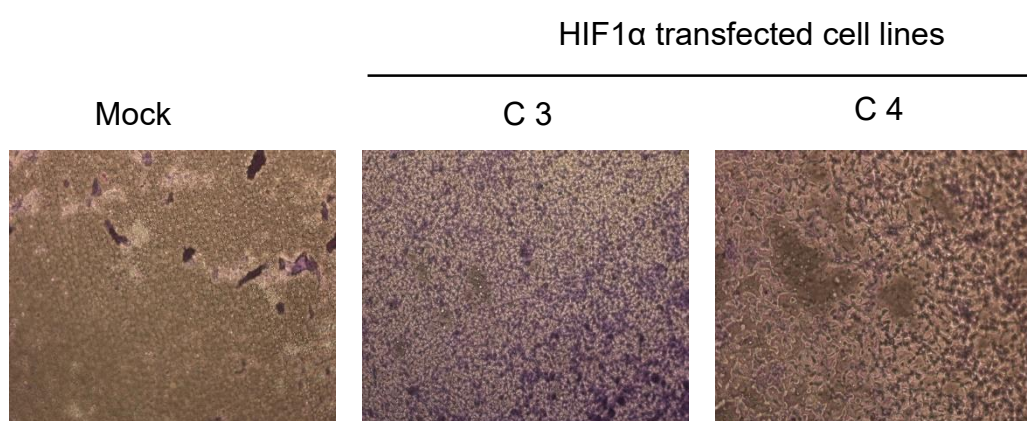


Figure 5.6. Representative Matrigel Invasion assay Images of Mock and HIF1 α transfected cells. Images (Magnification 20X) taken by light microscope after 3 days show that increase in HIF1 α activity increased invasive properties of HIF1 α positive clones C3 and C4 in comparison to Mock cells indicating EMT activation and mesenchymal properties

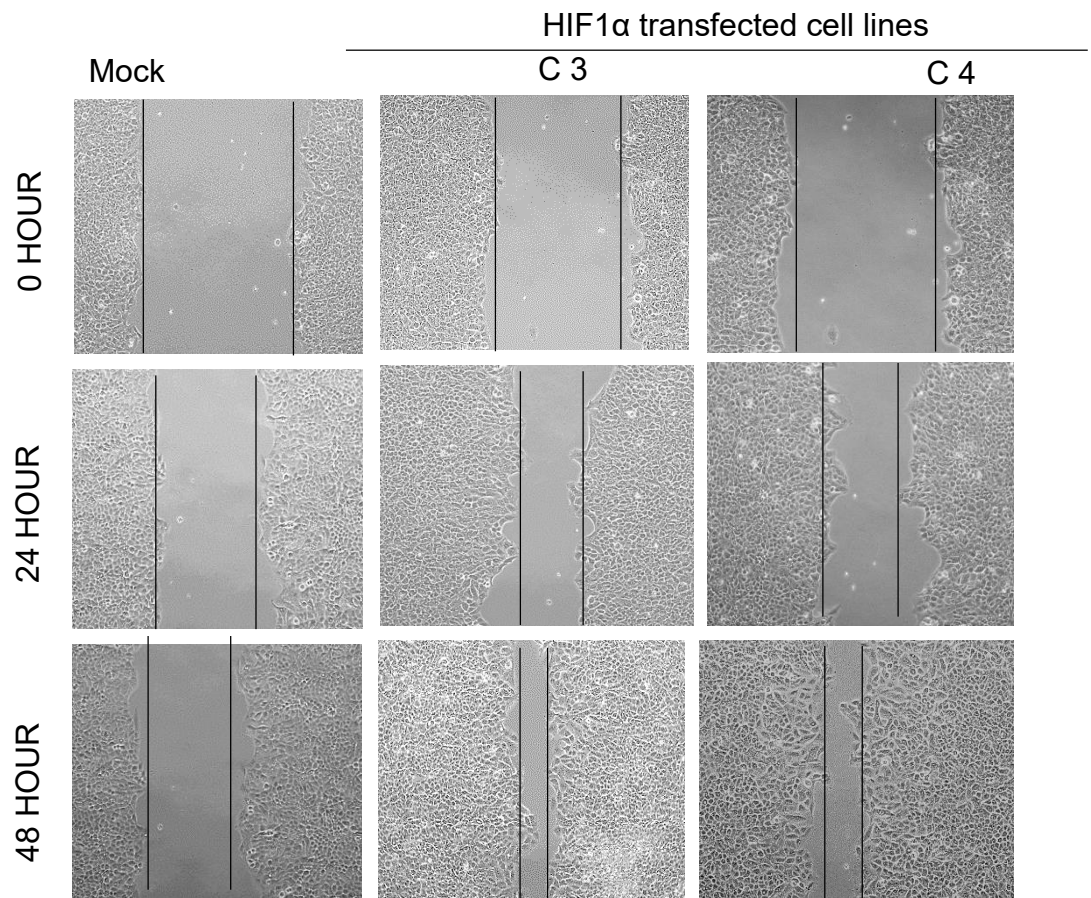


Figure 5.7. Representative Migration (wound healing) assay Images of Mock and HIF1 α transfected cells. Images (Magnification 10X) shows that increase in HIF1 α activity increased migratory properties of HIF1 α positive clones C3 and C4 in comparison to Mock cells after 48 hours indicating EMT activation and mesenchymal phenotype.

5.4.1 Stable transfection of HIF2 α in MDA-MB 231BC cell line

Mock cells and two clones (C4 and 6) with the highest expression of HIF1 α cultured in media containing 200 μ g/ml of G418 were chosen for further testing. Western blot results (Figure 5.8) show that clones 4 and 6 expressed higher levels of HIF1 α .

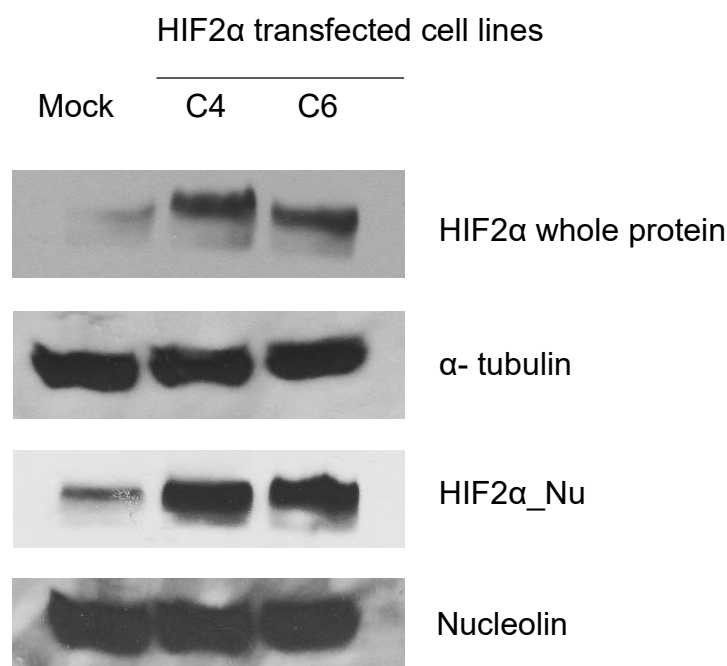


Figure 5.8. Representative Western Blots of Mock and HIF2 α transfection cells: MDA-MB 231 cell line was successfully transfected with pCMV6-HIF2 α to increase the expression of HIF2 α protein. Western blot analysis of whole cell lysates and nuclear protein from mock transfected cells and clones (C-4 and C-6) revealed an increase in expression and nuclear translocation of HIF2 α in the positive clones (C4 and C6) in comparison to that of Mock cells. Tubulin and Nucleolin was used as loading control.

5.4.2 Overexpression of HIF2 α in breast cancer cells induces higher expression of CSC markers.

Data from FACS analysis (Figure 5.9 and 5.10) showed that the HIF2 α overexpressing clones C4 and C6 have significantly higher expression of CSC markers (ALDH and CD 133) when compared to the mock similar to the finding for HIF1 α . The expression of embryonic stem cell markers Sox2, Oct4 and Nanog were also increased in the HIF2 α overexpressing clones compared to the mock cells (Figure 5.11).

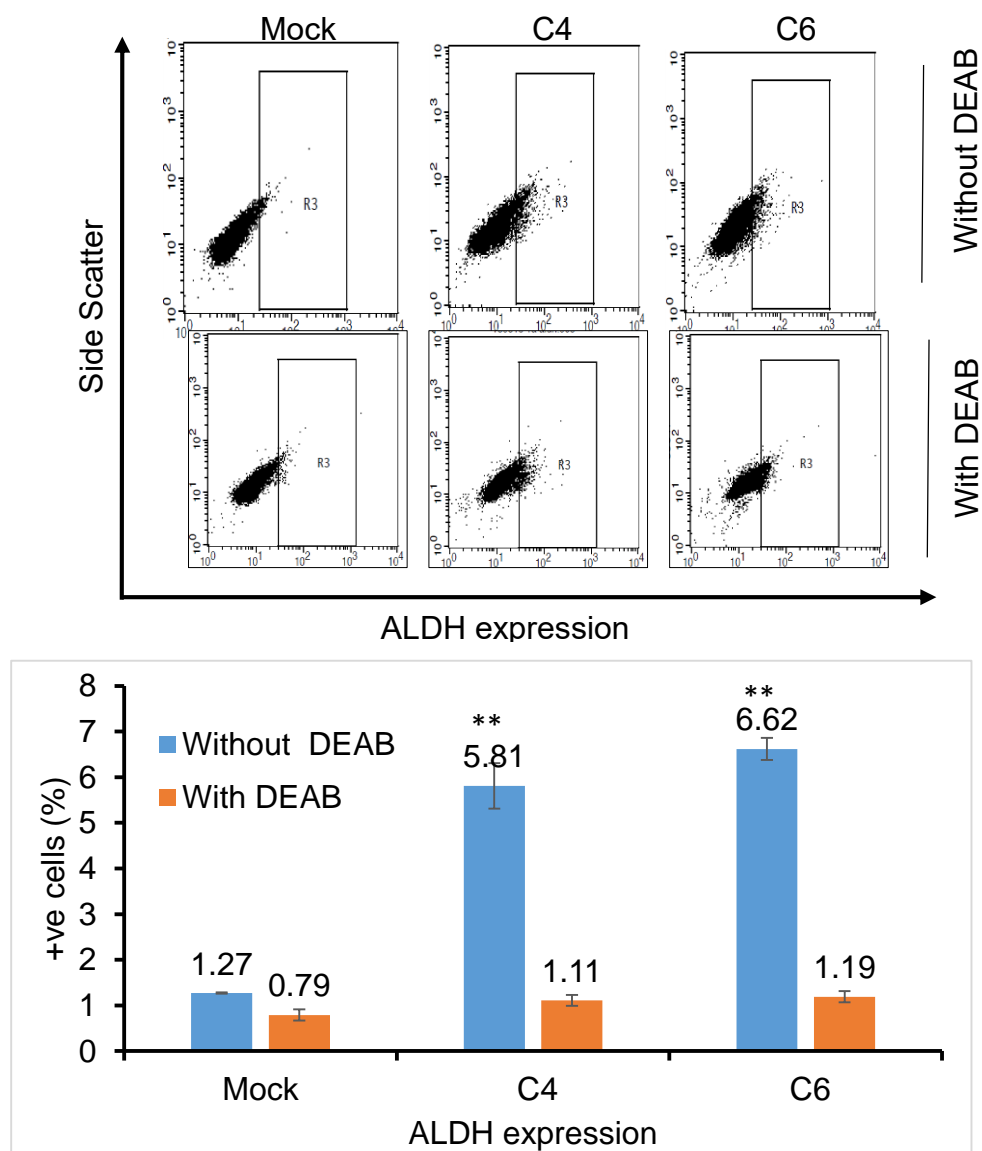


Figure 5.9. Representative FACS Plots of ALDH expression mock and HIF2 α transfected cells measured by ALDEFLUOR assay. FACS results shows ALDH expression in mock and HIF2 α transfected clones (C4 and C6) with and without treatment with DEAB (30 μ M). HIF2 α transfected clones (C4 and C6) expressed high percentage of ALDH⁺ compared to the mock cells before treatment with DEAB. Histograms (median \pm interquartile range) displays the statistically significant increase in the ALDH⁺ activity in HIF2 α transfected clones (C4 and C6) in comparison to mock cells (Kruskal-Wallis test, ** $p < 0.0001$, $n = 9$). After treatment with DEAB, there was no statistical difference in ALDH⁺ cell from mock and HIF2 α transfected clones (Kruskal-Wallis test, $p > 0.05$). (Abbreviations: DEAB: Diethylaminobenzaldehyde; ALDH: Aldehyde dehydrogenase).

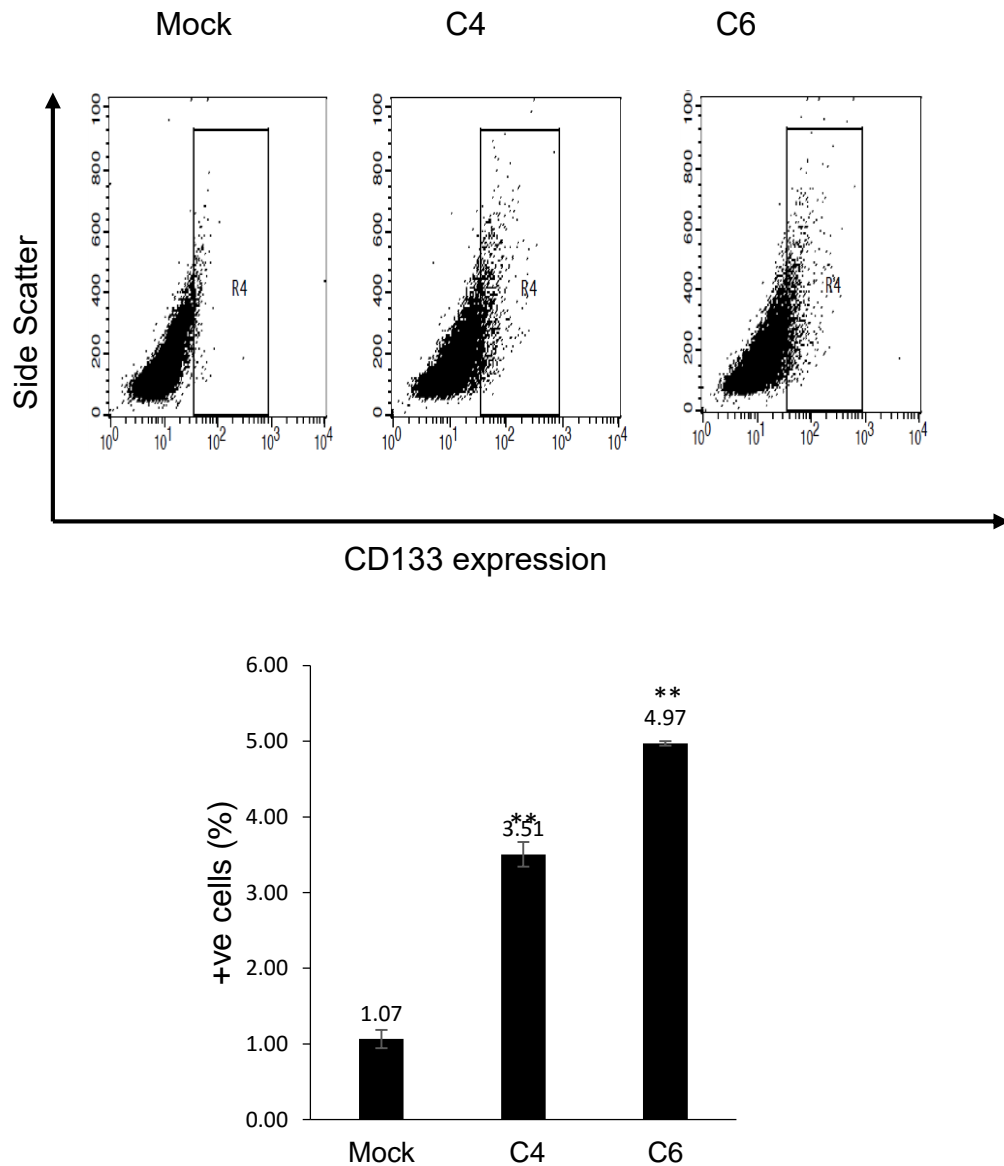


Figure 5.10. Representative FACS Plots of CD133 expression in MDA-MB 231 in mock and HIF2 α transfected cells measured by PE-CD133 immunostaining assay. Fluorescence Activated Cell Sorting (FACS) data shows CD133 expression in mock and HIF2 α transfected clones (C4 and C6). There was an increase in the expression of CD133 in the HIF2 α overexpressing clones (C4 and C6) compared to mock cells. Histograms (median \pm interquartile range) displays the statistically significant increase in the CD133 expression in HIF2 α positive clones C4 and C6 in comparison to mock transfected cells (Kruskal-Wallis test, ** $p < 0.05$ $n=9$).

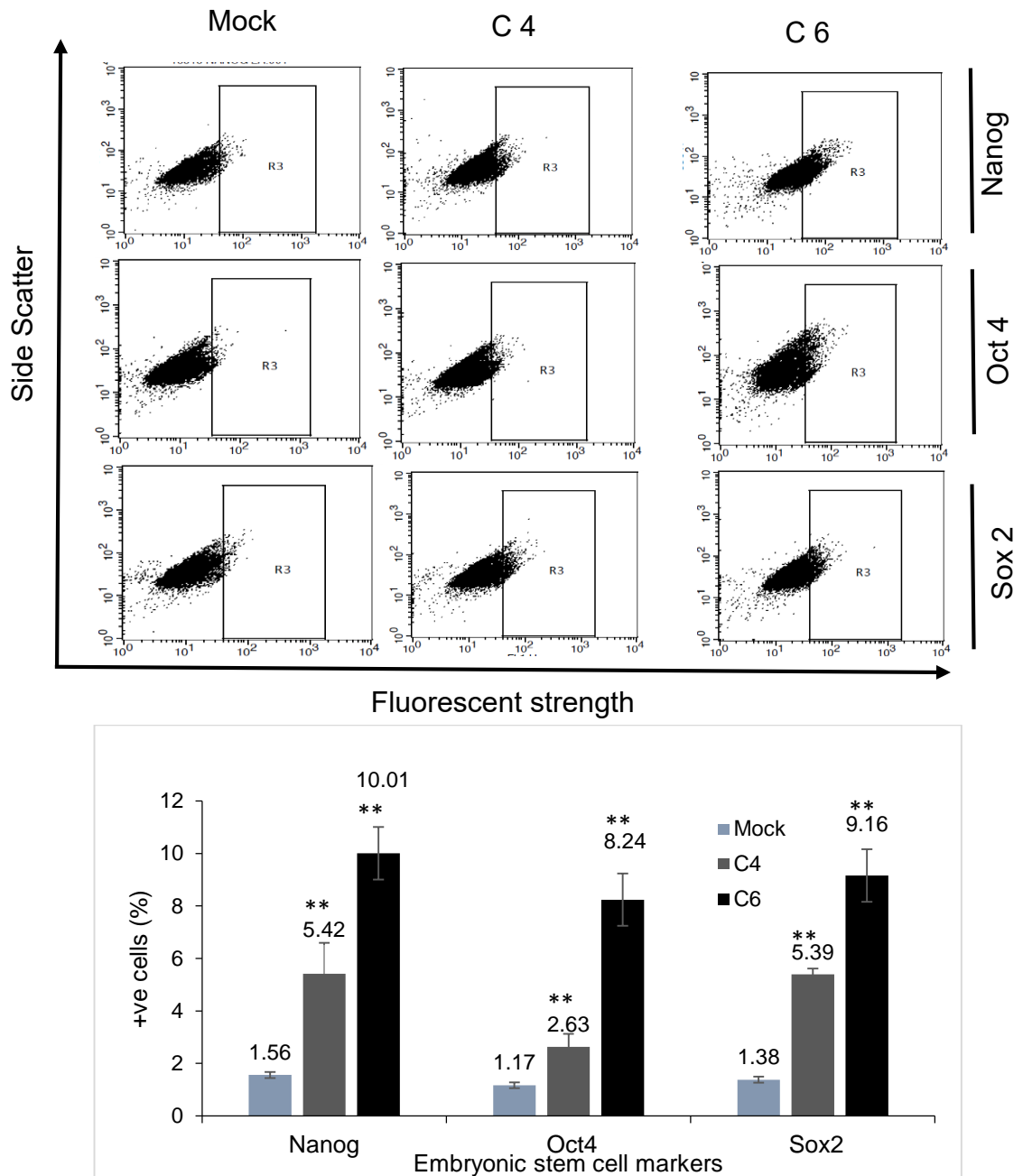
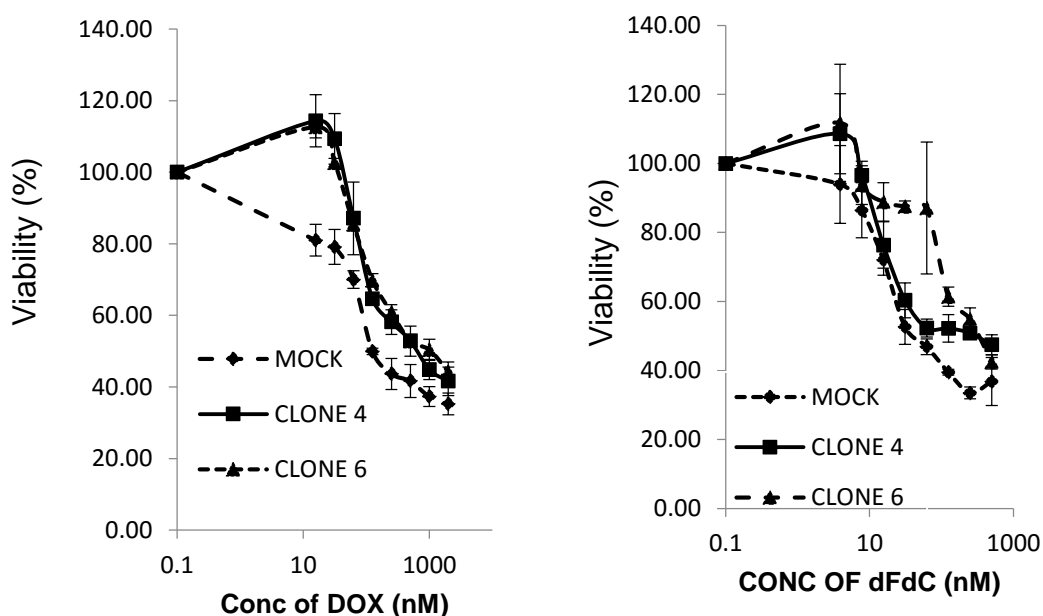


Figure 5.11. Representative FACS Plots of Embryonic Stem cell markers expression in MDA-MB 231 mock and HIF2 α transfected cell. FACS data shows that higher expression of embryonic stem cell markers (Nanog, Sox2 and Oct4) were displayed in HIF2 α transfected clones (C4 and C6) compared to mock cells. Histograms (median \pm interquartile range) above displays statistically significant increase in all three embryonic markers (Nanog, Oct4 and Sox2) markers in transfected transformed cells (4 and 6) when compared to the mock (Kruskal-Wallis test, ** $p < 0.05$ $n=9$).

5.4.3 Increase HIF2 α expression induces resistance to anticancer drugs

Drug sensitivity of HIF2 α clones to CDDP, a first line drug for TNBC and four other conventional anticancer drugs PTX, DOX, VCR and dFdC were tested. MTT cytotoxicity results showed that HIF2 α positive clones C4 and C6 were extremely resistant to all five anticancer drugs tested compared to the Mock cells. Figure 5.12 shows the cell viability curves for the IC₅₀ values for the five anticancer drugs indicating that increase HIF2 α protein is able to induce drug resistance in cells.



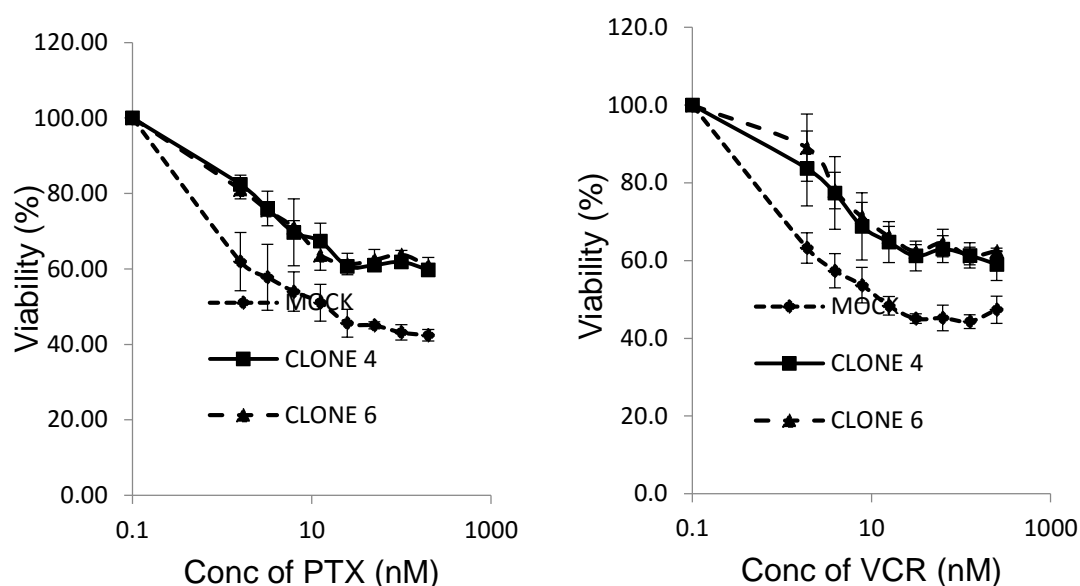


Figure 5.12 Representative Drug Concentration Response Curves of Mock and HIF2 α transfected cells after treatment with CDDP, VCR, PTX, dFdC and DOX. The cell viability curves show that HIF2 α transfected cells were highly resistant to these anticancer drugs. The transfected cells survived at higher concentrations of drugs compared to mock cells (Cisplatin: CDDP, vincristine: VCR, paclitaxel: PTX, gemcitabine (dFdC) and doxorubicin (DOX)).

Table 5.2 IC₅₀ values of 5 Anticancer Drugs in Mock and HIF2 α Transfected cells

Anti -cancer drug	IC ₅₀ Mock	IC ₅₀ HIF2 α C4	IC ₅₀ HIF2 α C6	H-value	p-value
Cisplatin (μ M)	201 \pm 40.32	> 500	> 500	17.83	0.001**
Paclitaxel (nM)	20.56 \pm 10.67	> 200	> 200	24.42	0.0001**
Vincristine (nM)	16.89 \pm 5.33	> 150	>150	27.57	0.0001**
Gemcitabine (nM)	30.49 \pm 9.81	> 500	> 500	36.18	0.0001**
Doxorubicin (nM)	300.11 \pm 8.73	> 1000	> 1000	29.90	0.0001**

Table 5.2 displays the results (median \pm interquartile range) of half maximum inhibitory concentration (IC₅₀) values of HIF2 α transfected cells (C3 and C4) and mock cells. The HIF2 α transfected cells were found to have higher IC₅₀ and were significantly resistant to these conventional anticancer drugs compared to the mock cells. (Kruskal-Wallis test, ** p<0.05, n=9).

5.4.3 Increase HIF2 α activity show mesenchymal properties.

Similar to the results for HIF1 α overexpressing cells, HIF2 α clones (C4 and C6) also expressed higher mesenchymal proteins vimentin and N-cadherin with a loss of the epithelial marker E-cadherin as seen from western blot analysis (Figure 5.13). In the mock cells the E-cadherin expression was high with decreased expression of vimentin and N-cadherin suggesting an epithelial phenotype in these cells.

Migration and invasion assay (Figure 5.14 and 5.15) further confirmed the increased migratory and invasiveness of HIF2 α overexpressing cells.

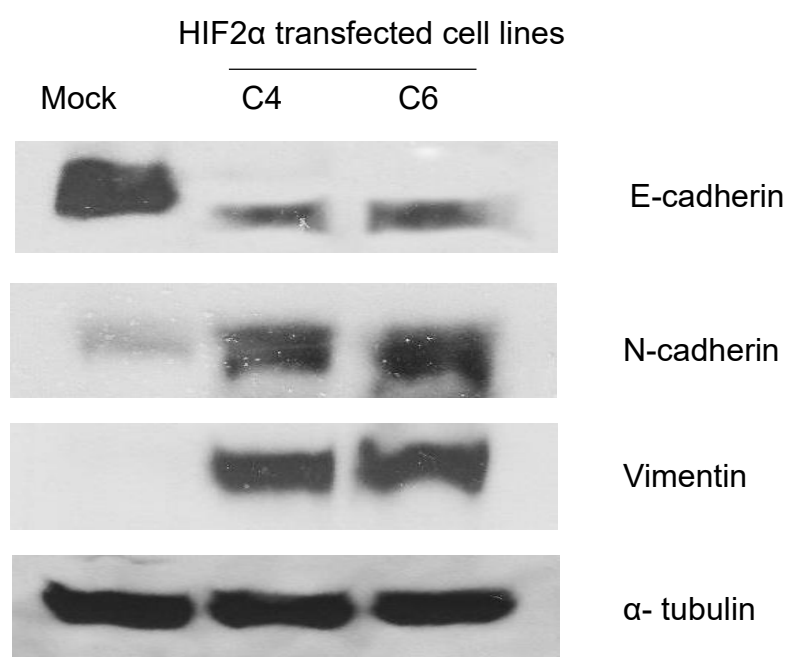


Figure 5.13. Representative Western Blots of EMT markers in Mock and HIF2 α transfected cells using whole cell lysates. The results show that HIF2 α transfection decreased expression of epithelial marker E-cadherin and increased expression of mesenchymal markers (N-cadherin and vimentin) in comparison to that of Mock cells indicating EMT activation in the hypoxic cells. Tubulin was used as loading control.

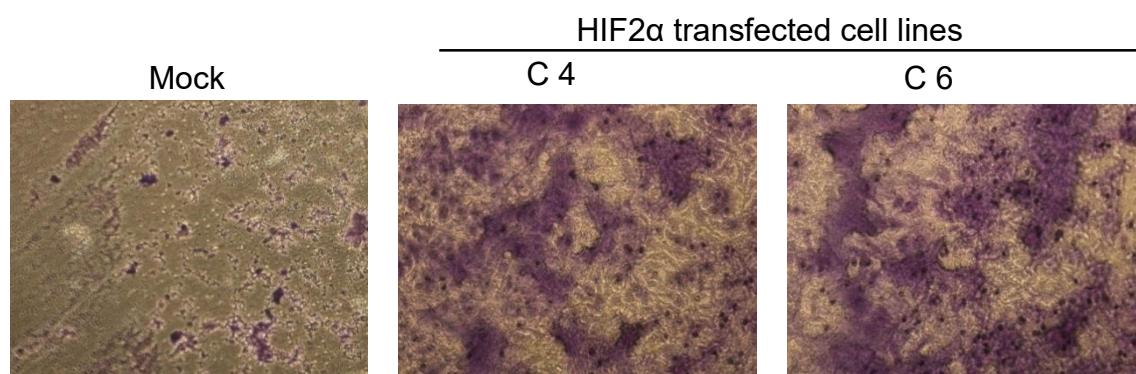


Figure 5.14. Representative Matrigel Invasion assay Images of Mock and HIF1 α transfected cells. Images (Magnification 20X) taken shows that increase in HIF2 α activity enhanced the invasive properties of HIF2 α positive clones C4 and C6 in comparison to Mock cells after 3 days indicating EMT activation and mesenchymal phenotype.

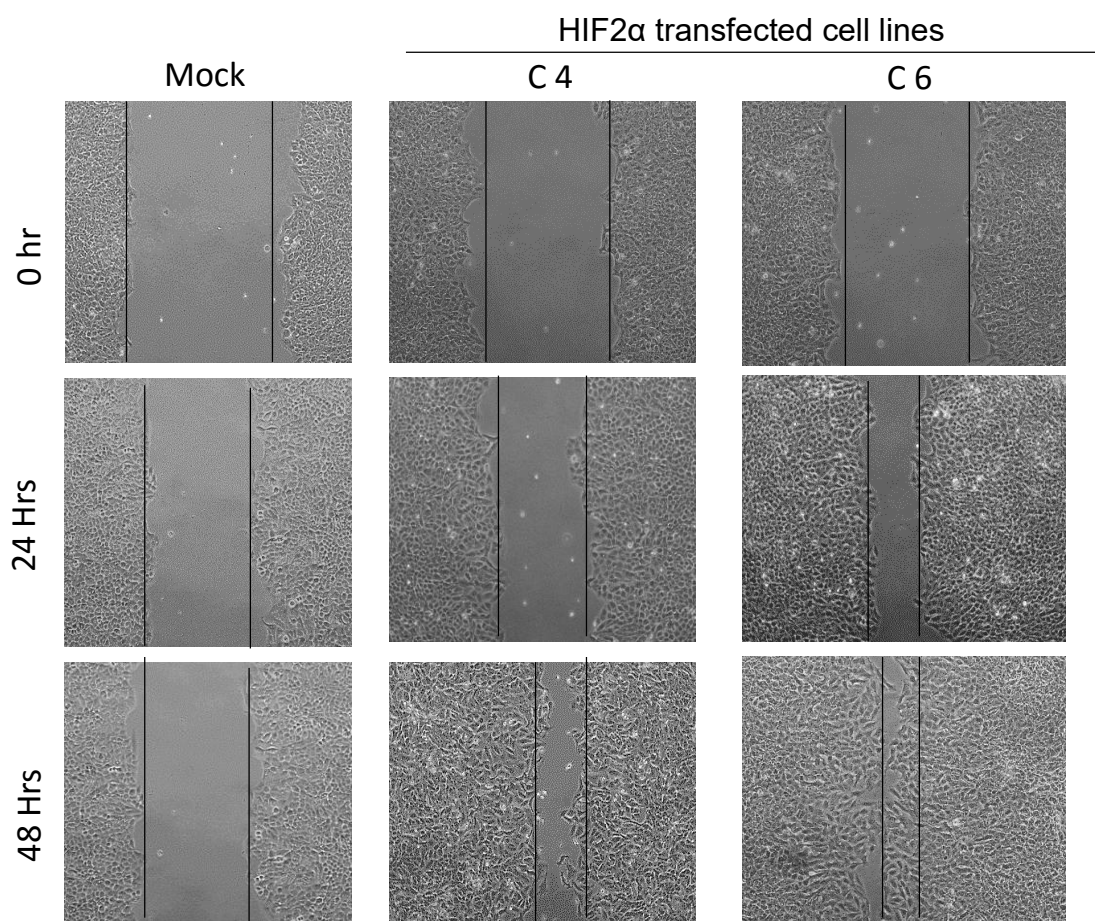


Figure 5.15. Representative Migration (wound healing) assay Images of Mock and HIF2 α transfected cells. Images properties (Magnification 10X) shows that increase in HIF2 α activity increased migratory properties of HIF2 α positive clones C4 and C6 in comparison to Mock cells even after 48 hours indicating EMT activation and mesenchymal.

5.5. Discussion

Cellular adaptation to environmental stresses such as hypoxia promotes the activation of several signalling pathways to ensure survival. Primary mediators of the hypoxic response of cells HIF1 α and 2 α are activated under hypoxic stress. Results from previous chapter (Chapter 3) show that both HIF1 α and 2 α nuclear translocation increased in BC cells cultured under hypoxia. It was hypothesized that either HIF1 α or 2 α may be responsible for the hypoxia-induced epithelial to mesenchymal transition (EMT) and resultant chemoresistance in BC cells. To this effect, the EMT and cancer stem cell (CSC) abilities of HIF1 α and 2 α were studied through over expression by stable transfection in MDA-MB 231 BC cell line. After successful transfection, several clones were picked and screened two clones with the highest expression and nuclear translocation of HIF were selected. These two positive clones and one mock transfected clone (control) was analysed for both HIF1 α and 2 α proteins using western blot.

HIF the master regulator of hypoxia is not normally expressed in breast tissues but is highly expressed in malignant breast cancer (Wang *et al.*, 2006). Hypoxia promotes EMT in BC cells via the induction of notch and twist pathways which are direct transcription target of HIF1 α (Higgins *et al.*, 2007). HIF2 α was shown to induce EMT by overexpression of 'snail' and 'vimentin' in mouse lung model (Li *et al.*, 2009). My results show that both HIF1 α and 2 α overexpressing clones have higher expression of vimentin and N-cadherin indicating a mesenchymal phenotype with associated loss of E-cadherin a hallmark of epithelial phenotypes. The migratory and invasive potential from these HIF overexpressing clones were also increased. It was hypothesized that the induction of CSCs-like traits by HIF may be responsible for this drug resistance. Multiple recent studies in CSC

isolated from GBM, neuroblastoma, renal cancer and non-small lung cancer show that HIF2 α is required for the maintenance of the CSC phenotype and its functions (Li *et al.*, 2009). Heddleston *et al.*, (2010) reported that HIF2 α activation increased expression of CSC factors like *cMyc*, *Nanog* and *Oct4*. Similar to the findings of these reports the HIF1 α and 2 α overexpressing cells also had higher expression of CSC markers ALDH a universal marker for stemness of cells, CD 133 and CD44 with accompanying low expression of CD24 all suggestive of CSC-like cell phenotype when compared to the mock. The expression of embryonic stem cell markers Sox2, Oct4 and Nanog were also increased in the HIF1 α and 2 α transfected cells when compared to the mock cells. The results from this study suggest that both HIF1 α and 2 α play important role in the activation of EMT and consequent maintenance of CSC phenotype.

Study by Teicher *et al.*, (2003) demonstrated that BC cells acquire resistance to doxorubicin under low-oxygen-induced hypoxia and CoCl₂-induced chemical hypoxia indicative that HIF play significant role in hypoxia induced chemoresistance. The focus of this study was to examine the effects HIF1 α and 2 α overexpression on chemoresistance and possibility understand the mechanism involved in this drug resistance. The results showed that both HIF1 α and 2 α overexpressing cells were significantly resistant to the 5 conventional anticancer drugs tested (cisplatin, paclitaxel, doxorubicin, vincristine and gemcitabine) which is in line with previously published study (Sullivan and Graham, 2009). Recent studies show that cancer stem-like cells play key roles in TNBC chemoresistance (Bhola *et al.*, 2013 and Samanta *et al.*, 2014). Bhola *et al.*, (2013) demonstrated that HIF-1 α is a central determinant of triple negative cancer stem-like cell chemo-resistance. These finding along with results obtained

from this study strongly suggest that HIF are important for induction of CSC traits in BC with associated EMT and chemoresistance.

Conclusion

The main aim of this study was to examine the role of HIF1 α and 2 α proteins in hypoxia-induced EMT and consequent chemoresistance. Data from my results show that both HIF1 α and 2 α can induce EMT and CSC traits. Therefore, development of pharmacological agents to inhibit these factors may hold promise for patients with TNBC as they lack targetable receptors.

Chapter Six

The cytotoxic mechanisms of Disulfiram in pan-chemoresistant breast cancer cell lines

6.0 Characterization of resistant breast cancer cell lines (T47D_{Dox100nM} and MDA-MB 231_{Gem 100nM}).

6.1. Introduction

Primary and acquired resistance represents a major challenge for the effectiveness of chemotherapeutic agents in breast cancer management. Doxorubicin (Dox) an anthracycline antibiotic is one of the most widely used chemotherapeutic agents for BC and is a preferred single agent as well as used in combination regimens for recurrent and metastatic BC (Gluck, 2005). Resistance to Dox can occur through several mechanisms such as decreased drug accumulation in which there is an increase drug efflux due to overexpression of multidrug resistance protein P-glycoprotein, alteration in drug targets proteins via cellular downregulation of topoisomerase II expression, cellular suppression of apoptosis by upregulation of GST and by enhanced capacity of drug-induced DNA repair (Nielsen *et al.*, 1996; Tubbs *et al.*, 2009).

Gemcitabine (dFdC) can be used as a single agent for advanced BC or in combination therapy with other chemotherapeutic drugs such as CDDP and PTX with even higher response rates. It is a first line drug for the treatment of BC and has a high initial activity against tumours but is prone to induce acquired resistance in cancer cells. Metabolism and chemoresistance mechanisms of dFdC have been discussed in detailed in chapter 1.

Many current cancer therapies are limited by the severity and frequency of adverse side effects associated with such treatments which has led to a search and high demand for non-toxic alternatives. One source of new therapies may be through repurposing of clinically approved drugs, where safety in patients has already been established. Disulfiram (DS) an anti-alcoholism drug used in clinic for over 60 years (Eneanya *et al.*, 1981) demonstrates anti-cancer effects in cancer cell lines (Cen *et al.*, 2004) as well as in a range of solid and haematological malignancies (Wickstrom *et al.*, 2007). The clinical use of DS over a long period of time has shown it to be a very safe drug with minimal and manageable toxic effects, even at fairly high doses of 300 to 500 milligrams daily (Sauna *et al.*, 2005).

The biological activity of disulfiram is attributed to its ability to bind divalent cations and consequently disrupt metal dependent processes, principally those involving copper (Cu) and zinc (Zn) (Marikovsky *et al.*, 2002; Shiah *et al.*, 2003). Several *in vitro* experiments indicate that the cytotoxicity of DS is entirely dependent on copper(II) (Cu) or some other transition bivalent metal ions in the culture medium (Cen *et al.*, 2004; Iljin *et al.*, 2009; Liu *et al.*, 2012).

Acquired resistance of initially sensitive cancer cells to chemotherapeutic drugs is a major challenge for successful treatment of BC cells. Previous chapters 3, 4 and 5 have revealed that CSCs, NF κ B and HIFs play vital roles in conferring resistance to BC cell. Therefore, it is necessary for development of drugs that counter these resistance in BC. However, no positive data has been published by clinical trials using oral version of DS plus copper gluconate in cancer treatment even with the promising laboratory data obtained from the *in vitro* and

in vivo experiments in cancer cell lines and animals respectively. Therefore, elucidating the disparity between the anticancer cytotoxicity of DS in laboratory and clinic is of great importance.

6.1.2. Rationale for the study

This study evaluates the drug sensitivity of MDA-MB 231_{GEM100nM} and T47D_{Dox100nM} to a number of conventional anticancer drugs and the possible mechanisms for drug resistance.

A recent study by Lewis *et al.*, (2014) proposed that the *in vitro* cytotoxicity of DS in cancer cells occurs by ROS generated from the reaction of DS and Cu rather than the final product, DDC-Cu. If this is the case, then DS and Cu may not be able to react near the cancer cells to execute anticancer cytotoxic action *in vivo* since the half-life of ROS is very short (D'Autreaux and Toledano 2007). Thus it will be virtual impossible to translate the *in vitro* anticancer cytotoxic effect of DS into clinic. Furthermore, if ROS generated by the reaction of DS and Cu is the major mechanism by which DS carries out its anticancer effect, then DDC-Cu will have no significant cytotoxic effect on cancer cells. The study was performed to examine the effect of DS-Cu induced ROS and to determine if DDC-Cu has any cytotoxic effects on cancer cells.

6.2. Experimental Design

General materials, products, labwares, manufacturers and methodologies used for the entire study have been described in details in chapter 2. Specific materials, methods and experimental design used for this part of this study are stated below.

6.2.1. MTT cytotoxicity assay in resistant cell lines

Drug sensitivity of the resistant cells lines (MDA-MB-231_{GEM100nM} and T47D_{Dox100nM}) and parental cell line (MDA-MB-231 and T47D) were analysed using MTT assays (refer to Chapter 2, page 71).

6.2.2. Time dependent Cytotoxicity of DDC-Cu and DS plus Cu (DS/Cu)

To examine the time-dependent cytotoxicity of DS/Cu reaction and DDC-Cu. MCF 7 breast cancer cells were exposed to DDC-Cu or DS/Cu (1:1 molar ratio) in a time dependent manner and then subjected to MTT assay (refer to Chapter 2, 72).

6.2.3. Determination of CSC markers in resistant cell lines

CSC markers ALDH, CD133, Sox2, Oct4 and Nanog were detected in the resistant and parental cell lines by flow cytometry (refer to Chapter 2, page 78).

6.2.4. Reactive Oxygen Species activity detection

To examine the effects of reactive oxygen species (ROS) generated by DS plus Cu reaction, extracellular ROS levels at different time intervals were determined in culture medium (refer to Chapter 2, page 93).

6.2.5. Determination of metabolic kinetics of DS/Cu and DDC-Cu

To examine the metabolic kinetics of DS plus Cu and DDC-Cu, medium and MCF7 cells lysate were subjected HPLC analysis after treated with equal molar ratio of DS and CuCl₂ or DDC-Cu (refer to Chapter 2, page 94).

6.3. Results

6.3.1. Morphological features

The drug resistance cells were observed to have a different phenotype than the wild type (WT) parental cells. The resistant cells were smaller and with less defined irregular multiple nuclei.

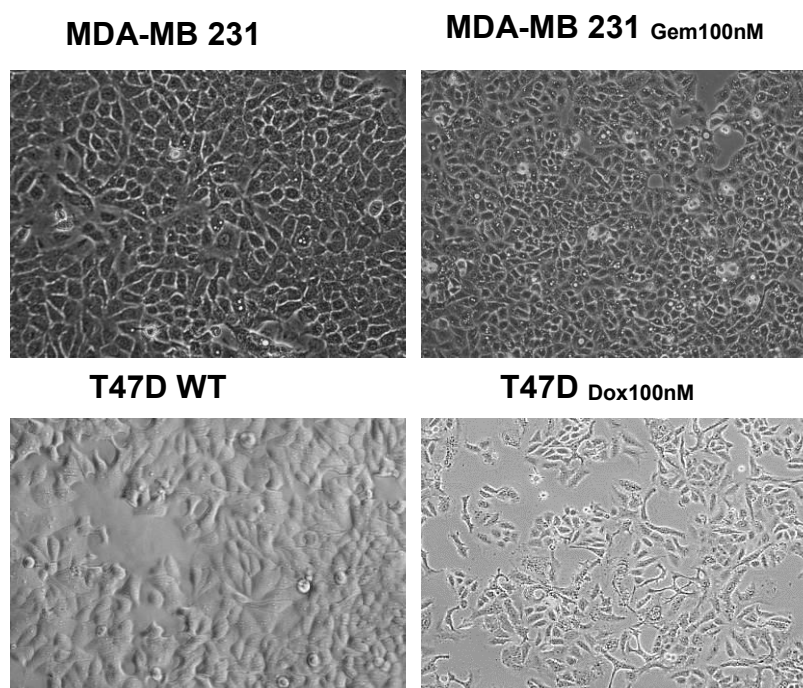


Figure 6.1 Representative Images of Morphology of wild type and resistant cells.

Images taken by light microscopy shows the morphology of parental and resistant cells (Magnification 20X) after culturing in normoxia. The resistant cells were smaller in size when compared to the parental cell lines (Abbreviations WT: wide type; MDA-MB-231_{GEM100nM}: MDA-MB231 gemcitabine resistant cell).

6.3.2. Resistant cell lines show cross and pan-resistance to anticancer drugs

Data from MTT cytotoxicity analysis showed that apart from being highly resistant to dFdC (Figure 6.3A), the MDA-MB 231_{GEM100nM} cell line is also cross resistant to other anticancer drugs e.g. CDDP, Dox, VCR and PTX (Figure 6.3B). The parental cell line has a much lower IC_{50s} compared to that of the resistant cell line

MDA-MB 231_{Gem100nM} (Table 6.1). Similar results were also obtained for the T47D_{Dox100nM} cell line, in which resistance to Dox was observed and cross resistance to other anticancer drug with various mechanism of action (Figure 6.4 A and B).

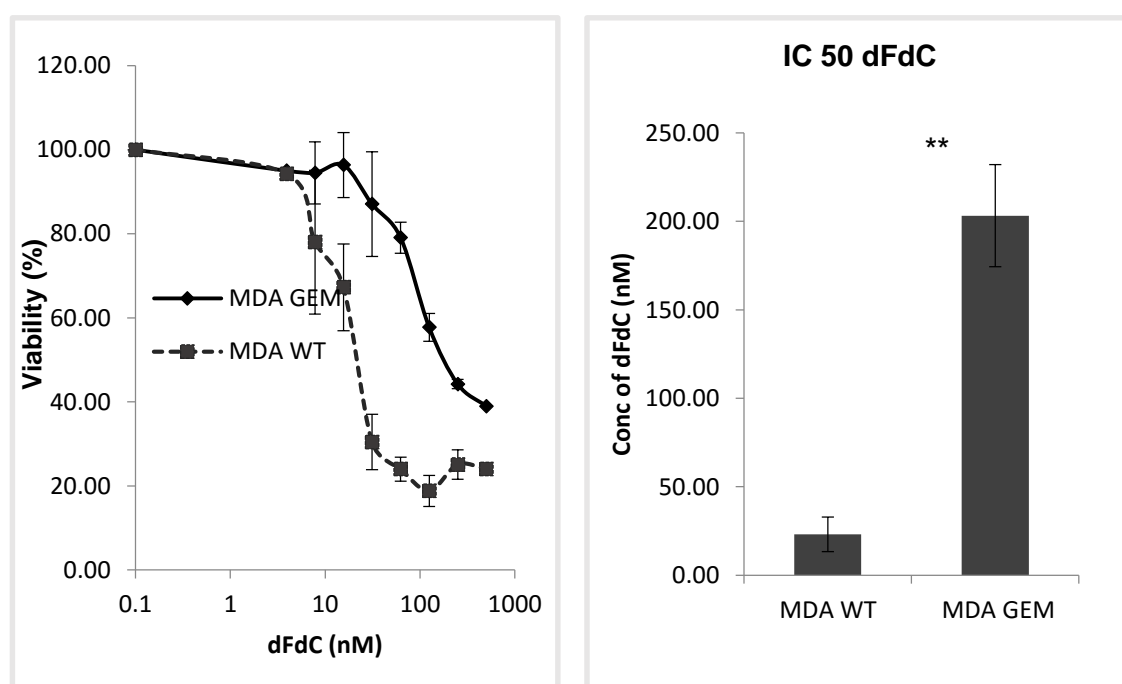
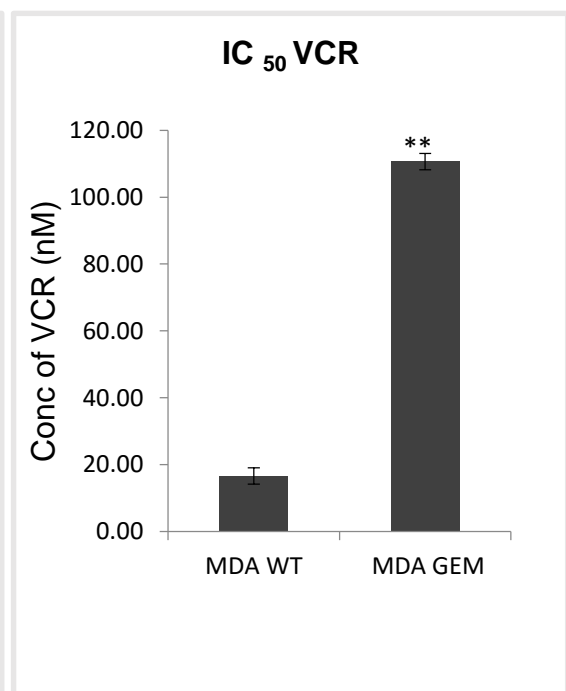
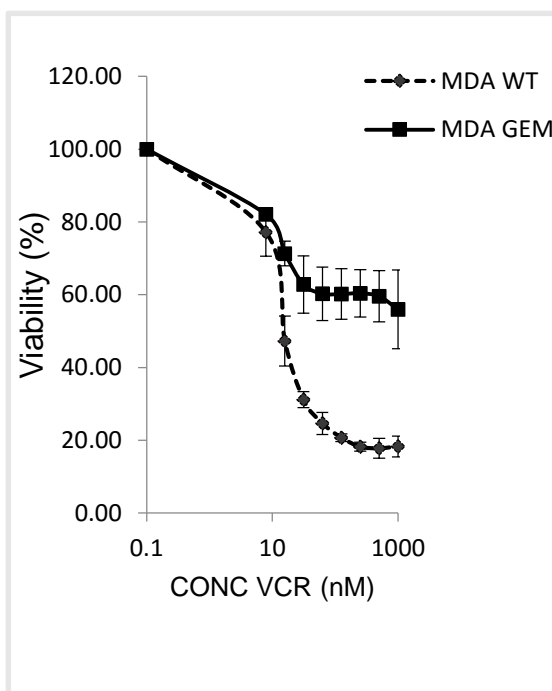
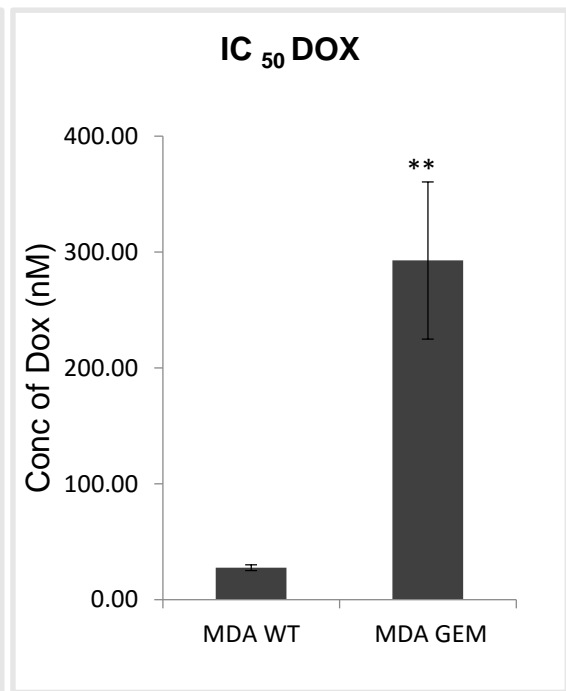
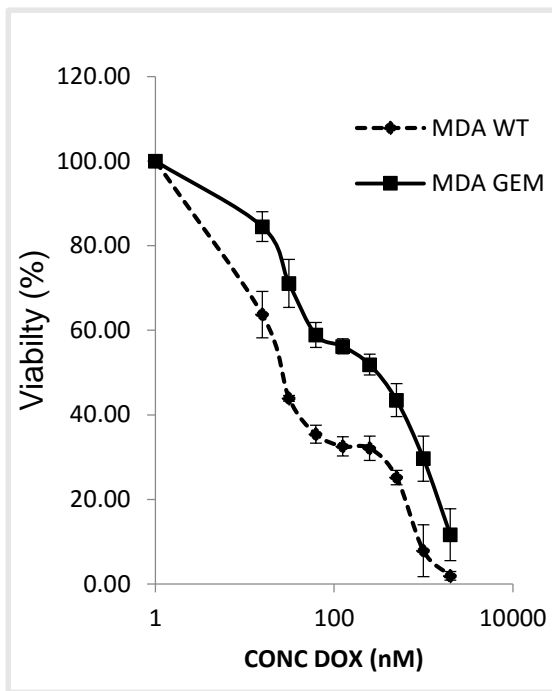


Figure 6.2(A). Representative Drug Concentration Response Curve of MDA-MB 231 and MDA-MB 231_{Gem100nM} cell line. Cell viability curve from MTT analysis shows difference in dose response between resistant cell (MDA GEM) and parental cell (MDA WT). The resistant cell displayed significant resistance to dFdC. Histogram (median \pm interquartile range) shows elevated half maximal inhibitory concentration (IC_{50}) values indicating increased drug resistance to gemcitabine (Mann and Whitney U test, resistance, $**p < 0.001$, $n=9$). (Abbreviations; MDA-WT: MDA-MB 231 wild type cell line, MDA GEM: MDA-MB 231 gemcitabine resistant cell line, dFdC: gemcitabine).



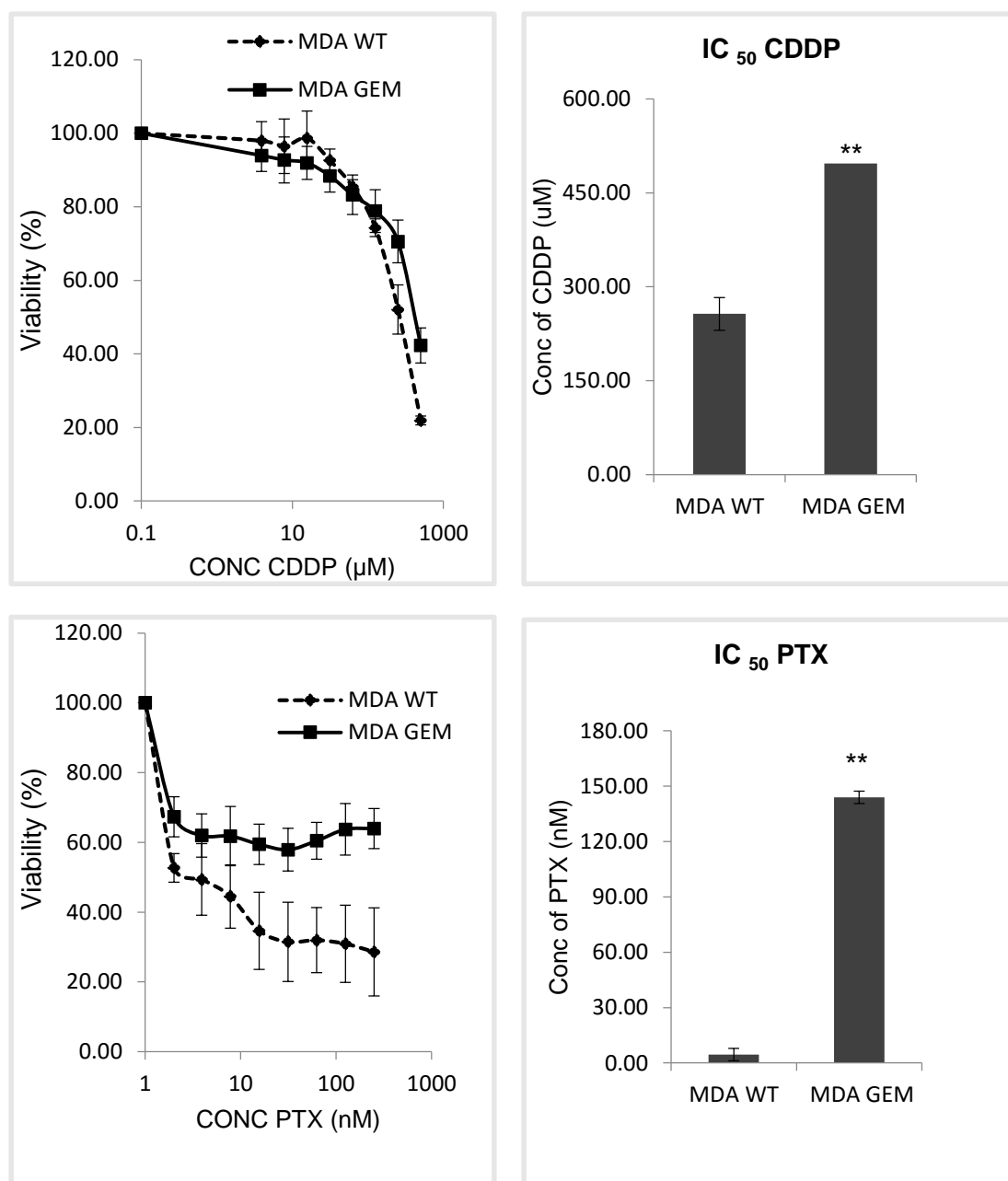


Figure 6.2(B). Representative Drug Concentration Response Curves of MDA-MB 231 and MDA-MB 231_{Gem100nM} cell line. Cell viability curve shows difference in dose response between resistant cell and parental cell lines. The resistant cell MDA-MB 231_{Gem100nM} displayed significant cross resistance to anticancer drugs (VCR, Dox, CDDP and PTX). Histogram (median \pm interquartile range) shows elevated half maximal inhibitory concentration (IC₅₀) values indicating increased drug resistance (MDA WT: MDA-MB 231 wild type cell line, MDA GEM: MDA-MB 231 gemcitabine resistance cell line, VCR: vincristine, Dox: doxorubicin, CDDP: cisplatin and PTX: paclitaxel).

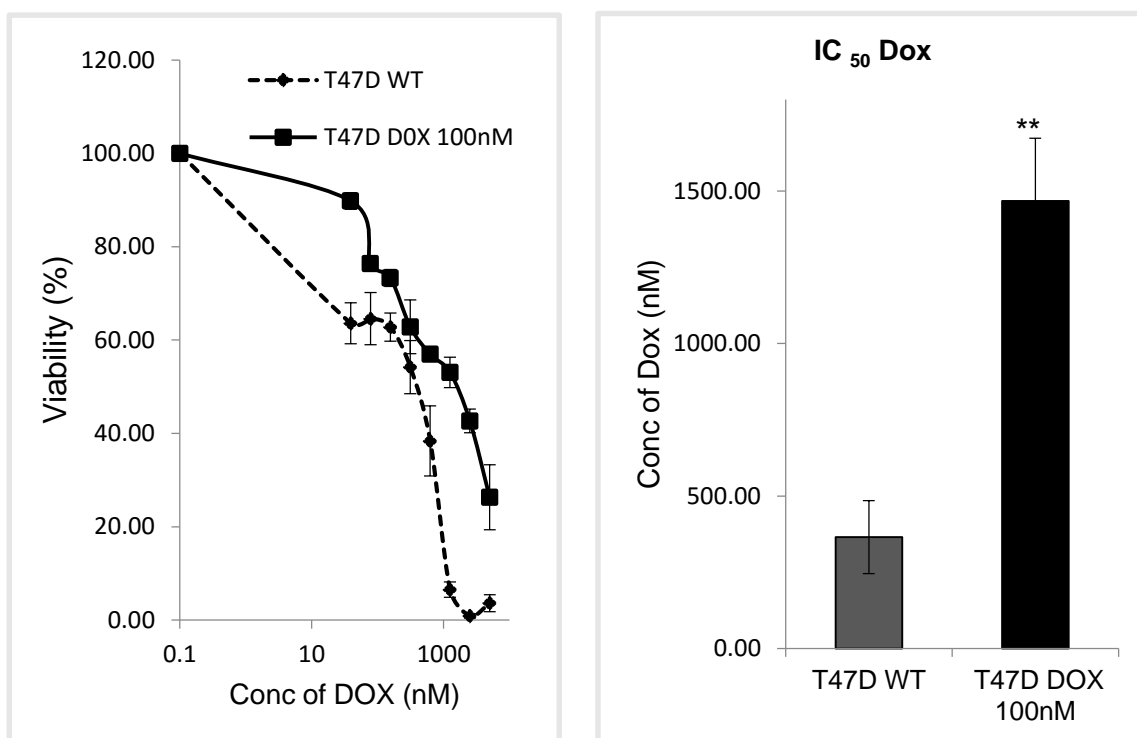


Figure 6.3. Representative Drug Concentration Response Curve of T47D and T47D_{Dox100nM} cell line. Cell viability curve from MTT analysis shows difference in dose response between resistant cell (T47D_{Dox100nM}) and parental cell (T47D WT). The resistant cell displayed significant resistance to Dox. Histogram (median \pm interquartile range) shows elevated half maximal inhibitory concentration (IC₅₀) values indicating increased drug resistance to doxorubicin (Mann and Whitney U test, resistance, ** $p < 0.001$, $n = 9$). (Abbreviations; T47D-WT: T47D wild type cell line, T47D DOX: T47D doxorubicin resistant cell line, Dox: doxorubicin).

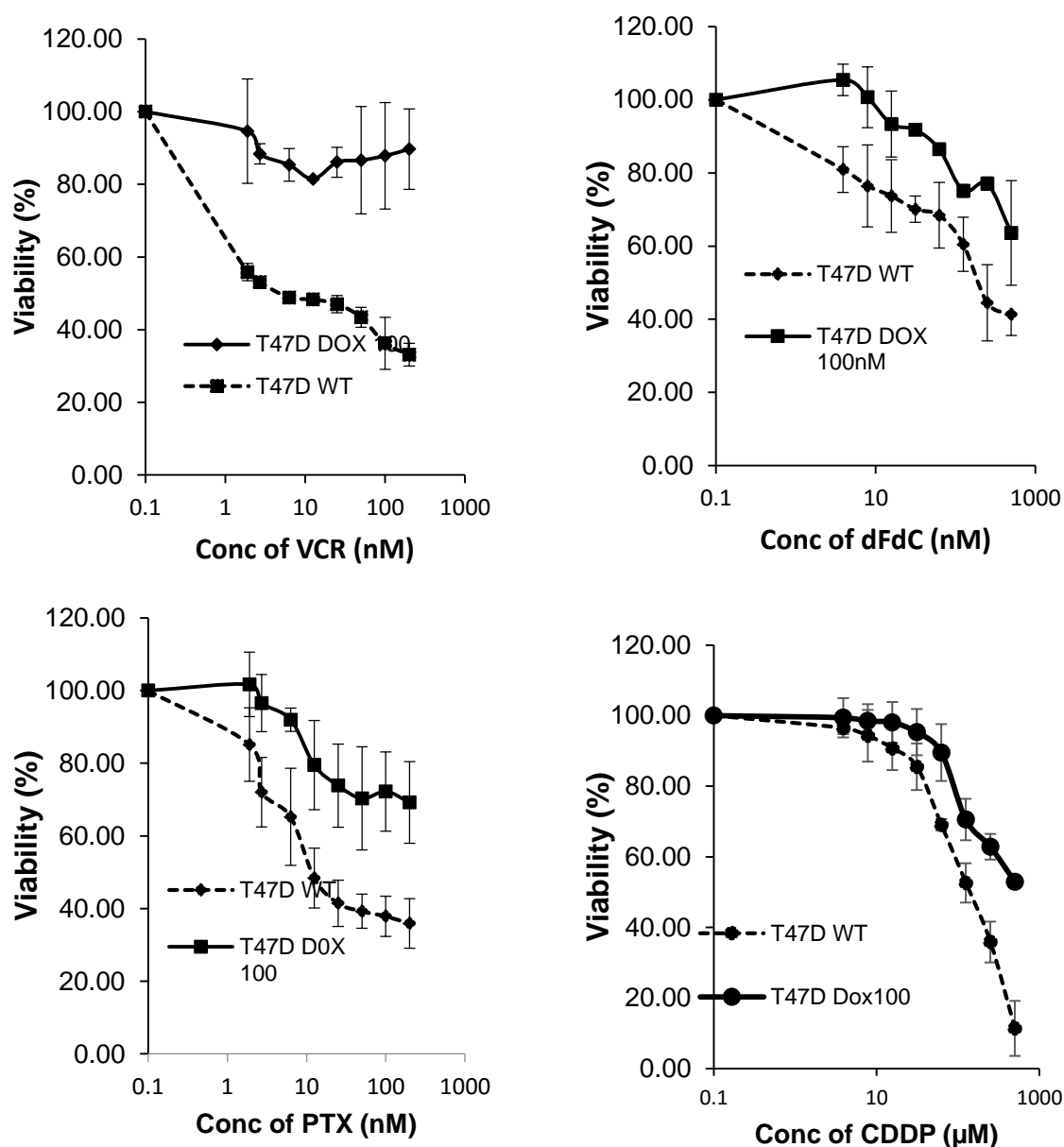


Figure 6.3.B Representative Drug Concentration Response Curves of T47D and T47D_{DOX100nM} cell line to conventional anticancer drugs. Cell viability curve shows difference in dose response between resistant cell (T47D_{DOX100nM}) and parental cell (T47D WT). The resistant cell T47D_{DOX100nM} displayed significant cross resistance to anticancer drugs (VCR, dFdC, CDDP and PTX). Histogram (median \pm interquartile range) shows elevated half maximal inhibitory concentration (IC₅₀) values indicating increased drug resistance in T47D_{DOX100nM} cell lines (Mann and Whitney U test, resistance, $**p < 0.001$, $n=9$). (Abbreviations; T47D-WT: T47D wild type cell line, T47D DOX: T47D doxorubicin resistant cell line, cisplatin (CDDP), paclitaxel (PTX), vincristine (VCR) and gemcitabine (dFdC)).

**Table 6.1 IC₅₀ Value from cell viability curve in Resistant Cell Line T47D_{Dox}
100nM and Sensitive Cell Line T47D WT**

Anti-cancer drug/ IC ₅₀	T47D WT	T47D _{Dox100nM}	U- value	p-value
Cisplatin (μM)	198.01 ± 5.89	> 600	17.12	0.0002**
Paclitaxel (nM)	7.69± 0.26	> 200	36.29	0.0001**
Vincristine (nM)	4.81 ± 3.56	> 250	31.97	0.0001**
Gemcitabine (nM)	224.54 ± 4.81	> 600	23.45	0.0001**
Doxorubicin (nM)	365.78 ± 108.73	> 1000	29.32	0.0001**

Table 6.1 displays the results (median ± interquartile range) of half maximum inhibitory concentration (IC₅₀) values of T47D wild type and T47D_{Dox 100nM} resistant cell line. The resistant cell line T47D_{Dox 100nM} were found to have higher IC₅₀ and were significantly resistant to these conventional anticancer drugs compared to the mock cells. (Mann and Whitney U test ** p<0.05, n=9). (Abbreviations: WT: wild type, IC₅₀: half maximum inhibitory concentration)

6.3.3. Resistant cell lines displayed an increase in CSC markers

Data from FACS analysis show that the resistant cell lines MDA-MB-231_{GEM100nM} (Figure 6.4 A and B) have higher expression of CSC markers (ALDH, CD 133) compared to the sensitive parental cell line MDA-MB 231 WT. Similar results were also obtained for T47D_{Dox100nM} resistant cells (Figure 6.5 A and B).

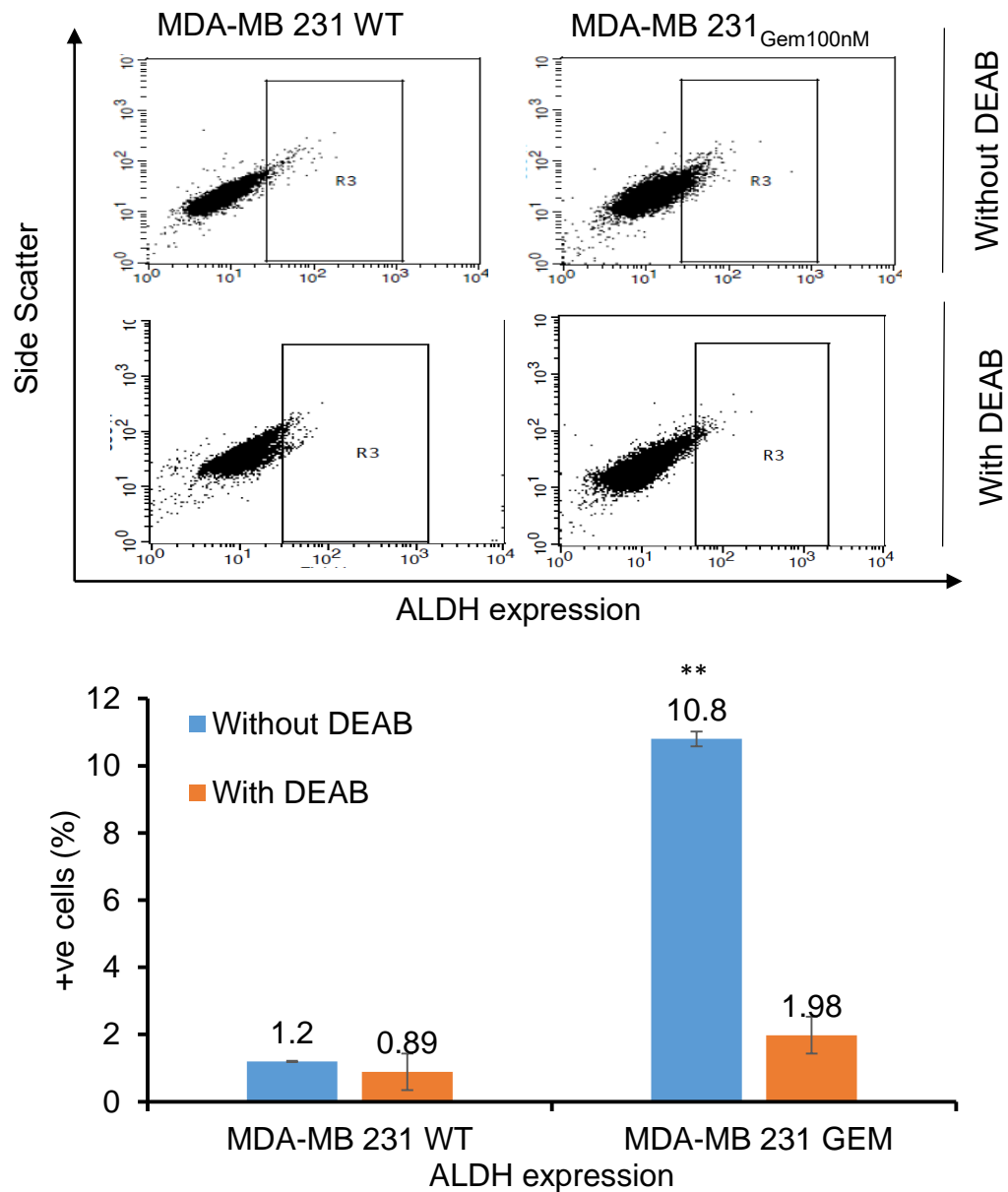


Figure 6.4(A) Representative FACS Plots of ALDH expression in MDA-MB 231 WT and MDA-MB 231_{GEM100nM} BC cell line. FASC results shows ALDH activity in MDA-MB 231 WT and MDA-MB 231_{GEM100nM} BC cells with and without treatment with DEAB (30μM). MDA-MB 231_{GEM100nM} expressed high percentage of ALDH⁺ compared to the mock cells before treatment with DEAB. Histogram (median ± interquartile range) displays the statistically significant increase in the ALDH⁺ activity in MDA-MB 231_{GEM100nM} in comparison to MDA-MB 231 WT (Mann and Whitney U test, ** $p < 0.0001$, $n = 9$). After treatment with DEAB, there was no statistical difference in ALDH⁺ cell from both cultures ($p > 0.05$). (Abbreviations WT: wild type, GEM100nM: gemcitabine resistance cell line, DEAB: Diethylaminobenzaldehyde; ALDH: Aldehyde dehydrogenase active).

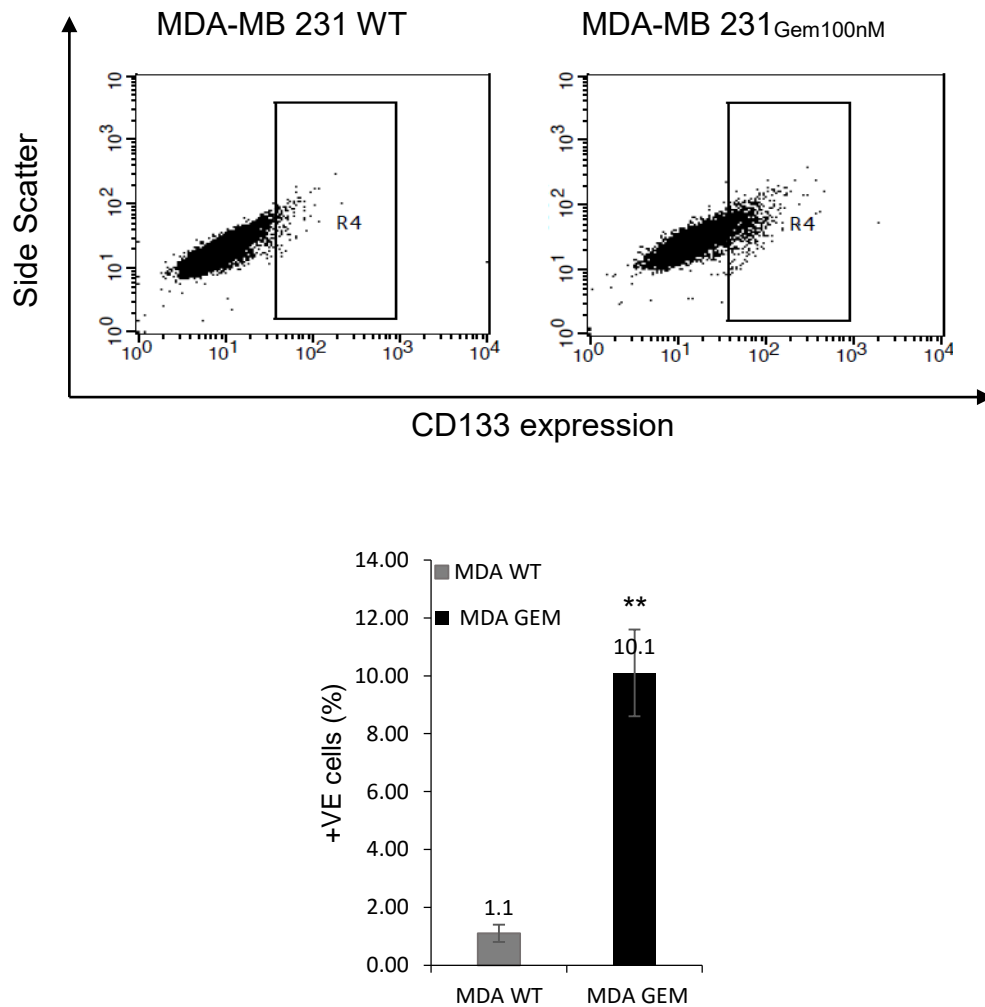


Figure 6.4(B). Representative FACS Plots of CD133 expression in MDA-MB 231 WT and MDA-MB 231GEM100nM BC cell line by PE-CD133 immunostaining assay.

FACS data shows CD133 expression in MDA-MB 231 WT and MDA-MB 231_{GEM100nM} cell lines. There was an increase in the expression of CD133 in the MDA-MB 231_{GEM100nM} compared to parental cell line MDA-MB 231 WT. Histograms (median \pm interquartile range) displays the statistically significant increase in the CD133 expression in MDA-MB 231_{GEM100nM} in comparison to sensitive MDA-MB 231 WT cell line (Mann and Whitney U test, $**p < 0.0001$, $n=9$) (Abbreviations: WT: wide type; GEM100nM: gemcitabine resistance cell).

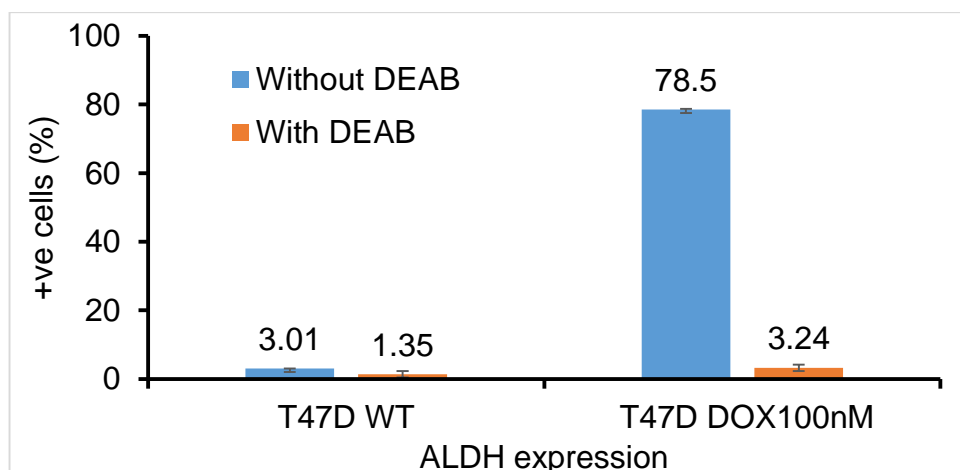
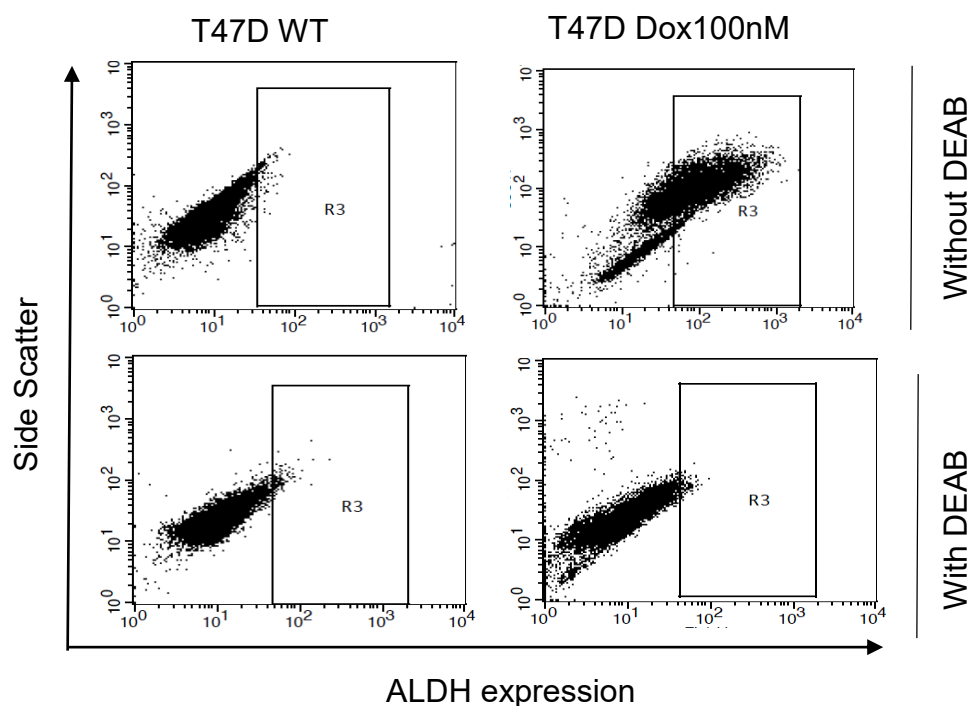


Figure 6.5(A). Representative FACS Plots of ALDH expression in T47D WT and T47D_{Dox100nM} BC cell line measured by ALDEFLUOR assay. FACS results shows ALDH expression in T47D WT and T47D_{Dox100nM} BC cells with and without treatment with DEAB (30μM). T47D_{Dox100nM} expressed high percentage of ALDH⁺ compared to the mock cells before treatment with DEAB. Histogram (median ± interquartile range) displays the statistically significant increase in the ALDH⁺ activity in T47D_{Dox100nM} in comparison to T47D WT (Mann and Whitney U test, ** $p < 0.0001$, $n = 9$). After treatment with DEAB, there was no statistical difference in ALDH⁺ cell from sensitive and resistant cell lines (Mann and Whitney U test, $p > 0.05$). (Abbreviations WT: wild type, Dox100nM: doxorubicin resistance cell, DEAB: Diethylaminobenzaldehyde; ALDH: Aldehyde dehydrogenase active).

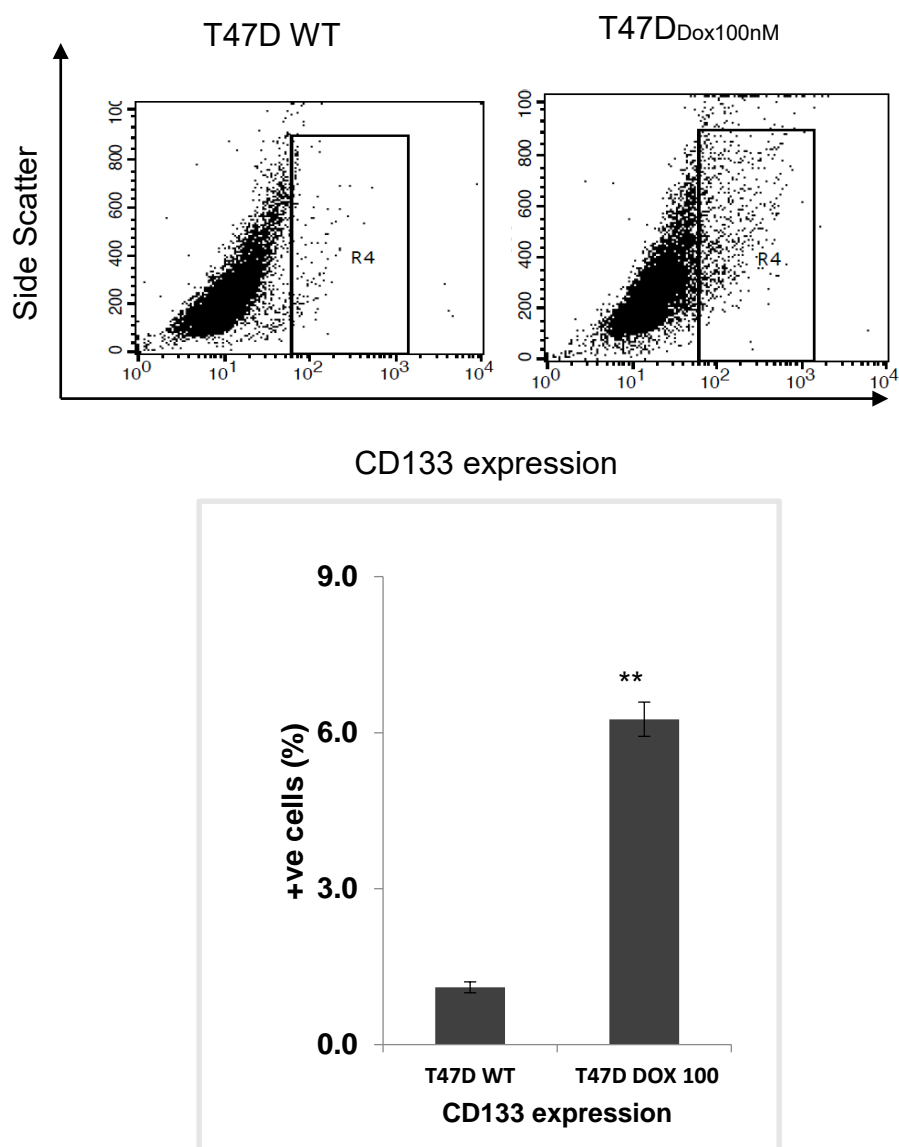


Figure 6.5B. Representative FASC Plots of CD133 expression in T47D WT and T47D_{Dox100nM} BC cell line measured by PE-CD133 immunostaining assay. FASC data shows CD133 expression in T47D WT and T47D_{Dox100nM} cell lines. T47D_{Dox100nM} cells displayed increase in CDD 133 expression compared to parental cell line T47D WT. Histogram (median \pm interquartile range) above displays statistically significant increase in CD133 in T47D_{Dox100nM} cells compared to the sensitive parental cell T47D WT (Mann and Whitney U test, $**p < 0.0001$, $n=9$). (Abbreviations: WT: wide type; Dox100nM: doxorubicin resistance cell, ALDH: aldehyde dehydrogenase).

6.3.4. Resistant cell lines displayed an increase in embryonic stem cell markers

The embryonic stem cells (Nanog, Sox2, Oct4) important for maintenance of stem cell, renewal and pluripotency were also significantly increased in the resistant cell lines MDA-MB-231_{GEM100nM} and T47D_{Dox100nM} in comparison to the parental cell MDA-MB-231 and T47D respectively. (Figure 6.6 (A)(B) and 6.7).

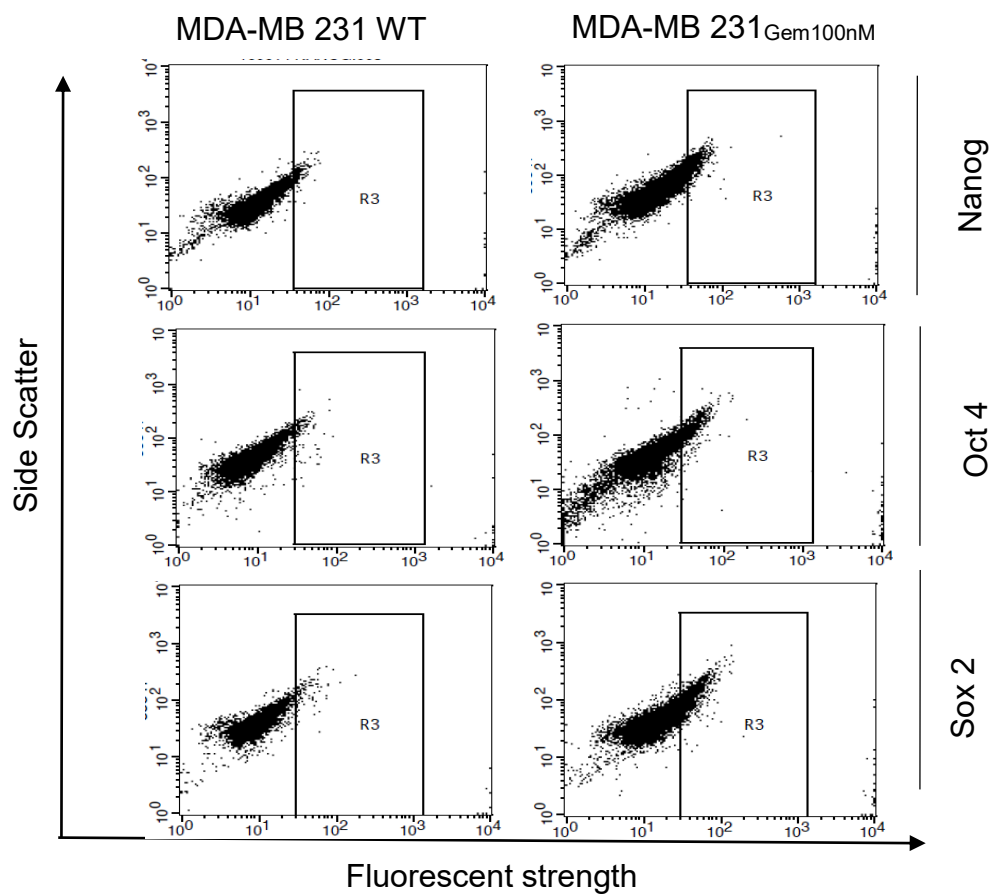


Figure 6.6(A). Representative FACS Plots of Embryonic Stem cell markers expression in MDA-MB 231 MDA-MB 231 Wild Type and MDA-MB 231_{GEM100nM} cell line. Fluorescence Activated Cell Sorting (FACS) data shows that higher expression of embryonic stem cell markers (nanog, Sox2 and Oct4) were displayed in MDA-MB 231_{GEM100nM} compared to parental cell MDA-MB 231.

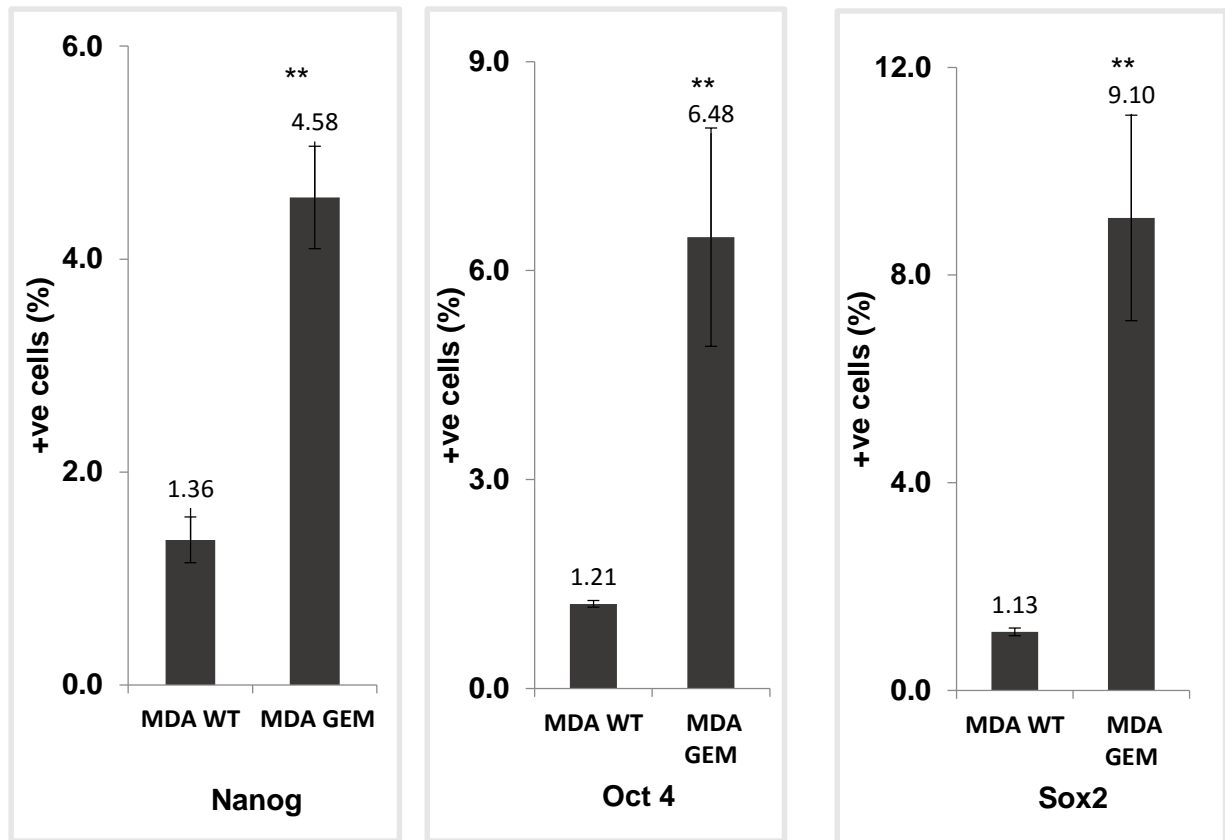


Figure 6.6B Bar chart Representation of embryonic stem cell markers expression in MDA-MB 231 WT and MDA-MB 231_{GEM100nM} BC cell line. Histograms (median \pm interquartile range) above displays statistically significant increase in all three embryonic markers (Nanog, Oct4 and Sox2) markers in MDA-MB 231_{GEM100nM} cells compared to the sensitive parent cell MDA-MB 231 WT (Mann and Whitney U test, ** $p < 0.05$, $n=9$). (Abbreviations: WT: wide type; GEM100nM: gemcitabine resistance cell).

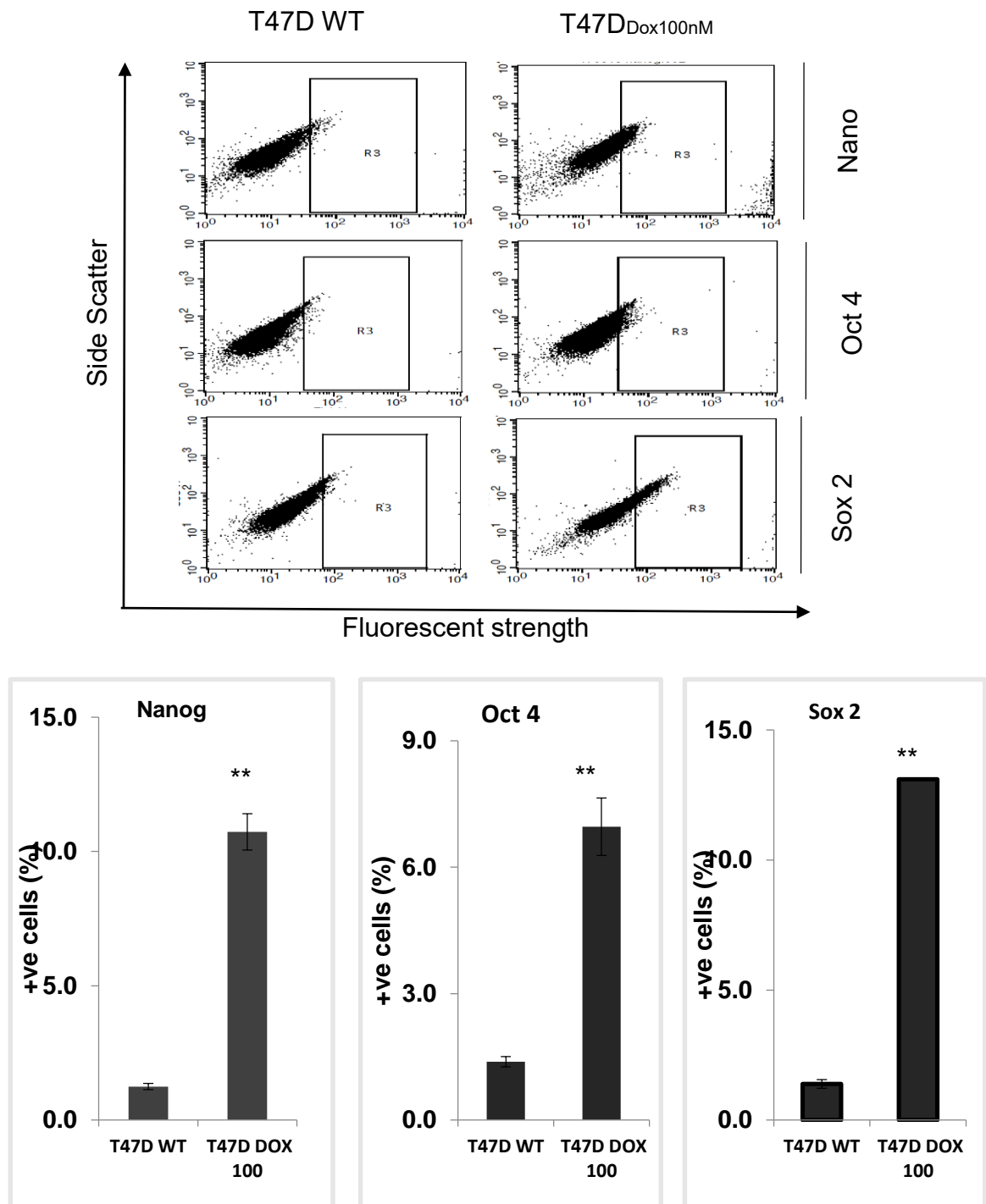


Figure 6.7. Representative FACS Plots of Embryonic Stem cell markers expression in T47D WT and T47D_{Dox100nM} cell line. Fluorescence Activated Cell Sorting (FACS) data shows that higher expression of embryonic stem cell markers (Nanog, Sox2 and Oct4) were displayed in T47D_{Dox100nM} compared to parental cell T47D. Histograms (median \pm interquartile range) above displays statistically significant increase in all three embryonic markers (Nanog, Oct4 and Sox2) markers in T47D_{Dox100nM} cells compared to the sensitive parent cell T47D wild type (Mann and Whitney U test, **p<0.05, n=9). (Abbreviations: WT: wide type; Dox100nM: doxorubicin resistance cell).

6.3.5. Resistant cell lines have longer doubling time

Quiescence is a common feature of drug resistant cancer cell lines. The cell growth of resistant cells MDA-MB-231_{GEM100nM} and T47D_{Dox100nM} were significantly slower compared to the parental wide type cells MDA-MB-231 and T47D respectively. Growth curves show that the resistant cells have a longer doubling time as shown in Figure 6.8.

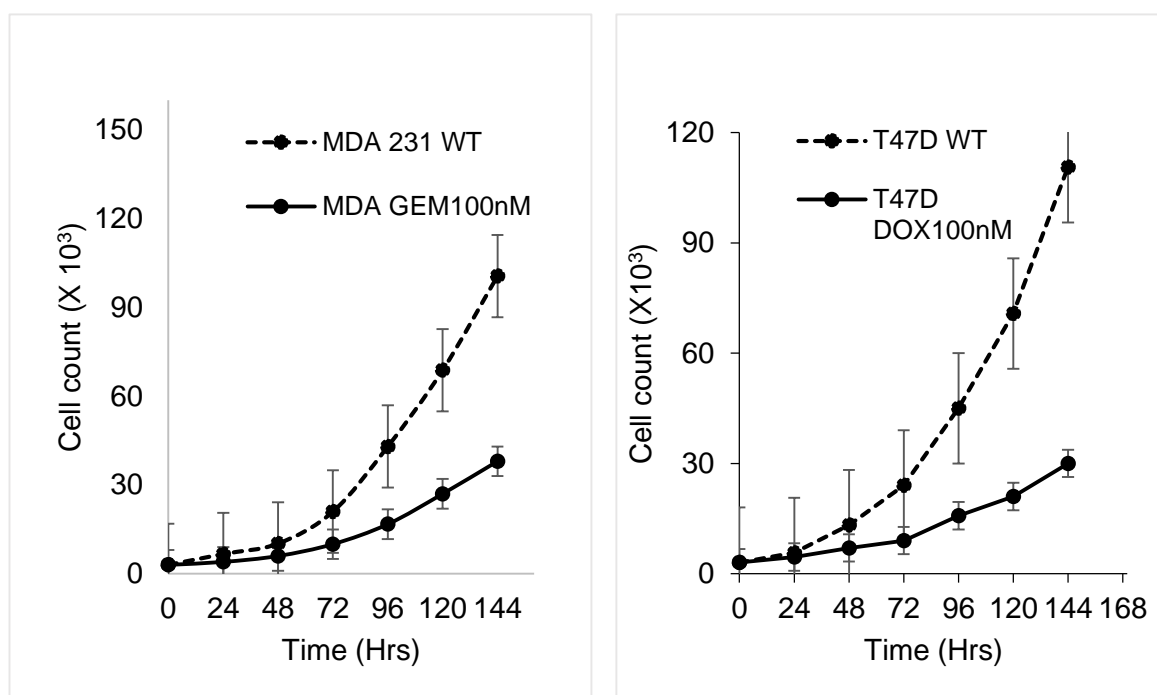


Figure 6.8. Representative Growth curves of MDA-MB-231 and MDA-MB-231_{GEM100nM} cells and T47D and T47D_{Dox100nM} cell lines. The figure shows the growth curve (Mean \pm SD) for wide type cells and resistant cells, MDA-MB-231_{GEM100nM} and T47D_{Dox100nM} cell lines proliferates slower than their respective wide type cells. (Abbreviations: WT: wide type; Dox100nM: doxorubicin resistance cell, ALDH: aldehyde dehydrogenase)

6.3.6. Western blot analysis of antiapoptotic proteins

Western blot analysis performed on whole cell lysate of T47D_{Dox100nM} resistant cell line show that expression of P-gp may be a major factor contributing to drug resistance in these cells.

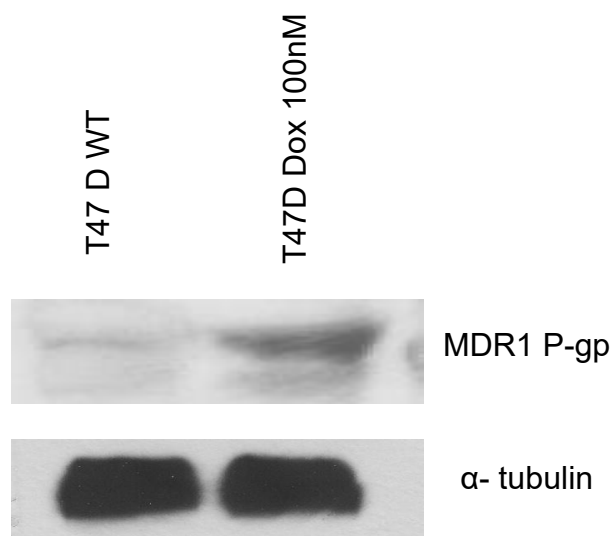


Figure 6.9. Representative Western Blot of MDR1 P-gp expression in T47D wild type and T47D_{Dox100nM}. Western blotting on whole cell lysates shows that T47D_{Dox100nM} resistant cell overexpresses multiple drug resistance1 (MDR1) P-glycoprotein compared to sensitive T47D wild type cell line.

6.3.7. Resistant cells exhibit reduce cytotoxic apoptotic induced death

Several morphological changes were observed in the resistant cell lines. Images captured using light microscope show that the MDA-MB 231_{GEM100nM} cells were smaller than the parental cell MDA-MB 231 cells. The T47D_{Dox100nM} appeared to have multiple nuclei, spindle like with elongated pseudopodia and have a less

cohesive appearance while parental T47D cells have a cobblestone appearance with single nuclei.

Cell death was observed in the parental cells MDA-MB 231 and T47D cells after exposure to 200nM and 700nM of dFdC and Dox respectively, while the resistant cells were tolerant to the anticancer drugs. Treatment of cells with Ds/Cu induced massive cell death.

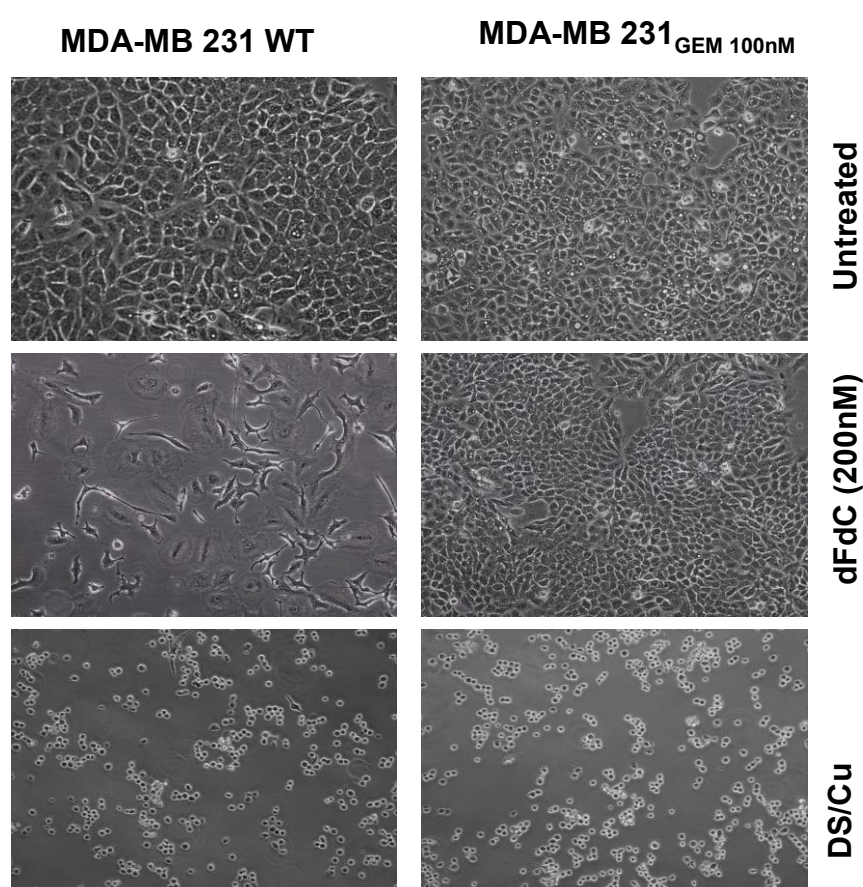


Figure 6.10.A. Representative Images of MDA-MB-231_{GEM100nM} cell line resistance to gemcitabine-induced apoptosis. Images shows the morphology (× 20 magnification) of MDA-231 WT and MDA-MB231_{GEM100nM} cells before and after treatment with dFdC (200nM). After 72 hours, cell death was observed in the MDA-MB 231 treated parental cells while the resistant cells survived. Treatment of MDA-231 WT and MDA-MB231_{GEM100nM} cell lines with DS plus Cu for 4 hours induced cell death in both resistant and sensitive cell lines. (Abbreviations: dFdC: gemcitabine, WT: wild type, GEM100nM: gemcitabine resistance cell, DS: disulfiram, Cu: copper).

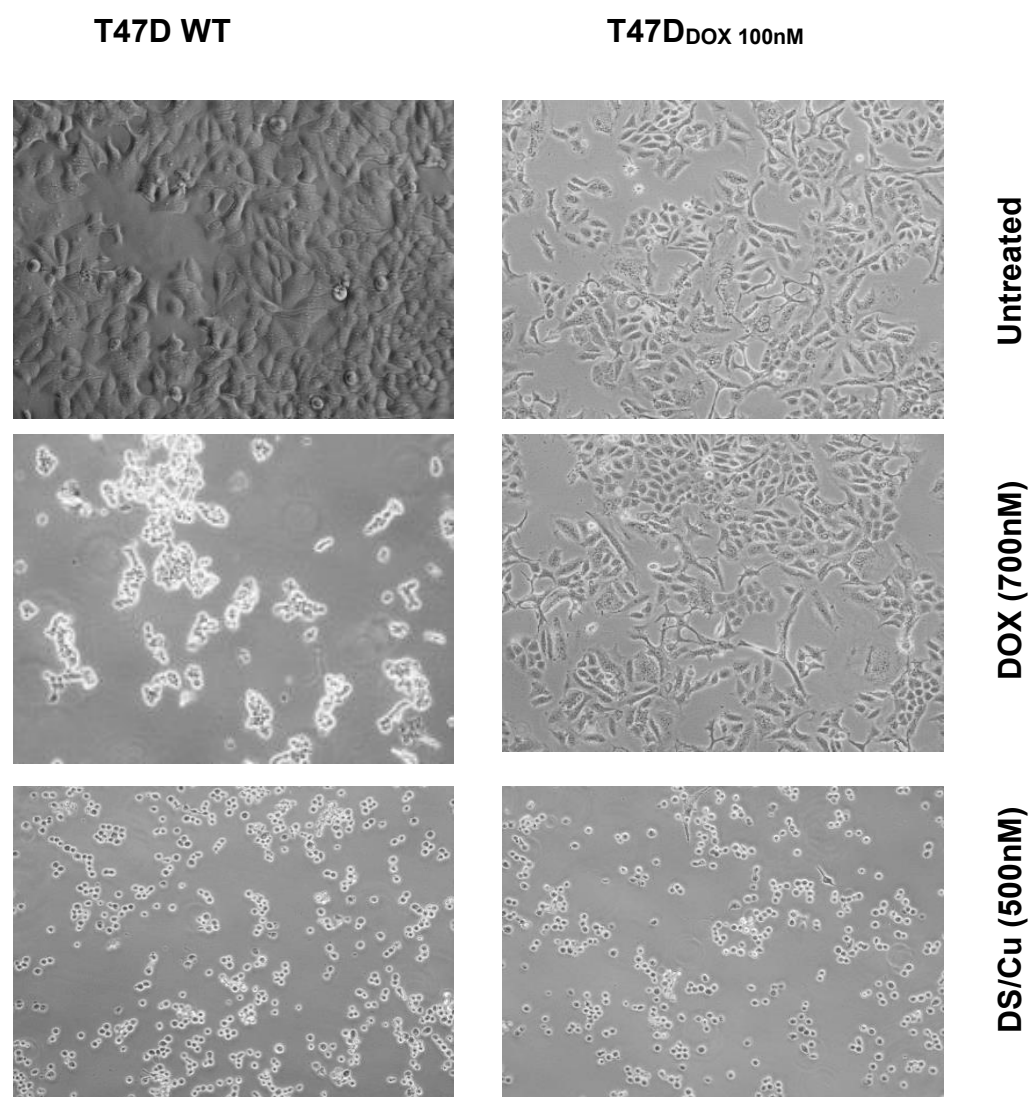


Figure 6.10B. Representative Images of T47D_{DOX100} cell line resistance to doxorubicin-induced apoptosis. Images shows the morphology (×20 magnification) of T47D wild type and T47D_{DOX100nM} cells before and after treatment with Dox (700nM). After 72 hours, cell death was observed in the MDA-MB 231 treated parental cells while the resistant cells survived. Treatment of T47D wild type and T47D_{DOX100nM} cell lines with DS plus Cu for 4 hours induced cell death in both resistant and sensitive cell lines. (Abbreviations: Dox: doxorubicin, WT: wild type, DOX100nM: doxorubicin resistance cell, DS: disulfiram, Cu: copper).

6.4.1 Cytotoxicity of DDC-Cu and DS plus Cu (DS/Cu) was observed in cancer cell lines.

After 72 hours exposure of DDC-Cu and DS/Cu, both showed high cytotoxic to MCF7 breast cancer cell line. The IC_{50} of DS/Cu was 449nM while that of DDC-Cu which was 238nM. Our results showed that DDC-Cu exhibited higher cytotoxicity than DS/Cu (Figure 6.11). This may indicate that the cytotoxicity of DS/Cu may not be solely due by the reaction between DS and Cu but DDC-Cu the final product of the reaction may play critical role in DS/Cu induced cell death.

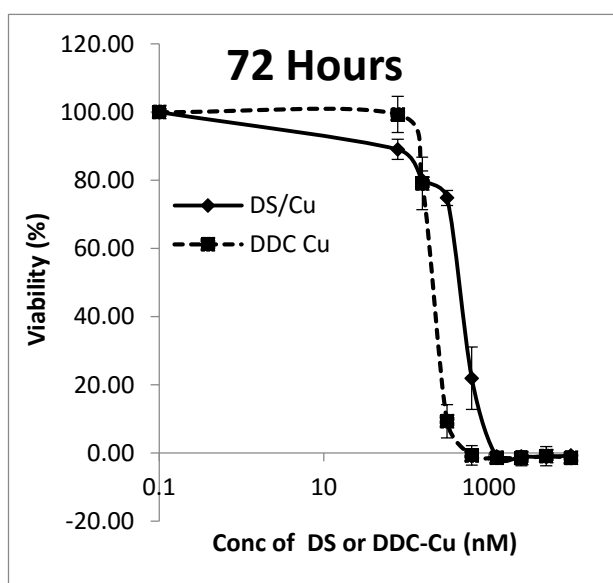


Figure 6.11. Representative Drug Concentration Response Curve of MCF7 cells treated with DS/Cu and DDC-Cu. Viability curve from the MTT analysis show that both DS/Cu and DDC-Cu are toxic to cancer cells. DDC-Cu complex induced more cell death in than DS plus Cu treated MCF 7 cell line (DS: disulfiram, Cu: copper, DDC-Cu: diethyldithiocarbamic copper complex).

6.4.2 Time dependent cytotoxicity of DDC-Cu and DS plus Cu (DS/Cu) in BC cancer cell lines.

The time dependent cytotoxicity of DS/Cu reaction and DDC-Cu was studied at different time interval. Viability curve from MTT analysis showed that there was massive cell death in cells exposed to DS/Cu after 30 minutes with more cell death detected at 60 minutes but levelled off after 180 minutes. This was in contrast to cell killing observed for DDC-Cu, at 30 and 60 minutes no significant cell death was observed until about 180 minutes (Figure 6.12). The viability curves for both DS/Cu and DDC-Cu was similar until after 72 hours where more killing was observed for DDC-Cu (Figure 6.11A). This results suggest that the DS is able to exhibit a rapid cytotoxic effect on cancer cells, followed a delayed cell killing by DDC-Cu.

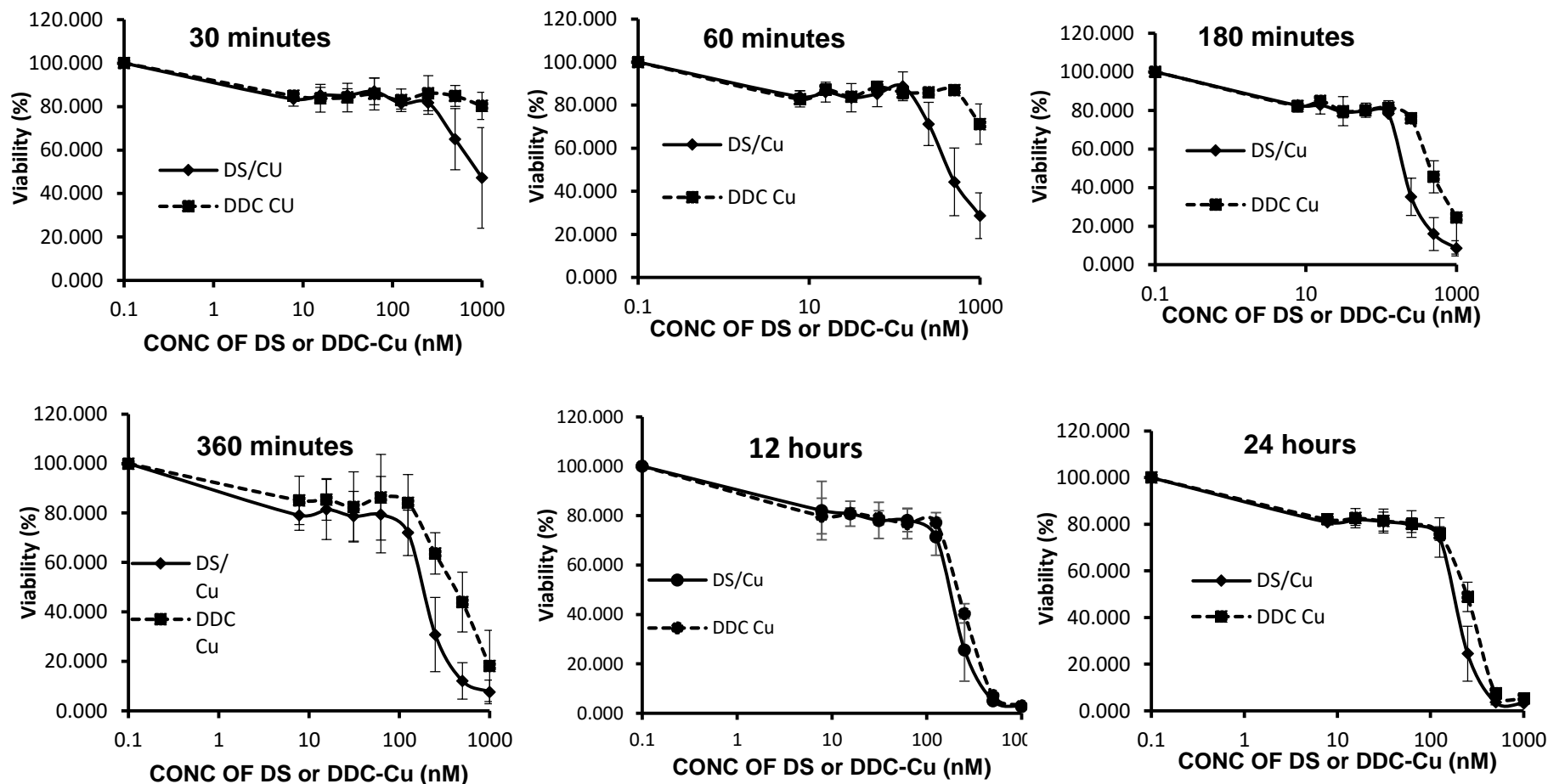


Figure 6.12. Representative Drug Concentration Response Curves of DS/Cu and DDC-Cu at different time points (30min, 60min, 180min, 360 min, 12 hours and 24 hours). Cell viability curve from MTT analysis for DS/Cu and DDC-Cu at different time interval show that both DS/Cu and DDC-Cu are toxic to cancer cells. DS plus Cu and DDC-Cu were both toxic to cancer cells in a time dependent trend.

6.4.3 ROS was responsible for the cytotoxic killing of DS/Cu

MTT analysis data show that DS/Cu and DDC-Cu are both toxic to cancer. According to a recent report by (Lewis *et al.*, 2014) the cytotoxic effect of DS in association with Cu was attributed to the generation of ROS. Extracellular ROS generation in medium was examined from the reaction of DS/Cu, DDC-Cu, DS alone, Cu alone and H₂O₂. The results showed that higher levels of ROS was detected at ordinary working concentration of DS at 10µM, the reaction between Ds/Cu generated significantly higher ROS than 20µM H₂O₂ and plateaued at about 3 hours. Lower levels of ROS were detected from 10mM of DS/Cu probably due to instant crystallization of DS and Cu at higher concentrations. No significant ROS was detected in DDC-Cu and DS only containing mediums (Figure 6.13), indicating that ROS may be responsible for the cytotoxicity of DS/Cu but not DDC-Cu.

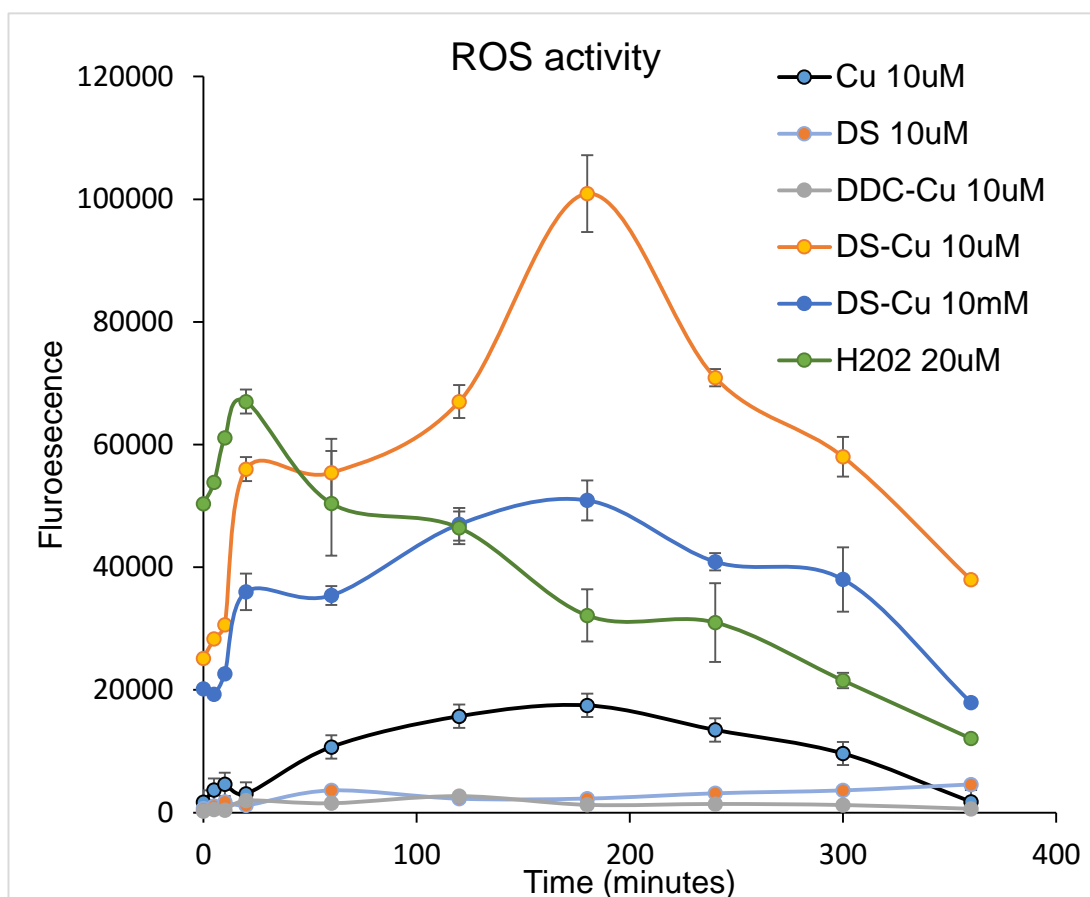


Figure 6.13. Representative Plots of ROS activity detected in DS, Cu, DS/Cu, DD-Cu and H₂O₂ containing cell culture medium. Extracellular ROS in medium containing DS/Cu and H₂O₂ generated higher ROS than medium containing DDC-Cu, DS alone, Cu alone suggestive that ROS generated by DS plus Cu reactive could be responsible for the rapid cell death. The intensity of the fluorescence represents the intensity of the ROS in the medium (ROS: reactive oxygen species, DS: disulfiram, Cu: copper, DDC-Cu: diethyldithiocarbamic copper complex).

6.4.4 DS/Cu is unstable in medium

The stability of DS/Cu and the metabolic kinetics of DS/Cu and DDC-Cu in MCF7 cell cultured was evaluated. Peak for pure standard DDC-Cu and DS were detected at retention time of 4.15 and 7.07 minutes respectively (Figure 6.14).

DDC-Cu was detected in both medium and cell lysate extracts from DS/Cu containing medium with a steady increase in concentration (Figure 6.15). Stable levels of DDC-Cu was detected in medium and cell lysate when pure DDC-Cu was added to culture medium(Figure 6.16), DS was detected in DS/Cu cultured medium but rapidly plunged to undetectable levels after 30 minutes while no DS was detected in cell lysate.

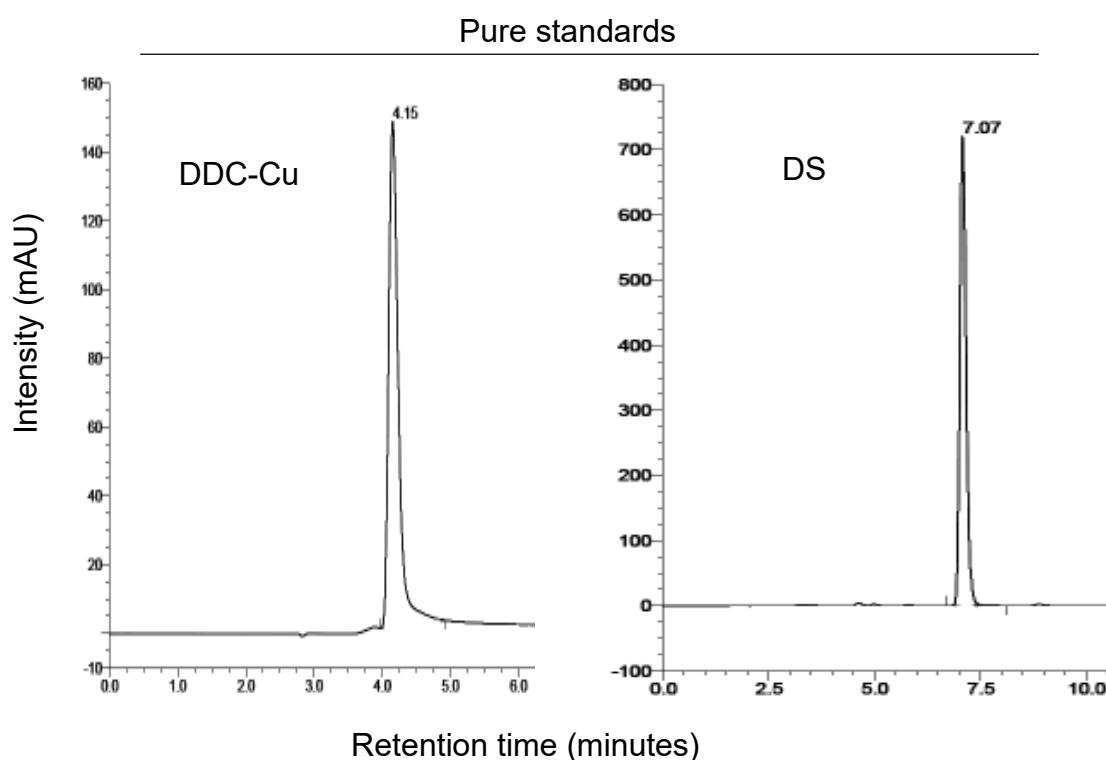


Figure 6.14(A). Representative HPLC Peaks DS and DDC-Cu in cell medium. Peaks for retention time of pure standards of DS and DDC-Cu measured by HPLC (DS: disulfiram, Cu: copper, DDC-Cu: diethyldithiocarbamic-copper complex, mAU: milliabsorbance unit).

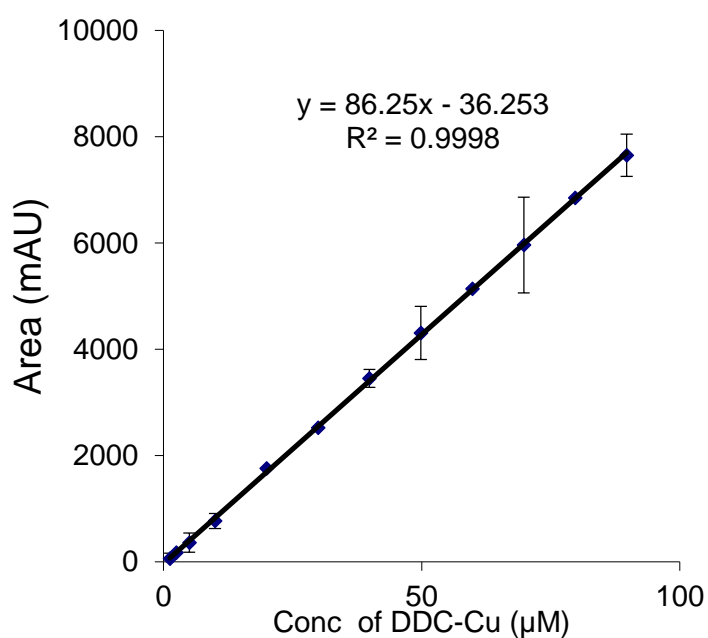
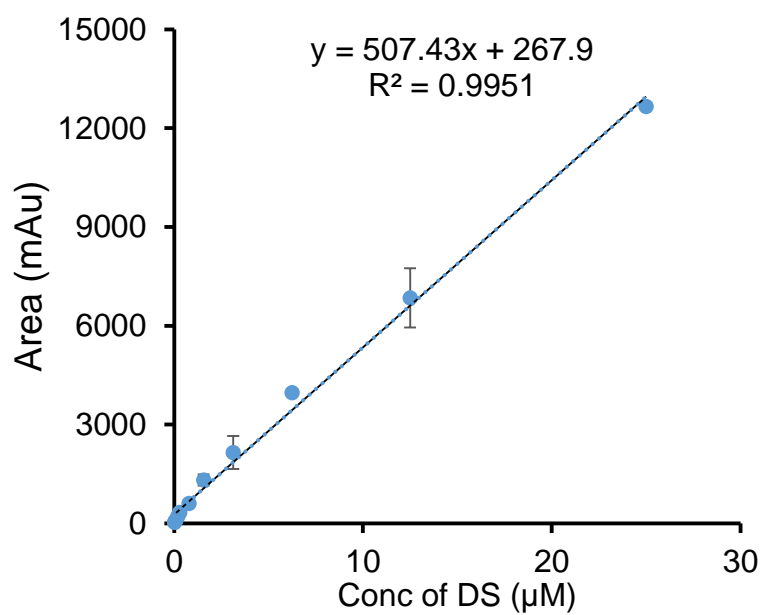


Figure 6.14(B). Representative Calibration Curves of DS and DDC-Cu in cell medium. The figure displays the standard calibration curve of Area (mAU) of pure standards of DS and DDC-Cu measured by HPLC (DS: disulfiram, DDC-Cu: diethyldithiocarbamic-copper complex, mAU: milliabsorbance unit).

Cell lysate

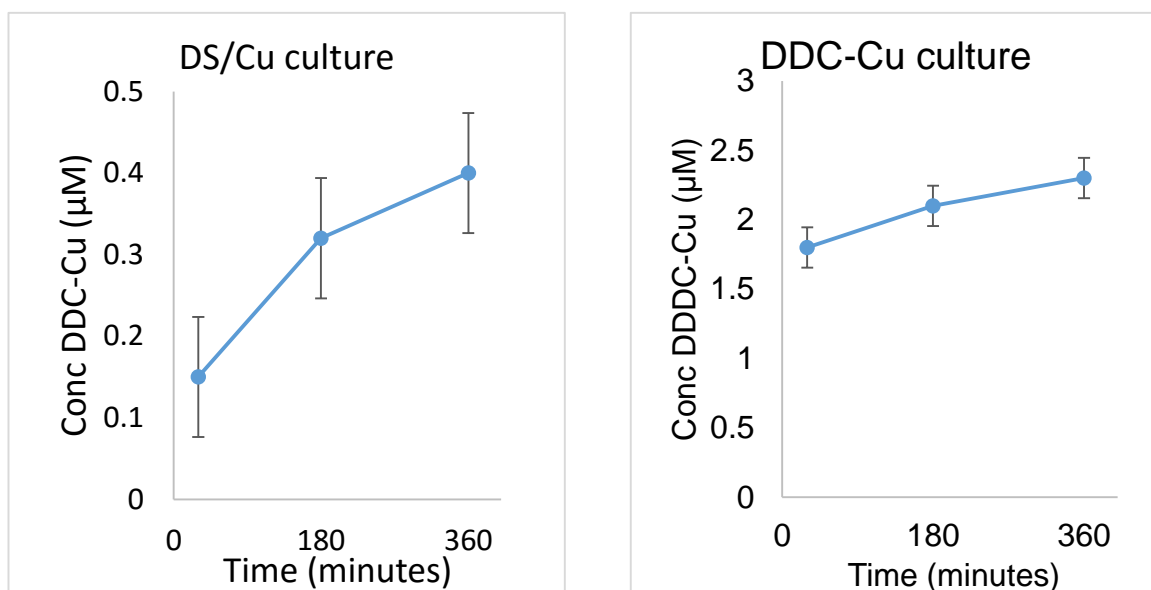


Figure 6.15 Representative HPLC profile Plots of DS/Cu and DDC-Cu. DS/Cu and DDC-DC detected from cell lysate of MCF7 cell line. The graph (median \pm interquartile range, n=6) show the HPLC profiles of DS and DDC-Cu in the time-dependent trend of DDC-Cu in the cell lysate. DS plus Cu was converted to DDC-Cu in cell lysate in a time dependent trend and DDC-Cu complex in cell lysate steadily increased.

Culture medium

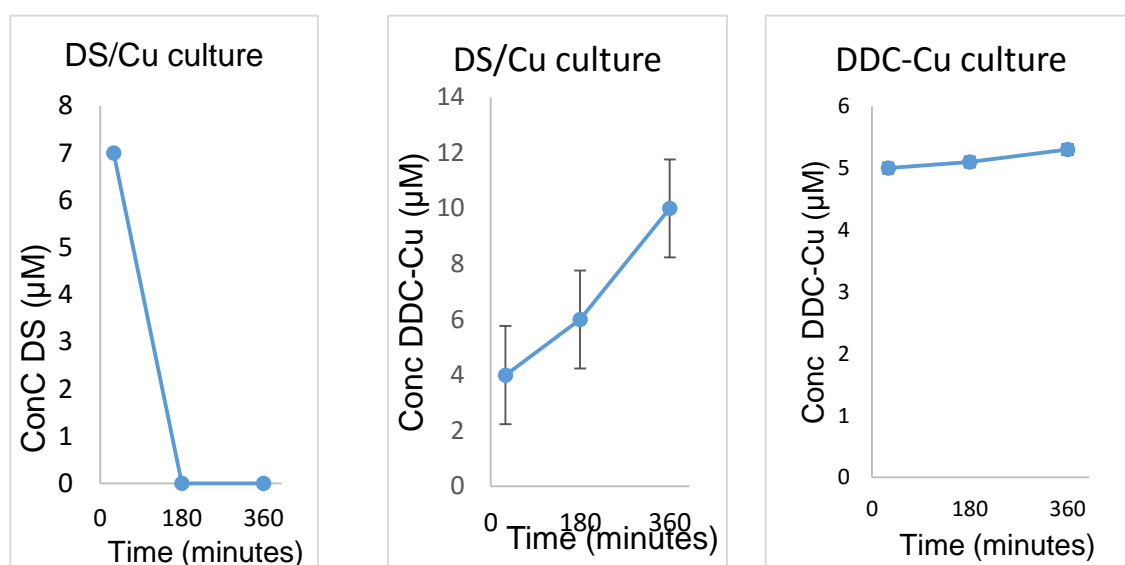


Figure 6.16. Representative Plots on Time dependent trend of DS-Cu and DDC-Cu in culture medium. The graph (median \pm interquartile range, n=6) shows the HPLC profiles of DS and DDC-Cu in the time-dependent trend of DDC-Cu in the culture medium. In cell culture DS rapidly degraded forming DDC-Cu complex (DS: disulfiram, Cu: copper, DDC-Cu: diethyldithiocarbamic-copper complex).

6.5. Discussion

Chemotherapy the use of cytotoxic drugs is one of the standard methods of treatment for many cancers. Chemotherapy induces cell death in tumours reducing the tumour bulk however many patients experience tumour recurrence and ultimately death. Resistance to these therapeutic drugs remains a major hurdle in the treatment and management of BC. In this study, two resistant cell lines MDA-MB-231_{GEM100nM} and T47D_{Dox100nM} were characterized for better understanding on the mechanisms of chemoresistance involved in resistance to dFdC and Dox respectively.

In this study, *in vitro* cytotoxicity assay showed that MDA-MB-231_{GEM100nM} cell lines were significantly resistant to dFdC-induced cytotoxicity compared to the sensitive parental MDA-MB 231 cell line. The resistant cell line was also cross resistant to four other conventional anticancer drugs (CDDP, VCR, PTX, Dox) all with different mechanism of action (Figure 6.2 A and B), indicative that acquired resistance to dFdC can induce pan-resistance to a range of anticancer drugs which is in agreement with the report by Faneyte *et al.*, (2001) which demonstrated that BC cells initially responsive to anticancer drugs frequently relapsed and acquired resistance to a broad spectrum of drugs.

Previous results show that CSCs play vital roles in the induction of chemoresistance in BC cells. To further understand the mechanism of resistance of dFdC, flow cytometry assay was performed in the MDA-MB 231 parental cell and MDA-MB 231_{GEM100nM} cell line. The resistant cell line MDA-MB 231_{GEM100nM} had higher expression of CSC markers suggestive that these cells had a stem-like phenotype which may be the cause for the chemoresistance.

Dox an anthracycline antibiotic is considered to be one of the most effective agent in the treatment of BC, however resistance to Dox leads to unsuccessful outcome in many patient. MTT cytotoxicity analysis showed that the T47D_{Dox100nM} resistant cells were also found to be resistance to Dox and other conventional anticancer drugs. Similar to the findings in dFdC resistant cells, the Dox resistant cells also displayed CSCs like phenotype as stem cell markers ALDH, CD44⁺/CD24⁻, CD 133 and embryonic markers (Nanog, Sox2 and Oct4) were all significantly increased in T47D_{Dox100nM} cells compared to the parental T47D wild type cell. Further confirming the involvement of stem cells in drug resistance.

Another mechanism of resistance in cancer cell is overexpression of MDR related ABC transporters which increase drug efflux from cells. Dox resistance is predominantly due to the expression of P-gp (Broxterman *et al.*, 1995). P-gp a multidrug efflux pump responsible for drug resistant in a number of cancer cancers was also slightly upregulated in the T47D_{Dox100nM} resistant cell line but was not detected in MDA-MB-231_{GEM100nM} cells, suggesting that P-gp could be responsible for the resistance in Dox resistant cells but was not the case for the dFdC resistant cells.

Several studies have shown that DS induced apoptosis in a number of cell lines (Cen *et al.*, 2002; Wang *et al.*, 2003; Brar *et al.*, 2004), others reveal that it has antiangiogenic effects on cancer cell (Shain *et al.*, 2003), inhibits DNA topoisomerase (Yakisich *et al.*, 2001) and inhibits NFκB activity. Cancer cells due to their rapid proliferation and metabolic rate possess higher ROS (a group of oxygen-containing free radicals with high reactive chemical properties) than normal cells but are quite tolerable to this increase in ROS because of their high antioxidant capability (Gupte and Mumper, 2009; Sporn and Liby, 2012). Further

increases in ROS exposure by ROS-generating agent can overwhelm and exhaust this cellular antioxidant capacity protecting cancer cells thus inducing apoptosis and ultimately death. Several studies have illustrated that DS facilitates the intracellular uptake of Cu in cancer cells and potentiate the cytotoxicity of several anticancer drugs in drug resistant and sensitive breast, colon and leukaemia cell lines (Wang *et al.*, 2003; Guo *et al.*, 2010; Liu *et al.*, 2014).

The reaction between DS and Cu is a strong ROS inducer (Nobel *et al.*, 1995). According to the report by Conticello *et al.*, (1995), DS in association with heavy metal can induce ROS mediated death in cells. Data from my MTT analysis show that DS/Cu and DDC-Cu were both significantly cytotoxic to BC cell lines (Figure 6.11A). I demonstrated that the cytotoxicity of DS may occurs in two phase, firstly an instant and short term action (Figure 6.13) in which higher ROS was generated from the reaction between DS/Cu. This was further confirmed by MTT results analysis in which instantaneous cell death was observed in cells after 30 minutes treatment with DS/Cu reaction, further killing also observed but levelled off after 180 minutes. No significant ROS was detected in DDC-Cu and DS only containing mediums, indicative that the cytotoxic effect of DDC-Cu was not mediated through ROS. DS can also exert a delayed toxic effect by its end product DDC-Cu with a higher cytotoxic effect.

After absorption of the parent drug DS or its Cu-complex DDC-Cu across the GIT mucosa into the blood stream, DS rapidly disappears below its limit of detection (Stromme, 1965; Cobby *et al.*, 1977) being reduced to DDC by endogenous thiols and glutathione reductase in the erythrocytes. The metabolic stability of free DS/Cu and DDC-Cu was examined; my result illustrated that DS was highly

unstable in medium and cell lysate while DDC-Cu was detected in both medium and cell lysate extracts from DS/Cu containing medium with a steady increase in concentration. DS has a very short half-life in serum less than 2 minutes (data from chapter 7). Due to this very short half-life of DS *in vivo* sufficient ROS will not be generated if the oral version of DS and Cu is administered to patient separately limiting the efficacy of DS as a potential chemotherapeutics. To resolve this problem, we recently protected DS from degradation in the bloodstream by encapsulation of DS into nanoparticles.

Conclusion

These resistant cell lines could be useful model to investigate the mechanisms of resistance in BC cells. My data show that the resistant cells were highly resistant to a range of anticancer drugs suggestive that acquired resistance can induce pan-resistance in BC cells. The resistant cells had slow proliferation rate as shown in the growth curve displaying senescence. We believe that the induction of stem-like cell features (increased stem cell markers) in these cells together with the several antiapoptotic genes were responsible for drug resistance, therefore development of drugs that can target these CSCs would be beneficial.

Cell death induced by DS/Cu may be biphasic via instant and delayed phases, with the instant killing caused the ROS generation from the reaction between DS and Cu and the delayed killing linked to the effects of DDC-Cu which interfere with molecular pathways within cancer cells inducing apoptosis.

Chapter Seven

Encapsulation of DS in Polymeric micelles

7.1. Introduction

There is a growing interest in the use of nanotechnology in the prevention, diagnosis and treatment of disease. The use of nanocarriers for cancer treatment could be quite advantageous the reason being that the encapsulated anticancer drug is protected from unfavourable conditions which prevent rapid degradation, improve biodistribution and pharmacokinetics and ultimately improving the efficacy of the anticancer drugs. The abnormal vasculature and reduced lymphatic drainage of tumours results in an increase in selective targeting by nanocarriers which can penetrate the leaky blood vessels of cancer cells with high local concentration of the encapsulated anticancer drug (Upreti *et al.*, 2013).

Nanocarriers used for delivery of chemotherapeutic agents include liposomes (Li *et al.*, 2009), polymeric micelles (Kim *et al.*, 2004) and PLGA (Torchilin, 2007). Liposomes have been used extensively in the clinic for drug delivery and their efficacy has been shown to reduce systematic effects and toxicity as well as attenuate drug clearance (Torchilin, 2005). The efficacy of DS encapsulated in liposome has been investigated by Prof. Wang Weiguang research group, although quite effective as a potential anticancer agent (Liu *et al.*, 2014) liposomes are subjected to several limitation such as low encapsulation efficiency, poor storage stability, fast burst release of drugs in the presence of blood components and lack of tunable trigger for drug release (Mohanraj and Chen, 2006).

Polymeric micelles are nanoscopic drug carriers with a core/shell structure formed by amphiphilic block polymers. The application of micelles as drug delivery is due to this unique amphiphilic core-shell architecture in which the hydrophobic core serves as a reservoir for the encapsulation of hydrophobic drugs and the hydrophilic brush like shell structure protects the hydrophobic part from biological invasion and minimizes opsonin adsorption contributing to a longer blood circulation time and blood stability of micelles (Gabizon *et al.*, 2003). Furthermore, the relatively small size polymeric micelles enables them evade scavenging by the mononuclear phagocytic system of the liver and bypass of filtration by the inter-endothelial cells of the spleen which increase the accumulation of micelles at tissue site with vascular abnormalities (Aliabadi, and Lavasanifar, 2006).

The cytotoxicity of DS in complex with Cu has long been reported in a number of breast cancer cells lines (Chen *et al.*, 2006; Yip *et al.*, 2011), however the translation of DS into clinical cancer treatment is severely limited because the half-life of DS in the blood stream is very short approximately 4 minutes (Cobby *et al.*, 1977; Johansson, 1992). The efficacy of liposomal DS has been investigated by Prof. Wang Weiguang research group in breast cancer models (Liu *et al.*, 2014), although effective liposome was only able to extend the half-life of DS to about 30 minutes.

7.1.2. Rationale and aims of this study

The objective of this study is to develop a long circulating polymeric micelle encapsulated DS all aimed at improving the anticancer efficacy of DS.

7.2. Experimental design

Detailed information on materials, products, manufacturers and methodologies used for the entire study have been described in chapter 2. The following are specific experimental designs and methods used for this part of the study.

7.2.1. Preparation and Characterization of Disulfiram loaded Polymeric Micelle

DS loaded polymeric micelles (PMDS) were prepared and characterized (refer to Chapter 2, page 94 and 95).

7.2.2. Cumulative release of Disulfiram and Measurement of the *in vitro* half-life of Disulfiram in Horse Serum

Cumulative release profile of free disulfiram (DS) in PBS and *in vitro* half-life of free DS and disulfiram loaded polymeric micelles (PM-DS) in horse serum were examined (refer Chapter 2, page 96).

7.3. Results

7.3.1. Physicochemical characterization of DS loaded PM nanoparticles

Data from pilot study show that PMDS ratio influence encapsulation efficiency (EE), drug loading content (DLC) and nanoparticle size (Table 7.1). The PMDS ratio of 2:1 (w/w) gave optimum results and was used for further preparations. The stabilized micelles have an average size of about 200nm, narrow distribution and negative zeta potential values (Table 7.2).

Table 7.1: Influence of PMDS ratio on Encapsulation Efficiency and Drug Loading Content.

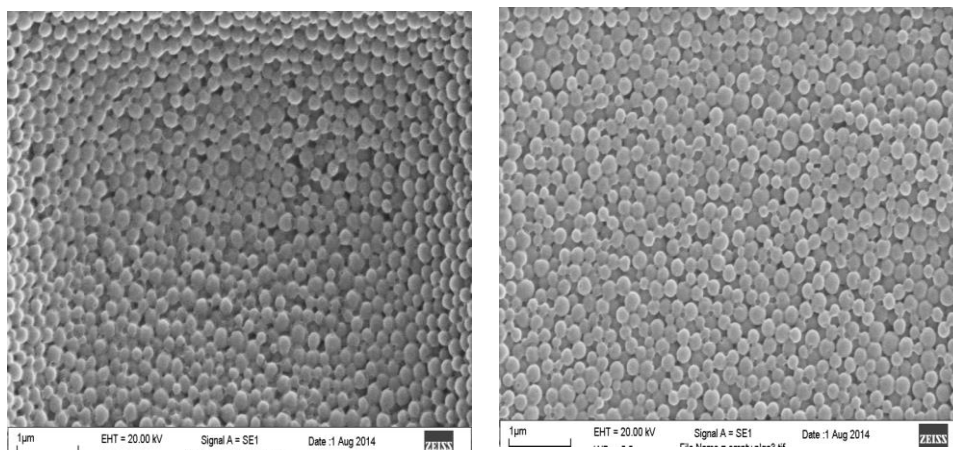
Parameter	Formulation			
PM (mg)	100	100	100	100
DS (mg)	10	30	50	70
DLC(%)	4.21±0.34	6.42±1.22	10.69±2.15	7.87±1.49
EE (%)	91.5±0.56	83.2±2.76	81.8±3.59	60.2±2.4

Table 7.1 show the encapsulation efficiency (EE) and drug loading content (DLC) of different ratio of DS encapsulated in polymeric micelles. The 2:1 ratio was the optimum ratio used for preparation for PMDS formulations because of the high DLC and EE obtained (DS –disulfiram, PM – polymeric micelles).

Table 7.2 Size, Polydispersity and Zeta Potential of PMDS

PM-DS	Aqueous dispersion	Lyophilized sample
Size (nm)	192 ± 8	223 ± 5
Polydispersity	0.25 ±0.01	0.30 ±0.02
Zeta potential (mV)	-17.2 ± 1.2	-20.4 ± 1.6

Table 7.2 show the size, polydispersity and zeta potential of dried and wet sample of PMDS. (DS –disulfiram, PM – polymeric micelles). The PMDS formulation were of uniform distribution and size. The negative zeta potential show the stability strength of PMDS.



Empty PM

PMDS

Figure 7.1. Representative Scan Electron Microscopy (SEM) images of PMDS. SEM images show that the PMDS is spherical in shape and have uniform size distribution. The empty PM and DS loaded PM were similar in size distribution and uniformity (DS: disulfiram, PM: polymeric micelle).

7.3.2. *In vitro* half-life of Disulfiram in Horse Serum

In vitro release profile of free DS and PMDS dispersed in horse serum showed that free DS was quickly degraded to undetectable levels within few minutes, while DS was slowly released from micelles with a half-life of approximately 3 hours (Figure 7.2 A and B).

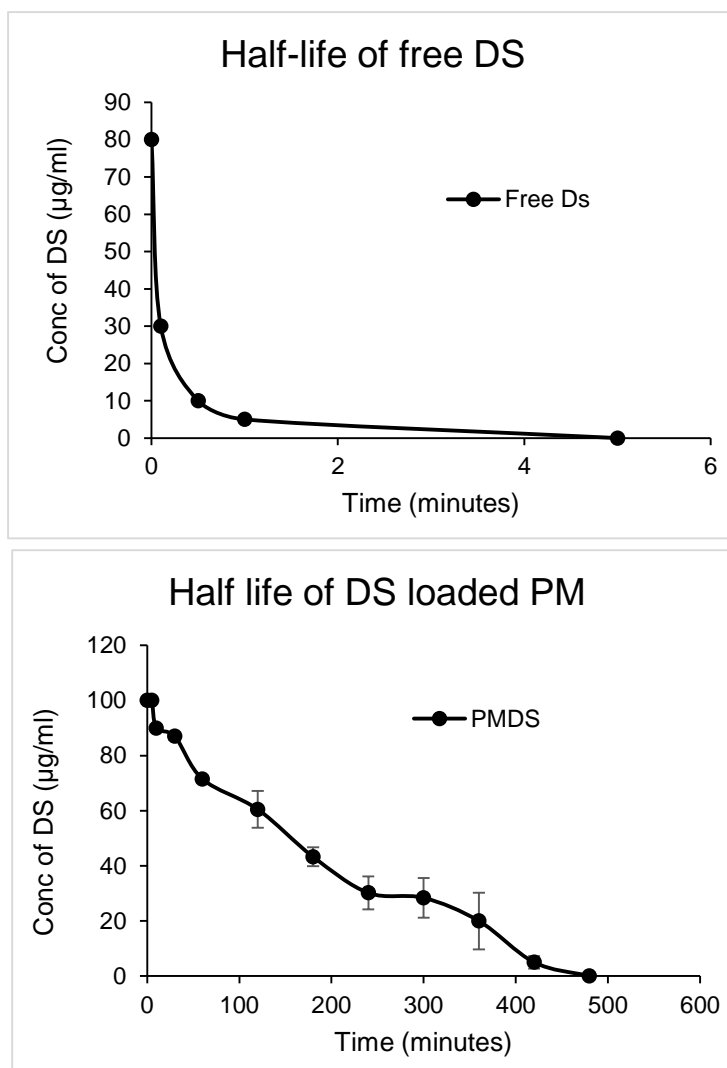


Figure 7.2(A). Representative Plots of *In vitro* half-life of free DS and DS loaded PM in horse serum. The half-life of free DS and DS loaded micelles measured at interval time points using HPLC. Free DS was rapidly degraded in horse serum, while the release of DS from PM was slowly released with a half-life of over 3 hours (DS: disulfiram, PM: polymeric micelle)

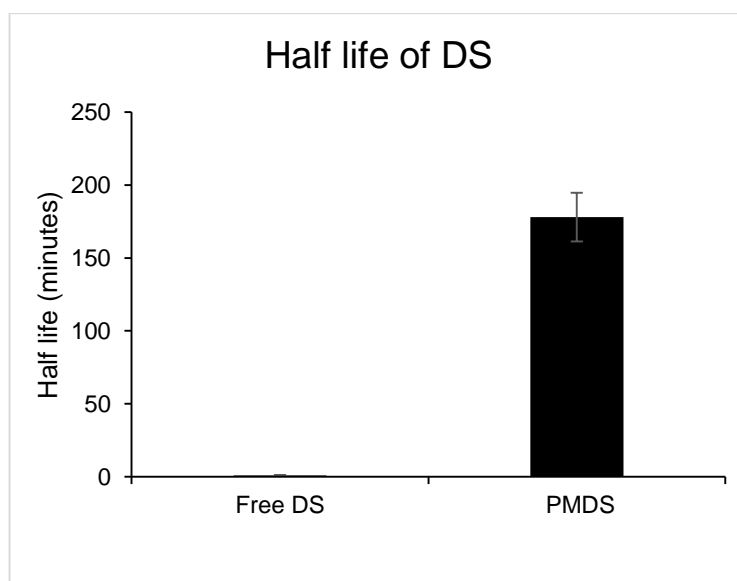


Figure 7.2B. Representative Bar chart of half-life of free DS and DS loaded PM in horse serum. *In vitro* release experiment on horse serum shows that DS is slowly released from PM with significant longer half-life whereas free DS was rapidly degraded. (n= 4, median \pm interquartile range). DS: disulfiram, PM: polymeric micelle.

7.3.3. *In vitro* release studies

The cumulative release profile of DS from PM in PBS (containing 0.5% Tween 80 (w/v) at pH 7.4 and 5 reveal that DS can be released from PM nanoparticle (Figure 7.3). The release was higher in acidic conditions suggesting that DS would be released from PM in higher amounts within the acidic tumour microenvironment compared to its release in the blood which is at physiological pH of 7.

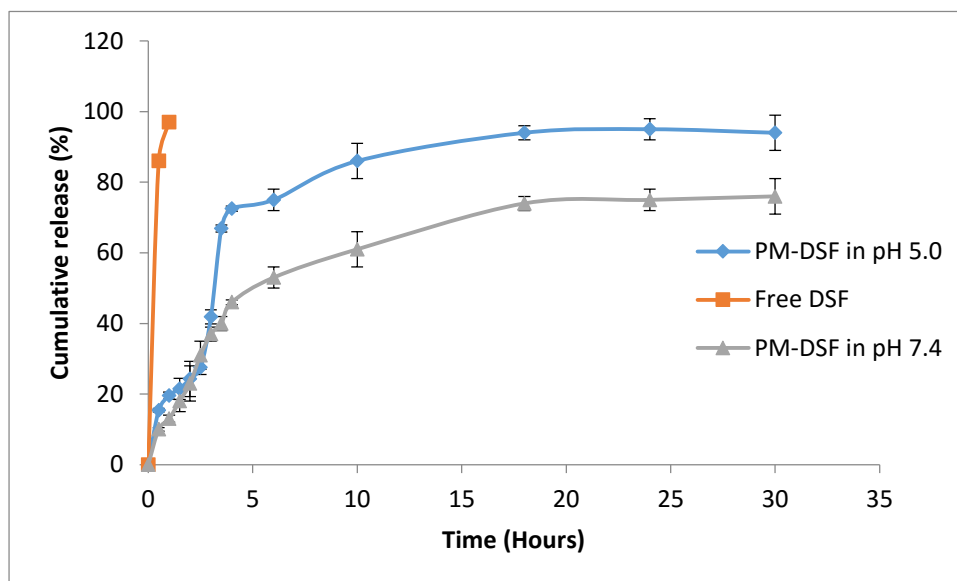


Figure 7.3. Representative Plots of *In vitro* cumulative release of DS from PM in PBS (containing 0.5% tween 80) at pH 5 and 7.4. DS can be released from PM in both acidic and alkaline conditions. Degradation of free DS occurred rapidly, while the release of DS from PM was sustained for over 25 hours. (DS –disulfiram, PM – polymeric micelles, PBS: phosphate buffer saline).

7.3.4. MTT cytotoxicity assay of PMDS in TNBC cell lines

The cytotoxicity of free DS and PMDS were examined in BC cell lines cultured in in hypoxia, transfected cell lines (HIF 1 α and HIF2 α transfect cells), NF κ Bp65 transfected cells and resistant cell lines. MTT assay showed that the *in vitro* cytotoxicity of PMDS supplemented with Cu (1 μ M) was comparable to that of free DS/Cu.

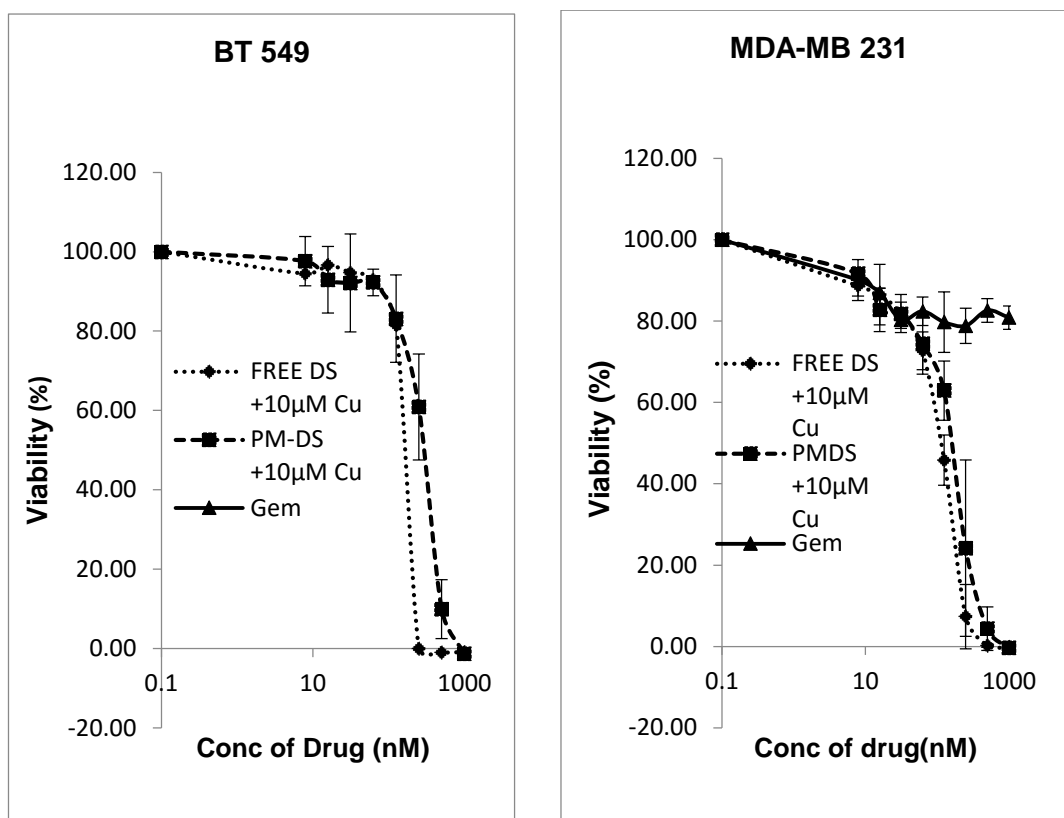


Figure 7.4(A). Representative Drug Concentration Response Curves of PMDS and Anticancer Drugs on cells in Hypoxic culture. Cell viability curve shows difference in dose response of Free DS, PM-DS and a first line anticancer drug (dFdC). Hypoxic cells resistant to dFdC were sensitive to DS plus Cu. DS induced cell death in the hypoxic cells which were resistant to dFdC. (Abbreviations: DS: disulfiram, PM: polymeric micelles, Gem100nM: Gemcitabine resistant cells, dFdC (gemcitabine)).

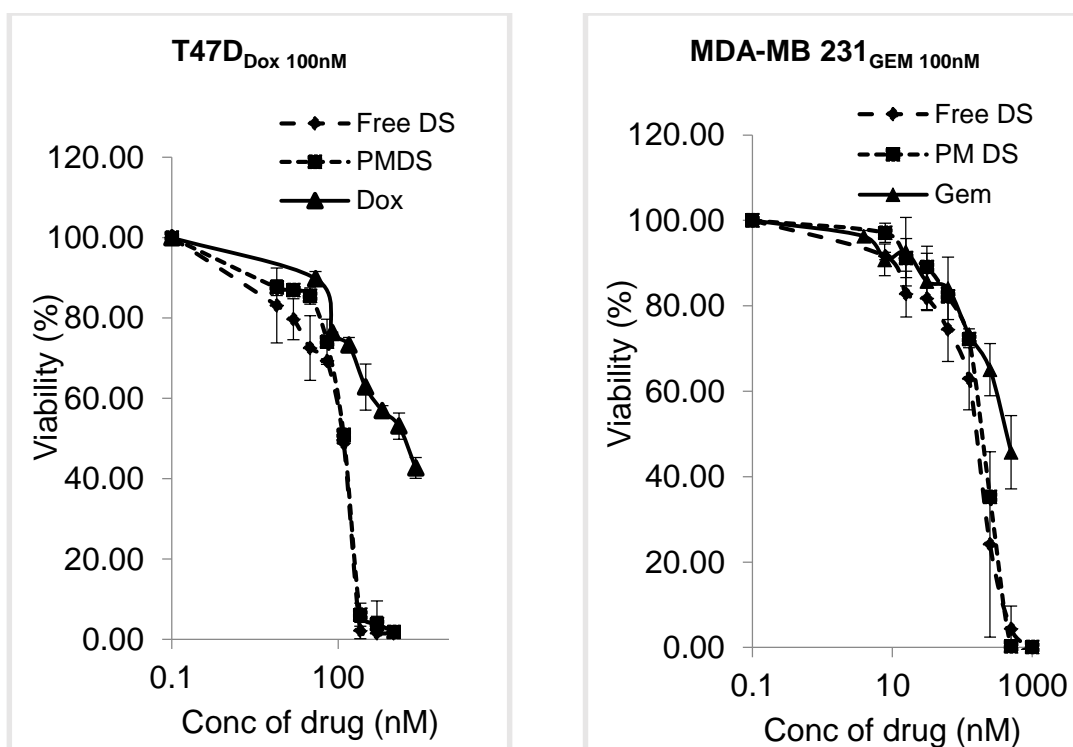


Fig 7.4(B). Representative Drug Concentration Response Curves of PMDS and Anticancer Drugs on cells in cells resistant cell lines. Cell viability curve shows difference in dose response of Free DS, PM-DS and first line anticancer drugs (gemcitabine and Dox). Resistant cell T47D_{DOX100nM} and MDA-MB 231_{GEM100nM} were sensitive to DS plus Cu. DS induced cell death in the resistant cell lines. (Abbreviations: DS: disulfiram, PM: polymeric micelles, Gem100nM: Gemcitabine resistant cells, Dox100nM: doxorubicin resistant cells, Dox: doxorubicin, dFdC: gemcitabine).

Table 7.3: IC₅₀ value of Several Resistant BC Cell Lines to First line Anticancer drugs

BC cell line/ IC ₅₀	Free DS/Cu (nM)	PMDS Cu (nM)	CDDP (μ M)	Gem (nM)	DOX (nM)
Hypoxic BT 549	141.06 (4.30)	249.46 (35.98)	826.22 (189.94)	600.1 (26.99)	1276.54 (157.01)
Hypoxia MDA-MB 231	111.81 (0.88)	149.88 (40.1)	993.98 (152.33)	> 1000	2405.22 (2.15.67)
NF κ B p65 transfected cell	91.89 (7.85)	100.22 (9.12)	535.47 (52.9)	940.22 (160.76)	> 2000
HIF 1 α transfected cell	110.43 (7.85)	120.22 (9.12)	> 900	> 500	> 1000
HIF 2 α transfected cell	105.19 (5.47)	124.77 (10.99)	> 900	>500	>1000
T47D _{Dox 100nM}	102.19 (11.12)	109.19 (8.87)	> 900	771 (38.81)	>1000
MDA-MB 231 _{Gem 100nM}	102.20 (15.43)	140.86 (9.21)	> 900	300 (5.67)	>1000

Table 7.4 shows the (median \pm interquartile range) of half maximum inhibitory concentration (IC₅₀) values of cells treated with free DS/Cu, PMDS/Cu and three first line anti-breast cancer drugs (dFdC, Dox and CDDP). The resistant cells (hypoxic cells, NF κ Bp65, HIF 1 α , HIF 2 α , T47D_{Dox 100nM} and MDA-MB 231_{Gem 100nM}) were resistant to conventional anticancer drugs (dFdC, Dox and CDDP). Free DS and PMDS induced cell death in these resistant cells (Mann and Whitney U test ** p<0.05, n=9). (DS: disulfiram, PM: polymeric micelle, dFdC: gemcitabine, DOX: doxorubicin, PTX: paclitaxel, CDDP: cisplatin, IC₅₀: half maximum inhibitory concentration).

7.4. Discussion

Numerous anticancer drugs such as Doxorubicin, cisplatin and paclitaxel have been encapsulated in nanocarriers and were found to be more effective than the free drug (Torchilin, 2005; Zhang *et al.*, 2005). Encapsulation of anticancer drugs in nanocarriers circumvents the problem of drug insolubility, increase precision of drugs on desired sites, protection against systemic adverse effects, control drug release and enhance transportation across barrier. Thereby increasing the efficacy, specificity and targeting ability of chemotherapeutic agents (Soppimath *et al.*, 2000).

Polymeric micelles are fast becoming powerful tools in nanomedicine for cancer therapeutics due to their small size, *in vivo* stability, ability to solubilize water insoluble anticancer drugs and prolonged blood circulation. Clinical trials with micellular formulations have demonstrated that they have numerous pharmacological advantages with reduced systemic toxicity and morbidity in patients compared to conventional drug formulation (Sutton *et al.*, 2007; Matsumura and Kataoka, 2009). Due to their unique size range < 200nm, micelles are able to avoid renal clearance and uptake by the liver and spleen thus preferentially accumulating in solid tumour via enhanced permeation and retention effects (EPR) (Maeda *et al.*, 2001; Torchilin, 2007). Compared with other nanocarriers, micelles are much easier to prepare and have a flexible structure for manipulation as drug delivery system (Moutinho *et al.*, 2012).

Liu *et al.*, (2014) have recently investigated the efficacy of a liposomal encapsulated DS on cancer cells. Liposome increased the half-life of DS to 30 minutes in blood, however liposome is subject to degradation in the bloodstream.

With these facts in mind, DS was encapsulated in polymeric micelles aimed at improving the *in vivo* efficiency of DS. Free DS is highly toxic to BC cells *in vitro* (Figure 7.5 A and B) having a biphasic cytotoxic effect on cancer cells, with rapid cell death caused by the generation of ROS by the interaction between DS and Cu and a delayed killing caused by a metabolite of DS DDC-Cu. However translation of DS into clinics is hampered due to its short half-life.

DS was successfully encapsulated in PM with a high encapsulation efficiency of over 80% with relatively small size (200nm) and even distribution as shown from Scan Electron Microscopy images (Figure 7.3). Cumulative *in vitro* release study performed on PMDS show that DS can be released from PM in both acidic and alkaline conditions in a pH dependent manner with higher release occurring in acidic pH, indicative that my formulation PMDS can preferentially target tumour cells (acidic milieu). Studies with miniature pH electrodes show that the pH within tumours varies from those of normal tissues having substantially more acidic values (Kallinowski and Vaupel, 1989; Huber *et al.*, 2010).

The short half-life of free DS in blood stream is the major hindrance preventing its clinical translation as an anticancer agent (Johansson, 1992). The result shows that free DS was rapidly degraded in horse serum with a half-life of less than 2 minutes consistent with the previous report (Cobby *et al.*, 1977). In contrast, the half-life of encapsulated DS in the PMDS formulation was markedly increased to over 3 hours (Figure 7.3 A and B) indicative that in the bloodstream DS can be slowly released from PM and in association with Cu induce cytotoxicity in cancer cells.

The cytotoxicity of PMDS was examined in several BC cells grown under hypoxia, resistant cells (MDA-MB-231_{GEM100nM} and T47D_{Dox100nM}) and transfected cells (HIF1 α , HIF2 α and NF κ Bp65 overexpressing cells). Results from MTT cytotoxicity assay have shown that cells grown under hypoxia are highly resistant to conventional anticancer drugs (CDDP, Dox, dFdC, PTX and VCR), similarly overexpression of both HIF 1 α and HIF2 α confer resistance to these transformed cells. NF κ Bp65 activation in cells also induced drug resistance BC cells as shown from previous results. The *in vitro* cytotoxic effect of PMDS was comparable to that of the free DS (Table 7.3). The IC_{50s} of PMDS and free DS were found to be very similar. DS alone, Cu alone and the empty PM did not induce cell death.

Conclusion

The clinical anticancer application of DS is severely limited due to the very short half-life as DS is very unstable in the bloodstream and rapidly degraded. Polymeric micelles hold great promise as drug delivery agents, DS was successfully encapsulated in micelle and this formulation protects DS from enzymatic degradation. This new formulation PMDS has a reasonable encapsulation efficiency, drug loading content, *in vitro* controlled release and half-life. PMDS in combination with Cu was significantly toxic to BC cells. Therefore the use of nanotechnology may improve the efficacy of DS as an anticancer agent translating it into an effective BC therapeutics.

Chapter Eight

8.1. General Discussion

In this study, results from growth curve analysis showed that monolayer TNBC cells grown under hypoxia have slower rate of proliferation compared to those grown in normoxia, indicating that hypoxia can induce quiescence in cells. Furthermore data from MTT analysis also show that hypoxia induced resistance to anticancer drugs as cells grown under hypoxia were significantly resistant to cisplatin (CDDP), gemcitabine (dFdC), vincristine (VCR), doxorubicin (Dox) and paclitaxel (PTX) compared to cells cultured in normoxic conditions in which cell death was induced at a much lower concentration.

Recent studies demonstrate that hypoxia induces expression of stem cell markers in cancer cells, decreases proliferation and such cells were highly resistant to conventional anticancer drugs (Bar *et al.*, 2010; Kolenda *et al.*, 2011). The identification of CSCs in BC (Al-Hajj *et al.*, 2003) opened an interest in the relevance of CSCs in cancer biology. These cells are believed to reside in the hypoxic niche and are mostly in a hypoxic state. Several studies suggest that hypoxia may be responsible for the persistence and maintenance of CSCs in tumours involved in the promotion of therapeutic failure and tumour relapse (Rosen and Jordan, 2009; Lin and Yun, 2010). According to the report by Bao *et al.*, (2012), hypoxia was a determinant of stemness in the stem cell niche and exposure of cells to hypoxia *in vitro* enhanced their tumourigenic potential *in vivo*. Hypoxia facilitate the emergence of malignant clones by maintaining cancer cells in their undifferentiated stem cell state, permitting self-renewal of cells and the accumulation of genetic and epigenetic changes resulting in a more aggressive

tumour. One aim of my study was to investigate the relevance of hypoxia in chemoresistance, monolayer of TNBC cells cultured in hypoxic condition were found to exhibit CSC-like characteristics with increase in CSC markers (ALDH and CD133) and embryonic markers (Nanog, Sox2, Oct4) compared to those grown in normoxia. These results suggest that hypoxia is able to induce these CSCs phenotype which may be responsible for the resistance to therapy.

Hypoxia can induce stem cell characteristics, however the molecular mechanisms and pathways linking hypoxia and CSCs are not fully understood. The HIF (HIF1 α and HIF2 α) are the most prominent and best understood hypoxia-induced signalling pathways. Evidence from several reports demonstrated that HIF activation is associated with an undifferentiated phenotype in several cancers; in primary pancreatic carcinomas, nuclear accumulation of HIF1 α protein was found mainly in poorly differentiated tumour cells (Couvelard *et al.*, 2005). Similar observations were seen in neuroblastomas as elevated levels of HIF1 α and HIF2 α proteins were found in stem cell-like populations (Li *et al.*, 2009; Pietras *et al.*, 2009). Covetto *et al.*, (2006) confirmed that Oct4, a stem cell transcription factor is a target for HIF2 α and HIF2 α activated Oct4 regulates self-renewal and differentiation in stem cells. Flow cytometry data analysis from my study showed that both HIF1 α and HIF2 α overexpression induced higher expression of CSC marker (ALDH and CD133) compared to the mock cells suggesting that HIF protein may induce these stem-like characters in cells. Embryonic stem cell markers indicating pluripotent phenotype (Nanog, Oct4, Sox2) were also expressed in the HIF transfected cells. These results are consistent with other reports which showed that elevated levels of these stem cell markers occurs in many somatic carcinomas (Jones *et al.*, 2004; Tai *et al.*, 2005).

Cancer with stem cell-like features displays higher resistance than the bulk mass of differentiated cancer cells to radiotherapy and chemotherapy. These cells were also observed to be significantly resistant to anti-cancer drugs.

Apart from the HIF activated pathways which play important cellular responses during hypoxia, other signalling pathways such as the NF κ B pathways are also activated during hypoxia. In this study, nuclear translocation of HIF1 α , HIF2 α and NF κ Bp65 proteins were detected in hypoxic monolayer cell indicative that NF κ B is activated in hypoxic cells. Evidence has revealed that NF κ B play pivotal roles in maintaining CSCs and chemoresistance in cancer cells (Liu *et al.*, 2010; Hinohara *et al.*, 2012; Myant *et al.*, 2013). To evaluate the role of NF κ B in maintenance of stemness and chemosensitivity, MDA-MB 231 cells were transfected with NF κ Bp65 subunits. High p65 protein level and transcriptional activities were detected in the transformed clones. These transformed cells have significantly higher population of CSCs (ALDH⁺ and CD133) and embryonic stem cell (Nanog, Oct4 and Sox2). In comparison to the mock-transfected cells, the cells overexpressing p65 were highly resistant to 5 first line anticancer drugs tested (CDDP, dFdC, VCR, Dox and PTX). Data from my result is in line with reports by Liu *et al.*, (2014), which showed that NF κ B plays a key role in hypoxia-induced CSCs and chemoresistance. The molecular mechanisms of how HIF pathway regulates NF κ B pathway remains unclear, HIF pathway activates NF κ B pathway mainly through the regulation of IKK signalling-mediated regulation of canonical NF κ B signalling (Cummins *et al.*, 2006) as HIF1 α protein have κ B site in its promoter region. Several reports have shown that there is a cross-talk between HIF and NF κ B pathways, HIF2 α subunits interacts with NF κ B

through I κ B nuclear factor kappa B essential modulator (NEMO) and NEMO is reported to shuttle between the nucleus and cytoplasm and compete with IKK α and p65 (Bracken *et al.*, 2005). I κ B kinase B, an upstream activator of NF κ B has been identified as a substrate of prolyl-hydroxylases and its activity was found to reduce upon hydroxylation (Cummins *et al.*, 2006). Inhibition of NF κ B was found to reduce the induction of HIF target cells (Fitzpatrick *et al.*, 2011) and the expression of HIF was directly regulated by NF κ B (Bonello *et al.*, 2007, van Uden *et al.*, 2008). Data from this study further confirm the existence of this cross-talk between NF κ B and HIF pathways as the HIF transfected cells overexpressed NF κ B and the NF κ B transfected clones overexpressed HIF1 α and HIF2 α proteins. Interactions of HIF and NF κ B pathways contribute to BC metastasis through the induction of EMT together with migration through p65-lysine acetylation and HDAC dependent epigenetic mechanism leading to the up-regulation NF κ B and HIF (Bendinelli *et al.*, 2009).

Approximately 90% of BC deaths are caused by local invasion and distant metastasis of tumours. During epithelial to mesenchymal transition (EMT) transformed epithelial cells acquire mesenchymal-like phenotype which enables tumour cells to disseminate from the primary tumour and penetrate extracellular matrix into the blood and lymphatic vessels to a secondary organ. Expression of classic EMT markers (Vimentin, N-cadherin, Twist and snail) is a feature of TNBC and is associated with evasion of apoptosis, senescence and resistance to chemotherapy (Polyak and Weinberg, 2009; Nieto, 2011). The connection between EMT and CSCs was demonstrated by Hollier *et al.*, (2009), they observed that EMT facilitated the generation of cancer cells with mesenchymal

traits as well as self-renewal of cells required for initiating secondary tumours. In this study, hypoxia induced EMT phenotype in BC cells as cells grown under hypoxia exhibited higher invasive and migratory potentials. Similarly, NF κ Bp65 and HIF transfected cells also showed higher migratory and invasive potentials. Interestingly these cells were also found to exhibit CSC-like cell features suggesting that there may be a link between EMT and stemness of cells.

Primary and acquired resistance represents a major challenge for the effectiveness of chemotherapeutic agents in Breast cancer (BC). Breast cancer becomes refractory to cytotoxic drugs and becomes typically incurable resulting in tumour relapse (Harris *et al.*, 2000). Cancer cells with reduced sensitivity to drugs after continuous exposure to anticancer drugs become cross resistant to other anticancer with different mechanism of action. In this study, two resistant cells lines MDA-MB-231_{GEM100nM} and T47D_{Dox100nM} were characterized. These resistant cells were significantly resistant to anticancer drugs which is in agreement with the reports from others studies (Faneyte *et al.*, 2001; AbuHammad and Zihlif, 2013). The resistant cell lines were also found to exhibit some CSC-like characteristics having higher expression of CSC markers suggestive that CSCs play important roles in the biology of BC cells.

Conventional therapeutic agents eradicate cells of the tumour bulk but spare the CSC sub-population. These surviving cells have stem cell-like phenotype and are proposed to be the cause for tumour recurrence and chemoresistance. Therefore targeting these CSCs may improve the long-term outcome of TNBC patients. The demand for an effective anticancer agent against BC especially in patients with TNBC is of great importance. Development of new therapies for cancer involves

a slow and costly process thus repurposing of old drugs would greatly reduce the time and cost for development of new drugs which benefits both the patient and the pharmaceutical industries as safety and pharmacokinetic profiles are ready well established. DS an anti-alcoholism drug used for the management and treatment of alcoholism have been shown to have cytotoxic effects against cancer cells (Wickstrom *et al.*, 2007; Cvek, 2011). The metabolism and clinical pharmacology of DS is well understood and is shown to have little or no cytotoxic effects on normal cell, thus DS can be repurposed as a potential anticancer agents. *In vitro* experiments show that DS is highly toxic to BC cells however its *in vivo* activity is sum worth limited because of its relatively short half-life in the blood stream been rapidly degraded and thus cancer cells are not sufficiently exposed to the cytotoxic effect of DS. The half-life of DS according to the reports by Cobby *et al.*, (1977) was only about 4 minutes, *in vitro* half-life experiments in horse serum showed a shorter half-life less than 2 minutes (Figure 7.2 A and B). The anticancer activity of DS requires the unmodified DS, therefore to translate DS into cancer therapeutics an efficacious delivery system to protect DS in the blood stream and transport it into cancer cells is necessary.

Nanotechnology the use of nanocarriers to encapsulate active ingredients may be a solution to this hurdle. Nanoparticles (NP) have distinctive advantages in delivering anticancer drugs to tumour sites by changing the pharmacokinetics and biodistribution of drugs which improves the efficacy and reduces systematic adverse effects. It was hypothesized that encapsulation of DS in NP will improve its anticancer efficacy and aid in its translation in clinics. To this effect I encapsulated DS in polymeric micelles. Polymeric micelles are FDA approved excipients for internal use and is considered as one of the most suitable

biocompatible polymer carrier for *in vivo* studies (Sahoo et al., 2007). The advantages of micelles as drug carriers are their relative small size, high structural stability and low toxicity. I successfully encapsulated DS in polymeric micelles. This formulation PMDS was able to increase the half-life of DS to over 3 hours in horse serum and a sustained release was obtained.

The cytotoxic effects of DS are dependent on copper (Cu) as shown from my results (Chapter 6, Figure 6.12). The unique electronic structure of Cu enables it to act as cofactors in a number of redox reactions of enzymes required for normal growth and development (Tapiero *et al.*, 2003). Tumour cells accumulate Cu to sustain their higher metabolic demand with resultant increase in Cu levels compared to non-malignant cells (Gupte and Mumper, 2009). DS is a chelator of divalent metallic ions such as Cu and Zn and enables the transportation of Cu into cells bypassing the CTr1 regulator inducing a phenomenon known as Cu overload which depletes the glutathione antioxidant defences systems of tumour cells inducing cell death. In this study, Cu alone did not induce cell death in cancer cells. Results from my study indicate the cytotoxicity of Cu on cancer cells occurs in two phases. Firstly an instant and short-term action induced by the reaction between DS and Cu generating of ROS as shown in Chapter 6 (Figure 6.12 and 6.13). Secondly, delayed toxic effects induced by DDC-Cu an end product in DS metabolism (Figure 6.13). Data from my results reveal that the cytotoxicity of DDC-Cu was even higher than that occurring with ROS generation by DS and Cu alone (Figure 6.11).

The most important and novel findings in my study are that DS was successfully encapsulated in polymeric micelles, this encapsulated DS is protected from rapid

degradation and can target CSCs which are the main reason for chemotherapeutic failure and cancer relapse. I was also able to show that the cytotoxic effect of DS occurs in two phases, a rapid ROS induced cell death followed by a delayed and more effective cytotoxic effect induced by DDC-Cu.

8.2. Conclusion

This study has shown that hypoxia plays fundamental role in Breast Cancer biology by inducing stem-like characters in TNBC. It provides a suitable environment 'stem cell niche' for the maintenance of these CSCs which are responsible for therapeutic failure and tumour recurrence. To maintain cellular homeostasis during hypoxic insult several signalling pathway such as the HIF and NF κ B pathway are activated during hypoxia, these transcriptional factors were also shown to induce stem-like traits and chemoresistance in BC. Chemotherapy still remains the gold standard treatment of TNBC as patients with this form of BC have the worst prognosis and outcome due to the lack of targetable receptors. This study have shown that these CSCs are the key factor responsible for chemoresistance as hypoxic cells as well as transfected cells were all shown to have high expression of CSC markers. Therefore targeting these CSC could improve the prognosis of patients with TNBC. DS shows strong anticancer activity *in vitro*, DS in association with Cu is a strong ROS inducer, it is also a potent inhibitor of NF κ B which is the principle antiapoptotic transcription factor activated in many types of tumours. More importantly DS is an inhibitor of ALDH a functional marker of CSCs. Therefore combination of DS with Cu will induce cell death preferentially in tumour cells while sparing normal tissues, because cancer cell with their high metabolic rate already have high Cu, and

increase in Cu load will induce more ROS which can be counteracted by the high antioxidant capacity of cancer cells. Fortunately DS as an ALDH inhibitor can exhaust the antioxidants within cancer cells thus making them vulnerable to ROS induced cell death. DS though effective as an anticancer agent *in vitro* is highly unstable and rapidly degraded in the blood stream. To improve the efficacy of DS as a BC therapeutic *in vivo*. DS was successfully encapsulated in polymeric micelles and our formulation enhanced the stability and half-life of DS in serum. My results show that PMDS was able to induce cell death in hypoxic and overexpressing cells, thus reversing the chemoresistance induced the CSCs.

8.2.3. Recommendation and future work

As proven in this study, DS in combination with Cu have potent anticancer effects in BC cells. The targeted delivery of DS in nanoparticles needs further development to speed up the emergence of DS as a chemotherapeutics in clinical use for the treatment of TNBC patients.

Having developed this formulation polymeric micelle enabled disulfiram (PMDS), the next phase of this study is to further increase the pharmacodynamic properties of this formulation by modifying the ratio of hydrophilic/hydrophobic block, improving the stability and drug loading content.

DS clearly has been shown to be very effective *in vitro* as an anticancer agent, however behaviour of treatment systems differs in *in vitro* and *in vivo* studies. Therefore, *in vivo* studies would be carried out for further evaluation of the effects of PMDS in tumour mice models. Firstly, tissue distribution studies needs to be done in mice to examine the stability of PMDS *in vivo*. The anticancer efficacy of

PMDS *in vivo* needs to be studied. Xenograft experiments would be carried out in nude immunodeficient mice. Resistant cells (5×10^5) would be subcutaneously injected at one front flank of the mice. When the tumour volume (V) reaches $\sim 200 \text{ mm}^3$, the tumour bearing mice would be randomly subdivided into 6 groups (8 mice/group): control; copper gluconate (CuGlu), empty PMDS i.v.; PMDS 2.5mg/kg i.v. + CuGlu 6mg/kg; PMDS 5mg/kg i.v. + CuGlu 6mg/kg.; PMDS 10mg/kg i.v. + CuGlu 6mg/kg. The animals would then be for treated 3 times/week for successive 3 weeks. The xenograft size would be monitored weekly and tumour volume calculated. The animals would be sacrificed after 3 weeks. The tumours removed, photographed and subjected to further analysis.

Modification of the formulation polymeric enabled disulfiram (PMDS) would also be done to improve the drug loading content and to test their effects on other cancers especially human brain cancers. Polymeric micelles may be an effective drug carrier due to its small size and can target cancer cells. This formulation PMDS may be a successful therapy against chemoresistant GBM stem cells opening an area for novel effective therapy in brain tumours.

Flow cytometry results would also be reanalysed to show the cell count versus the forward light scatter height showing the degree of increase or decrease in fluorescence intensities. Images from western blot, invasive and migratory assays would also be quantified using image J software.

The half maximum inhibitory concentration (IC_{50}) for some of the resistant cells were not obtained because the highest concentrations of drug tested did not induce cell death in these cells. Higher concentrations of anticancer drugs would be used to treat these cells.

References

- AbuHammad, S. and Zihlif, M. (2013). "Gene expression alterations in doxorubicin resistant MCF7 breast cancer cell line." *Genomics* 101(4): 213-220.
- Afify, A., Purnell, P. and Nguyen, L. (2009). "Role of CD44s and CD44v6 on human breast cancer cell adhesion, migration, and invasion." *Exp Mol Pathol* 86(2): 95–100.
- Albain, K. S., Nag, S., Calderillo-Ruiz, G., Jordaan, J. P., Llombart, A. C., Pluszanska, A., Rolski, J., Melemed, A. S., reyes-Vidal, J. M., Sekhon, J. S., Simmins, L. and O'Shaughnessy, J. (2008). "Global phase III study of gemcitabine plus paclitaxel (GT) vs. paclitaxel (T) as frontline therapy for metastatic breast cancer (MBC): First report of overall survival." 26(24): 3950-3957.
- Al-Hajj, M. and Clarke, M. F. (2004). "Self-renewal and solid tumour stem cells." *Oncogene* 23: 7228–7274.
- Al-Hajj, M., Wicha, M. S., Benito-Hernandez, A., Morrison, S. J. and Clarke, M. F. (2003). "Prospective identification of tumorigenic breast cancer cells." *Proc. Natl. Acad. Sci. USA* 100 (7), 3983–3988.
- Aliabadi, H. M. and Lavasanifar A. (2006). "Polymeric micelles for drug delivery." *Expert Opin. Drug Delivery* 3(1): 139.
- Anders, C. K. and Carey, L. A. (2009). "Biology, metastatic patterns, and treatment of patients with triple-negative breast cancer." *Clin Breast Cancer* 9(2): 73-81.
- Arlt, A. and Schafer, H. (2002). "Nfkapab-dependent chemoresistance in solid tumours." *Int J Clin Pharmacol Ther* 40: 336-347.
- Arlt, A., Gehrz, A., Muerkoster, S., Vorndamm, J., Kruse, M. L., Folsch, U. R. and Schafer, H. (2003). "Role of NF-kappaB and Akt/PI3K in the resistance of pancreatic carcinoma cell lines against gemcitabine-induced cell death." *Oncogene* 22(21): 3243–3251.

Azim, H. A. Jr., Michiels, S., Bedard, P. L., Singhal, S. K., Criscitiello, C., Ignatiadis, M., Haibe-Kains, B., Piccart, M. J., Sotiriou, C. and Loi, S. (2012). "Elucidating prognosis and biology of breast cancer arising in young women using gene expression profiling." *Clin Cancer Res* 18(5): 1341–1351.

Badve, S. and Nakshatri, H. (2012). "Breast cancer stem cells-beyond semantics." *Lancet Oncol* 13 (1):43-48.

Bao, B., Azmi, A. S., Ali, S., Ahmad, A., Li, Y., Banerjee, S., Kong, D. and Sarkar, F. H. (2012). "The biological kinship of hypoxia with CSC and EMT and their relationship with deregulated expression of miRNAs and tumor aggressiveness." *Biochim Biophys Acta* 1826(2): 272–296.

Bar, E. E., Lin, A., Mahairaki, V., Matsui, W. and Eberhart, C. G (2010). "Hypoxia increases the expression of stem-cell markers and promotes clonogenicity in glioblastoma neurospheres." *Am J Pathol* 177(3):1491-1502.

Barnes, M. J., Estlin, E. J, Taylor, G. A., Aherne, W., Hardcastle, A., McGuire, J. J., Calvete, J. A., Lunee, J., Pearson, A. D. J and Newll, D. R. (1999). "Impact of polyglutamation on sensitivity to raltitrexed and methotrexate in relation to drug-induced inhibition of de novo thymidylate and purine biosynthesis in CCRF-CEM cell lines." *Clin Cancer Res* 5: 2548–2558.

Basseres, D. and Baldwin, A. S. (2006). "Nuclear factor-kappaB and inhibitor of kappaB kinase pathways in oncogenic initiation and progression." *Oncogene* 25: 6817–6830.

Bendinelli, P., Matteucci, E., Maroni, P. and Desiderio, M. A. (2009). "NF-kappaB activation, dependent on acetylation/deacetylation, contributes to HIF-1 activity and migration of bone metastatic breast carcinoma cells." *Mol Cancer Res* 17(8): 1328-1341.

Bergman, A. M., Eijk, P. P., Ruiz van Haperen, V. W., Smid, K., Veerman, G., Hubeek, I., van den Ijssel, P., Ylstra, B. and Peters, G. J. (2005). "In vivo induction of resistance to gemcitabine results in increased expression of ribonucleotide reductase subunit M1 as the major determinant." *Cancer Res* 65(20): 9510-9516.

Bertout, J. A., Patel, S. A. and Simon, M. C. (2008). "The impact of O₂ availability on human cancer." *Nature Rev. Cancer* 8(12): 967–975.

Bharti, A.C., Donato, N., Singh, S. and Aggarwal, B. B. (2003). "Curcumin (diferuloylmethane) down-regulates the constitutive activation of nuclear factor-kappa B and IkappaBalpha kinase in human multiple myeloma cells, leading to suppression of proliferation and induction of apoptosis." *Blood* 101: 1053–1062.

Bhat-Nakshatri, P., Sweeney, C. J. and Nakshatri, H. (2002). "Identification of signal transduction pathways involved in constitutive NF-kappaB activation in breast cancer cells." *Oncogene* 21(13): 2066-2078.

Bhola, N. E, Balko, J. M, Dugger, T. C, Kuba, M. G., Sanchez, V., Sanders, M., Stanford, J., Cook, R. S. and Arteaga, C. L. (2013). "TGF-beta inhibition enhances chemotherapy action against triple-negative breast cancer." *J Clin Invest* 123(3):1348-1358.

Biswas, D. K, Cruz, A. P., Gansberger, E. and Pardee, A. B. (2000). "Epidermal growth factor-induced nuclear factor kappa B activation: a major pathway of cell-cycle progression in oestrogen-receptor negative breast cancer cells." *Proc Natl Acad Sci USA* 97(15): 8542-8547.

Biswas, D. K., Shi, Q., Baily, S., Strickland, I., Ghosh, S., Pardee, A. B and Ighehart, J. D. (2004). "NF-kappa B activation in human breast cancer specimens and its role in cell proliferation and apoptosis." *Proc Natl Acad Sci USA*. 101(27): 10137–10142.

Blagosklonny M.V. (2001). "Paradox of Bcl-2 and p53: why may apoptosis-regulating proteins be irrelevant to cell death?" *Bioessay* 23: 947–953.

Bokoch, G. M. and Knaus, U. G. (2003). "NADPH oxidases: not just for leukocytes anymore." *Trends Biochem. Sci.* 28: 502-508.

Bonello, S., Zahringer, C., Belaiba, R.S., Djodjevic, T., Hess, J., Michiels C., Kietzmann, T. and Gorlach, A. (2007). "Reactive oxygen species activate the HIF-1 alpha promoter via a functional Nfkappa B site." *Arterosc. Thromb. Vasc. Biol.* 27(4), 755-761.

Bonizzi, G. and Karin, M. (2004). "The two NF-kappaB activation pathways and their role in innate and adaptive immunity." *Trends Immunol* 25(6): 280-288.

Bonnet, D. and Dick, J. E. (1997). "Human acute myeloid leukaemia is organized as a hierarchy that originates from a primitive hematopoietic cell." *Nature Med.* 3(7): 730–737.

Boonstra, J. and Post, J. A. (2004). "Molecular events associated with reactive oxygen species and cell cycle progression in mammalian cells." *Gene* 337: 1-13.

Borchert, P. and Wattenberg L. W. (1976). "Inhibition of macromolecular binding of benzo(a)pyrene and inhibition of neoplasia by disulfiram the mouse forestomach." *J Natl. Cancer Inst.* 57(1): 173-179.

Bos, R., van der Groep, P., Greijer, A. E., Shvarts, A., Meijer, S., Pinedo, H. M., Semenza, G L., van Diest, P.J. and van der Wall, E. (2003). "Levels of hypoxia-inducible factor-1alpha independently predict prognosis in patients with lymph node negative breast carcinoma." *Cancer*, 97(6):1573–1581.

Bourguignon, L. Y., Spevak, C. C., Wong, G., Xia, W. and Gilad, E. (2009). "Hyaluronan-cd44 interaction with protein kinase c(epsilon) promotes oncogenic signaling by the stem cell marker nanog and the production of microrna-21, leading to down-regulation of the tumour suppressor protein pdcd4, anti-apoptosis, and chemotherapy resistance in breast tumour cells." *J Biol Chem* 284 (39):26533–26546.

Bracken, C. P, Whitelaw, M. L. and Peet, D. J. (2005). "Activity of hypoxia-inducible factor 2alpha is regulated by association with the NF-kappaB essential modulator." *J Biol Chem* 280(14):14240-14251.

Brahimi-Horn, M.C., Chiche, J. and Pouyssegur, J. (2007). "Hypoxia and cancer." *J Mol Med (Berl)* 85(12):1301–1307.

Brar, S. S., Grigg, C., Wilson, K. S., Holder, W. D., Dreau, D., Austin, C., Foster, M., Ghio, A. J., Whorton, A. R., Stowell, G. W., Whittall, L. B., Whittle, R. R., White, D. P and Kennedy, T. P. (2004). "Disulfiram inhibits activating transcription factor/cyclic AMP-responsive element binding protein and human melanoma

growth in a metal-dependent manner in vitro, in mice and in a patient with metastatic disease." *Mol Cancer Ther*, 3 (9):1049–1060.

Brar, S. S., Grigg, C., Wilson, K. S., Holder, W. D., Jr., Dreau, D., Austin, C., Foster, M., Ghio, A. J., Whorton, A. R., Stowell, G. W., Whittall, L. B., Whittle, R. R., White, D. P. and Kennedy, T. P. (2004). "Disulfiram inhibits activating transcription factor/cyclic AMP-responsive element binding protein and human melanoma growth in a metal-dependent manner in vitro, in mice and in a patient with metastatic disease." *Mol Cancer Ther* 3(9): 1049-1060.

Broxterman. H. J., Giaccone, G. and Lankelma, J. (1995). "Multidrug resistance proteins and other drug transport-related resistance to natural product agents." *Current Opinion in Oncology* 7(6): 532-540.

Burris, H. A, Moore, M. J., Andersen J., Green, M. R., Rothenberg, M. L., Modiano, M. R., Cripps, M. C., Portenoy, R. K., Storniolo, A. M., Tarassoff, P., Nelson, R., Dorr, F. A., Stephens, C. D. and Von Hoff DD (1997). "Improvements in survival and clinical benefit with gemcitabine as first-line therapy for patients with advanced pancreas cancer: A randomized trial." *J Clin Oncol* 15(6): 2403–2413.

Byrski, T., Gronwald, J., Huzarski T., Grzybowska, E., Budryk, M., Stawicka, M., Mierzwa, T., Szwiec, M., Wisniowski, R., Siolek, M., Dent, R., Lubinski, J. and Narod, S. (2010). "Pathologic complete response rates in young women with BRCA1-positive breast cancers after neoadjuvant chemotherapy." *J Clin Oncol* 28(3): 375–379.

Byrski, T., Huzarski, T., Dent, R., Gronwald, J., Zuziak, D., Cybulski, C., Kladny, J., Gorski, B., Lubinski, J. and Narod S. A. (2009). "Response to neoadjuvant therapy with cisplatin in BRCA1-positive breast cancer patients." *Breast Cancer Res Treat* 115(2): 359–363.

Cabral, H., Nishiyama, N. and Kataoka, K. (2007). "Optimization of (1,2-diaminocyclohexane)platinum(II)-loaded polymeric micelles directed to improved tumor targeting and enhanced antitumor activity." *J Control Release* 121(3):146–155.

Cardoso, F., Harbeck, N., Fallowfield, L., Kyriakides, S., Senkus, E. (2012). "Locally recurrent or metastatic breast cancer: ESMO clinical practice guidelines for diagnosis, treatment and follow-up." *Ann. Oncol.* 23(7): 11-19.

Carey, L. A, Perou, C. M, Livasy, C. A, Dressler, L. G, Cowan, D., Conway, K., Karaca, G., Troester, M. A., Tse, C. K., Edmiston, S., Deming, S. L., Geradts, J., Cheang, M. C., Nielsen, T. O., Moorman, P. G., Earp, H. S and Millikan, R. C. (2006). "Race, breast cancer subtypes, and survival in the Carolina Breast Cancer Study." *JAMA*, 295(21): 2492-2502.

Carroll, V.A. and Ashcroft, M. (2006). "Role of hypoxia-inducible factor (HIF)-1alpha versus HIF 2alpha in the regulation of HIF target genes in response to hypoxia, insulin-like growth factor-I, or loss of von Hippel-Lindau function: implications for targeting the HIF pathway." *Cancer Res* 66(12): 6264-6270.

Cen, D., Brayton, D., Shahandeh, B., Meyskens, Jr. F. L and Farmer, P. J., (2004). "Disulfiram facilitates intracellular Cu uptake and induces apoptosis in human melanoma cells." *J Med Chem* 47 (27): 6914–6920.

Cen, D., Cui, Q. C., Yang H. and Dou, Q. P. (2006). "Disulfiram, a clinically used anti-alcoholism drug and copper-binding agent, induces apoptotic cell death in breast cancer cultures and xenografts via inhibition of the proteasome activity." *Cancer Res.* 66(21):10425–10433.

Chan, A., Wong, F. and Arumanayagam, M. (1993). "Serum ultrafiltrable copper, total copper and ceruloplasmin concentrations in gynecological carcinoma." *Ann Clin Biochem* ;30(6): 545–549.

Charafe-Jauffret, E., Ginestier, C., Iovino, F., Wicinski, J., Cervera, N., Finetti, P., Hur, M. H., Diebel, M. E, Monville, F., Dutcher, J., Brown, M., Viens, P., Xerri, L., Bertucci, F., Stassi, G., Dontu, G., Birnbaum, D. and Wicha, M. S. (2009). "Breast cancer cell lines contain functional cancer stem cells with metastatic capacity and a distinct molecular signature." *Cancer Res* 69 (4):1302–1313.

Cheang, M. C., Voduc, D., Bajdik, C., Leung, S., McKinney, S., Chia, S. K., Perou, C. M. and Nielsen, T. O. (2008). "Basal- like breast cancer defined by five

biomarkers has superior prognostic value than triple-negative phenotype.” *Clin Cancer Res* 14(5); 1368-1376.

Chen, Y. C, Chen, Y. W, Hsu, H. S, Tseng, L. M., Huang, P. I., Lu, K. H., Chen, D. T., Tai, L. K., Yung, M. C., Chang, S. C., Ku, H. H., Chiou, S. H. and Lo, W. L (2009). “Aldehyde dehydrogenase 1 is a putative marker for cancer stem cells in head and neck squamous cancer.” *Biochem Biophys Res Commun* 385(3): 307–313.

Chen, Y. C, Hsu, H. S., Chen, Y. W., Tsai, T. H., How, C. K., Wang, C. Y., Hung, S. C., Chang, Y. L., Tsai, M. L., Lee, Y. Y., Ku, H. H and Chiou, S. H (2008) “Oct-4 expression maintained cancer stem-like properties in lung cancer-derived CD133-positive cells.” *PLoS ONE* 2008 3(7): 2637.

Chevillard, S., Pouillart, P., Beldjord, C., Asselain, B., Beuzebou, P., Magdelenat, H and Vielh, P. (1996). “Sequential assessment of multidrug resistance phenotype and measurement of S-phase fraction as predictive markers of breast cancer response to neoadjuvant chemotherapy.” *Cancer* 1996; 77(2): 292–300.

Chia, S. K., Speers, C. H., D'yachkova, Y., Kang, A., Malfair-Taylor, S., Barnett, J., Coldman, A., Gelmon, K A., O'reilly, S. E and Olivotto, I. A (2007). “The impact of new chemotherapeutic and hormone agents on survival in a population-based cohort of women with metastatic breast cancer.” *Cancer*, 110(5): 973-979.

Chorawala, M.R., Oza, P.M., Shah G.B. (2012). “Mechanisms of Anticancer Drugs Resistance: An Overview.” *Intern J. of Pharm Sci and Drug Res* 4(1): 01-09.

Chretien, D., Metoz, F., Verde, F., Karsenti, E. and Wade, R. H. (1992). "Lattice defects in microtubules: protofilament numbers vary within individual microtubules." *J Cell Biol* 117(5): 1031-1040.

Christofori, G. (2006). “New signals from the invasive front.” *Nature* 441(7092): 444–450.

Chua, H. L, Bhat-Nakshatri, P., Clare, S. E., Morimiya, A., Badve, S. and Nakshatri, H. (2007) “NF-kappaB represses E-cadherin expression and

enhances epithelial to mesenchymal transition of mammary epithelial cells: potential involvement of ZEB-1 and ZEB-2." *Oncogene* 26(5):711–724.

Clarke, M. F and Fuller, M. (2006). "Stem cells and cancer: two faces of eve." *Cell* 124:1111-1115.

Clarke, M., Collins, R., Darby, S., Davies, C., Elphinstone, P., Evans, V., Godwin, J., Gray, R., Hicks, C., James, S., MacKinnon, E., McGale, P., McHugh, T., Peto, R., Taylor, C. and Wang Y (2005). "Early Breast Cancer trialists' collaborative Group (EBCTCG). Effects on radiotherapy and of difference in the extent of surgery for early breast cancer on local recurrence and 15-year survival, an overview of the randomized trials." *Lancet*; 366(9503): 2087-2106.

Clay, M. R., Tabor, M., Owen, J. H., Carey, T. E., Bradford, C. R., Wolf, G. T., Wicha, M. S. and Prince, M. E. (2010). "Single-marker identification of head and neck squamous cell carcinoma cancer stem cells with aldehyde dehydrogenase." *Head Neck* 32(9): 1195-1201.

Cobby, J., Mayersohn, M. and Selliah, S. (1977). "The rapid reduction of Disulfiram in blood and plasma." *J Pharmacol Exp Ther* 202(3): 724-731.

Cogswell, P. C., Guttridge, D. C., Funkhouser. W. K., Baldwin. A. S. Jr. (2000). "Selective activation of NF-kappa B subunits in human breast cancer: potential roles for NF-kappa B2/p52 and for Bcl-3." *Oncogene* 19 (9):1123–1131.

Coker, A. K. and Allan A. L (2008). "Cancer stem cells: Implications for the progression and treatment of metastatic disease." *J Cell Mol Med* 12: 374-390.

Collins, L. C., Martyniak, A., Kandel, M. J., Stadler, Z. K., Masciari, S., Miron, A., Richardson, A. L., Schnitt, S. J. and Garber, J. E. (2009). "Basal Cytokeratin and epidermal growth factor receptor expression are not predictive of BRCA1 mutation status in women with triple-negative breast cancers." *Am J Surg Pathol* 33(7): 1093-1097.

Conticello, C., Martinetti, D., Adamo, L., Buccheri, S., Giuffrida, R., Parrinello, N., Lombardo, L., Anastasi, G., Amato, G., Cavalli, M., Chiarenza, A., De Maria, R., Giustolisi, R., Gulisano, M. and Di Raimondo, F. (2012). "Disulfiram, an old drug

with new potential therapeutic uses for human hematological malignancies.” *Int. J. Cancer* 131(9): 2197–2203.

Cortes-Funes, H. and Coronado, C. (2007). “Role of anthracyclines in the era of targeted therapy.” *Cardiovasc Toxicol* 7(2):56–60.

Couvelard A, O’Toole D, Turley H, Leek R, Sauvanet A, Degott C, Ruzniewski P, Belghiti J, Harris AL, Gatter K, Pezzella F (2005). “Microvascular density and hypoxia-inducible factor pathway in pancreatic endocrine tumours: negative correlation of microvascular density and VEGF expression with tumour progression.” *Br J Cancer* 92(1): 94–101.

Covello, K. L., Kehler, J., Yu, H., Gordon, J. D., Arsham, A. M., Hu, C. J., labosky, P. A., Simon, M. C. and Keith, B. (2006). “HIF-2alpha regulates Oct-4: effects of hypoxia on stem cell function, embryonic development, and tumour growth.” *Genes Dev.* 20(5): 557-577.

Croker, A. K. and Allan, A. L. (2012). "Inhibition of aldehyde dehydrogenase (ALDH) activity reduces chemotherapy and radiation resistance of stem-like ALDHhigh CD44 (+) human breast cancer cells." *Breast Cancer Res Treat* 133(1): 75-87.

Cummins, E.P., Berra, E., Comerford, K.M., Ginoves, A., Fitzgerald, K.T., Seeballuck, F., Godson, C., Nielsen, J.E., moynagh, P., Pouyssegur, J., Taylor, C.T (2006). “Prolyl hydroxylase-1 negatively regulates Ikb kinase β , giving insight into hypoxia-induced NFkB activity.” *Proc. Natl Acad. Sci* 103 (48), 18154-18159.

Curigliano, G. and Goldhirsch, A. (2011). “The triple-negative subtype: new ideas for the poorest prognosis breast cancer.” *J Natl Cancer Inst Monogr* 2011(43): 108–110.

Cvek, B. (2011). “Targeting malignancies with disulfiram (Antabuse): multidrug resistance, angiogenesis, and proteasome.” *Curr Cancer Drug Targets* 11(3): 332–337.

Cvek, B. and Dvorak, Z. (2007). "Targeting of nuclear factor kappa B and proteasome by dithiocarbamate complexes with metals." *Curr Pharm Des*, 13(30): 3155-3167.

Cvek, B. and Dvorak, Z. (2008). "The value of proteasome inhibition in cancer. Can the old drug, disulfiram, have a bright new future as a novel proteasome inhibitor?" *Drug Discovery Today*, 13(15-16): 716– 722.

Dafni, U., Grmani, I., Xyrafas, A., Eleftheraki, A.G and Fountizilas G (2010). "Fifteen-year trends in metastatic breast cancer survival in Greece." *Breast Cancer Res Treat* 119:621.

Dalerba, P., Cho, R. W. and Clarke, M. F. (2007). "Cancer stem cells: models and concepts." *Annu Rev Med* 58: 267-284.

D'Arpa, P. and Liu, L. F. (1989). "Topoisomerase-targeting antitumor drugs." *Biochim Biophys Acta* 989(2): 163-177.

Das, B., Tsuchida, R., Malkin, D, Koren, G., Baruchel, S. and Yeger, H. (2008). "Hypoxia enhances tumor stemness by increasing the invasive and tumorigenic side population fraction." *Stem Cells* 26(7):1818–1830.

D'Autreaux, B. and Toledano, M. B. (2007). "ROS as signalling molecules: mechanisms that generate specificity in ROS homeostasis." *Nat Rev Mole cell Biol* 8(10): 813-814.

Dave, B. and Chang, J. (2009). "Treatment resistance in stem cells and breast cancer." *J Mammary Gland Biol Neoplasia* 14(1):79-82.

Davies, K. J. (1999). "The broad spectrum of responses to oxidants in proliferating cells: a new paradigm for oxidative stress." *IUBMB Life* 48(1): 41-47.

De Milito, A. and Fais, S. (2005). "Tumour acidity, chemoresistance and proton pump inhibitors." *Future Oncol* 1(6): 779-86.

Deitrich, R.A., Petersen, D. and Vasiliou, V. (2007). "Removal of acetaldehyde from the body." *Novartis Foundation Symposia*, 285: 23-40.

Dematteis. F. (1974). "Covalent binding of sulfur to microsomes and loss of cytochrome P450 during the oxidative desulfuration of several chemicals." *Mol Pharmacol* 10:849–854.

Dent, R., Trudeau, M., Pritchard, K. I, Hanna, W. M., Kahn, H. K, Sawka, C. A., Lickley, L. A., Rawlinson, E., Sun, P., Narod, S. A (2007). "Triple-negative breast cancer: clinical features and patterns of recurrence." *Clin Cancer Res* 13(15):4429-4434.

Diez, M., Arroyo, M., Cerdan, F.J., Munoz, M., Martin, M. A and Balibrea, J L (1989). "Serum and tissue trace metal levels in lung cancer." *Oncology* 46(4):230–234.

Dolle, J. M., Daling, J. R., White, E., Brinton, L. A., Doody, D. R., Porter, P. L. and Malone, K. E. (2009). "Risk factors for triple negative breast cancer in women under the age of 45 years." *Cancer Epidemiol Biomarkers Prev* 18(4): 1157–1166.

Dylla, S. J., Beviglia, L., Park, I. K., Chartier, C., Raval, J., Ngan, L., Pickell, K., Aguilar, J., Lazetic, S., Smith-Berdan, S., Clarke, M. F., Hoey, T., Lewicki, J. and Gurney, A. L. (2008). "Colorectal cancer stem cells are enriched in xenogeneic tumours following chemotherapy." *PLoS One* 3(6): e2428.

Early Breast Cancer Trialists' Collaborative Group (EBCTCG) (2005). "Effects of radiotherapy and of differences in the extent of surgery for early breast cancer on local recurrence and 15-year survival: an overview of the randomised trials." *Lancet*, 366: 2087–2106.

Edwards JE, Alcorn J, Savolainen J, Anderson BD, McNamara PJ (2005). "Role of P-glycoprotein in distribution of nelfinavir across the blood-mammary tissue barrier and blood-brain barrier." *Antimicrob Agents Chemother* 49(4):1626–1628.

Eneanya, D. I., Bianchine, J. R., Duran, D. O. and Andresen, B. D. (1981). "The actions of metabolic fate of Disulfiram." *Annu Rev Pharmacol Toxicol* 21: 575-596.

Engelmann, K., Shen, H. and Finn, O. J (2008). "MCF7 side population cells with characteristics of cancer stem/progenitor cells express the tumour antigen muc1." *Cancer Res* 68 (7): 2419–2426.

Evans, A. J., Russell, R. C., Roche, O., Burry, T. N., Fish, J. E., Chow, V. W., Kim, W. Y., Saravanan, A., Maynard, M. A, Gervais. M. L, Sufan, R. I., Roberts, A. M., Wilson, L. A., Betten, M., Vandewalle, C., Berx, G., Marden, P.A., Irwin, M.S., The, B.T., Jewett, M. A. and Ohh, M. (2007). "VHL promotes E2 boxdependent E-cadherin transcription by HIF-mediated regulation of SIP1 and snail." *Mol Cell Biol*, 27(1):157–169.

Ezashi, T., Das, P. and Roberts, R. M. (2005). "Roberts Low O₂ tensions and the prevention of differentiation of hES cells". *Proc. Natl. Acad. Sci.* 102 (13): 4783–4788.

Faiman, M. D., Haya, K. and Ewing, J. A. (1978). "Disulfiram and CS₂ toxicity." *Am J Psychiatry* 135(5): 623-624.

Faneyte, I. F., Kristel, P. M and van de Vijver, M. J. (2001). "Determining MDR1/P-glycoprotein expression in breast cancer." *Int J Cancer* 2001, 93(1):114-122.

Farokhzad, O. C., and Langer, R. (2009). "Impact of nanotechnology on drug delivery." *ACS Nano* 3(1): 16-20.

Fathi, M., and Mohebbi, M. (2010). "Increasing food safety using nanotechnology." *Magazine of Nanotechnology Initiative Council*, 143: 16-18.

Ferlay J, Soerjomataram I, Ervik M, Dikshit R, Eser S, Mathers C, Rebelo M, Parkin DM, Forman D, Bray, F.GLOBOCAN 2012 v1.0 (2013) "Cancer Incidence and Mortality Worldwide:" IARC Cancer Base No. 11 [Internet]. Lyon, France: *International Agency for Research on Cancer*. Available from: <http://globocan.iarc.fr>, accessed on day/month/year.

Fink, D., Aebi, S., Howell, S. B. (1998). "The role of DNA mismatch repair in drug resistance." *Clin Cancer Res* 4(1): 1–6.

Fitzpatrick, S.F., Tambuwala, M.M., Bruning, U., Schaible, B., Scholz, C.C., Byrne, A., O'connor, A., Gallagher, W.M., lenihan, C.R., Garvey, J.F., Howell, K., Fallon, P.G., cummins, E.P., Taylor, C.T (2011). "An intact canonical NF-kappaB pathway is required for inflammatory gene expression in response to hypoxia." *J. Immuni.*, 186(2), 1091-1096.

Fortuna, A., Alves, G. and Falcao, A. (2011). "In vitro and in vivo relevance of the P-glycoprotein probe substrates in drug discovery and development: focus on rhodamine 123, digoxin and talinolol". *J Bioequiv S2*.

Franovic, A., Holterman, C. E., Payette, J. and Lee, S. (2009). "Human cancers converge at the HIF-2alpha oncogenic axis". *Proc. Natl. Acad. Sci.* 106(50): 21306–21311.

Fuertes, M. A., Alonso, C. and Perez, J. M. (2002). "Biochemical modulation of cisplatin mechanisms of action: enhancement of antitumor activity and circumvention of drug resistance." *Chem Rev*;103: 645-62.

Gabizon, A., Horowitz, A. T., Goren, D., Tzemach, D., Shmeeda, H., Zalipsky, S. (2003). "In vivo fate of folate-targeted polyethylene-glycol liposomes in tumor-bearing mice." *Clin. Cancer Res* 9(17): 6551– 6559.

Galmarini, C. M., Clarke, M. L., Jordheim, L., Santos, C. L., Cros, E., Mackey, J. R. and Dumontet, C. (2004). "Resistance to gemcitabine in a human follicular lymphoma cell line is due to partial deletion of the deoxycytidine kinase gene." *BMC Pharmacol* 4: 8.

Gandhi, V. and Plunkett, W. (1990). "Modulatory activity of 2',2'-difluorodeoxycytidine on the phosphorylation and cytotoxicity of arabinosyl nucleosides." *Cancer Res* 50: 3675–3680.

Ganguly, A., Yang, H. and Cabral, F. (2010). "Paclitaxel-dependent cell lines reveal a novel drug activity." *Mol Cancer Ther* 9(11): 2914-2923.

Garber, J. F., Richardson, A. and Harris LN (2006). "Neo-adjuvant cisplatin (CDDP) in 'triple negative' breast cancer (BC)". *Breast Cancer Res Treat* 100(1):S32.

Gascoigne K.E. and Taylor S. (2009). "How do anti-mitotic drugs kill cancer cells?" *J Cell Sci.* 122: 2579–2585.

Gennari, A., Conte, P., Rosso, R., Orlandini, C and Bruzzi, P. (2005). "Survival of metastatic breast carcinoma patients over a 20-year period: a retrospective analysis based on individual patient data from six consecutive studies." *Cancer* 104(8): 1742.

Gessner, T. and Jakubowski, M. (1972). "Diethyldithiocarbamic acid methyl ester. A metabolite of Disulfiram." *Biochem Pharmacol* 21(2): 219-230.

Gewirtz, D. A. (1999). "A critical evaluation of the mechanisms of action proposed for the antitumor effects of the anthracycline antibiotics adriamycin and daunorubicin." *Biochem Pharmacol* 57(7):727–741.

Ghosh, A., Mandal, A. K., Sarkar, S., Panda, S., and Das, N. (2009). "Nanoencapsulation of quercetin enhances its dietary efficacy in combating arsenic-induced oxidative damage in liver and brain of rats." *Life Sci* 84(3-4): 75-80.

Ghosh, S. and Karin, M. (2002). "Missing pieces in the NF-kappaB puzzle." *Cell* 109 Suppl: S81-96.

Giaccone, G. (2000). "Clinical perspectives on platinum resistance." *Drugs* 59 (4), 9–17.

Gidding, C. E., Kellie, S. J., Kamps, W. A., de Graaf, S. S. (1999). "Vincristine revisited." *Crit Rev Oncol Hematol* 29(3):267–287.

Gilmore, T. D. (2006). "Introduction to NF-κB: players, pathways, perspectives." *Oncogene* 25:6680-6684.

Ginestier, C., Hur, M. H., Charafe-Jauffret, E., Monville, F., Dutcher, J., Brown, M., Jacquemier, J., Viens, P., Kleer, C. G., Liu, S., Schott, A., Hayes, D., Birnbaum, D., Wicha, M. S. and Dontu, G. (2007). "ALDH1 is a marker of normal and malignant human mammary stem cells and a predictor of poor clinical outcome." *Cell Stem Cell* 1(5): 555-567.

Gluck, S. (2005). "Adjuvant chemotherapy for early breast cancer: optimal use of epirubicin." *Oncologist*. 10(10):780-91.

Goldhirsch, A., Wood, W. C, Gelber, R. D., Coates, A. S, Thurlimann, B. and Senn HJ (2007). "Panel members. Progress and promise: highlights of the international expert consensus on the primary therapy of early breast cancer." *Annals Onco*. 18:1133–1144.

Gonzalez, V. M., Fuertes, M. A, Alonso, C. and Perez JM (2001). "Is cisplatin-induced cell death always produced by apoptosis?" *Mol Pharmacol* 59:657-663.

Gordan, J. D., Lal, P., Dondeti, V. R., Letrero, R., Parekh, K. N., Oquendo, C. E., Greenberg, R. A., Flaherty, K. T., Rathmell, W. K., Keith, B., Simon, M. C. and Nathanson, K. L. (2008). "HIF-alpha effects on c-Myc distinguish two subtypes of sporadic VHL-deficient clear cell renal carcinoma." *Cancer Cell* 14(6): 435-446.

Gordon R. M. and. Seaton, D. R. (1942). "Observations on the Treatment of Scabies." *Brit. Med. J.* 1(4248) 685-687.

Gottesman, M. M. (2002). "Mechanisms of cancer drug resistance." *Annu Rev Med* 53: 615-627.

Grodzki, M. (1881). "Über äthylirte Sulfoharnstoffe" *Ber. Dtsch. Chem. Ges.*14: 2754-2758.

Gudjonsson, T. and Magnusson, M. K. (2005). "Stem cell biology and the cellular pathways of carcinogenesis." *APMIS* 113:922-999.

Guo, X., Xu, B., Pandey, S., Goessl, E., Brown, J., Armesilla, A. L., Darling, J. L. and Wang, W. (2010). "Disulfiram/copper complex inhibiting NFkappaB activity and potentiating cytotoxic effect of gemcitabine on colon and breast cancer cell lines." *Cancer Lett* 290(1): 104-113.

Gupta, G. P. and Massague, J. (2006). "Cancer metastasis: building a framework." *Cell* 127(4):679-695.

Gupte, A. and Mumper, R. J. (2009). "Elevated copper and oxidative stress in cancer cells as a target for cancer treatment." *Cancer Treat Rev* 35(1): 32-46.

Hambardzumyan, D., Squatrito, M. and Holland, E. C. (2006). "Radiation resistance and stem-like cells in brain tumors." *Cancer Cell* 10:454-456.

Hammarstrom, A. K and Gage, P. W. (2002). "Hypoxia and persistent sodium current." *Eur. Biophys J* 31: 323-330.

Han, W., Jung, E. M., Cho, J., Lee, J. W., Hwang, K. T, Yang, S. J., Kang, J. J., Bae, J. Y., Jeon, Y. K., Park, I. A., Nicolau, M., Jeffrey, S. S. and Noh, D. Y. (2008). "DNA copy number alterations and expression of relevant genes in triple-negative breast cancer." *Genes Chromosomes Cancer* 47(9):490-499.

Hanahan, D. and Weinberg, R. A (2000): "The hallmarks of cancer." *Cell* 100(1): 57–70.

Harris, A. L. (2002). "Hypoxia—A key regulatory factor in tumour growth." *Nat Rev Cancer* 2(1):38–47.

Harris, J. R., Lippman, M. E and Morrow, C.K. (2000). "Osborne Treatment of metastatic breast cancer, Diseases of the Breast" (2nd ed.), Lippincott Williams & Wilkins, Philadelphia pp. 749.

Harris, Z.H. and Gitlin, J.D. (1996). "Genetic and molecular basis of copper toxicity" *Am J Clin Nutr*, 63(5): 836–841.

Hastak, K., Alli, E. and Ford, J. M. (2010). "Synergistic chemosensitivity of triple-negative breast cancer cell lines to poly(ADP-Ribose) polymerase inhibition, gemcitabine, and cisplatin." *Cancer Res.* 70:7970–7980.

Hayden, M. S and Ghosh, S. (2004). "Signaling to NF- κ B." *Genes Dev* 18: 2195-2224.

Hayden, M. S and Ghosh, S. (2008). "Shared principles in NF-kappa B signalling." *Cell* 132(3):344–362.

Hedenfalk, I. A., Ringner, M., Trent, J. M and Borg, A. (2002). "Gene expression in inherited breast cancer." *Adv Cancer Res* 84: 1–34.

Hellsten, R., Johansson, M., Dahlman, A., Sterner, O. and Bjartell, A. (2011). "Galiellalactone inhibits stem cell-like ALDH-positive prostate cancer cells." *PLoS One* 6(7): e22118.

Henderson IC: Chemotherapy for metastatic disease, in Harris JR, Hellman S, Henderson IC, et al, eds: Breast Diseases. pp 604- 665. 2nd ed, J.B. Lippincott Company, Philadelphia, 1991.

Higgins, D. F, Kimur, K., Bernhardt, W. M., Shrinmanker, N., Akai, Y., Hohenstein, B., Saito, Y., Johnson R. S., Kretzler M., Cohen, C. D., Exkardt, K., Iwano, M. and Haase V. H. (2007). "Hypoxia promotes fibrogenesis in vivo via HIF1 stimulation of epithelial to mesenchymal transition." *J Clin Invest* 117(12):3810-3820.

Hill, R. P., Marie-Egyptienne, D. T. and Hedley, D. W. (2009.) "Cancer stem cells, hypoxia and metastasis." *Semin Radiat Oncol.*19(2):106–111.

Himes, R. H. (1991). "Interactions of the catharanthus (Vinca) alkaloids with tubulin and microtubules." *Pharmacol Ther* 51:257–267.

Hinohara, K., Kobayashi, S., Kanauchi, H., Shimizu, S., Nishioka, K., Tsuji, E., Tada, K., Umezawa, K., Mori, M., Ogawa, T., Inoue, J., Tojo, A. and Gotoh, N. (2012). "ErbB receptor tyrosine kinase/NF-kappaB signaling controls mammosphere formation in human breast cancer." *Proc Natl Acad Sci USA* 109(17):6584–6589.

Hoffmann, A., Natoli, G. and Ghosh, G (2006). "Transcriptional regulation via the NFkB signalling module." *Oncogene.* 18: 6867-6874.

Hollier, B. G., Evans, K. and Mani, S. A. (2009). "The epithelial-to-mesenchymal transition and cancer stem cells: a coalition against cancer therapies." *J Mammary Gland Biol Neoplasia.* 14(1):29–43.

Howell, A., Cuzick, J., Baum, M., Buzdar, A., Dowsett, M., Forbes, J. F., Hochtin-Boes, G., Houghton, J., Locker, G. Y. and Tobias, J. S. (2005). "Results of the ATAC (Arimidex, Tamoxifen, Alone or in Combination) trial after completion of 5 years' adjuvant treatment for breast cancer." *Lancet* 365(9453): 60-62.

Hu, X., Stern, H. M., Ge, L., O'Brien, C., Haydu, L., Honchell, C. D., Haverty, P. M., Peter, B. A., Wu, T. D., Amler, L. C., Chant, J., Stokoe, D., Lackner, M. R. and Cavet, G. (2009). "Genetic alterations and oncogenic pathways associated with breast subtypes." *Mol Cancer Res* 7(4): 511-522.

Huber, M. A., Azoitei, N., Baumann, B., Grünert, S., Sommer, A., Pehamberger, H., Kraut, N., Beug, H. and Wirth, T. (2004). "NF- κ B is essential for epithelial-mesenchymal transition and metastasis in a model of breast cancer progression." *J Clin Invest* 114(4): 569–581.

Huber, M. A., Kraut, N. and Beug, H (2005). "Molecular requirements for epithelial mesenchymal transition during tumour progression." *Curr Opin Cell Biol* 17(5):548–558.

Huber, V., de Milito, A., Harguindey, S., Reshkin, S. J., Wahl, M. L., Rauch, C., Chiesi, A., Pouyssegur, J., Gatenby, R. A., Riviltini, L and Fais S (2010). "Proton dynamics in cancer." *J. Transl. Med.* 8: 57.

Ilijin, K., Ketola, K., Vainio, P., Halonen, P., Kohonen, P., Fey, V., Grafstrom, R. C, Perala M. and Kallioniemi O. (2009). "High-throughput cell-based screening of 4910 known drugs and drug-like small molecules identifies disulfiram as an inhibitor of prostate cancer cell growth." *Clin Cancer Res* 15(19): 6070-6078.

Irving, C. C. Daniel, D. S. and Murphy, W. M. (1983). "The effect of disulfiram on the carcinogenicity of N-butyl-N-(3-carboxypropyl) nitro-samine in the rat." *Carcinogenesis* 4: 617-620.

Irving, C. C., Tice, A. J. and Murphy, W. M. (1979). "Inhibition of N-n-butyl- N-(4-hydroxybutyl) nitrosamine-induced urinary bladder cancer in rats by administration of disulfiram in the diet." *Cancer Res* 39:3040-3043.

Ishikawa, F., Yoshida, S., Saito, Y., Hijikata, A., Kitamura, H., Tanaka, S., Nakamura, R., Tanaka, T., Tomiyama, H., Saito, N., Fukata, M., Miyamoto, T., Lyons, B., Ohshima, K., Uchida, N., Taniguchi, S., Ohara, O., Akashi, K., Harada, M. and Shultz, L. D. (2007). "Chemotherapy-resistant human aml stem cells home to and engraft within the bone-marrow endosteal region." *Nat Biotechnol* 25(11): 1315–1321.

Ivan, M., Kondo, K., Yang, H., Kim, W., Valiando, J., Ohh, M., Salic, A., Asara, J. M., Lane, W. S. and Kaelin, W. G. Jr. (2001). "HIF α targeted for VHL-mediated destruction by proline hydroxylation: implications for O₂ sensing." *Science* 292(5516): 464–468.

Jacobson, M.D., Weil, M. and Raff M.C. (1997). "Programmed cell death in animal development". *Cell* 88 (3): 347–354.

Jiang F, Qiu Q, Khanna A, Todd, N. W., Deepak, J., Xing, L., Wang, H., Liu, Z., Su, Y., Stass S. A. and Katz, R. L. (2009). "Aldehyde dehydrogenase 1 is a tumor stem cell-associated marker in lung cancer." *Mol Cancer Res* 7(3): 330–338.

Johansson, B. (1992) "A review of the pharmacokinetics and pharmacodynamics of disulfiram and its metabolites." *Acta Psychiatrica Scandinavica*, 362: 15-26.

Jones, T. D., Ulbright, T. M., Eble, J. N. and Cheng, L. (2004). "OCT4: a sensitive and specific biomarker for intratubular germ cell neoplasia of the testis." *Clin Cancer Res* 10(24): 8544–8547.

Jordan, C. T. (2004). "Cancer stem cell biology: from leukemia to solid tumors." *Curr Opin Cell Biol* 16: 708-712.

Juliano, R.L. and Ling, V. (1976). "A surface glycoprotein modulating drug permeability in Chinese hamster ovary cell mutants." *Biochim Biophys Acta* 455(1): 152-162.

Kakarala, M. and Wicha, M. S. (2008). "Implications of the cancer stem-cell hypothesis for breast cancer prevention and therapy." *J Clin Oncol* 26 (17):2813–2820.

Kallinowski, F and Vaupel, P. (1989). "pH distribution in spontaneous and isografted rat tumours." *Br. J. Cancer*. 58: 314-321.

Kalluri, R. and Weinberg, R. A. (2009). "The basics of epithelial-mesenchymal transition." *J Clin Invest* 119(6):1420–1428.

Karin, M. (2006). "Nuclear factor-kappaB in cancer development and progression." *Nature* 441(7092):431–436.

Karin, M. and Ben-Neriah, Y. (2000). "Phosphorylation meets ubiquitination: the control of NF-[kappa]B activity." *Annu Rev Immunol* 18: 621-663.

Karin, M. and Lin, A. (2002). "NF-kappa B at the crossroads of life and death." *Nat Immunol.* 3(3):221–227.

Karin, M., Cao, Y., Greten, F. R. and Li, Z.W. (2002). "NF-kappaB in cancer: from innocent bystander to major culprit." *Nat. Rev. Cancer* 2(4): 301–310.

Kato, T. Jr., Delhase, M., Hoffmann, A. and Karin, M. (2003). "CK2 is a C-terminal IkappaB kinase responsible for NF-kappaB activation during the UV response." *Mol Cell*, 12(4): 829-839.

Keith, B. and Simon, M. C. (2007). "Hypoxia-inducible factors, stem cells, and cancer." *Cell* 129(3): 465–472.

Kim, R., Emi, M. and Tanabe, K. (2006). "Role of mitochondria as the gardens of cell death." *Cancer Chemother Pharmacol* , 57:545-553.

Kim, T. Y., Kim, D. W., Chung, J. Y., Shin, S. G., Kim, S., Hoe, D. S., Kim, N.K. and Bang, Y. J. (2004). "Phase I and pharmacokinetic study of Genexol-PM, a cremophor-free, polymeric micelle-formulated paclitaxel, in patients with advanced malignancies." *Clin. Cancer Res.*10 (11): 3708–3716.

Kim, M. Y., Kim, K. S., McConnell, F. and Lane, P. (2009). "Lymphoid tissue inducer cells: Architects of CD4 immune responses in mice and men." *Clin Exp Immunol* 157(1):20–26.

Kolenda, J., Jensen, S. S., Aaberg-Jessen, C., Christensen, K., Andersen, C., Brunner, N. and Kristensen BW (2011). "Effects of hypoxia on expression of a panel of stem cell and chemoresistance markers in glioblastoma-derived spheroids." *J Neurooncol* 103(1):43-58.

Kostrzewa-Nowak, D., Paine, M. J., Wolf, C. R. and Tarasiuk, J. (2005). "The role of bioreductive activation of doxorubicin in cytotoxic activity against leukaemia HL60-sensitive cell line and its multidrug-resistant sublines." *Br J Cancer* 93: (1):89–97.

Krishna, R. and Mayer, L. D. (2000). "Multidrug resistance (MDR) in cancer. Mechanisms, reversal using modulators of MDR and the role of MDR modulators in influencing the pharmacokinetics of anticancer drugs." *Eur J Pharm Sci* 11(4): 265–283.

Kufe D.W., Pollock R.E., Weichselbaum R.R., Bast R.C., Gansler T.S., Holland J.E. and Frei E. (2003). "Cancer Medicine", 6th ed. Hamilton, Ontario. B.C: Decker Inc., pp. 585-604.

Kuo, K. W, Chen, S. F., Wu, C. C., Chen, D. R. and Lee, J. H. (2002). "Serum and tissue trace elements in patients with breast cancer in Taiwan." *Biol Trace Elem Res* 89(1):1–11.

Kwon GS. (2003). "Polymeric micelles for delivery of poorly watersoluble compounds." *Crit Rev Ther Drug Carr Syst* 20:357–403.

Lai, P. S., Lou, P. J., Peng, C. L., Pai, C. L, Yen, W. N., Huang, M. Y., Young, T. H and Shieh, M. J. (2007). "Doxorubicin delivery by polyamidoamine dendrimer conjugation and photochemical internalization for cancer therapy." *J Control Release* 122(1): 39–46.

Le, Q.T., Denko, N.C. and Giaccia, A.J. (2004). "Hypoxic gene expression and metastasis." *Cancer Metastasis Rev.*, 23(3-4): 293-310.

Leamon CP, Reddy JA. (2004). "Folate-targeted chemotherapy." *Adv. Drug Deliv. Rev* 56(8): 1127–1141.

Lehmann, B., Bauer, J. and Chen, X. (2010). "Transcriptome analysis of triple negative breast cancers identifies six distinct biological subgroups and reveals therapeutic strategies. 'In Supplement to Cancer Research 33rd Annual San Antonio Breast Cancer Symposium: December 8-12; San Antonio, TX: San Antonio Breast Cancer Symposium, PD01-PD07.

Lewis, D. J., Deshmukh, P., Tedstone, A. A., Tuna F. and O'Brien P. (2014). "On the interaction of copper(II) with disulfiram." *Chem comm*, 50(87): 13334-13337.

Lewis, R., Bagnall, A. M., Forbes, C., Shirran, E., Duffy, S., Kleijnen, J., Riemsma, R. and ter Riet, G. (2002). "The clinical effectiveness of trastuzumab for breast cancer: a systematic review." *Health Technol Assess* 6(13): 1-71.

Lewison, E. F. (1977). "Spontaneous regression of breast cancer." *Prog Clin Biol Res* 12:47–53.

Li, Q. and Verma, I. M. (2002). "NFkB regulation in the immune system." *Nat Rev Immunol*. 2(10): 725–734.

Li, Z. and Rich, J. N. (2010). "Hypoxia and hypoxia inducible factors in cancer stem cell maintenance." *Curr Top Microbiol Immunol* 345: 21-30.

Li, Z., Bao, S., Wu, Q., Wang, H., Eyler, C., Sathornsumetee, S., Shi, Q., Cao, Y., Lathia, J., McLendon, R. E., Hjelmeland, A. B. and Rich, J. N. (2009). Hypoxia-inducible factors regulate tumorigenic capacity of glioma stem cells. *Cancer Cell* 15(6):501–513.

Li, Z., Bao, S., Wu, Q., Wang, H., Eyler, C., Sathornsumetee, S., Shi, Q., Cao, Y., Lathia, J., McLendon, R. E., Hjelmeland, A. B. and Rich, J. N. (2009) "Hypoxia-inducible factors regulate tumorigenic capacity of glioma stem cell." *Cancer Cell*; 15(6): 501-513.

Li. C., Heidt, D. G., Dalerba, P., Burant, C. F., Zhang, L., Adsay, V., Wicha, M., Clarke, M. F. and Simeone, D. M. (2007). "Identification of pancreatic cancer stem cells." *Cancer Res* 67 (3):1030–1037.

Liang, Y., Zhou, Y and Shen P. (2004). NF-Kappa B and its regulation on the immune system". *Cellular and molecular immunology* 1(5): 343-350.

Liedtke, C., Mazouni, C., Hess, K. R., André, F., Tordai, A., Mejia, J. A., Symmans, W. F., Gonzalez-Angulo, A. M., Hennessey, B., Green, M., Cristofanilli, M., Hortobagyi, G. N. and Pusztai, L. (2008). Response to neoadjuvant therapy and long-term survival in patients with triple-negative breast cancer. *J Clin Oncol* 26(8): 1275-1281.

Lim, S. C. (2005). "CD24 and human carcinoma: tumour biological aspects." *Biomed Pharmacother* 59(2): 351–354.

Lin, Q. and Yun, Z. (2010). "Impact of the hypoxic tumour microenvironment on the regulation of cancer stem cell characteristics." *Cancer Biol Ther* 9(12): 949–956.

Lipsky, J. J, Shen, M. L. and Naylor, S. (2001). "In vivo inhibition of aldehyde dehydrogenase by disulfiram." *Chem Biol Interact* 130–132:(1-3): 93–102.

Liu, M., Sakamaki, T., Casimiro, M. C., Willmarth, N. E., Quong, A. A., Ju, X., Ojeifo, J., Jiao, X., Yeow, W. S., Katiyar, S., Shirley, L. A., Joyce, D., Lisanti, M. P., Albanese, C. and Pestell RG. (2010). "The canonical NF-kappaB pathway governs mammary tumorigenesis in transgenic mice and tumour stem cell expansion." *Cancer Res.* 70(24): 10464–10473.

Liu, P., Brown, S., Goktug, T., Channathodiyil, P., Kannappan, V., Hugnot, J. P., Guichet, P. O., Bian, X., Armesilla, A. L., Darling, J. L. and Wang, W. (2012). "Cytotoxic effect of Disulfiram/copper on human glioblastoma cell lines and ALDH-positive cancer-stem-like cells." *Br J Cancer* 107(9): 1488-1497.

Liu, P., Wang, Z., Brown, S., Kannappan, V., Tawari, P. E., Jiang, J., Irache, J. M., Tang, J. Z., Armesilla, A. L., Darling, J. L., Tang X. and Wang. W. (2014) "Liposome encapsulated Disulfiram inhibits NFkB pathway and targets breast cancer stem cells *in vitro* and *in vivo*". *Oncotarget*, 5(17): 7471–7485.

Lodish, H., Berk, A., Matsudaira, P., Kaiser, C. A., Krieger, M., Scott, M. P., Zipursky, S. L. and Darnell, J. (2004). "Molecular cell biology" (5th ed.). New York: W.H. Freeman and CO. pp. 66–72.

Longley, D. B. and Johnston, P. G. (2005). "Molecular mechanisms of drug resistance." *J Pathol* 205(2): 275-292.

Loo, T. W. and Clarke, D. M. (2000). "Blockage of drug resistance *in vitro* by disulfiram, a drug used to treat alcoholism." *J. Natl. Cancer Inst.* 92(11): 898-902.

- Loo, T. W., Bartlett, M. C. and Clarke, D. M. (2004). "Disulfiram metabolites permanently inactivate the human multidrug resistance P-glycoprotein." *Mol. Pharm.* 1(6): 426-433.
- Lu, X. and Kang, Y. (2011). "Hypoxia and hypoxia-inducible factors: master regulators of metastasis." *Clin Cancer Res* 16(24):5928-5935.
- Lynch, M. D., Cariati, M. and Purushotham, A. D. (2006). "Breast cancer, stem cells and prospects for therapy." *Breast Cancer Res* 8:211
- Ma, J. D, Tsunoda, S. M., Bertino, J. S. Jr., Trivedi, M., Beale, K. K. and Nafziger, A. N. (2010). "Evaluation of in vivo P-glycoprotein phenotyping probes: a need for validation." *Clin Pharmacokinet.* 49(4): 223–237.
- Ma, S., Chan, K. W., Lee, T. K., Tang, K. H., Wo, J. Y., Zheng, B. J. and Guan XY (2008). "Aldehyde dehydrogenase discriminates the CD133 liver cancer stem cell populations." *Mol Cancer Res* 6(7):1146–1153.
- Madjd, Z., Mehrjerdi, A. Z., Sharifi, A. M., Molanaei, S., Shahzadi, S. Z. and Asadi-Lari, M. (2009) "Cd44+ cancer cells express higher levels of the anti-apoptotic protein bcl-2 in breast tumours." *Cancer Immun* 9:4.
- Maeda, H., Sawa, T. and Konno, T. (2001). "Mechanism of tumour-targeted delivery of macromolecular drugs, including the EPR effect in solid tumor and clinical overview of the prototype polymeric drug SMANCS." *J Controlled Release.* 74(1–3):47–61.
- Makino, Y. Cao, R., Svensson, K., Bertilsson, G., Asman, M., Tanaka, H., Cao, Y., Berkenstam, A. and Poellinger L. (2001). "Inhibitory PAS domain protein is a negative regulator of hypoxia-inducible gene expression." *Nature* 414, 550-554.
- Marhaba, R. and Zoller, M. (2004). "CD44 in cancer progression: adhesion, migration and growth regulation." *J Mol Histol* 35:211–31.
- Marikovsky, M., Nevo, N., Vadai, E. and Harris-Cerruti C. (2002). "Cu/Zn superoxide dismutase plays a role in angiogenesis." *Int J Cancer*, 97(1): 34–41.

- Marin, A., Sun, H., Hussein, G. A., Pitt, W. G., Christensen, D. A. and Rapoport, N. Y. (2002). "Drug delivery in pluronic micelles: effect of high-frequency ultrasound on drug release from micelles and intracellular uptake." *J Control Release* 84(1-2):39–47.
- Martindale, J. L. and Holbrook, N. J. (2002). "Cellular response to oxidative stress: signaling for suicide and survival." *J Cell Physiol* 192(1): 1-15.
- Matsumura, Y. and Kataoka, K. (2009). "Preclinical and clinical studies of anticancer agent-incorporating polymer micelles." *Cancer Science* 100(4):572–579.
- Matsuno, T., Kariya, R. and Yano, S. (2012). "Diethyldithiocarbamate induces apoptosis in HHV-8- infected primary effusion lymphoma cells via inhibition of the NF-kappaB pathway." *Int J Oncol* 40 (4):1071-1078.
- Maynard, M. A., Qi, H., Chung, J., Lee E. H. L., Kondo, Y., Hara, S., Conaway, R. C., Conaway, J. W. and Ohh M. (2003) "Multiple splice variants of the human HIF-3 alpha locus are targets of the von Hippel-Lindau E3 ubiquitin ligase complex." *J of Biol Chem* 278, 11032-11040.
- McArthur, H. L. and Hudis, C. A. (2007). "Breast cancer chemotherapy." *Cancer J* 13(3): 141-147.
- Medema JP (2013) "Cancer stem cells: The challenges ahead." *Nat Cell Biol* 15(4): 338–344.
- Melaine, N., Liénard, M. O, Dorval, I., Le Goascogne, C., Lejeune, H. and Jégou, B. (2002) "Multidrug resistance genes and P-glycoprotein in the testis of the rat, mouse, guinea pig, and human." *Biol Reprod.* 67(6):1699–1707.
- Mersin, H., Yildirim, E., Berberoglu, U. and Gulben, K. (2008). "The prognostic importance of triple negative breast carcinoma. " *Breast* 17(4):341–346.
- Metzen, E., Stiehl, D. P., Doege, K., Marxsen, J. H., Hellwig-Burgel, T. and Jelkmann, W. (2005). "Regulation of the prolyl hydroxylase domain protein 2

(phd2/egln-1) gene: identification of a functional hypoxia-responsive element.” *Biochem J* 2005, 387(Pt 3):711-717.

Miki J, Furusato B, Li H, Gu, Y., Takahashi, H., Egawa, S., Sesterhenn, I. A., McLeod, D. G., Srivastava, S. and Rhim, J. S. (2007). “Identification of putative stem cell markers, CD133 and CXCR4, in hTERT-immortalized primary nonmalignant and malignant tumor-derived human prostate epithelial cell lines and in prostate cancer specimens.” *Cancer Res* 67(7): 3153–3161.

Milani, M. and Harris, A. L. (2008). “Targeting tumour hypoxia in breast cancer.” *Eur J Cancer* 44(18):2766–2773.

Mimeault, M., Hauke, R. and Batra, S. K. (2007). "Stem cells: a revolution in therapeutics-recent advances in stem cell biology and their therapeutic applications in regenerative medicine and cancer therapies." *Clin Pharmacol Ther* 82(3): 252-264.

Mini, E., Nobili, S., Caciagli, B., Landini, I. and Mazzei, T. (2006). "Cellular pharmacology of gemcitabine." *Ann Oncol* 17 (Suppl 5): 7-12.

Miraglia, S., Godfrey, W., Yin, A.H, Atkins, H., Warnke, R., Holdn J. H., Bray, R.A (1997). “Novel five-transmembrane hematopoietic stem cell antigen: iso and molecular cloning.” *Blood* 90: 5013-5021.

Mohanraj V. J., Chen, Y. (2006) “Nanoparticles – a review”. *Trop J Pharma Res* 5(1): 561–573.

Montagut, C., Tusquets, I. and Ferrer, B. (2003). “Activation of nuclear factor – kappa B is linked to resistance to neoadjuvant chemoresistance in breast cancer patients.” *Endocr Relat Cancer* 13:607-616.

Monteiro, H. P. and Stern, A. (1996). “Redox modulation of tyrosine phosphorylation-dependent signal transduction pathways.” *Free Rad Biol Med* 21:323–333.

Moreb, J. S. (2008) “Aldehyde dehydrogenase as a marker for stem cells.” *Curr Stem Cell Res Ther* 3 (4):237–246.

Morrison, B. W., Doudican, N. A., Patel, K. R. and Orlow, S. J. (2010). "Disulfiram induces copper-dependent stimulation of reactive oxygen species and activation of the extrinsic apoptotic pathway in melanoma." *Melanoma Res* 20(1): 11-20.

Moulder, S. and Hortobagyi, G. N. (2008). "Advances in the treatment of breast cancer." *Clin Pharmacol Ther* 83(1): 26-36.

Moutinho, C. G., Matos, C. M., Teixeira, J. A. and Balcao, V. M. (2012). "Nanocarrier possibilities for functional targeting of bioactive peptides and proteins: state-of-the-art." *J. Drug. Target.* 20(2):114–141.

Moynagh, P. N. (2005). "The NFκB pathway." *J Cell Sci.* 118 (20): 4389-4392.

Mozafari, M. R. (2006). "Bioactive entrapment and targeting using nanocarrier technologies: an introduction." In M. R. Mozafari (Ed.), *Nanocarrier technologies* (pp. 1-16). Netherlands: Springer.

Muller, C.A. and Banas, R. (2011). "Disulfiram: An anticraving substance?" *Am J of Psychiatry* 168(1): 98.

Myant, K. B., Cammareri, P., McGhee, E. J., Ridgway, R. A., Huels, D. J., Cordero, J. B., Schwitalla, S., Kalna, G., Ogg, E. L., Athineos, D., Timpson, P., Vidal, M., Murray, G. I., Greten, F. R., Anderson, K. I. and Sansom, O. J. (2013). "ROS production and NF-κB activation triggered by RAC1 facilitate WNT-driven intestinal stem cell proliferation and colorectal cancer initiation." *Cell Stem Cell* 12(6):761–773.

Nakshatri, H. and Goulet, R. J., Jr (2002). "NF-κB and breast cancer." *Curr Probl Cancer* 26(5): 282–309.

Nakshatri, H., Bhat-Nakshatri, P., Martin, D. A., Goulet, R. J. Jr., Sledge, G. W., Jr (1997). "Constitutive activation of NFκB during progression of breast cancer to hormoneindependent growth." *Mol Cell Biol* 17(7):3629–3633.

Nechushtan, H., Hamamreh, Y., Nidal, S., Gotfried, M., Baron, A., Shalev, Y. I., Nisman, B., Peretz, T. and Peylan-Ramu, N. (2015). "A phase IIb trial assessing

the addition of disulfiram to chemotherapy for the treatment of metastatic non-small cell lung cancer." *Oncologist*. 20(4):366-367.

Neethirajan, S. and Jayas, D. (2011). "Nanotechnology for the Food and Bioprocessing Industries." *Food and Bioprocess Technology* 4: 39-47.

Nielsen, D., Maare, C. and Skovsgaard, T. (1996). "Cellular resistance to anthracyclines." *Gen Pharmacol* 27(2):251-255.

Nieto, M. A. (2011). "The ins and outs of the epithelial to mesenchymal transition in health and disease." *Annu Rev Cell Dev Biol* 27: 347–376.

Niu, L., Meng, L. and Lu, Q. (2013). "Folate-conjugated PEG on single walled carbon nanotubes for targeting delivery of doxorubicin to cancer cells." *Macromol Biosci* 13(6): 735–744.

Nobel, C. I., Kimland, M., Lind, B., Orrenius, S. and Slater, A. F. (1995). "Dithiocarbamates induce apoptosis in thymocytes by raising the intracellular level of redox-active copper." *J Biol Chem* 270(44): 26202-26208.

Nofech-Mozes, S., Trudeau, M., Kahn, H. K., Dent, R., Rawlinson, E., Sun, P., Narod, S. A. and Hanna, W. M. (2009). "Patterns of recurrence in the basal and non-basal subtypes of triple-negative breast cancers." *Breast Cancer Res Treat* 118(1):131–137.

Oakman, C., Viale, G. and Di Leo, A. (2010). "Management of triple negative breast cancer." *Breast* 19(5): 312–321.

O'Brien, C. A., Pollett, A., Gallinger, S. and Dick, J. E. (2007). "A human colon cancer cell capable of initiating tumour growth in immunodeficient mice." *Nature*, 445(7123):106–110.

Oeckinghaus, A. and Ghosh, S. (2009). "The NF-kappaB family of transcription factors and its regulation." *Cold Spring Harb Perspect Biol* 1(4): 34.

Ohh, M., Park, C. W, Ivan, M., Hoffman, M. A, Kim, T. Y, Huang, L. E, Pavletich, N, Chau, V. and Kaelin WG (2000) "Ubiquitination of hypoxia-inducible factor

requires direct binding to the beta-domain of the von Hippel-Lindau protein." *Nat Cell Biol* 2 (7): 423–427.

Ozols, R. F. (1991). "Ovarian cancer: new clinical approaches." *Cancer Treat. Rev.*, 18 (Suppl A), 77–83.

Panchision, D. M. (2009). "The role of oxygen in regulating neural stem cells in development and disease." *J Cell Physiol* 220(3): 562-568.

Panta, G. R, Kaur, S., Cavin, L. G., Cortés, M. L., Mercurio, F., Lothstein, L., Sweatman, T. W., Israel, M., Arsura, M. (2004). "ATM and the catalytic subunit of DNA-dependent protein kinase activate NF-kappaB through a common MEK/extracellular signal-regulated kinase/p90^{rsk} signaling pathway in response to distinct forms of DNA damage." *Mol Cell Biol*, 24(5): 1823-1835.

Pardal, R., Clarke, M. F. and Morrison, S. (2003). "Applying the principles of stemcell biology to cancer." *Nat Rev Cancer* 3(12): 895–902.

Park, E. K., Kim, S. Y., Lee, S. B. and Lee YM (2005). "Folate conjugated methoxy poly(ethylene glycol)/poly(qcaprolactone) amphiphilic block copolymeric micelles for tumor-targeted drug delivery." *J Control Release* 109(1-3):158–168.

Penault-Llorca, F. and Viale, G. (2012). "Pathological and molecular diagnosis of triple-negative breast cancer: a clinical perspective." *Ann Oncol* 23 (6): vi19–vi22.

Perou, C. M., Sorlie T, Eisen M. B., van de Rijn M, Jeffrey S.S., Rees C. A., Pollack J. R., Ross D. T., Johnsen H, Akslen L. A., Fluge O, Pergamenschikov A, Williams C, Zhu S. X., Lonning P. E., Borresen-Dale A. L., Brown P. O., Botstein D (2000)."Molecular portraits of human breast tumours". *Nature*; 406: 747-752.

Pescador, N., Cuevas, Y., Naranjo, S., Alcaide, M., Villar, D., Landazuri, M., Del Peso, L. (2005). "Identification of a functional hypoxia-responsive element that regulates the expression of the egl nine homologue 3 (egln3/phd3) gene." *Biochem J* 390(Pt 1):189-197.

- Phillips, T. M., McBride, W. H. and Pajonk, F. (2006). "The response of cd24(-/low)/cd44+ breast cancer-initiating cells to radiation." *J Natl Cancer Inst* 98 (24): 1777–1785.
- Pietras, A., Gisselsson, D., Ora, I., Noguera, R., Beckman, S., Navarro, S. and Pahlman, S. (2008). "High levels of HIF-2 α highlight an immature neural crest-like neuroblastoma cell cohort located in a perivascular niche." *J Pathol* 214 (4):482–488.
- Pike, M. G., Mays, D. C., Macomber, D. W. and Lipsky, J. J. (2001). "Metabolism of a disulfiram metabolite S-methyl N,N-diethyldithiocarbamate by flavinmonooxygenase in human renal microsomes." *Drug Metab & Disposition*, 29(2): 127-132.
- Plumb, J. A, Strathdee, G., Sludden, J., Kaye, S. B and Brown R (2000). "Reversal of drug resistance in human tumour xenografts by 2'-deoxy-5-azacytidine-induced demethylation of the hMLH1 gene promoter." *Cancer Res* 60 (21): 6039–6044.
- Polyak, K. and Hahn, W. C. (2006). "Roots and stems: stem cells in cancer." *Nat Med*. 12(3): 296-300.
- Polyak, K. and Weinberg, R. A. (2009). "Transitions between epithelial and mesenchymal states: acquisition of malignant and stem cell traits." *Nat Rev Cancer*, 9: 265–273.
- Prat, A. and Perou, C. M. (2011). "Deconstructing the molecular portraits of breast cancer." *Mol Oncol* 5(1): 5-23.
- Prat, A., Parker, J., Karginova, O., Fan, C., Livasy, C., Herschkowitz, J. I., He, X. and Perou, C. M. (2010). "Phenotypic and molecular characterization of the claudin-low intrinsic subtype of breast cancer." *Breast Cancer Res* 12(5): R68.
- Prince, M. E., Sivanandan, R., Kaczorowski, A., Wolf, G. T., Kaplan, M. J., Dalerba, P., Weissman, I. L., Clarke, M. F. and Ailles, L. E. (2007). "Identification of a subpopulation of cells with cancer stem cell properties in head and neck squamous cell carcinoma." *Proc Natl Acad Sci USA*.104(3): 973-978.

- Proulx, M. E, Desormeaux, A., Marquis, J. F., Olivier, M. and Bergeron MG (2001). "Treatment of visceral leishmaniasis with sterically stabilized liposomes containing camptothecin." *Antimicrob. Agents Chemother.* 45(9): 2623–2627
- Rae, C., Tesson, M., Babich, J. W., Boyd, M., Sorensen, A. and Mairs, R. J. (2013) "The role of copper in disulfiram-induced toxicity and radiosensitization of cancer cells." *J Nucl Med* 54(6): 953-960.
- Raina, K. and Agarwal, R. (2007). "Combinatorial strategies for cancer eradication by silibinin and cytotoxic agents: efficacy and mechanisms." *Acta Pharmacol Sin* 28(9): 1466-1475.
- Rankin, E. B. and Giaccia, A. J. (2008). "The role of hypoxia-inducible factors in tumorigenesis." *Cell Death Differ.* 15(4): 678-685.
- Raval, R. R., Lau, K. W., Tran, M. G. B., Sowter, H. M., Mandriota, S. J., Li, J.-L., Pugh, C. W., Maxwell, P. H., Harris A. L. and Ratcliffe, P. J. (2005). "Contrasting Properties of Hypoxia-Inducible Factor 1 (HIF-1) and HIF-2 in von Hippel-Lindau-Associated Renal Cell Carcinoma." *Molecular and Cellular Biology*, 25(13): 5675–5686.
- Reya, T., Morrison, S. J., Clarke, M. F. and Weissman, I. L. (2001). "Stem cells, cancer and cancer stem cells." *Nature* 414 (6859):105–111.
- Ritzel, M. W., Ng, A. M., Yao, S. Y., Graham, K., Loewen, S. K, Smith, K. M, Hyde R. J., Karpinski, E., Cass, C. E, Baldwin, S. A., Young, J. D. (2001). "Recent molecular advances in studies of the concentrative-dependent nucleoside transporter (CNT) family: identification and characterization of novel human and mouse proteins (hCNT3 and mCNT3) broadly selective for purine and pyrimidine nucleosides (system cib)." *Mol Membr Biol* 18(1): 65–72.
- Rofstad, E. K., Mathiesen, B., Kindem, K. and Galappathi, K. (2006). "Acidic extracellular pH promotes experimental metastasis of human melanoma cells in athymic nude mice." *Cancer Res.* 2006; 66(13): 6699–6707.
- Rosen, J. M and Jordan, C. T. (2009). "The increasing complexity of the cancer stem cell paradigm." *Science* 324(5935): 1670–1673.

Rosenberg, B., Vancamp, L., and Krigas, T. (1965). "Inhibition of cell division in *Escherichia coli* by electrolysis products from a platinum electrode." *Nature* 205(4972): 698–699.

Ross, D. D and Cuddy, D. P (1994). "Molecular effects of 2',2'-difluorodeoxycytidine (Gemcitabine) on DNA replication in intact HL-60 cells." *Biochem Pharmacol*; 48 pp 1619–1630.

Rowinsky, E. K., Onetto, N., Canetta, R. M. and Arbuck, S. G. (1992). "Taxol: the first of the taxanes, an important new class of antitumor agents." *Semin Oncol* 19(6): 646-662.

Sahoo, S.K., Labhasetwar, V in: Amiji, M. (ed) (2007). "Biodegradable PLGA/PLA Nanoparticles for Anticancer Therapy", CRC Press, pp. 243–250.

Samanta, D., Gilkes, D. M., Chaturvedi, P., Xiang, L. and Semenza, G. L. (2014). "Hypoxia-inducible factors are required for chemotherapy resistance of breast cancer stem cells." *Proc Natl Acad Sci USA* 2014, 111(50):5429-5438.

Sandler, A. B, Nemunaitis, J., Denham, C., von Pawel, J., Cormier, Y., Gatzemeier, U., Mattson, K., Manegold, C., Palmer, M. C., Gregor, A., Nguyen, B., Niyikiza, C. and Einhorn, L. H. (2000). "Phase III trial of gemcitabine plus cisplatin vs. cisplatin alone in patients with locally advanced or metastatic non-small cell lung cancer." *J Clin Oncol* 18(1): 122–130.

Sano, A., Kato, H., Sakurai, S., Sakai, M., Tanaka, N., Inose, T., Saito, K., Sohda, M., Nakajima, M., Nakajima, T. and Kuwano, H. (2009). "CD24 expression is a novel prognostic factor in oesophageal squamous cell carcinoma." *Ann Surg Oncol* 16 (2):506–514.

Sauna, Z. E., Peng, X. H., Nandigama, K., Tekle S. and Ambudkar, S. V. (2004). "The molecular basis of the action of disulfiram as a modulator of the multidrug resistance-linked ATP binding cassette transporter MDR1 (ABCTB1) and MRP1 (ABCC1)." *Mol. Pharmacol* 65(3): 675–684.

Sauna, Z. E., Shukla, S. and Ambudkar, S. V. (2005). "Disulfiram, an old drug with new potential therapeutic uses for human cancers and fungal infections." *Mol Biosyst* 1(2): 127-134.

Scadden, D.T. (2006). "The stem-cell niche as an entity of action." *Nature* 441 (7097): 1075–1079.

Schafer, F. Q. and Buettner, G. R. (2001). "Redox environment of the cell as viewed through the redox state of the glutathione disulfide/glutathione couple." *Free Radic Biol Med* 30(11): 1191-1212.

Scheidereit, C. (2006). "I κ B kinase complexes: gateways to NF κ B activation and transcription." *Oncogene*. 25(51): 6685–6705.

Schindl, M., Schoppmann, S. F., Samonigg, H., Hausmaninger, H., Kwasny, W., Gnant, M., Jakesz, R., Kubista, E., Birner, P. and Oberhuber G (2002): "Overexpression of hypoxia-inducible factor 1 α is associated with an unfavourable prognosis in lymph node positive breast cancer." *Clin Cancer Res* 8(6):1831–1837.

Schneider, B. P., Winer, E. P., Foulkes, W. D., Garber, J., Perou. C. M., Richardson, A., Sledge, G. W. and Carey, L. A. (2008). "Triple-negative breast cancer: risk factors to potential targets." *Clin Cancer Res*, 14 (24): 8010-8018.

Schnitt, S. J. (2010). "Classification and prognosis of invasive breast cancer: from morphology to molecular taxonomy." *Mod Pathol* 23(2):60–64.

Scortegagna, M., Cataisson, C., Martin, R. J., Hicklin, D. J., Schreiber, R. D., Yuspa, S. H. and Arbeit, J. M. (2008). "HIF-1 α regulates epithelial inflammation by cell autonomous NF κ B activation and paracrine stromal remodeling." *Blood* 111(7): 3343-3354.

Semenza, G. L. (2000). "Hypoxia, clonal selection, and the role of HIF-1 in tumour progression." *Crit. Rev. Biochem. Mol. Biol* 35(2): 71-103.

Semenza, G. L. (2007). "Evaluation of HIF-1 inhibitors as anticancer agents." *Drug Discov Today* 12(19–20):853–859.

Semenza, G. L. (2009). "Regulation of cancer cell metabolism by hypoxia inducible factor 1." *Semin Cancer Biol.* 19(1):12–16.

Semenza, G. L. (2010). "Defining the role of hypoxia-inducible factor 1 in cancer biology and therapeutics." *Oncogene* 2010, 29(5): 625-634.

Semenza, G. L. (2012). "Hypoxia-inducible factors: mediators of cancer progression and targets for cancer therapy." *Trends Pharmacol Sci* 33 (4):207-214.

Semenza, G. L. (2002). "HIF-1 and tumour progression: pathophysiology and therapeutics." *Trends Mol. Med* 8(4): 62-67.

Sen, R. and Baltimore, D. (1986). "Multiple nuclear factors interact with the immunoglobulin enhancer sequences." *Cell* 46(5): 705-716.

Shah, A. N., Summy, J. M., Zhang, J., Park, S. I., Parikh, N. U. and Gallick, G. E. (2007). "Development and characterization of gemcitabine-resistant pancreatic tumour cells." *Ann Surg Oncol* 14(12): 3629-3637.

Shiah, S. G.; Kao, Y. R.; Wu, F. Y.; Wu, C. W. (2003). "Inhibition of invasion and angiogenesis by zinc-chelating agent disulfiram." *Mol.Pharmacol.* 64(5): 1076-1086.

Shimoni, E. (2009). "Nanotechnology for foods: delivery systems." In BC. Gustavo, M. Alan, L. David, S. Walter, B. Ken, & C. Paul (Eds.), *Global issues in food science and technology* (pp. 411-424). San Diego: Academic Press

Silver, D. P, Richardson, A. L, Eklund, A. C, Wang, Z. C, Szallasi, Z, Li, Q., Juul, N., Leong, C. O., Calogrias, D., Buraimoh, A., Fatima A, Gelman RS, Ryan PD, Tung NM, De Nicolo A, Ganesan S, Miron A, Colin C, Sgroi DC, Ellisen LW, Winer EP, Garber JE. (2010). "Efficacy of Neoadjuvant Cisplatin in Triple-Negative Breast Cancer." *J Clin Oncol.* 28(7): 1145–1153.

Simsek, T., Kocabas, F., Zheng, J., Deberardinis, R. J., Mahmoud, A. I., Olson, E. N., Schneider, J. W., Zhang, C. C. and Sadek, H. A. (2010). "The distinct

metabolic profile of hematopoietic stem cells reflects their location in a hypoxic niche." *Cell Stem Cell* 7(3): 380-390.

Simon, M. C and Keith, B. (2008). "The role of oxygen availability in embryonic development and stem cell function." *Nat Rev Mol Cell Biol* 9 (4): 285–296.

Singh, S. K., Hawkins, C., Clarke, I. D., Squire, J. A., Bayani, J., Hide, T., Henkelman, R. M., Cusimano, M. D. and Dirks, P. B. (2004). "Identification of human brain tumour initiating cells." *Nature* 432 (7015):396–401.

Sinha, R., Kim, G. J., Nie, S. and Shin DM. (2006). "Nanotechnology in cancer therapeutics: bioconjugated nanoparticles for drug delivery." *Mol. Cancer Ther* 5(8): 1909–1917.

Smith, A. M., Duan, H., Mohs, A. M. and Nie, S. (2008). "Bioconjugated quantum dots for *in vivo* molecular and cellular imaging." *Adv. Drug Deliv Rev* 60(11): 1226–1240.

Soppimath, K. S., Aminabhavi, T. M., Kulkarni, A. R., Rudzinski, W. E.(2001). "Biodegradable polymeric nanoparticles as drug delivery devices." *J Control Release* 70(1-2):1–20.

Sorlie, T., Tibshirani, R., Parker, J., Hastie, T., Marron, J. S., Nobel, A., Deng, S., Johnsen, H., Pesich, R., Geisler, S., Demeter, J., Perou, C. M., Lonning, P. E., Brown, P. O., Borresen-Dale, A. L and Botstein D (2003). "Repeated observation of breast tumour subtypes in independent gene expression data sets. *Proc Natl Acad Sci USA*." 100 (14): 8418-8423.

Sovak, M. A., Bellas, R. E., Kim, D. W., Zanieski, G. J., Rogers, A. E., Traish, A. M. and Sonenshein, G. E. (1997). "Aberrant nuclear factor-kappa B/Rel expression and the pathogenesis of breast cancer." *J Clin Invest* 100(12): 2952-2960.

Sporn, M. B. and Liby, K. T. (2012). "NRF2 and cancer: the good, the bad and the importance of context." *Nat Rev Cancer*, 12 (8): 564-571.

.

Steeg, P. S. (2006). "Tumour metastasis: mechanistic insights and clinical challenges." *Nat Med*. 12(8): 895-904.

Storms, R. W., Trujillo, A. P., Springer, J. B., Shah, L., Colvin, O. M., Ludeman, S. M. and Smith, C. (1999). "Isolation of primitive human hematopoietic progenitors on the basis of aldehyde dehydrogenase activity." *Proc Natl Acad Sci USA* 96 (16): 9118–9123.

Storz, P. (2005). "Reactive oxygen species in tumour progression." *Front Biosci* 10: 881–896.

Stromme, J. H. (1965). "Interaction of disulfiram and diethyldithiocarbamate with serum proteins studied by means of a gel-filtration technique." *Biochem. Pharmacol.* 14: 381-391.

Stromme, J. H. and Eldjarn, L. (1966). "Distribution and chemical forms of diethyldithiocarbamate and tetraethylthiuram disulphide (disulfiram) in mice in relation to radioprotection." *Biochem Pharmacol* 15(3): 287-297.

Strume, J. H. (1965). "Metabolism of Disulfiram and Diethyldithiocarbamate in Rats with Demonstration of an in Vivo Ethanol-Induced Inhibition of the Glucuronic Acid Conjugation of the Thiol." *Biochem Pharmacol* 14: 393-410.

Sullivan, R and Graham, C. H. (2007). "Hypoxia-driven selection of the metastatic phenotype." *Cancer Metastasis Rev* 26(2):319–331.

Sullivan, R. and Graham, C. H. (2009). "Hypoxia prevents etoposide-induced DNA damage in cancer cells through a mechanism involving hypoxia-inducible factor 1." *Mol Cancer Ther* 8(6):1702-1713.

Sutton, D., Nasongkla, N., Blanco, E. and Gao, J. (2007). "Functionalized micellar systems for cancer targeted drug delivery." *Pharmaceutical Research* 24(6):1029–1046.

Szatrowski, T. P. and Nathan, C. F. (1991). "Production of Large Amounts of Hydrogen Peroxide by Human Tumor-Cells." *Cancer Research* 51(3): 794-798.

Tai, M. H., Chang, C. C., Kiupel, M., Webster, J. D., Olson, L. K. and Trosko, J. E (2005). "Oct4 expression in adult human stem cells: evidence in support of the stem cell theory of carcinogenesis." *Carcinogenesis* 26 (2):495–502.

Takase, O., Yoshikawa, M., Idei, M., Hirahashi, J., Fujita, T., Takato, T., Isagawa, T., Nagae, G., Suemori, H., Aburanti, H. and Hishikawa, K. (2013). "The Role of NF- κ B Signaling in the Maintenance of Pluripotency of Human Induced Pluripotent Stem Cells." *PLoS ONE* 8(2), e56399.

Takeda, A. L., Jones, J., Loveman, E., Tan, S. C. and Clegg, A. J. (2007). "The clinical effectiveness and cost-effectiveness of gemcitabine for metastatic breast cancer: a systematic review and economic evaluation." *Health Technol Assess* 11(19): iii, ix-xi, 1-62.

Talks, K. L., Turley, H., Gatter, K. C., Maxwell, P. H., Pugh, C. W., Ratcliffe, P. J. and Harris, A. L. (2000). "The expression and distribution of the hypoxia-inducible factors HIF-1 α and HIF-2 α in normal human tissues, cancers, and tumor-associated macrophages." *Am J Pathol* 157(2): 411- 421.

Tang, C., Chua, C. L and Ang, B. T. (2007). "Insights into the cancer stem cell model of glioma tumorigenesis." *Ann Acad Med* 36 (5):352–357.

Tang, P., Skinner, K. A. and Hicks, D. G (2009). "Molecular classification of breast carcinomas by immunohistochemical analysis: are we ready?" *Diagn Mol Pathol* 18(3):125–132.

Tapiero, H., Townsend, D. M. and Tew, K. D. (2003). "Trace elements in human physiology and pathology Copper." *Biomed Pharmacother*, 57(9): 386–398.

Tatum, J.L., Kelloff, G.J., Gillies, R.J., Arbeit, J.M., Brown, J.M., Chao, K.S., Chapman, J.D., Eckelman, W.C., Fyles, A.W., Giaccia, A.J., Hill, R.P., Koch, C.J., Krishna, M.C., Krohn, K.A., Lewis, J.S., Mason, R.P., Melillo, G., Padhani, A.R., Powis, G., Rajendran, J.G., Reba, R., Robinson, S.P., Semenza, G.L., Swartz, H.M., Vaupel, P., Yang, D., Croft, B., Hoffman, J., Liu, G., Stone, H., Sullivan, D. (2006) "Hypoxia: Importance in tumour biology, noninvasive measurement by imaging, and value of its measurement in the management of cancer therapy." *Int J Rad Biol* 82(10): 699-757.

Tawari, E. P., Wang, Z., Najlah, M., Tsang, C. W., Kannappan, V., Liu, P., McConville, C., He, B., Armesilla, A. L and Wang, W. (2015). "The cytotoxic mechanisms of disulfiram and copper(II) in cancer cells." *Toxicol. Res.* 4 (6): 1439-1442.

Taylor, C. T (2008). "Interdependent roles for hypoxia inducible factor and nuclear factor-kappaB in hypoxic inflammation." *J. Physiol* 586(17): 4055–4059.

Teicher, A. M, Bouchier-Hayes, D. J., Condrón, C. M. and Toomey, D. (2003). "Tumour hypoxia, chemotherapeutic resistance and hypoxia-related therapies." *Cancer Treat Rev.* 29 (4): 297–307.

Tergaonkar, V. (2006). "NFkB pathway: A good signaling paradigm and therapeutic target." *Int J Biochem Cell Biol.* 38 (10): 1647–1653.

The Independent UK Panel on Breast Cancer Screening (2012). "The benefits and harms of breast cancer screening: an independent review." *Lancet* 380 (9855): 1778-86.

Thiery, J. P. (2002). "Epithelial-mesenchymal transitions in tumour progression." *Nat Rev Cancer* 2 (6): 442–454.

Thiery, J. P., Acloque, H., Huang, RY. and Nieto, M. A. (2009). "Epithelial-mesenchymal transitions in development and disease." *Cell* 139 (5):871–890

Thomas, H. and Coley, H. M. (2003). "Overcoming multidrug resistance in cancer: an update on the clinical strategy of inhibiting p-glycoprotein." *Cancer Control*; 10 (2): 159–165.

Tian, X. S., Cong, M. H, Zhou, W. H., Zhu, J., Chen, Y. Z. and Liu, Q. (2008). "Clinicopathologic and prognostic characteristics of triple-negative breast cancer." *Onkologie* 31(11):610–614.

Tirino, V., Desiderio, V., Paino, F., De Rosa, A., Papaccio, F., Fazioli, F., Pirozzi, G. and Papaccio, G. (2011). "Human primary bone sarcomas contain CD133+ cancer stem cells displaying high tumorigenicity in vivo." *FASEB J* 25(6): 2022-2030

Torchilin, V. P. (2007). "Micellar nanocarriers: pharmaceutical perspectives." *Pharmaceutical Research*. 24(1):1–16.

Torchilin, V. P. (2005). "Recent advances with liposomes as pharmaceutical carriers." *Nat. Rev. Drug Discov*. 4 (2): 145–160.

Tsang, J., Lai, T. L., Lau, D. H., Au, G. K. and Chua, D. T. (2009). "Triple-negative breast cancer in Hong Kong Chinese patients." *J Clin Oncol* 27: 22127.

Tubbs, R., Barlow, W. E., Budd, G. T., Swain, E., Porter, P., Gown, A., Yeh, I. T., Sledge, G., Shapiro, C., Ingle, J., Haskell, C., Albain, K. S., Livingston, R. and Hayes D. F. (2009). "Outcome of patients with early-stage breast cancer treated with doxorubicin-based adjuvant chemotherapy as a function of HER2 and TOP2A status." *J Clin Oncol*. 27(24): 3881-3886.

Twiss, D., Bazier, S. A. and Thomas, F. (1922). "The Dithiocarbamate Accelerators of Vulcanization." *J Soc Chem Ind*. 41: 81-88.

Ucar, D., Cogle, C. R., Zucali, J. R., Ostmark, B., Scott, E. W., Zori, R., Gray, B. A. and Moreb, J. S. (2009). "Aldehyde dehydrogenase activity as a functional marker for lung cancer." *Chem Biol Interact* 178(1-3): 48-55.

Ueno, H., Kiyosawa, K. and Kaniwa, N. (2007). "Pharmacogenomics of gemcitabine: can genetic studies lead to tailor-made therapy?" *Br J Cancer* 97(2): 145-151.

Upreti, M., Jyoti, A. and Sethi, P. (2013). "Tumour microenvironment and nanotherapeutics." *Transl cancer res* 2(4): 309–319.

Valko, M., Izakovic, M., Mazur, M., Rhodes, C. J. and Telser J (2004). "Role of oxygen radicals in DNA damage and cancer incidence." *Mol Cell Biochem* ;266 (1-2): 37–56.

Valko, M., Morris, H. and Cronin, M. T. D (2005). "Metals, toxicity and oxidative stress." *Curr Med Chem* 12 (10): 1161–208.

van Uden, P., Kenneth, N.S. and Rocha, S (2008). "Regulation of hypoxia-inducible factor-1 alpha by NF-kappaB." *Biochem. J* 412 (3): 477-484.

van Vlerken, L.E., Vyas, T. K and Amiji, M. M (2007). "Poly(ethylene glycol)-modified nanocarriers for tumour-targeted and intracellular delivery." *Pharm. Res.* 24(8): 1405-1414.

Vaupel, P. and Mayer, A. (2007). "Hypoxia in cancer: significance and impact on clinical outcome." *Cancer Metastasis Rev.*, 26 (2): 225-239.

Vaupel, P., Kallinowski, F., and Okunieff P (1989). "Blood flow, oxygen and nutrient supply, and metabolic microenvironment of human tumours: a review." *Cancer Res* 49 (23): 6449–6465.

Vaupel, P., Mayer, A. and Höckel, M. (2004). "Tumour hypoxia and malignant progression." *Methods Enzymol.* 381 pp 335–354.

Vergis, R., Corbishley, C. M., Norman, A. R., Bartlett, J., Jhavar, S., Borre, M., Heeboll, S., Horwich, A., Huddart, R., Khoo, V., Eeles, R., Cooper, C., Sydes, M., Dearnaley, D. and Parker, C. (2008). "Intrinsic markers of tumour hypoxia and angiogenesis in localised prostate cancer and outcome of radical treatment: a retrospective analysis of two randomised radiotherapy trials and one surgical cohort study". *Lancet Oncol* 9 (4): 342-251.

Verrelle, P., Meissonnier, F., Fonck, Y., Feillel, V., Dionet, C., Kwiatkowski, F., Plagne, R. and Chassagne, J. (1991). "Clinical relevance of immunohistochemical detection of multidrug resistance P-glycoprotein in breast carcinoma." *J Natl Cancer Inst.* 83 (2): 111–116.

Viale, G. (2012) "The current state of breast cancer classification". *Ann Oncol* 23(10): 207-210.

Wang, C. Y., Mayo, M. W., Korneluk, R. G., Goeddel, D. V. and Baldwin, A. S. Jr (1998). "NF-kappaB antiapoptosis: induction of TRAF1 and TRAF2 and c-IAP1 and c-IAP2 to suppress caspase-8 activation." *Science* 281(5383): 1680–1683.

Wang, L., Munch-Petersen, B., Herrstrom Sjöberg, A., Hellman, U., Bergmen, T., Journvall, H and Eriksson S. (1999). "Human thymidine kinase 2: molecular cloning and characterisation of the enzyme activity with antiviral and cytostatic nucleoside substrates." *FEBS Lett* 443 (2): 170–174.

Wang, T and Guo, Z. (2006). "Copper in medicine: homeostasis, chelation therapy and anti-tumour drug design." *Curr Med Chem* 13(5): 525–537.

Wang, T. C., Cardiff, R. D., Zukerberg, L., Lees, E., Arnold, A. and Schmidt, E. V. (1994). "Mammary hyperplasia and carcinoma in MMTV-cyclin D1 transgenic mice." *Nature* 369(6482): 669-671.

Wang, W., McLeod, H. L. and Cassidy, J. (2003). "Disulfiram-mediated inhibition of NF-kappaB activity enhances cytotoxicity of 5-fluorouracil in human colorectal cancer cell lines." *Int J Cancer* 104(4): 504-511.

Wang, Y., Zhao, R. and Goldman I. D. (2003). "Decreased expression of the reduced folate carrier and folypolyglutamate synthetase is the basis for acquired resistance to the pemetrexed antifolate (LY231514) in an L1210 murine leukemia cell line." *Biochem Pharmacol* 65 pp 1163–1170.

Wani, M. C., Taylor, H. L., Wall, M. E., Coggon, P. and McPhail, A. T. (1971). "Plant antitumor agents. VI. The isolation and structure of taxol, a novel antileukemic and antitumor agent from *Taxus brevifolia*." *J Am Chem Soc* 93(9): 2325-2327.

Weigelt, B. and Reis-Filho, J. S. (2009). "Histological and molecular types of breast cancer: is there a unifying taxonomy?" *Nat Rev Clin Oncol* 6(12): 718-730.

Weinberg, R. A (2007) Garland Science. Taylor and Francis Group, LLC London. The biology of cancer. pp 316-321.

Wickstrom, M., Danielsson, K., Rickardson, L., Gullbo, J., Nygren, P., Isaksson, A., Larsson R., and Lovborg H (2007). "Pharmacological profiling of disulfiram using human tumour cell lines and human tumour cells from patients" *Biochem Pharmacol* 73: 25–33.

Woodruff, H. B. and Waksman, S. A. (1960). "The actinomycins and their importance in the treatment of tumors in animals and man. Historical background." *Ann N Y Acad Sci* 89 pp 287-298.

- Wu, M.X., Ao, Z., Prasad, K.V., Wu, R. and Schlossman, S. F. (1998) "IEX-1L, an apoptosis inhibitor involved in NF-kappaB-mediated cell survival." *Science* 281 (5379): 998–1001.
- Wu, Y., Deng, J., Rychahou, P. G., Qiu, S., Evers, B. M., Zhou, B. P (2009). "Stabilization of snail by NF-kappaB is required for inflammation-induced cell migration and invasion." *Cancer Cell* 15 (5): 416–428.
- Wu, Y., Sefah, K., Liu, H., Wang, R. and Tan, W. (2010). "DNA aptamer-micelle as an efficient detection/delivery vehicle toward cancer cells." *Proc. Natl Acad Sci* 107 (1): 5–10.
- Xia, X., Lemieux, M. E., Li, W., Carroll, J.S., Brown, M., Liu, X. S. and Kung, A. L. (2009). "Integrative analysis of HIF binding and transactivation reveals its role in maintaining histone methylation homeostasis." *Proc Natl Acad Sci USA* 106 (11): 4260–4265.
- Yakisich, J.S., Siden, A., Eneroth, P. and Cruz M. (2001). "Disulfiram is a potent in vitro inhibitor of DNA topoisomerases." *Biochem Biophys Res Commun*, 289(2): 586–590.
- Yen, W. C., Corpuz, M. R., Prudente, R. Y., Cooke, T. A., Bissonnette, R. P., Negro-Vilar, A. and Lamph, W.W. (2004). "A selective retinoid X receptor agonist bexarotene (Targretin) prevents and overcomes acquired Paclitaxel (Taxol) resistance in human non-small cell lung cancer." *Clin Cancer Res* 10 (24): 8656-8664.
- Yinjun, L., Jie, J. and Yungui, W. (2005). "Triptolide inhibits transcription factor NF-kappaB and induces apoptosis of multiple myeloma cells." *Leuk. Res.* 29 (1): 99–105.
- Yip, N. C., Fombon, I. S., Liu, P., Brown, S., Kannappan, V., Armesilla, A. L., Xu, B., Cassidy, J., Darling, J. L. and Wang, W. (2011). "Disulfiram modulated ROS-MAPK and NFkappaB pathways and targeted breast cancer cells with cancer stem cell-like properties." *Br J Cancer* 104(10): 1564-1574.

Yu, Q., Geng, Y. and Sicinski, P. (2001). "Specific protection against breast cancers by cyclin D1 ablation." *Nature* 411(6841): 1017-1021.

Zaman, G. J., Flens, M. J., van Leusden, M. R., de Haas, M., Mülder, H. S., Lankelma, J., Pinedo, H. M., Scheper, R. J., Baas, F. and Broxterman, H. J. (1994). "The human multidrug resistance-associated protein MRP is a plasma membrane drug-efflux pump." *Proceedings of the National Academy of Sciences of the United States of America*, 91(19): 8822–8826.

Zhang, J. A., Anyarambhatla, G., Ma, L., Ugwu, S., Xuan, T., Sardone, T. and Ahmad, I. (2005). "Development and characterization of a novel cremophor EL free liposome-based paclitaxel (LEP-ETU) formulation". *Eur. J. Pharm. Biopharm.* 59 (1): 177–187.

Zhang, Q., Shi, S., Yen, Y., Brown, J., Ta, J. Q. and Le, A. D. (2009). "A subpopulation of CD133(+) cancer stem-like cells characterized in human oral squamous cell carcinoma confer resistance to chemotherapy". *Cancer Lett* 289 (2): 151–160.

Zhao, Y., Yan, Q., Long, X., Chen, X. and Wang, Y. (2008): "Vimentin affects the mobility and invasiveness of prostate cancer cells". *Cell Biochem Funct*, 26 (5): 571-577.

Zhou, S., Schuetz, J. D., Bunting, K. D., Colapietro, A. M., Sampath, J., Morris, J. J., Lagutina, I., Grosveld, G. C., Osawa, M., Nakauchi, H. and Sorrentino, B. P. (2001). "The ABC transporter Bcrp1/ABCG2 is expressed in a wide variety of stem cells and is a molecular determinant of the side-population phenotype." *Nature Medicine* 7(9): 1028–1034.

Appendices

Appendix I

Peer-reviewed Publications

1. **Tawari, E. P.**, Wang, Z., Najlah, M., Tsang, C. W., Kannappan, V., Liu, P., McConville, C., He, B., Armesilla, A. L and Wang, W. (2015). "The cytotoxic mechanisms of disulfiram and copper(II) in cancer cells". *Toxicology Research* 4 (6): 1439-1442.
2. Iwona Zembko, Iram Ahmed, Aneesa Farooq, Jagdeep Dail, **Patricia Tawari**, Weiguang Wang and Christopher McConville (2014). Development of Disulfiram-loaded PLGA Wafers for the Localised Treatment of Glioblastoma Multiforme: A Comparison of Manufacturing Techniques. *Journal of Pharmaceutical Sciences J Pharmaceutical Sci* 104(3).
3. Liu, P., Wang, Z., Brown, S., Kannappan, V., **Tawari, P.E.**, Jiang, W., Irache, J.M., Tang, J.Z., Armesilla, A.L., Darling, J.L., Tang, X., Wang, W. (2014) Liposome encapsulated Disulfiram inhibits NFkB pathway and targets breast cancer stem cells *in vitro* and *in vivo*. *Oncotarget* 5(17):7471-85.
4. Liu, P., Kumar, I. S., Brown, S., Kannappan, V., **Tawari, P. E.**, Tang, J. Z, Jiang, W., Armesilla, A. L., Darling, J. L. and Wang, W. (2013). "Disulfiram targets cancer stem-like cells and reverses resistance and cross-resistance in acquired paclitaxel-resistant triple-negative breast cancer cells." *Br J Cancer*. 1109(7):1876-1885.
5. Christopher McConville, **Patricia Tawari**, Weiguang Wang (2015). Hot melt extruded and injection moulded disulfiram-loaded PLGA millirods for the treatment of glioblastoma multiforme via stereotactic injection. *International Journal of Pharmaceutics* 494(1): 73–82.

Appendix II

Presentations

Patricia Erebi Tawari, Zhipeng Wang, Vinodh Kannappan, Christopher Mcconville, Angel L Armesilla and Weiguang Wang NF κ B: A key factor involved in hypoxia-induced chemoresistance in breast cancer cells. BACR Special Meeting - Breast Cancer - Bridging gaps in our knowledge to improve patient outcome, New Castle 5th- 7th October, 2015.

Tawari, E. P., Liu, P., Wang, Z., Kannappan, V., Mcconville, C., Armesilla, A. L., Darling, J. L., Irache, J., Yoncheva, K., Petrov, P. and Wang, W Pluronic micelle-encapsulated Disulfiram targets cancer stem-like cells and reverses pan-resistance in acquired resistant breast cancer cell lines. AACR Annual Meeting 2015 in Philadelphia, PA, USA.

Patricia Erebi Tawari, Vinodh Kannappan, Zhipeng Wang, Peng Liu, Angel L Armesilla, John L Darling, Weiguang Wang. An acquired gemcitabine-resistant triple-negative breast cancer cell line expresses cancer stem-like cell markers and cross-resistant to anticancer drugs. NCRI Cancer Conference, 4-7 November 2014, BT Convention Centre, Liverpool, UK.

Tawari, E.P., Irache, J., Larranta, E., Yoncheva, K. and Wang, W. Encapsulation of Disulfiram in Pluronic Micelles: increasing its efficacy as a potential anticancer agent. 19th International symposium of microencapsulation held on the 9th- 11th September, 2013 at the University of Navarra, Pamplona, Spain.

Liu, P., Kumar, I.S., Brown, S., Kannappan, V., **Tawari, P.E.**, Wang, Z., Tang, J.Z., Wang, W. Disulfiram targets cancer stem-like cells and reverses chemoresistance in an acquired paclitaxel resistant triple negative breast cancer cell line. UK PharmSci 2013, the Science of Medicines Conference, 2nd - 4th September 2013, Heriot-Watt University, Edinburgh UK.

P Liu, Z Wang, S Brown, V Kannappan, **E.P. Tawari**, J.Z. Tang, A.L. Armesilla, J.L. Darling, W Wang. Disulfiram – An anti-alcoholism medicine giving breast cancer patients new hope. BACR Advances in Cancer Drug Discovery Conference, Cambridge 30th March – 1st April 2014.

Kannappan, V., Wang, Z., Liu, P., Brown, S., **Tawari, E.P.**, Bian, X., Armesilla, A.L., Darling, J.L. and Wang, W. Disulfiram – An anti-alcoholism drug targets glioblastoma stem cells by modulating hypoxia-NF-kB pathway. BACR Advances in Cancer Drug Discovery Conference, Cambridge 30th March – 1st April 2014.

Vinodh Kannappan, Zhipeng Wang, **Patricia Erebi Tawari**, Peng Liu, Sarah Brown, Ziuwu Bian, Angel L Armesilla, John L Darling, Weiguang Wang. Disulfiram targets cancer stem cells by modulating hypoxia-NF-kB pathway to reverse chemoresistance in glioblastoma multiforme. NCRI Cancer Conference, 4-7 November 2014, BT Convention Centre, Liverpool, UK.

Liu, P., Wang, Z., Brown, S., Kannappan, V., **Tawari, P.E.**, Tang, J.Z., Armesilla, A., Darling, J.L and Wang, W. Repurposing Disulfiram into breast cancer therapeutics: Nano-encapsulation may bridge the gap between ‘bench’ and ‘bed’. 19th International symposium of microencapsulation held on the 9th- 11th September, 2013 at the University of Navarra, Pamplona, Spain.